Activities of the

Oil Implementation Task Force

Reporting Period March–August 1991

Contracts for field projects
and supporting research on . . .

Enhanced Oil Recovery

Reporting Period October–December 1990

65

DOE/BC-91/1
(DE91002231)
PROGRESS REVIEW
Quarter Ending December 31, 1990

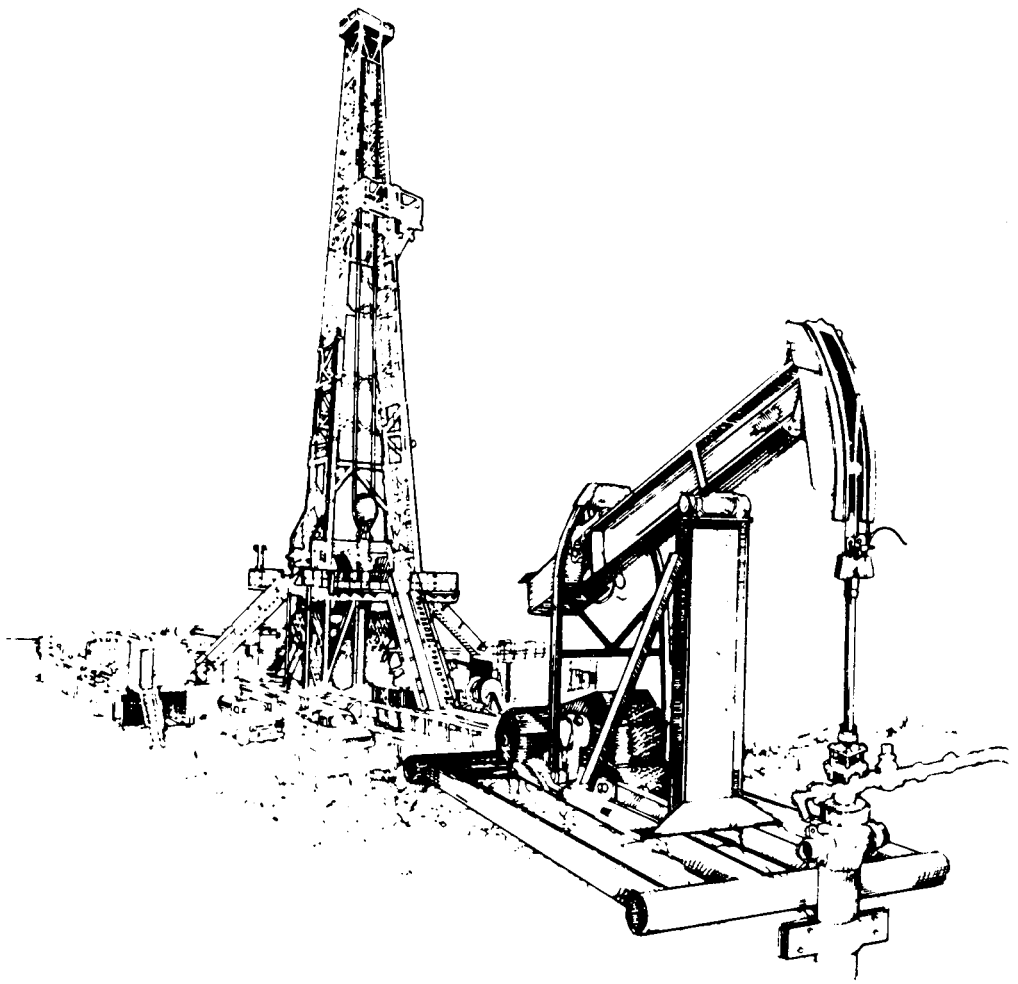

United States Department of Energy
Office of Oil, Gas, and Shale Technology
and Bartlesville Project Office

DISCLAIMER

Available to DOE and DOE contractors from the Office of Scientific and Technical Information, P.O. Box 62, Oak Ridge, Tennessee 37831; prices available from (615)576-8401, FTS 626-8401.

Available to the public from the National Technical Information Service, U.S. Department of Commerce, 5285 Port Royal Rd., Springfield, Virginia 22161.

Printed in the United States of America

SECTION INDEX

SECTION I

Oil Implementation Task Force – Final Report

U.S. Department of Energy
Washington, D.C. 20545

LINDA G. STUNTZ
Acting Assistant Secretary for Fossil Energy
Room 4G-084 Forrestal Building
Telephone Number (202) 586-4695

MARVIN SINGER
Deputy Assistant Secretary for Oil, Gas, Shale, and Special Technologies

ROBERT L. FOLSTEIN
Director, Oil Implementation Task Force

Bartlesville Project Office
P.O. Box 1398
Bartlesville, Oklahoma 74005
Telephone No. 918/337-4401

THOMAS C. WESSON
Director

EDITOR:
HERBERT A. TIEDEMANN
Project Manager for Technology Transfer

DOE/BC-91/1
(DE91002231)
Distribution Category UC-122

PROGRESS REVIEW NO. 65

OIL IMPLEMENTATION TASK FORCE

Final Report

Date Published - October 1991

UNITED STATES DEPARTMENT OF ENERGY

INDEX

OIL IMPLEMENTATION TASK FORCE – FINAL REPORT

Quarterly Progress Reviews #62 (December 1990) and #63 (March 1991) contained reports covering activities of the Oil Implementation Task Force (OITF) from its organization in September 1990 through February 1991. During this six-month period the Task Force accomplished a number of tasks critical to implementation of DOE's National Energy Strategy — Advanced Oil Recovery Program (NES-AORP).

- Using DOE's Tertiary Oil Recovery Information System (TORIS), OITF provided baseline data for:
  - classification, geographic distribution of reservoirs
  - determination of urgency relative to abandonment
  - identification of applicable recovery processes
  - prioritization of reservoir classes
  - estimated impact of R&D successes and failures on increasing the economic producibility of the known remaining oil resources in each reservoir class.
- Initiated processes for:
  - selection of reservoir classes for study
    - selected Class 1, unstructured, fluvial-dominated deltaic reservoirs
    - selected Class 2, shelf carbonate reservoirs
  - solicitation of industry and other public input regarding technical constraints to improved production and mechanisms for overcoming those constraints for each class of reservoirs
    - first public input meeting held in Dallas TX (January 1991) for Class 1 reservoirs.
  - implementing near-term demonstrations of conventional technology that will assist operators in maintaining production and preventing abandonment of oil resources
  - conducting research to better characterize the reservoirs in each class
    - Study of five deltaic reservoir plays included in January 1991 Class 1 meeting report
  - implementing field demonstrations of advanced technology to overcome the reservoir constraints identified in the characterization research
    - database of supporting research compiled containing 327 current and past EOR-related projects

During the continuation of these reservoir class-related activities throughout the period of March-August 1991, several additional tasks were completed.

- The report on the January Class 1 meeting in Dallas was published (DOE/BC–91/6/SP) "Opportunities to Improve Oil Productivity in Unstructured Deltaic Reservoirs," and was distributed to interested members of the petroleum community.
- A comprehensive literature review and field case history study was compiled to define the research needed to achieve NES-AORP goals.
- A presolicitation meeting was held in Dallas (August 1991) for public comment on draft Public Opportunity Notices (PONs) for near- and mid-term research, de-

velopment and demonstration projects for Class 1 deltaic reservoirs.

The Oil Implementation Task Force completed its assigned tasks during June 1991. Activities of the NES-AORP are continuing as separate efforts for each selected reservoir class, tailoring the procurement and research activities to the specific needs of the reservoir class.

NES-AORP Reservoir Class activities scheduled for the near future include:

- Following incorporation of public comments from the August meeting, the Class 1 PONs are scheduled for issuance in October 1991. A pre-procurement meeting to provide information and clarify issues regarding the final procurement documents will be held several weeks after the PONs are issued.
- Class 2 Shelf Carbonate Reservoir regional workshops are scheduled to be held in November and December 1991 to provide information on the reservoirs and to receive public input and comments on the Class 2 program.

As other reservoir classes are added, each class will initiate a series of public input, procurement, project research, technology transfer and implementation actions. Throughout the next fiscal year (FY 1992) activity, principally in the area of procurement for Class 1 and 2 reservoirs, will be reported in the Quarterly Progress Review, starting with #66, tentatively scheduled for publication in December 1991 or January 1992. Reporting will continue as the activities enter into the research, demonstration and application stages for the various reservoir classes.

For further information regarding the NES-AORP Reservoir Class activities, contact:

Herbert A. Tiedemann
U.S. Department of Energy
Bartlesville Project Office
P.O. Box 1398
Bartlesville OK 74005
918-337-4293 FTS 745-4293
FAX 918-337-4418

SECTION II

Enhanced Oil Recovery
Progress Reviews

U.S. Department of Energy
Washington, D.C. 20545

LINDA G. STUNTZ
Assistant Secretary
for Fossil Energy
Room 4G-084 Forrestal Building
Telephone Number (202) 586-4695

MARVIN SINGER
Deputy Assistant Secretary for Oil,
Gas, Shale, and Special
Technologies

JAMES D. BATCHELOR
Director for Oil, Gas,
and Shale Technology

ARTHUR HARTSTEIN
Deputy Director of Oil, Gas,
and Shale Technology

J. J. STOSUR
Enhanced Oil Recovery Program Manager
Mail Stop D-116, Germantown
Telephone Number (301) 353-2749

Bartlesville Project Office
P.O. Box 1398
Bartlesville, Oklahoma 74005

Telephone No. 918/337-4401

THOMAS C. WESSON
Director

R. M. RAY
Deputy Director

FRED W. BURTCH
Program Coordinator,
Enhanced Oil Recovery

HERBERT A. TIEDEMANN
Project Manager for
Technology Transfer

DOE/BC-91/1
(DE91002231)
Distribution Category UC-122

PROGRESS REVIEW NO. 65

CONTRACTS FOR FIELD PROJECTS AND SUPPORTING RESEARCH ON ENHANCED OIL RECOVERY

Date Published - October 1991

UNITED STATES DEPARTMENT OF ENERGY

PUBLICATIONS LIST

Bartlesville Project Office
Thomas C. Wesson, Director

AVAILABILITY OF PUBLICATIONS

The Department of Energy makes the results of all DOE-funded research and development efforts available to DOE and DOE contractors from the **Office of Scientific and Technical Information, P.O. Box 62, Oak Ridge, TN 37831; prices available from (615) 576-8401, FTS 626-8401.**

Available to the public from the **National Technical Information Service, U.S. Department of Commerce, 5285 Port Royal Road, Springfield, VA 22161; prices available from (703) 487-4650.**

Give the full title of the report and the report number.

Sometimes there are slight delays between the time reports are shipped to NTIS and the time it takes for NTIS to process the reports and make them available. Accordingly, if NTIS advises you that a specific report is not yet available, we will provide one copy of any individual report as long as our limited supply lasts. Please help us in our effort to eliminate wasteful spending on government publications by requesting only those publications needed. Order by the report number listed at the beginning of each citation and enclose a self-addressed mailing label. Available from **DOE Bartlesville Project Office, ATTN: Herbert A. Tiedemann, P.O. Box 1398, Bartlesville, OK 74005; (918) 337-4293.**

Quarterly Reports

DOE/BC–90/2 **Activities of the Oil Implementation Task Force. Reporting Period September-November 1990. Contracts for Field Projects and Supporting Research on Enhanced Oil Recovery. Progress Review No. 62. Quarter ending March 31, 1990. Order No. DE90000262.** In Section I, the first report of the Oil Implementation Task Force is summarized. The introduction explains the shift in program direction and the reservoir classification system. Further discussion includes the Tertiary Oil Recovery Information System; field research, development and demonstration, and research support – the characterization of Class 1 reservoirs. In Section II, status reports are given for various enhanced oil recovery and gas recovery projects sponsored by the Department of Energy. The field tests and supporting research on enhanced oil recovery include chemical flooding, gas displacement, thermal/heavy oil, resource assessment, geoscience technology, microbial technology, novel technology, and environmental technology.

Chemical Flooding

NIPER–466 **Critical Factors in the Design of Cost-Effective Alkaline Flooding. Topical Report. National Institute for Petroleum and Energy Research. February 1991. 20 pp. Order No. 91002224.** A review of major alkaline flooding projects highlights the recognized fact that alkali consumption and scale formation are serious deterrents when strong alkalis are used. The review also confirms that there are several mechanisms of oil mobilization besides reducing interfacial tension. Even oils of low acid number may be amenable to alkaline flooding. Moreover, alkalis in a lower pH range – which have minimal reaction with reservoir minerals – can often mobilize oil, especially when enhanced with a low concentration of surfactant. However, the future of alkaline flooding depends critically on improved reservoir analysis, which includes factors that have often been neglected: (1) thorough mineralogical analysis; (2) evaluation of ion-exchange properties; and (3) assessment of carbon dioxide content.

NIPER–488 **Effects of Degree of Hydrolysis and Shear on Gelation Reaction Kinetics and Gel Strength. Topical Report. National Institute for Petroleum and Energy Research. February 1991. 24 pp. Order No. DE91002225.** Gelation tests were conducted to investigate the effect of the degree of hydrolysis on gelation reaction kinetics and gel strength using four low-molecular-weight polyacrylamides (MW = 400,000 daltons), which were 10% (HPAM1-10), 20% (HPAM1-20), 30% (HPAM1-30), and 40% (HPAM1-40) hydrolyzed, and Cr(III) (pH = 4.8) and Al(III) (pH = 7.0) crosslinkers. Results showed that for polymer/Cr(III) gel systems, samples prepared with a low-molecular-weight polyacrylamide polymer, which was 20% hydrolyzed, gelled at a faster rate and retained higher gel strength than those prepared with a low-molecular-weight polyacrylamide polymer, which was 10% hydrolyzed. Under the screening conditions, no viscosity enhancement was observed in samples prepared with polymers having a degree of hydrolysis equal to or greater than 30%. For polymer/Al(III) gel systems, samples prepared with a low-molecular-weight polyacrylamide polymer, which was 20% hydrolyzed, gelled at the fastest rate and retained the strongest gel strength among the polymer/Al(III) gel systems prepared with four low-molecular weight polyacrylamide polymers, which were 10, 20, 30, and 40% hydrolyzed, respectively. Gelation tests of gel systems in glass bead packs showed that high shear favored the gelation of a gel system that had a fast rate of gelation, but had an adverse effect on the gelation of three gel systems that had a slow rate of gelation. Weak gels were found to be injectable through porous media. Weak gels were degradable under high shear condition and regained viscosity under low shear conditions.

NIPER–498 **Modeling of Asphaltene and Wax Precipitation. Topical Report. National Institute for Petroleum and Energy Research. January 1991. 48 pp. Order No. DE91002217.** Organic deposition has been shown to be a major problem associated with oil recovery by gas flooding. Industry is looking for ways of controlling organic deposition and economic methods that can remedy the problem. A predictive technique is crucial to the solution of this problem, and this research project was designed to focus on the development of a predictive technique. A thermodynamic model has been developed to describe the effects of temperature, pressure, and composition on asphaltene precipitation. The model employs a polymer solution theory for asphaltene-oil solution and treated asphaltene as a polydispersed medium. The proposed model combines regular solution theory with Flory-Huggins polymer solutions theory to predict maximum volume fractions of asphaltene dissolved in oil. The model requires evaluation of vapor-liquid equilibria, first using an equation of state followed by calculations of asphaltene solubility in the liquid-phase. A state-of-the-art technique for C_7 – fraction characterization was employed in developing this model. The preliminary model developed in this work was able to predict qualitatively the trends of the effects of temperature, pressure, and composition. Since the mechanism of paraffinic wax deposition is different from that of asphaltene deposition, another thermodynamic model based on the solid-liquid solution theory was developed to predict the wax formation. This model is simple and can predict the wax appearance temperature with reasonable accuracy. In addition to the modeling work, experimental studies were conducted to investigate the solubility of asphaltene in oil and solvents and to examine the effects of oil composition, CO_2, and solvent on asphaltene precipitation and its properties. This research focused on the solubility reversibility of asphaltene in oil and the precipitation caused by CO_2 injection at simulated reservoir temperature and pressure conditions. These experiments have provided many observations about the properties of asphaltenes for further improvement of the model, but more detailed information about the properties of asphaltenes in solution is needed for the development of more reliable asphaltene characterization techniques.

NIPER–506 **The Effect of Alkaline Additives on the Performance of Surfactant Systems Designed to Recover Light Oils. Topical Report. National Institute for Petroleum and Energy Research. February 1991. 52 pp. Order No. DE91002226.** Surfactant flooding is flexible because of the ability to optimize formulations for a wide range of reservoir conditions and crude oil types. The objective for this work was to determine if the addition of alkaline additives will allow the design of surfactant formulations that are effective for

the recovery of crude oil, while, at the same time, maintaining the surfactant concentration at a much lower level than has previously been used for micellar flooding. Specifically, the focus of the work was on light, mid-continent crudes that typically have very low acid contents. These oils are typical of much of the midcontinent resource. The positive effect of alkaline additives on the phase behavior of surfactant formulations and acidic crude oils is well known. The extension to nonacidic and slightly acidic oils is not obvious. Three crude oils, a variety of commercial surfactants, and several alkaline additives were tested. The oils had acid numbers that ranged from 0.13, which quite low, to less than 0.01 mg KOH/g of oil. Alkaline additives were found to be very effective in recovering Delaware-Childers (OK) oil at elevated temperatures, but much less effective at reservoir temperatures. Alkaline additives were very effective with Teapot Dome (WY) oil. With Teapot Dome oil, surfactant/alkali systems produced ultralow IFT values and recovered 60% of the residual oil that remained after waterflooding. The effect of alkaline additives on recovering Hepler (KS) oil was minimal. The results of this work indicate that alkaline additives do have merit for use in surfactant flooding of low acid crude oils; however, no universal statement about applicability can be made. Each oil behaves differently with this treatment, and the effect of alkaline additives must be determined (at reservoir conditions) for each oil.

NIPER–507 **Surfactant-Enhanced Alkaline Flooding with Weak Alkalis. Topical Report. National Institute for Petroleum and Energy Research. February 1991. 24 pp. Order No. DE91002227.** The objective of this project was to develop cost-effective and efficient chemical flooding formulations using surfactant-enhanced, lower pH (weak) alkaline chemical systems. Chemical systems were studied that mitigate the deleterious effects of divalent ions. The experiments were conducted with carbonate mixtures and carbonate phosphate mixtures of pH 10.5, where most of the phosphate ions exist as the monohydrogen phosphate species. Orthophosphate did not further reduce the deleterious effect of divalent ions on IFT behavior in carbonate solutions, where the deleterious effect of the divalent ions is already very low. When added to a carbonate mixture, orthophosphate did substantially reduce the adsorption of an anionic surfactant, which was an unexpected result; however, there was no correlation between the amount of reduction and divalent ion levels. For acidic oils, a variety of surfactants are available commercially that have potential for use between pH 8.3 and pH 9.5. Several of these surfactants were tested with oil from Wilmington (CA) field and found to be suitable for use in that field. Two low-acid crude oils, with acid numbers of 0.01 and 0.27 mg KOH/g of oil, were studied. It was shown that surfactant-enhanced alkaline flooding does have merit for use with these low-acid crude oils. However, each low-acid oil tested was found to behave differently, and it was concluded that the applicability of the method must be experimentally determined for any given low-acid crude oil.

DOE/BC/14432–5 **Interactions of Structurally Modified Surfactants With Reservoir Minerals: Calorimetric, Spectroscopic and Electrokinetic Study. Final Report. Columbia University. March 1991. 44 pp. Order No. DE91002228.** The goal of this project was to develop an understanding of the adsorption of structurally modified surfactants and their interactions in the bulk and at the solid/liquid interface. A multi-pronged approach consisting of surface tensiometry, adsorption determination, microcalorimetry and electrokinetics measurement was used in this project to elucidate the effect of surfactant structure, specifically the effect of the position of sulfonate and methyl groups on the aromatic ring of alkyl xylene sulfonates on their adsorption. The study revealed that small changes in the position of the above functional groups have marked effect on their adsorption behavior; particularly the position of sulfonate relative to the methyl groups was found to play an important role. Microcalorimetric studies showed that hemimicellization of the surfactants was entropy driven and that the difference in the adsorption of the surfactants was because of differences in the steric hindrance to the packing of the molecules in the aggregates. The electrokinetic effects of the surfactants was investigated by measuring changes in the zeta potential of the mineral as a result of the surfactant adsorption and the studies indicated that the charge characteristics of the surfactants were not affected by the change in the position of the functional groups.

Thermal Recovery Processes

DOE/BC/14600–3 **Large Scale Averaging of Drainage at Local Capillary Control. Topical Report. University of Southern California. February 1991. 44 pp. Order No. DE91002221.** Large scale averaging is important for the description of displacement processes in heterogeneous porous media. For immiscible displacement, key objective is the determination of effective (psuedo) capillary pressure and phase permeabilities. Present continuum models rely on volume averaging and homogenization methods, typically under the premise of capillary control. However, such methods are intrinsically unable to provide the local saturation distribution, which is needed for the computation of effective flow properties. In this paper, paralleling pore-level approaches, a percolation method is proposed for the derivation of large scale properties in a drainage process at low flow rates. Percolation concepts are applied to a macroscopically heterogeneous region with a random and uncorrelated permeability distribution. Appropriate modifications of ordinary and invasion percolation, and percolation with trapping are developed for the determination of the large scale averages. Analytical results are also presented for certain simple cases. At conditions of local capillary control, when a local description is possible, the large scale capillary pressure curve is a non-trivial average of the individual curves. Large scale capillary trapping is predicted and a corresponding large scale trapped saturation is calculated. Large scale phase permeabilities are also derived. It is found that capillary heterogeneity renders a system more strongly wet in a macroscopic sense.

DOE/BC/14201–5 **Development of Methods for Controlling Premature Oxygen Breakthrough During Fireflooding. Final Report for the Period June 1, 1989 through October 1, 1990. Union Carbide Industrial Gases Inc. February 1991. 104 pp. Order No. DE91002220.** The overall objective of this study was to characterize the reservoir mechanisms that cause premature oxygen breakthrough, and develop practical tools for controlling it. The focus was on those conditions most likely to be encountered in moderate-depth to deep reservoirs; candidates included gas override, high-permeability streaks, and water underlie. Mitigation measures were selected based on due consideration of the cost of implementing them and their potential application to a wide range of specific problems. An overriding consideration was practicality for field use.

DOE/BC/91002214 **Injection Monitoring with Seismic Arrays and Adaptive Noise Cancellation. Final Report. Lawrence Livermore National Laboratory. January 1991. 32 pp. Order No. 91002214.** This report describes the results of a short field experiment conducted to test both the application of seismic arrays for in-situ reservoir stimulation monitoring and the active noise cancellation technique in a real reservoir production environment. Although successful application of these techniques to in-situ reservoir stimulation monitoring would have the greatest payoff in the oil industry, the proof-of-concept field experiment site was chosen to be the Geysers geothermal field in northern California. This site was chosen because of known high seismicity rates, a relatively shallow production depth, cooperation and some cost sharing with the UNOCAL Oil Corporation, and the close proximity of the site of LLNL. The body of this report describes the Geyser field experiment configuration, then discusses the results of the sesmic array processing and the results of the seismic noise cancellation.

Gas Displacement Technology

DOE/BC–91/2/SP **Miscible Applied Simulation Techniques for Energy Recovery – Version 2.0. User's Guide and Technical Manual. Morgantown Energy Technology Center. February 1991. 192 pp. Order No. 91002222.** MASTER was developed on a Digital Computer System (VAX 8650) and was written in standard FORTRAN 77. The simulator should run with minor or no modification on machines designed to handle standard FORTRAN 77. The User's Guide serves as a manual for users of the multicomponent, pseudomiscible simulator, MASTER. In Section 2, "Model Overview," the development history of MASTER and the type of problems that can be simulated are discussed. In Section 3, "Data Preparation and Description," the required format for the input file is shown, while in Section 4, "Interpretation of Model Output," various output formats are shown. In Section 5, "Conventional Model Features," and in Section 6, "Special Model Features," certain options and calculations in the code that the user should know to make the correct choice of variable values and options are discussed. Lastly, Section 7, "Example Problems" validation runs and examples of correct input and output files are presented. The information contained in this manual should be sufficient for the user to complete a successful simulation run with MASTER. The technical manual is divided into six parts. The first section discusses the relation of pseudomiscible simulators to black-oil simulators. The second presents the partial differential equations solved by MASTER and explains the discretization technique. The third section discusses the

implicit-in-pressure, explicit-in-saturation (IMPES) solution technique in general terms, and the fourth and fifth sections discuss the IMPES technique as it is applied to saturated and undersaturated blocks, respectively. The sixth section contains closing comments about the simulator. Appendix A discusses calculation of fluid properties and Appendix B discusses the operation of well models in MASTER.

Fundamental Petroleum Chemistry

NIPER-509 **The Thermodynamic Properties of 2, 3-Benzothiophene. Topical Report. National Institute for Petroleum and Energy Research. January 1991. 48 pp. Order No. DE91002218.** Measurements leading to the calculation of the ideal-gas thermodynamic properties for 2,3-benzothiophene are reported. Experimental methods included adiabatic heat-capacity calorimetry, comparative ebulliometry, inclined-piston gauge manometry, and differential-scanning calorimetry (d.s.c.). The critical temperature and critical density were determined with the d.s.c., and the critical pressure was derived. Entropies, enthalpies, and Gibbs energies of formation were derived for the ideal gas for selected temperatures between 260 K and 750 K. These values were derived by combining the reported measurements with values published previously for the enthalpy of combustion, the enthalpy of fusion, and the absolute entropy and enthalpy of the liquid at the triple-point temperature Measured and derived quantities were compared with available literature values.

NIPER-B06807-26 **Crude Oil and Finished Fuel Storage Stability: An Annotated Review – 1990 Revision. National Institute for Petroleum and Energy Research. January 1991. 92 pp. Order No. DE91002213.** The current update of the 1983 publication is brief and concise in both the narrative discussions and the annotated bibliography. Abstracts are meant to help readers determine the relevance of specific articles. To the extent possible, complete references are provided, as they were derived from the computer printout obtained from the various databases. The lack of uniformity among the citation formatting provided from the databases has made it necessary to provide all references in upper case print while abstracts were rewritten and reworded to avoid any possible copyright infringement. References in each of the subject sections are listed chronologically, starting with the oldest and working up through 1990. Papers covering more than one subject were not relisted under other subject headings to avoid redundancy and a complex numbering system. An alphabetical senior (first) author listing with the page number(s) on which citations can be found is provided at the end of this publication for reader convenience.

Geoscience Technology

NIPER-485 **Imaging Techniques Applied to the Study of Fluids In Porous Media–Topical Report. National Institute for Petroleum and Energy Research. January 1991. 36 pp. Order No. DE91002215.** The dynamics of fluid flow and trapping phenomena in porous media was investigated using a number of rock-fluid imaging techniques. Miscible and immiscible displacement experiments in heterogeneous Berea and Shannon sandstone samples were monitored using X-ray computed tomography (CT scanning) to determine the effect of heterogeneities on fluid flow and trapping. Thin sections were cut from these sandstone samples from areas exhibiting different flow and trapping characteristics. The statistical analysis of pore and pore throat sizes in these thin sections enabled the delineation of small-scale spatial distributions of porosity and permeability. Multiphase displacement experiments were conducted with micromodels constructed using thin slabs of the sandstones. The combination of the CT scanning, thin section, and micromodel techniques enables the investigation of how variations in pore characteristics influence fluid front advancement, fluid distributions, and fluid trapping. Plugs cut from the sandstone samples were investigated using high resolution nuclear magnetic resonance imaging (NMRI). NMRI permitted the visualization of oil, water or both within individual pores. The integration of how small-scale rock heterogeneities influence fluid flow and trapping. The application of these insights will aid in the proper interpretation of relative permeability, capillary pressure, and electrical resistivity data obtained from whole core studies.

NIPER-484 **Selection and Initial Characterization of a Second Barrier Island Reservoir System and Refining of Methodology for Characterization of Shoreline Barrier Reservoirs–Topical Report. National Institute for Petroleum and Energy Research. January 1991. 180 pp. Order No. DE91002216.** Generalization of shoreline barrier reservoir characteristics is a primary objective of this project. The Upper Cretaceous Almond formation in Patrick Draw oil field, southwestern Wyoming, has been selected from 18 primary candidates for comparison with the Lower Cretaceous Muddy formation in Bell Creek field, southeastern Montana. Both oil productive reservoirs selected for broadening geological and engineering understanding of the system represent a combination of "end-member" models of shoreline barriers developed under different hydrodynamic conditions. The hydrodynamic conditions primarily involve changes in sea level and the dominant tide and wave regime of a coastline. The productive Muddy formation in Bell Creek field predominantly consists of fine-grained littoral (intertidal) and neritic (shallow marine) sandstones deposited as shoreface and foreshore facies in a shoreline barrier system, whereas the Almond formation in Patrick Draw field contains two distinct units consisting of fine- to medium-grained estuarine sandstones deposited in a tidal channel/tidal delta environment associated with migrating tidal inlets within a barrier-island coastline and some fine to very fine-grained littoral and shallow neritic sandstones. For broadening comparative aspects of these oil-productive shoreline barrier systems, geologic information on a number of well documented outcrops and several representatives of the Holocene barriers have also been collected.

Resource Assessment Technology

NIPER–513 **Applications of EOR Technology in Field Projects–1990 Update. Topical Report. National Institute for Petroleum and Energy Research. January 1991. Order No. DE91002219.** Trends in the type and number of U.S. enhanced oil recovery (EOR) projects are analyzed for the period from 1980 through 1989. The analysis is based on current literature and news media and the Department of Energy (DOE) EOR Project Data Base, which contains information on over 1,348 projects. The National Institute for Petroleum and Energy Research maintains this data base and analyzes trends in the data. The characteristics of the EOR projects are grouped by starting date and process type to identify trends in reservoir statistics and applications of process technologies. Twenty-two EOR project starts were identified for 1989 and 10 project starts for 1988. An obvious trend over recent years has been the decline in the number of project starts since 1981 until 1988. An obvious trend over recent years has been the decline in the number of project starts since 1981 until 1988 which corresponds to the oil price decline during the period. There was a modest recovery in 1989 of project starts, which lags the modest recovery of oil prices in 1987 that was reconfirmed in 1989. During the time frame of 1980 to 1989, there has been a gradual improvement in costs of operation for EOR technology. The perceived average cost of EOR has gone down from a $30 bbl range to a low $20 bbl. These costs of operation seem to stay just at the price of oil or slightly above to result in marginal profitability. The use of polymer flooding has drastically decreased both in actual and relative numbers of project starts since the oil price drop in 1986. Production from polymer flooding is down more than 50%. Long-term plans for large, high-cost projects such as CO_2 flooding in West Texas, steamflooding in California, and hydrocarbon flooding on the North Slope have continued to be implemented. EOR process technologies have been refined to be more cost effective as shown by the continued application and rising production attributable to EOR.

Novel Recovery

DOE/BC/14458-1 **The Drilling of a Horizontal Well in a Mature Oil Field. Final Report. Rougeot Oil and Gas Corporation. January 1991. 60 pp. Order No. DE91002212.** This report documents the drilling of a medium radius horizontal well in the Bartlesville Sand of the Flatrock field, Osage County, Oklahoma. The report includes the rationale for selecting the particular site, the details of drilling the well, the production response, conclusions reached, and recommendations made for the future drilling of horizontal wells. Planning the well was difficult as there is very little publicly available data that provides details of horizontal drilling. The principal source of data was directional drilling vendors. The vendors projected job requirements were drastically different and somewhat contradictory. Vendor job cost estimates varied up to 300%. The well plan called for the placement of a 1,000' horizontal wellbore at a vertical depth of 1400'. The drill target was 10' thick and 200' wide. The spacing of the two rows of producing wells between which the horizontal wellbore is centered is 510'. In June 1990, Rougeot drilled the horizontal well (Wilson 25) attaining 1,050' of horizontal wellbore at a total cost of $150,532. The drilling problems that occurred were minor

and are readily available in the future. The well's productivity was tested with a rod pumping system before any wellbore clean-up or stimulation. The stabilized production rate after three months of production was 6 barrels of oil per day and 0.84 barrels of water per day, providing a very low water cut for this field. This level of oil production is 200 to 600% greater than a typical unstimulated vertical well. The production data for the well indicates that with wellbore clean-up/stimulation and increased wellbore length, future horizontal drilling in the Flatrock field could be economically viable.

INDEX

COMPANIES AND INSTITUTIONS

CONTENTS BY EOR PROCESS

DOE Technical Project Officers for Enhanced Oil Recovery

DIRECTORY

Name	Phone number	Name of contractor
U. S. Department of Energy Oil, Gas, and Shale Technology Mail Stop, D-116 GTN, Washington, D.C. 20545		
J. J. Stosur	301/353-2749	
Bartlesville Project Office P. O. Box 1398 Bartlesville, Oklahoma 74005		
Edith C. Allison	918/337-4390 - FTS 745-4390	Appalachian Oil and Natural Gas Research Consortium Brookhaven National Laboratory Fairleigh Dickinson Laboratory Idaho National Engineering Laboratory INJECTECH, Inc. National Institute for Petroleum and Energy Research Sandia National Laboratories University of Oklahoma University of Texas
Jerry F. Casteel	918/337-4412 - FTS 745-4412	National Institute for Petroleum and Energy Research
Alex Crawley		National Institute for Petroleum and Energy Research
Robert E. Lemmon	918/337-4405 - FTS 745-4405	National Institute for Petroleum and Energy Research Pennsylvania State University Sandia National Laboratories University of Alaska
Chandra M. Nautiyal	918/337-4409 - FTS 745-4409	Geological Survey of Alabama Kansas Geological Survey National Institute for Petroleum and Energy Research Southwest Research Institute University of Michigan University of Texas at Austin
R. Michael Ray	918/337-4403 - FTS 745-4403	Geological Survey of Alabama Illinois Department of Energy and Natural Resources Oklahoma Geological Survey
Thomas B. Reid	918/337-4233 - FTS 745-4233	Lawrence Livermore National Laboratory National Institute for Petroleum and Energy Research Stanford University Petroleum Research Institute University of Southern California
Metairie Site Office 900 Commerce Road, East New Orleans, Louisiana 70123		
Jerry Ham		Louisiana State University University of Oklahoma
E. B. Nuckols		Mississippi State University University of Oklahoma University of Texas
Rhonda Patterson		K&A Energy Consultants, Inc. Texas A&M University University of Tulsa
Eugene Pauling		University of Oklahoma
Morgantown Energy Technology Center P. O. Box 880 Morgantown, W. Va. 26505		
Royal J. Watts	304/291-4218 - FTS 923-4218	Morgantown Energy Technology Center New Mexico Institute of Mining and Technology Stanford University

CHEMICAL FLOODING—SUPPORTING RESEARCH

DEVELOPMENT OF IMPROVED SURFACTANT FLOODING METHODS

Cooperative Agreement DE-FC22-83FE60149, Project BE4A

National Institute for Petroleum and Energy Research
Bartlesville, Okla.

Contract Date: Oct. 1, 1983
Anticipated Completion: Sept. 30, 1991
Funding for FY 1990: $600,000

Principal Investigator:
Leo A. Noll

Project Manager:
Jerry F. Casteel
Bartlesville Project Office

Reporting Period: Oct. 1–Dec. 31, 1990

Objective

The objective of this year's work is to develop more effective surfactant flooding systems that have broader tolerance to chemical composition in reservoirs. The focus is to mitigate problems that have been shown to have adverse effects on the performance and economics of surfactant flooding processes, to improve the economics of surfactant-enhanced oil recovery through the development of effective oil recovery systems that contain very low concentrations of synthetic surfactants and alkaline additives, and to investigate the application or extension of current chemical flooding technology to near-term problem solving for near-wellbore permeability improvement.

Summary of Technical Progress

Mixed Surfactant Systems

In FY90 the evaluation of mixed surfactant systems that have broader tolerance to variation of chemical conditions in the reservoir was initiated. Most of the studies that have been conducted involved the use of carboxymethylated ethoxylated surfactants (CME) as additives to primary surfactant components in the system. The CME surfactants were chosen because they exhibited significant tolerance for high salinity ranges.[1] Economics is a major constraint in the use of these surfactants. Overall, from the results of the work conducted in FY90, the CME surfactants tested were not considered as potential candidates for the conditions tested. This year's emphasis is also on the study of mixed surfactant systems that include different combinations of various types of surfactants, synthetic sulfonates combined

with ionic and/or nonionic surfactants, that can also be economically applied. An example of the benefits of using mixed surfactant systems is the addition of an ethoxylated sulfonate to a petroleum sulfonate that resulted in an increase in the overall optimal salinity range of the surfactant system.[2]

Several surfactant system combinations are currently being tested with *n*-decane and with North Burbank Unit (NBU) crude oil. One of the systems being studied contains TRS 10-410 and isobutanol (IBA). Phase behavior measurements have been performed with this surfactant system, with the IBA component being substituted by several ethoxylated sulfonate surfactants (PPG's BSA-74 and GAF's SE-463) to determine improvement in salinity tolerance. The TRS 10-410 and IBA system has been fairly well studied in the past by other researchers for use with NBU crude oil.[3-4] The alcohol component was replaced with the ethoxylated sulfonate to help enhance the salinity tolerance of the overall system. The salinity limit of the surfactant solutions as a function of the ethoxylated surfactant substitution was determined. The results indicate that, in almost all cases, the substitution of the alcohol component resulted only in increasing salinity tolerance to about 3 to 4% NaCl at room temperature and at 50°C. Additional combinations will also be tested.

Phase inversion temperature (PIT) and salinity gradient phase inversion experiments were also conducted for the TRS 10-410 and IBA system to observe the change in solution conductivity and determine any relationship that may exist with respect to the behavior that was exhibited in the phase tubes. The width of the three-phase region for this surfactant system with the two oils has been determined by previous researchers.[3-4] The salinity gradient tests involved monitoring the electrical conductivity of the solution as a function of salinity at a fixed temperature. Results of these tests are shown in Fig. 1. The results from the salinity gradient tests indicate that the peak in solution conductivity

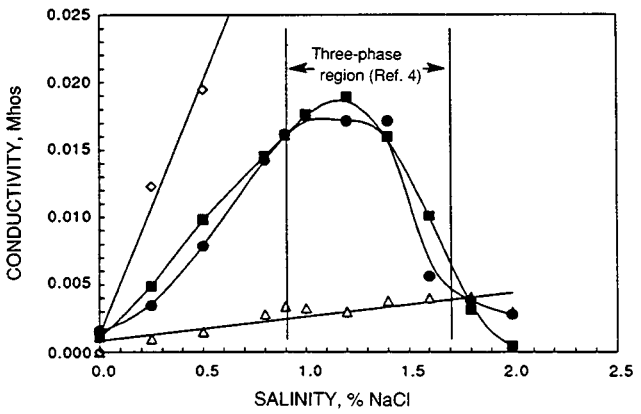

Fig. 1 Salinity gradient measurements using TRS 10-410 and isobutanol (IBA) system with North Burbank Unit (NBU) crude oil at 50°C. —△—, deionized water + *n* – C_{10}. —■—, surfactant + *n* – C_{10}. —●—, surfactant + NBU. —◇—, deionized water.

appears to coincide with the estimated midpoint of the three-phase region of this surfactant system.

Other surfactant systems that are also being evaluated include combinations of Stepan's B-100, B-105, B-110, and B-120 surfactants. The results from preliminary phase behavior screening conducted in FY90 showed that the B-105 had a fairly high salinity tolerance (up to 140% NBU brine strength). Additional tests with the B-105 surfactant showed a high salinity tolerance (up to 200% NBU brine strength tested), and the system exhibited three-phase behavior between 140 and 180% NBU strength. The B-105 surfactant formulation is a mixture of a high-molecular-weight (MW) alkyl aryl sulfonate and an ether sulfate.[5] The combinations using the B-105 and the other surfactants are being tested to shift the three-phase window closer to 100% NBU strength at 50°C. The addition of the other surfactants to B-105 can alter the proportion of the sulfonate and sulfate in the overall formulation, which will result in tolerance for conditions closer to NBU conditions. The B-105–B-110 combination resulted in the formation of a three-phase fluid at 100% NBU strength at a fixed proportion of the two surfactants (80:20 up to 90:10 of B-105:B-110). Interfacial tension (IFT) measurements indicated ultralow values ($<10^{-3}$ mN/m) of IFT between the aqueous phase and the oil. A coreflood experiment is being planned using this formulation.

Alkaline-Enhanced Mixed Surfactant Systems

Combined alkaline–surfactant chemical flooding methods show promise for improving cost-effectiveness of chemical enhanced oil recovery (EOR). A synergistic effect in lowering IFT using alkaline–surfactant mixtures allows the use of lower concentrations of the expensive surfactant chemicals. Mixed surfactant systems with added alkali have been evaluated to combine efforts to broaden surfactant salinity tolerance and reduce costs for the chemical flooding technique.

Phase behavior and IFT measurements have been conducted for a surfactant–alkaline system (0.25% Petrostep B-110, 0.15% Petrostep B-105, 0.095*N* $NaHCO_3$, and 0.095*N* Na_2CO_3 in 1% NaCl brine) with the Hepler and NBU crude oil. This system is being evaluated for reservoir conditions for the Hepler oil, and the use of NBU oil is for comparative purposes only. Previous results of IFT measurements using the Hepler oil have shown relatively low IFT values (6–10 μN/m) at room temperature.[6] Similar IFT values (10–12 μN/m) were measured with the NBU oil under the same conditions. Phase behavior experiments using this surfactant–alkaline system have indicated the formation of liquid crystals and fine-textured macroemulsions (observed using a video-enhanced microscopy apparatus) with the Hepler and NBU oil, respectively.

Coreflooding experiments have been conducted with this system with the use of Hepler and NBU crude oil. Initial evaluation of the incremental oil production for Hepler oil appeared to indicate that productivity decreased sharply

with a decrease in core permeability, as shown in Fig. 2. Similar results were found for other surfactant systems in Berea corefloods, although better correlations were made between recovery and oil permeability when native-state cores were used.[7]

Oil cuts for both Hepler and NBU oil recovery tests appeared to show a bimodal distribution as shown in Fig. 3. The initial production results from surfactant mobilization of the oil. Efficient polymer mobility control was necessary to observe the second kick in oil production. The presence of the surfactant was also required, however, to observe this additional production. Several corefloods were performed that demonstrated the effectiveness of the combined surfactant and polymer slugs. First, no incremental oil production was observed when only polymer was used. Next, production using another less effective alkaline–surfactant system (Petrostep B-120) was minimal with no second kick caused by the polymer. Finally, production of NBU oil increased from 36 to 54% of residual oil saturation when a higher concentration polymer slug (1000 and 3500 ppm biopolymer, respectively) was used.

Analysis of all the oil production curves indicated that two factors influenced the total recovery for the corefloods using the B-105/B-110 surfactant system. First, the production that resulted from surfactant mobilization without the aid of polymer mobility was proportional to the residual oil in place after the waterflood. This result was independent of core permeability (1250 to 50 mD) and oil type (Hepler and NBU oil). The correlation is shown in Fig. 4. Second, the production from the polymer kick was dependent on core permeability and/or polymer concentration. For the high-concentration polymer, injectivity was adversely affected by the low-permeability core (50 mD). Polymer filtered out on the face of the core. For intermediate permeability cores (250 mD), some polymer was also observed on the coreface after completion of the test, although the effect was not so great as with the low-permeability cores. Polymer filtration affects the mobility-control characteristics of the polymer slug, which, in turn, affects overall recovery efficiency. This is probably the reason total recovery appeared to be a function of core permeability as shown in Fig. 2.

The importance of good polymer mobility can probably be related to the observation that the surfactant–oil system formed liquid crystals or macroemulsions at this salinity. These are more viscous than microemulsions. Without good mobility control, these phases can be trapped in the core.

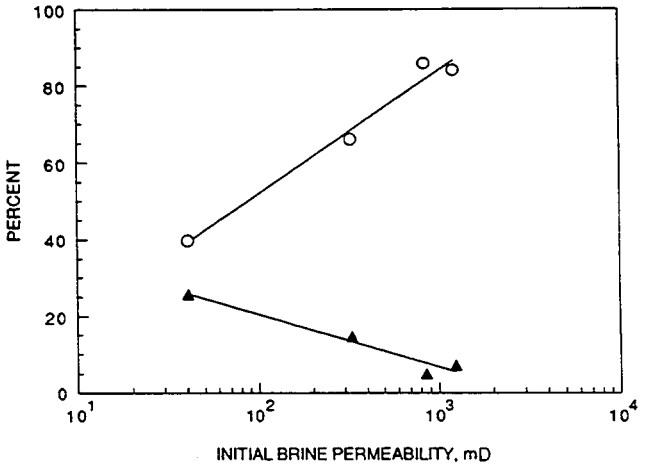

Fig. 2 Oil recovery and residual oil saturation after the chemical flood as a function of initial core permeability for Hepler oil using the surfactant system Petrostep B-110 and B-105 in alkaline brine. —○—, oil recovery, % residual oil. —▲—, residual oil after chemical flood.

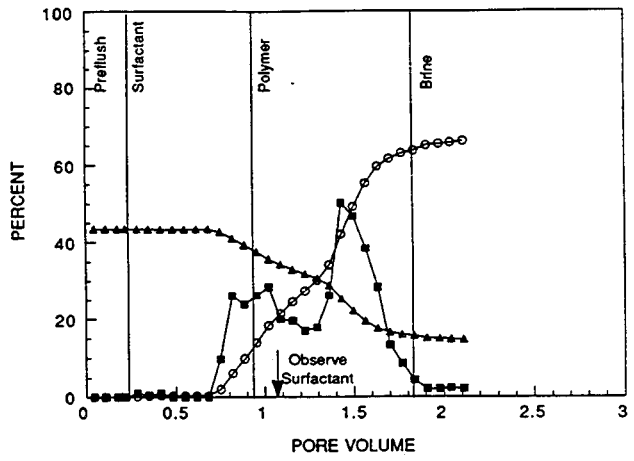

Fig. 3 Oil production for Hepler oil using an alkaline–surfactant system (B-105/B-110) showing effect of polymer mobility control to produce a second oil production peak. Initial brine permeability, 330 mD. —▲—, S_{ocf}. —○—, oil recovery, %. —■—, oil cut, %.

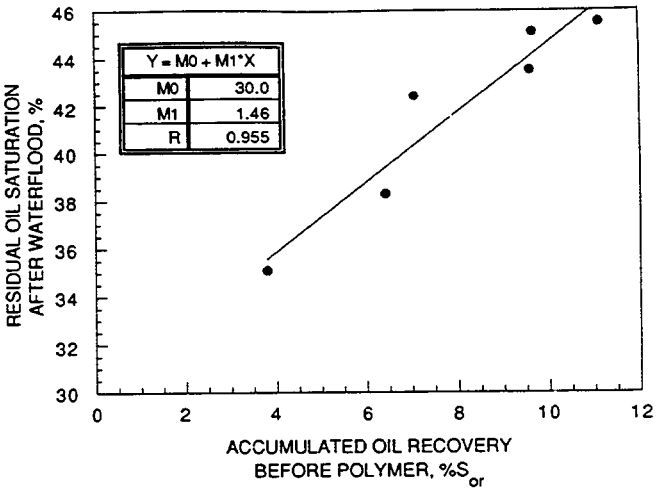

Fig. 4 Accumulative oil production before polymer kick as a function of residual oil saturation (S_{or}) after waterflood for corefloods using alkaline–surfactant (B-105/B110). Results are independent of core permeability and oil type.

These observations suggest that even though the potential for oil recovery with this surfactant system is high, there may be problems applying the technology in the field, either because the potential for phase trapping is high or because high polymer concentrations may make the chemical treatment uneconomical. Studies for the improvement of slug mobility and for the evaluation of other mixed surfactant systems to minimize liquid crystal and macroemulsion formation are continuing.

Surfactant-Based Well Treatments

Information has been gathered from the literature addressing the problems associated with loss of permeability in the near-wellbore region as well as paraffin problems in tubular goods. This information is presently being analyzed to determine which types of permeability impairment are amenable to chemical remediation treatments.

Paper SPE 21032, *The Effect of Temperature, Salinity, and Alcohol on the Critical Micelle Concentration of Surfactants*, was submitted to the Society of Petroleum Engineers (SPE) and will be presented at the 1991 International Symposium on Oilfield Chemistry. Galley proofs of the paper, "Flow Adsorption Calorimetry of Surfactants as a Function of Temperature, Salinity and Wettability," by Noll and Gall have been corrected and returned to *Colloids and Surfaces* for publication.

References

1. A. Strycker, *Selection and Design of Ethoxylated Carboxylates for Chemical Flooding*, DOE Report NIPER-449, September 1989.
2. V. K. Bansal and D. O. Shah, The Effect of Ethoxylated Sulfonates on Salt Tolerance and Optimal Salinity of Surfactant Formations for Tertiary Oil Recovery, *Soc. Pet. Eng. J.*, 18: 167-172 (June 1978).
3. G. R. Glinsmann, *Aqueous Surfactant Systems for In-Situ Multi-Phase Microemulsion Formation*, U.S. Patent No. 4,125,156, Nov. 14, 1978.
4. D. F. Boneau and R. L. Clampitt, A Surfactant System for the Oil-Wet Sandstone of the North Burbank Unit, *J. Pet. Technol.*, 29: 501-506 (May 1977).
5. Stepan Chemical Co., personal communication, 1990.
6. T. R. French, C. B. Josephson, and D. B. Evans, *The Effects of Alkaline Additives on the Performance of Surfactant Systems Designed To Recover Light Crude Oil*, DOE Report NIPER-506, 1991.
7. J. M. Maerker and W. W. Gale, *Surfactant Flood Process Design for Loudon*, paper SPE/DOE 20218 presented at the SPE/DOE Seventh Symposium on Enhanced Oil Recovery, Tulsa, Okla., Apr. 22–25, 1990.

DEVELOPMENT OF IMPROVED ALKALINE FLOODING METHODS

Cooperative Agreement DE-FC22-83FE60149, Project BE4B

National Institute for Petroleum and Energy Research
Bartlesville, Okla.

Contract Date: Oct. 1, 1983
Anticipated Completion: Sept. 30, 1991
Funding for FY 1991: $150,000

Principal Investigator:
Troy French

Project Manager:
Thomas B. Reid
Bartlesville Project Office

Reporting Period: Oct. 1–Dec. 31, 1990

Objectives

The objective of this project is to develop cost-effective and efficient chemical flooding formulations with surfactant-enhanced, weakly alkaline systems. Specific objectives for FY91 are: (1) to compare injection strategies and (2) to perform studies designed to support a field test.

Summary of Technical Progress

Application to Enhanced Oil Recovery

The emerging technology in alkaline flooding of heavy oil is the use of a combination of surfactant and alkali. Development of the proper design of injection strategy can be viewed as near-term as well as long-term research. In the near term, this research will support the design of a proposed surfactant-enhanced alkaline flooding field pilot test that will be conducted under the supplemental government project (SGP).

Discussion

One of the objectives of project BE4B is to develop improved alkali–surfactant flooding systems. Another objective is to provide support for the SGP field project. Injection strategy is an aspect of optimization that needs to be addressed. Some of the tests are being performed with crude oil from one of the sites proposed for the SGP project.

One of the candidate reservoirs identified is the Hepler (Kansas) oil field.[1] Favorable reservoir characteristics are low salinity and low divalent ion levels. The acid number of the oil is essentially zero. The chemical system composed of 0.25% Petrostep B-110 surfactant, 0.15% Petrostep B-105 surfactant, 0.095*N* $NaHCO_3$, 0.095*N* Na_2CO_3, 3500 ppm Flocon 4800-CX biopolymer, and 1.0% NaCl (optimal salinity) has been shown to be effective for mobilization of this oil. Several injection strategies with

this chemical system are being tested with laboratory corefloods, and the following results address this problem.

In situ oil viscosity is 76 cP; therefore a relatively high concentration of polymer is needed to achieve a favorable mobility ratio. Interfacial tension (IFT) experiments were conducted with alkali, surfactant, and polymer mixtures to separate the effects of the different chemicals on dynamic IFT behavior. Figure 1 shows the effect of polymer on the IFT obtained with the previously mentioned mixture of surfactant and alkali. The effect of polymer was to increase both initial and equilibrium IFT values.

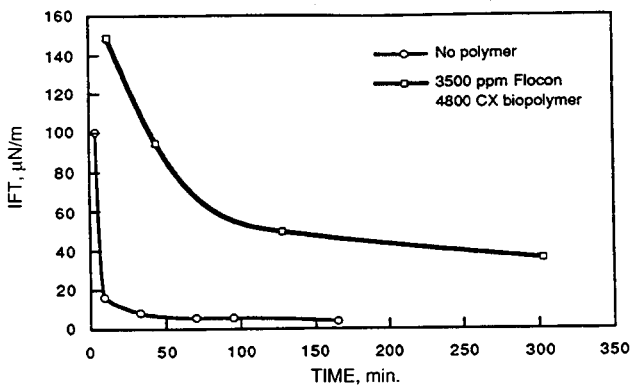

Fig. 1 Effect of polymer on dynamic interfacial tension (IFT) of Hepler (Kansas) oil and a chemical formulation composed of 0.25% Petrostep B-110, 0.15% B-105, 0.095*N* $NaHCO_3$, 0.095*N* Na_2CO_3, and 1% NaCl, 22°C.

Injections of a mixture of alkali + surfactant in one slug and polymer in a separate slug would be expected, on the basis of IFT measurements, to produce more incremental oil than combining alkali, surfactant, and polymer into one slug. This prediction was, however, not substantiated by corefloods conducted for comparing injection strategies.

Results of all corefloods conducted with the Hepler (Kansas) oil are tabulated in this report for project SGP41. Table 1 of that report shows that the injection of polymer as a part of a surfactant + alkali + polymer slug produced nearly as much incremental oil as the injection of separate surfactant + alkali and polymer slugs. The combined injection (coreflood RP-6) produced 78.9% of the oil that remained after waterflooding. This compares with 85.0 ± 0.9% for the injection of separate polymer and alkali + surfactant formulations. Coreflood RP-6 results are also considered important because the experiment was conducted in a core with a permeability similar to that of the reservoir.

An advantage of including the polymer in the alkali–surfactant slug is shown in Fig. 2. Tertiary oil production occurred significantly sooner in the coreflood (RP-6) conducted with the single slug of alkali + polymer + surfactant. Another advantage is that the surfactant and alkali should

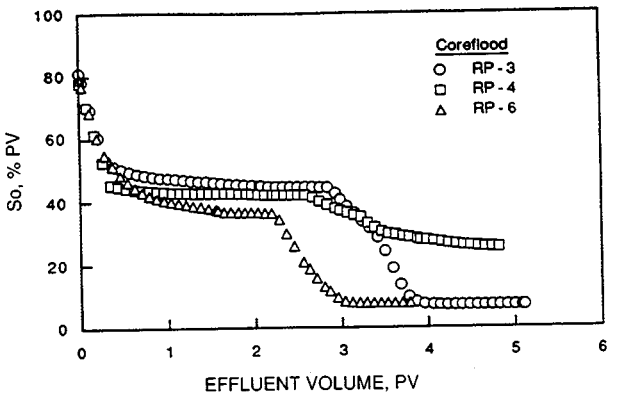

Fig. 2 Changes in oil saturation during corefloods conducted with Hepler (Kansas) oil.

sweep more of the reservoir when polymer is contained in the same slug as the surfactant and alkali.

Dynamic IFT experiments were also used to determine optimal salinity for surfactant (without alkali) and Hepler oil. This work is also being done as part of the injection strategy study. The results of a salinity scan performed with the above-mentioned surfactant mixture (no alkali) are shown in Fig. 3. The optimal salinity was determined to be approximately 2.0% NaCl. This compares to an optimal salinity of 1.0% with alkali present in the formulation.[1] A coreflood was performed to compare oil recovery with and without alkali in the chemical formulation. Since the initial and minimum IFT values were very nearly the same with and without alkali (optimal salinities different, of course) for this oil, it is predicted that oil recovery for the two different chemical systems will be similar. A coreflood to test this prediction is in progress.

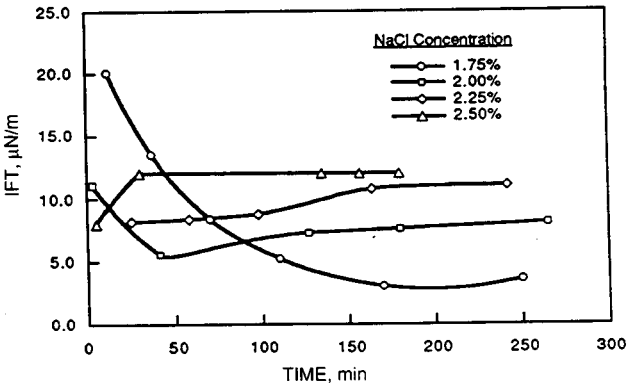

Fig. 3 Dynamic interfacial tension (IFT) of 0.25% Petrostep B-100, 0.15% B-105, and Hepler (Kansas) oil, 22°C.

Conclusions

1. In corefloods, total tertiary oil production is not affected by adding polymer to a surfactant–alkali slug, as opposed to injection of the polymer as a separate slug.

2. Including the polymer in the same slug as the alkali and surfactant results in faster production of incremental oil and, in petroleum reservoirs, should improve the sweep efficiency of a chemical slug.

Reference

1. National Institute for Petroleum and Energy Research, *Quarterly Technical Report for July 1–September 30, 1990,* Vol. II, Energy Production Research, DOE Report NIPER-501, pp. 87-91, October 1990.

DEVELOPMENT OF IMPROVED MOBILITY-CONTROL METHODS

Cooperative Agreement DE-FC22-83FE60149, Project BE4C

National Institute for Petroleum and Energy Research
Bartlesville, Okla.

Contract Date: Oct. 1, 1983
Anticipated Completion: Sept. 30, 1991
Funding for FY 1991: $200,000

Principal Investigators:
Troy R. French
Hong W. Gao

Project Manager:
Jerry F. Casteel
Bartlesville Project Office

Reporting Period: Oct. 1–Dec. 31, 1990

Objectives

The objectives of this project are to determine the applicability of low-molecular-weight polymer gels for mobility-control applications and to investigate the effect of a gel treatment on oil recovery in a polymer flood.

Summary of Technical Progress

Application to EOR

Mechanical degradation of high-molecular-weight polyacrylamides is a problem in field applications. A mobility-control system based on cross-linking a low-molecular-weight polyacrylamide may be much less susceptible to mechanical degradation. A permeability modification simulator is very useful to facilitate the design of treatments and assess potential fields for permeability modification treatments using gelled polymers.

Flow Behavior of Gel Systems in Porous Media

Residual resistance factor (RRF) was measured on a weak gel system that contained 15,000 ppm of HPAM1-10 (MW = 400,000 daltons, 10% hydrolyzed) and 25 ppm of Cr(III) in 53 meq/L NaCl at pH 4.8 in a glass bead pack (0.4 cm in diameter and 7.5 cm in length) to determine how the permeability was reduced by the gel system. Before measurements, the gel system (about 73 mL) had been continuously injected through the glass bead pack at an apparent shear rate of higher than 1,000 s^{-1} for more than 23 times (5,000 PV). During this injection period, the effluent showed no increase in viscosity. After 2,700 mL (8,180 PV) of brine (pH 4.8) was injected through the glass bead pack, RRF decreased from 84 at 0.408 mL/min to 28 at 0.71 mL/min. This RRF is about 15 times that of a solution of 1,500-ppm Pusher 500 in 53 meq/L NaCl in a Berea core (RRF 1.9). After the glass beads and interstitial fluid were pushed out of the glass tubing, gel was retained in the first quarter of the glass bead pack. The retained gel that accounted for the high-permeability reduction could be triggered by the adsorption of the gel system on the surfaces of the glass beads.

For the reduction of the adsorption effect on the flow behavior of a gel system in a porous medium, tests were then conducted in a polystyrene bead pack (0.4 cm in diameter and 7.62 cm in length) with a porosity of 45%. The beads used to pack the bead pack ranged in size from 60 to 120 mesh. Brine permeability of the bead pack used for testing a gel system that contained 15,000 ppm of HPAM1-10 and 50 ppm of Cr(III) in 53 meq/L NaCl at pH 4.8 was 45 darcys, and that used for testing a gel system that contained 15,000 ppm of HPAM1-10 and 75 ppm of Cr(III) in 53 meq/L NaCl at pH 4.8 was 40 darcys. A reciprocating pump was used to circulate the gel system continuously through the bead pack. The total volume of each gel sample used was about 60 mL. Before injection of the gel system into the bead pack, the pH of the interstitial fluid was adjusted to 4.8 with brine.

Figure 1 shows the test results of the gel system that contained 50 ppm of Cr(III) at both high and low shear conditions. Initially, the gel system was injected at 1.34 mL/min (apparent shear rate, 960 s^{-1}). After 5.75 h, the flow rate measured was 1.55 mL/min (1100 s^{-1}). The effluent viscosity measured with a Contraves viscometer decreased from 6.25 to 6.15 cP at a shear rate of 20 s^{-1}. At this time, the effluent had passed the bead pack 8 times (equivalent to having passed a 61-cm bead pack in about 2.5 min). One pore volume of the bead pack was 0.43 mL. After continuously circulating the gel system through the bead pack overnight, the flow rate itself changed from

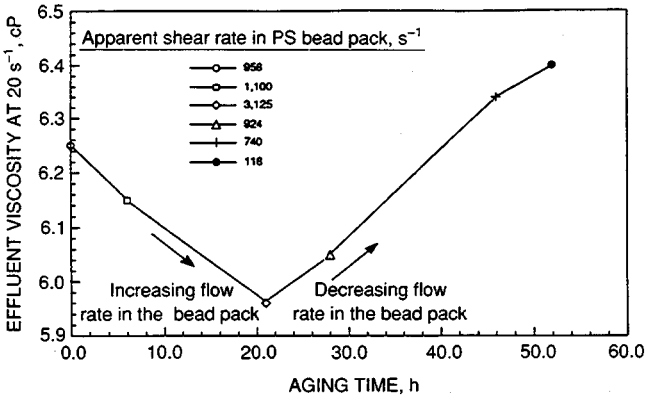

Fig. 1 Effect of shear on the gelation of a 15,000-ppm HPAM1-10/50-ppm Cr(III) gel system in 53 meq/L NaCl at pH 4.8 in a polystyrene (PS) bead pack. PS bead pack length, 7.62 cm; permeability, 45 darcys; porosity, 45%.

1.55 mL/min (1100 s^{-1}) to 3.13 mL/min (3125 s^{-1}), and the effluent viscosity decreased to 5.96 cP at 20.4 s^{-1}, as shown in Fig. 1, which indicates that some of the cross-linking bonds were broken. This indicated that high shear rates (higher than 960 s^{-1}) had an adverse effect on the gelation of the gel system in the porous medium. The flow rate was then decreased to about 1.56 mL/min to simulate decreasing flow rate of the fluid that flows into the reservoir. After the gel sample circulated for another 6 h, the flow rate itself decreased to 1.3 mL/min (925 s^{-1}), and the effluent viscosity increased to 6.05 cP at 20 s^{-1}. After the gel system circulated continuously through the bead pack overnight, the flow rate itself further decreased to 0.99 mL/min (740 s^{-1}), and the effluent viscosity further increased to 6.34 cP at 20.4 s^{-1} as shown in Fig. 1. These results indicate that low shear (lower than 960 s^{-1}) favored the gelation of this gel system in a porous medium. Although there was no way to distinguish between rehealing of the broken cross-linking bonds and gelation, the increase in viscosity was believed to have been caused by a combination of both. Previously, the effect of low shear on gelation reaction and rehealing of broken cross-linking bonds was observed in a Brookfield viscometer and in a tube flow,[1] but not in a porous medium because of adsorption effect.

Figure 2 shows the test results of another gel system that contained 15,000 ppm of HPAM1-10 and 75 ppm of Cr(III) in a 40-darcy bead pack at high shear conditions (apparent shear rates higher than 1,000 s^{-1}). During the 16 passes (equivalent to having passed a 122-cm bead pack), the flow rate was maintained most of the time in the range of 1.4 to 1.5 mL/min (apparent shear rates between 1,054 and 1,130 s^{-1}). As shown in Fig. 2, the effluent viscosity increased after each pass, which indicates that high shear favored the gelation of this system. This implies that this system and systems that have a faster rate of gelation than this one have the potential to exhibit higher viscosity after passing through the near-wellbore regime where the shear is high. As the gel system flows into the reservoir, an even higher viscosity can be obtained through continuous gelation reaction. Gel systems that have this characteristic will not have a mechanical degradation problem and will provide a better injectivity than do conventional high-molecular-weight polyacrylamides.

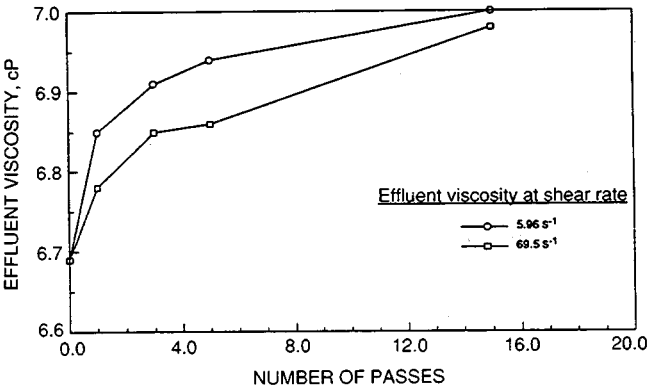

Fig. 2 Effect of high shear on the gelation of a 15,000-ppm HPAM1-10/75-ppm Cr(III) gel system in 53 meq/L NaCl at pH 4.8 in a polystyrene (PS) bead pack. Apparent shear rate in PS bead pack, >1000 s^{-1}; bead pack length, 7.62 cm; permeability, 40 darcys; porosity, 45%.

Reference

1. H. W. Gao, *Effects of Degree of Hydrolysis and Shear on Gelation Reaction Kinetics and Gel Strength*, DOE Report NIPER-488, October 1990 (NTIS order No. DE91002224).

SURFACTANT-ENHANCED ALKALINE FLOODING FIELD PROJECT

Cooperative Agreement DE-FC22-83FE60149, Project SGP41

National Institute for Petroleum and Energy Research
Bartlesville, Okla.

Contract Date: July 18, 1990
Anticipated Completion: Sept. 30, 1993
Funding for FY 1991: $318,000

Principal Investigator:
Troy French

Project Manager:
Thomas B. Reid
Bartlesville Project Office

Reporting Period: Oct. 1–Dec. 31, 1990

Objectives

The objectives of this pilot project are to: (1) obtain information and data that will help to demonstrate the applicability of surfactant-enhanced alkaline flooding as a cost-effective enhanced oil recovery (EOR) method, (2) transfer the surfactant-enhanced alkaline flooding technology that has been developed under the sponsorship of the Department of Energy (DOE) to the petroleum industry, and (3) obtain information regarding procedures for designing and applying this technology that will assist independent producers in sustaining production from mature producing oil fields rather than abandoning marginal wells.

Summary of Technical Progress

Several field sites are under consideration for the field project. A chemical system was designed and tested for possible use at the Hepler (Kansas) proposed test site. High mobilization of residual oil was achieved in corefloods conducted with the chemical system. The coreflood results are encouraging; however, problems remain as a result of the low permeability and heterogeneity of the site.

Application to EOR

Commercial and technological benefits will be achieved for all participants in the project if it is a success. The project will help move surfactant-enhanced alkaline flooding toward a commercial reality, increase oil production in the United States, and reduce the rate of resource abandonment in the United States.

Discussion

The most likely site for the field test is in the Hepler (Kansas) oil field; however, several other sites with favorable reservoir characteristics are being investigated. Several fields with favorable reservoir characteristics were identified in the Gulf Coast region. These fields are Government Wells, Loma Novia, Ganado West, and Coletto Creek. All these fields have high-permeability sands and low salinities and were selected as a result of a database search. Several operators in these fields have been contacted. One operator in Government Wells field has expressed enough interest to furnish samples for evaluation, and oil and brine samples should be received soon.

A sample of field core from the Hepler site was analyzed for mineral content with X-ray diffraction. The analysis is encouraging because the clay content is low. Kaolinite, the clay most detrimental to alkaline flooding, was present at the 3% level, which is acceptable.[1]

As previously reported, a chemical system composed of 0.25% Petrostep B-110 surfactant, 0.15% Petrostep B-105 surfactant, 0.095*N* $NaHCO_3$, 0.095*N* Na_2HCO_3, and 3500 ppm Flocon 4800-CX biopolymer is effective for mobilization of oil from the Hepler site.[2] The minimum interfacial tension (IFT) achieved was about 6 μN/m. The recovery during this chemical flood (coreflood RP-2) was 85.9% of the residual oil that remained after waterflood. The oil saturation after the chemical flood was 5.0%. Oil cuts during tertiary recovery were as high as 63% oil. This coreflood was repeated to verify the high oil recovery. The flooding strategy and results are summarized in Table 1. Oil recovery from the repeat coreflood (coreflood RP-3) was 84.1% of the oil that remained after waterflood. Figure 1 shows that the final oil saturation after tertiary flooding was 7.2% PV. Figure 2 shows that both alkali and surfactant were propagated through the Berea core at similar rates. The results from the two corefloods are very close and verify the high recovery efficiency potential of the chemical system when applied to recover Hepler oil.

Evaluation of core logs near the proposed site in Hepler (Kansas) field revealed that the pay zone of this field is heterogeneous, with permeabilities in the zone below 200 mD; some lower than 60 mD. Therefore corefloods are being performed in low-permeability cores.

Two low-permeability Berea cores (RP-4 and RP-6) and one core from the Bartlesville sandstone (RP-5) were used. The Bartlesville core is believed to be similar to that from the Hepler site. The floods are described and summarized in Table 1, and the oil recovery results are shown in Fig. 3. The injection strategy was different for coreflood RP-6, and this aspect of the results is reported elsewhere. Oil recovery was high in cores with permeabilities as low as 120 mD, which is within the range of permeability in the pay zone. Oil recovery was much lower in the 41- and 80-mD cores. Oil recovery and effluent analysis are shown in Fig. 4 for the 120-mD core (coreflood RP-6). Viscosity measurements indicate polymer did pass through the core. There was little indication of polymer plugging.

Lowest oil recovery resulted when a recently acquired polyacrylamide polymer sample was substituted for the biopolymer used in the other corefloods. The oil recovery in this experiment may have been adversely affected by the change in polymer since the sample of polyacrylamide polymer used may have been improperly labeled by the manufacturer. This sample of polymer was unexpectedly difficult to disperse in the brine and appeared to have very little salt tolerance. Nevertheless, the oil recovery appears to be much lower in the very tight cores. Coreflood RP-4 (conducted with the tightest core) produced 39.7% of the oil that remained after waterflood. There was evidence of polymer plugging at the face of this core.

Because of the low permeability range of the Hepler pay zone and the apparent problem of propagating polymer in the tight cores, two commercially available polymers with lower molecular weights are being tested.

Conclusions

1. A chemical system was identified that is effective for mobilization of oil from the Hepler (Kansas) site.

TABLE 1

Summary of Coreflood Injection Strategies and Results for Hepler (Kansas) Oil

Coreflood	Core type*	K, mD	Preflush solution		First chemical formulation injected	
			Composition	Vol., PV	Composition	Vol., PV
RP-1	Berea sandstone	796	None		2.12 g NaCl + 0.2 g B-120/100 mL + pH 9.5 carbonate + 3500 ppm Flocon 4800 CX	0.75
RP-2	Berea sandstone	855	1.0 g NaCl/100 mL pH 9.5 carbonate mixture	0.25	1.0 g NaCl + 0.25 g B-110 + 0.15 g B-105 + 2.03 g 2-butanol/ 100 mL + pH 9.5 carbonate	0.75
RP-3	Berea sandstone	1240	1.0 g NaCl/100 mL pH 9.5 carbonate mixture	0.25	1.0 g NaCl + 0.25 g B-110 + 0.15 g B-105 + 2.03 g 2-butanol/ 100 mL + pH 9.5 carbonate	0.75
RP-4	Berea sandstone	41	1.0 g NaCl/100 mL pH 9.5 carbonate mixture	0.25	1.0 g NaCl + 0.25 g B-110 + 0.15 g B-105 + 2.03 g 2-butanol/ 100 mL + pH 9.5 carbonate	0.75
RP-5	Bartlesville sandstone	80	1.0 g NaCl/100 mL pH 9.5 carbonate mixture	0.25	1.0 g NaCl + 0.25 g B-110 + 0.15 g B-105 + 2.03 g 2-butanol/ 100 mL + pH 9.5 carbonate	0.75
RP-6	Berea sandstone	120	1.0 g NaCl/100 mL pH 9.5 carbonate mixture	0.25	1.0 g NaCl + 0.25 g B-110 + 0.15 g B-105 + 2.03 g 2-butanol/ 100 mL + pH 9.5 carbonate + 3500 ppm Flocon 4800 CX polymer	0.75

Coreflood	Second chemical formulation injected		Recovery efficiency,† %
	Composition	Vol., PV	
RP-1	None		18.2
RP-2	3500 ppm Flocon 4800 CX biopolymer	1.0	85.9
RP-3	3500 ppm Flocon 4800 CX biopolymer	1.0	84.1
RP-4	3500 ppm Flocon 4800 CX biopolymer	1.0	39.7
RP-5	3000 ppm C4331D polyacrylamide	1.0	29.6
RP-6	3500 ppm Flocon 4800 CX biopolymer	0.25	78.9

*Cores were saturated with synthetic brine containing 1.022 g NaCl, 0.033 g $CaCl_2$, and 0.0694 g $MgCl_2 \cdot 6H_2O$/100 mL.
†Recovery efficiency = (oil produced during chemical flood/oil remaining after waterflood) × 100.

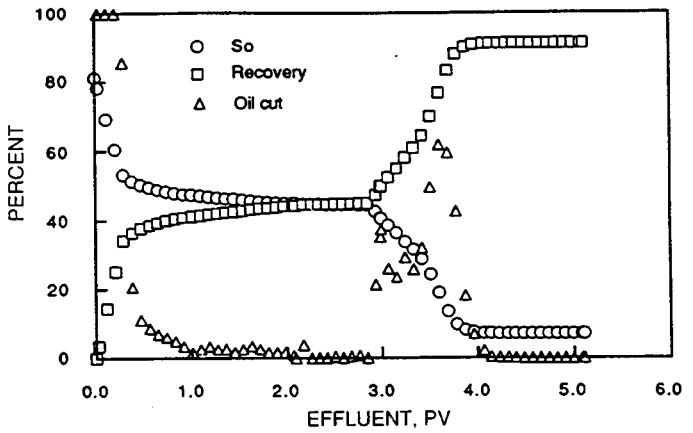

Fig. 1 Oil recovery from coreflood RP-3.

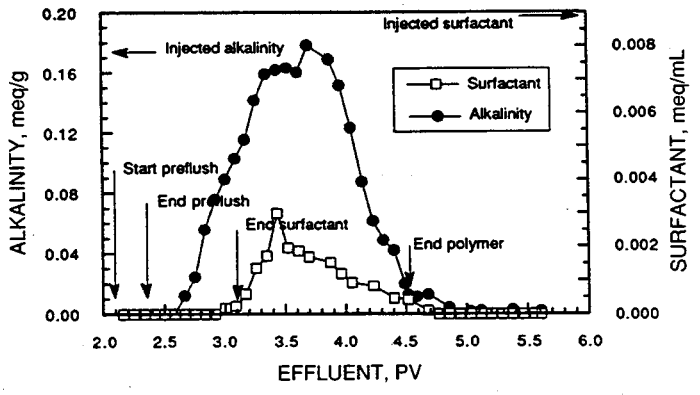

Fig. 2 Effluent analysis from coreflood RP-2.

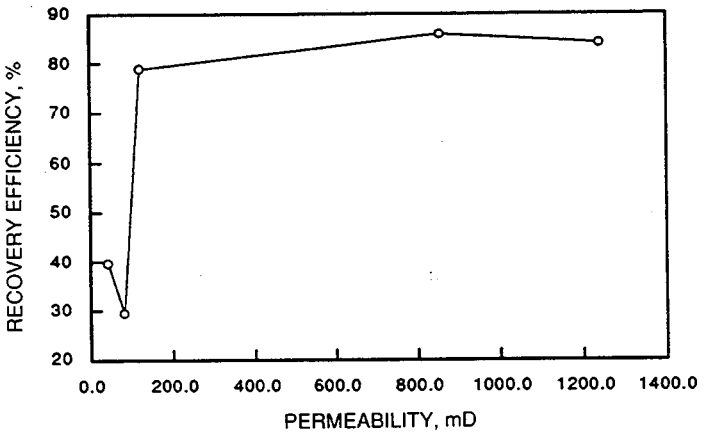

Fig. 3 Tertiary oil recovery from corefloods with Hepler (Kansas) oil.

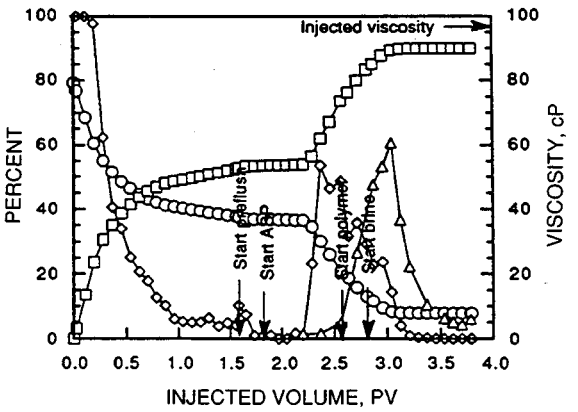

Fig. 4 Oil recovery and effluent analysis from coreflood RP-6. —Δ—, viscosity, cP. —○—, oil saturation, %PV. —□—, oil recovery, %OIP. —◊—, oil cut, %.

2. Oil recovery by the chemical system was lower when tight cores were used. This was due, in part, to problems associated with polymer injection.

3. Polymer with lower molecular weight should be tested for use in chemical formulations designed for use in Hepler (Kansas) field.

References

1. P. B. Lorenz and D. A. Peru, Guidelines Help Select Reservoirs for $NaHCO_3$ EOR, *Oil & Gas J.*, 87(37): 53-57 (Sept. 11, 1989).
2. National Institute for Petroleum and Energy Research, *Quarterly Technical Report for July 1–September 1990*, Vol. II, Energy Production Research, DOE Report NIPER-501, pp. 28-32, October 1990.

GAS DISPLACEMENT— SUPPORTING RESEARCH

GAS-MISCIBLE DISPLACEMENT

Cooperative Agreement DE-FC22-83FE60149, Project BE5A

National Institute for Petroleum and Energy Research
Bartlesville, Okla.

Contract Date: Oct. 1, 1983
Anticipated Completion: Sept. 30, 1991
Funding for FY 1991: $200,000

Principal Investigator:
Ting-Horng Chung

Project Manager:
Jerry F. Casteel
Bartlesville Project Office

Reporting Period: Oct. 1–Dec. 31, 1990

Objectives

The objectives of this project are to (1) develop methods to mitigate the deleterious effects of solid precipitation in gas flooding and (2) determine the effect of porous media on gas–oil phase behavior.

Summary of Technical Progress

Effect of Porous Media on CO_2–Oil Phase Behavior

Gas-miscible displacement is related to the phase behavior of the injected gas and the reservoir oil. That injected gas reaches equilibrium with reservoir oil instantaneously upon contact is assumed. However, in porous media, oil is stored inside pores of diameters in the range of several micrometers. In this situation, the dissolution of gas into oil occurs through the process of diffusion. Molecular diffusion is a slow process, especially when a water phase blocks an oil phase from gas. There is still no answer about how long injected gas must soak before equilibrium is reached. This is a very important factor for gas enhanced oil recovery (EOR) process design. This research was designed to study this problem. Carbon dioxide gas was used in this study.

Two coreflooding experiments have been performed to test oil recovery under two different CO_2 injection rates: 15 and 80 mL/h. A 10-in.-long, 1.5-in.-diameter Berea sandstone core was used in the CO_2-flooding tests. The core was saturated with light oil (52 °API gravity). The coreflooding was conducted at a miscible condition of 120°F and 1500 psig. Oil recoveries are compared in Fig. 1. There is significant difference in oil recovery, even with a homogeneous core. For example, at 1.5 PV injection of CO_2, the slow injection rate recovers about 55% of the in-place oil,

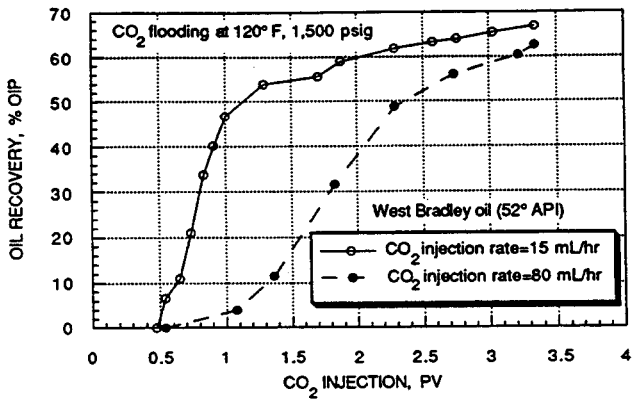

Fig. 1 Oil recovery in CO_2 flooding tests.

whereas the high injection rate recovers only about 20%, although both cases eventually will reach the same oil recovery after 3.5 PV injection. The efficiency of CO_2 use is higher at the lower injection rate. At a low injection rate CO_2 gas has more time to diffuse into the oil in place. Analysis of the CO_2 production rate in Fig. 2 shows that in the low injection rate CO_2 had already penetrated deeply into the core when the oil started producing. Figures 1 and 2 also show that CO_2 gas comes out simultaneously with the oil. This means that the CO_2 gas was already dissolved into the oil and released after oil produced. At the high injection rate, CO_2 flowed or fingered through the core at a relatively faster rate.

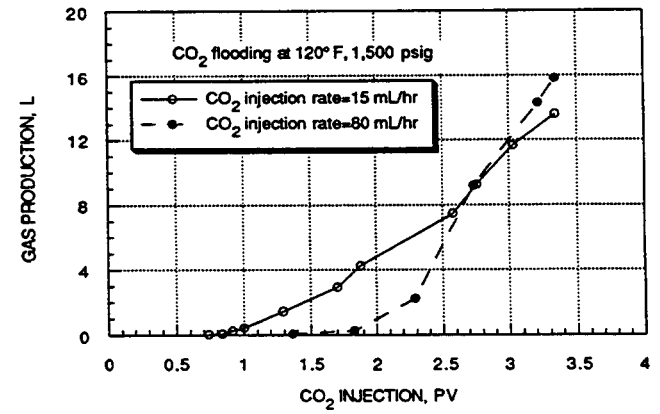

Fig. 2 Gas production in CO_2 flooding tests.

An experimental method was designed to study the diffusion rate of CO_2 in oil. Oil was introduced into a small-diameter glass tube ($^1/_{16}$ in. inner diameter) that was installed inside a pressure-volume-temperature (PVT) cell. The original oil height was measured by a cathetometer, and CO_2 was then injected into the PVT cell. The apparatus is shown in Fig. 3. Because the oil will be swollen by CO_2 dissolution, the oil–gas interface will move as more CO_2 dissolves into the oil, and the CO_2 diffusion rate can be estimated by monitoring the change in oil volume. A mathematical model to describe this problem is needed to determine the diffusion coefficient by matching the measured volume change curve. Initial tests were conducted to measure the time for CO_2 to saturate the oil of different lengths. Figure 4 shows the oil swelling as a function of time for two different-length oil columns. One is about

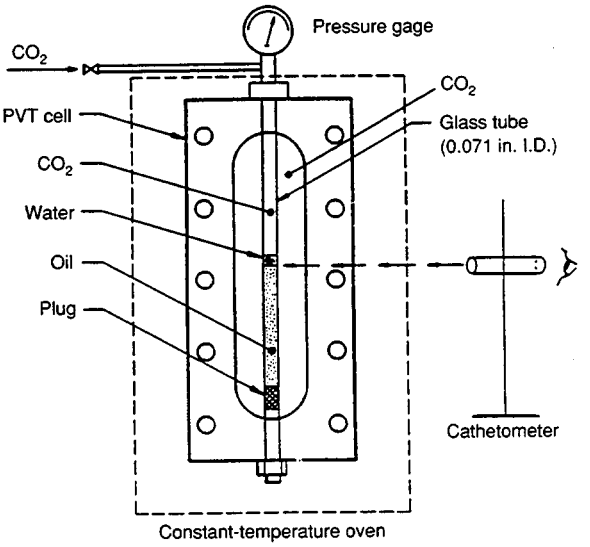

Fig. 3 Apparatus for CO_2 diffusion study.

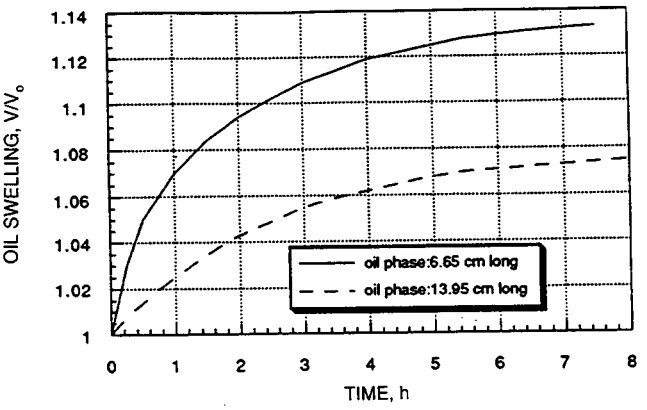

Fig. 4 Oil swelling rates.

twice as long as the other. Since the oil swelling factor is a linear function of CO_2 solubility, the amount of CO_2 that dissolved in the oil from the oil swelling can be estimated. Figure 4 shows that it will take much longer for CO_2 to saturate the oil inside a longer pore than a shorter pore, and the saturation time is not proportional to the oil column length. This experiment is designed to measure the linear molecular diffusivity for CO_2 in the sample oil. In porous media, the linear molecular diffusivity has to be modified by the mass tortuosity (τ_m), which can be measured from experiments or estimated from the relations[1]

$$\tau_m = \frac{1}{\tau} - 1$$

where τ is the flow tortuosity. The flow tortuosity has been related to the formation factor F_R and the bulk porosity as

$$\tau = F_R\phi$$

The oil used in this experiment is from New London (Arkansas) oil field and has 34 °API gravity. The phase behavior for the CO_2 with this oil at the testing condition shows three phases (L_1, L_2, and V). The second liquid phase started to form after about 12 h. The volume of the second liquid phase is small (about 4.5% of the original oil volume).

Reference

1. W. F. Ramirez, P. J. Shuler, and F. Friedman, Convection, Dispersion, and Adsorption of Surfactants in Porous Media, *Soc. Pet. Eng. J.*, 430-438 (December 1980).

DEVELOPMENT OF METHODS TO IMPROVE MOBILITY CONTROL AND SWEEP EFFICIENCY IN GAS FLOODING

Cooperative Agreement DE-FC22-83FE60149, Project BE5B

National Institute for Petroleum and Energy Research
Bartlesville, Okla.

Contract Date: Oct. 1, 1983
Anticipated Completion: Sept. 30, 1991
Funding for FY 1991: $440,000

Principal Investigators:
Clarence Raible
Ting-Horng Chung

Project Manager:
Jerry F. Casteel
Bartlesville Project Office

Reporting Period: Oct. 1–Dec. 31, 1990

Objectives

The objectives of this project are (1) for entrainers—address the critical issues that remain before their application in field trials can be justified (these issues include identifying the best class of compounds from which to choose the most cost-effective entrainers and identifying the best injection strategy for entrainers in gas flooding; for the latter, cyclic CO_2 processes will also be tested for potential near-term applications); (2) for other additives—evaluate unique approaches to improving sweep efficiency in gas flooding enhanced oil recovery (EOR) processes (this year, precipitation of polymers and perfluorinated alkanes will be evaluated for potential mid-term applications); and (3) for foam—initiate studies to evaluate foam flow behavior in radial corefloods (although many researchers have studied foam for mobility control, very few have actually studied the flow of foam under radial flow conditions—conditions more typical of oilfield environments).

Summary of Technical Progress

Previous work with CO_2 corefloods[1] has shown that certain entrainer additives, such as isooctane and 2-ethylhexanol, can increase oil recovery. These additives were injected as a small liquid slug or as a CO_2–additive mixture followed by CO_2 displacement. An improvement in oil displacement efficiency (a 10 to 15% increase in oil recovery) was measured for cores saturated with a relatively heavy crude oil (22.7 °API gravity). Also, a delay in gas breakthrough using additive slugs indicated improved mobility control, which was partly responsible for increased oil recovery.

This report summarizes initial experiments performed to determine if additive slugs would effectively increase oil production in reservoirs with lighter crude oils. Small slugs of suitable additives may improve carbon dioxide displacement efficiency by achieving improved mobility control. It was previously demonstrated that additive entrainers with appreciable solubility in the CO_2 gas phase increased the viscosity and density of the gas phase.[2] The increase in gas phase viscosity would improve mobility control of a CO_2 flood. Also, a number of oil reservoirs would be amenable to CO_2 flooding if their reservoir pressures were not below that required for miscibility.[3] Previous work demonstrated that a suitable additive slug resulted in hydrocarbon extraction of components present in crude oil in the gaseous phase. Improved displacement efficiency for some reservoirs would be possible if sufficient lighter crude oil components were extracted to achieve multiple contact miscibility in the frontal displacement zone. For these experiments, isooctane was used as the test additive, which was one of the compounds used in previous studies.

Experimental Test Conditions

A Ruska displacement pump was used to inject an oil at a constant rate into floating piston pressure vessels containing CO_2 and CO_2 plus additive mixtures. For tests with liquid isooctane injection, a $^1/_8$-in.(0.318-cm)-diameter

injection loop filled with a measured quantity of isooctane was used.

A 2.0-in.(5.0-cm)-diameter Berea core was used for corefloods. The core was 56.9 cm long with a pore volume (PV) of 216 cm^3, porosity of 19.3%, and a permeability of 40 mD. The test temperature was 150°F (65.5°C), and the injection pressure was 1600 psi.

A watered-out core was used for these tests where residual oil saturation was obtained by flooding the core with 1.25 PV each of crude oil and brine. The crude oil was Delaware–Childers (33.6 °API gravity). Following a CO_2 displacement test, the core was flushed with several PV of a 50:50 mixture of Stoddard solvent and propyl alcohol to remove the remaining oil. The solvent mixture was then removed by flushing with several PV of propyl alcohol and brine. During solvent extraction step, the core was cyclically pressurized to 1000 psi with solvent to assist in removing oil and CO_2 trapped in the smaller pores.

Experimental Results and Discussion

At the temperature and pressure conditions of these experiments, CO_2 was not miscible with the crude oil. The tests were terminated after produced fluids contained largely gas with virtually no production of oil or brine. For duplicate tests, CO_2 displacement produced an average of 45.5% of the tertiary oil or oil in place (OIP).

Two other experiments were conducted with an isooctane additive. For computation of oil recovery, the isooctane liquid volume was included with the tertiary oil volume to obtain OIP. For one coreflood experiment, a premixed CO_2 plus isooctane blend was injected followed by CO_2 displacement. The blend was 20 mol % of isooctane. This test produced 53% of the OIP. For another experiment, a 10.7-cm^3 slug of liquid isooctane was injected in front of the CO_2 displacement. This test produced 57% of the OIP.

The isooctane additive corefloods produced 9.5% greater oil recovery than tests with pure CO_2 displacement. Although both experiments with isooctane produced greater oil recoveries, the increase in oil recovery was largely offset by the quantity of injected isooctane. Also, the test with the liquid isooctane additive showed a delay in produced gas relative to the start of oil production. This would indicate an improvement in gas mobility with the use of the isooctane additive.

References

1. F. M. Llave and F. T. H. Chung, *The Use of Entrainers for Improving Mobility Control and Displacement Efficiency,* DOE Report NIPER-362, September 1988 (NTIS order No. DE89000704).
2. F. M. Llave, F. T. H. Chung, and T. E. Burchfield, Use of Entrainers in Improving Mobility Control of Supercritical CO_2, *SPE Reservoir Evaluation,* 47-51 (February 1990).
3. S. Haynes and R. B. Alston, *The Study of the Mechanisms of Carbon Dioxide Flooding and the Applications to More Efficient EOR Projects,* SPE/DOE paper 20190, presented at the SPE/DOE Enhanced Oil Recovery Symposium, Tulsa, Okla., Apr. 22–25, 1990.

SCALEUP OF MISCIBLE FLOOD PROCESSES

Contract No. DE-FG21-89MC26253

Stanford University
Stanford, Calif.

Contract Date: July 1989
Anticipated Completion: July 1992
Government Award: $756,000

Principal Investigator:
F. M. Orr, Jr.

Project Manager:
Royal J. Watts
Morgantown Energy Technology Center

Reporting Period: Oct. 1–Dec. 31, 1990

Objective

The objective of this research effort is to develop improved procedures for scaling predictions of miscible flood performance from laboratory scale, where the process is experimentally accessible, to field scale, where more accurate performance predictions are needed.

Summary of Technical Progress

Phase Behavior, Fluid Properties, and Flow

Additional results have been obtained that confirm the correctness of the analytical solutions obtained by Monroe et al.[1] for displacement of oils containing methane (CH_4), normal butane (C_4), and decane (C_{10}). The new results have important implications for the development of miscibility for oils containing dissolved CH_4, and they allow solutions to be constructed much more simply.

The following questions are examined:

1. Are the four-component solutions obtained by the method of characteristics (MOC) continuous with respect to initial composition data?

2. Is it possible for more than one tie line to intersect oil compositions that lie in the CH_4–C_4–C_{10} base of the quaternary diagram?

3. How is miscibility developed for oils containing dissolved CH_4?

Answers to the first two questions demonstrate that the flow problems considered by Monroe et al. are well posed. The resulting analysis can then be used to clarify the effect of dissolved CH_4 on minimum miscibility pressure (MMP).

Continuity

To demonstrate that solutions of the type given by Monroe et al.[1] are continuous with respect to the initial data, a three-component problem that raises exactly the same issue of continuity is considered. If the solution for three-component flow is to be continuous with respect to the initial data, it must reduce smoothly to the solution for two-component flow since the initial concentration of one of the components is reduced to zero. The displacement of mixtures of CH_4 and C_{10} by CO_2 is considered. To restrict the discussion to essentials, the phase behavior is described by constant K-values: $K_{CO_2} = 1.5$, $K_{CH_4} = 2.8$, $K_{C_{10}} = 0.01$. The resulting phase diagram is shown in Fig. 1. As comparison of (dashed) tie lines calculated with the Peng–Robinson equation of state (EOS) with (solid) tie lines obtained with the constant K-values indicates, the approximate phase diagram actually agrees quite well with the predictions of the Peng–Robinson EOS.

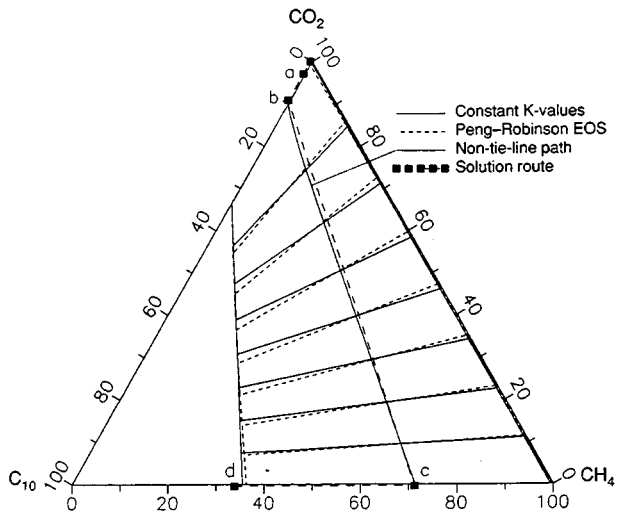

Fig. 1 Phase behavior of methane–butane–decane (CO_2–CH_4–C_{10}) mixtures and method of characteristics (MOC) solution route for displacement of mixture d by pure CO_2.

In the discussion that follows, the effects of volume change as components transfer between phases are ignored, and the assumption is made that the components all have the same molar density. Under those assumptions, volume fractions equal mole fractions. The question of continuity applies equally whether or not volume change is included. The analysis given here is extended in the Appendix to account for such effects. For the example solutions, the simple fractional flow expression is used.

$$f_g = \frac{S_g^2}{S_g^2 + (1 - S_g)^2} \tag{1}$$

In Eq. 1, the phase viscosities have been assumed to be constant and equal.

The MOC solution[2,3] for displacement of pure C_{10} by CO_2 is shown in Fig. 2. As Fig. 2 indicates, there is a

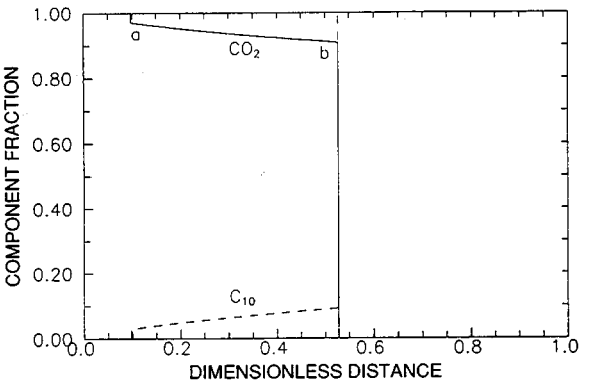

Fig. 2 Composition profile at 0.5 pore volume injected for displacement for pure C_{10} by pure CO_2.

leading shock from pure C_{10} to a point **b** in the two-phase region. Point **b** is also shown on the CO_2–C_{10} axis in Fig. 1. That point is determined from a material balance on CO_2 across the shock. The velocity of the shock is equal to the tie-line eigenvalue on the upstream side of the shock.

$$\lambda_t^b = \frac{F_l^b - F_l^{init}}{C_l^b - C_l^{init}} = \frac{df_g^b}{dS_g} \tag{2}$$

$$\text{where } C_i = \sum_{j=1}^{n_p} c_{ij} S_j \quad \text{and} \quad F_i = \sum_{j=1}^{n_p} c_{ij} f_j$$

In this case, however, $F_l^{init} = C_l^{init} = 0$ because there is no CO_2 present initially, and hence

$$\lambda_t^b = \frac{F_l^b}{C_l^b} = \frac{df_g^b}{dS_g} \tag{3}$$

The leading shock is followed by a zone of continuous variation in which the wave velocity of a given overall composition, C_l, is

$$\lambda_t = \frac{df_g}{dS_g} \tag{4}$$

The trailing shock shown in Fig. 2 satisfies

$$\lambda_t^a = \frac{1 - F_1^a}{1 - C_1^a} = \frac{df_g^a}{dS_g} \tag{5}$$

Point **a** is also shown in Fig. 1.

Solutions for initial compositions that contain CH_4 reduce uniformly to the solution given in Fig. 2 in the limit as the CH_4 concentration goes to zero.

The solution for displacement by pure CO_2 of a CH_4–C_{10} mixture with initial composition, $CO_2 = 0$, $CH_4 = 0.34$, $C_{10} = 0.66$, is shown in Fig. 3. The extension of tie lines shown in Fig. 1 indicates that the only tie line that intersects any composition on the CH_4–C_{10} base is the CH_4–C_{10} axis itself. That statement is true for constant K-values so long as $K_{CH_4} > K_{CO_2} > 1$. Thus the question of path uniqueness is not an issue for this phase diagram. That question is addressed for the four-component system.

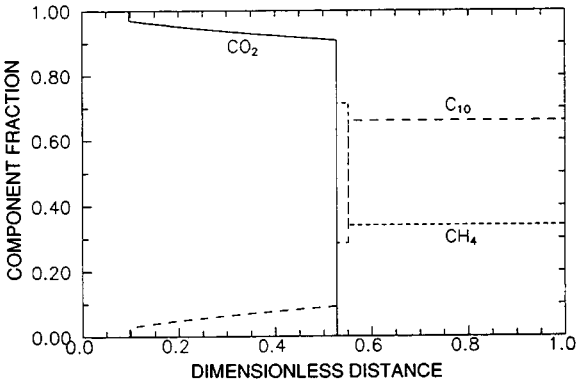

Fig. 3 Composition profile at 0.5 pore volume injected for displacement of mixture d by pure CO_2.

The trailing shock in Fig. 3 satisfies Eq. 5; it is identical to that obtained in the binary solution. The composition route from the trailing shock proceeds with a continuous variation along the injection tie line. The solution route must reach the initial tie line either by continuous variation along a non-tie-line path or via a shock. The only feasible continuous variation is along the non-tie-line path shown in Fig. 1. That path is obtained by integration along eigenvector directions from the point on the injection tie line where the tie-line and non-tie-line eigenvalues are equal. All other paths are ruled out because they require a switch from a fast path upstream to a slow path downstream, which violates the physical constraint that compositions with high velocities must lie downstream of slower ones.[4] In fact, a continuous variation along the non-tie-line path is also not allowed because non-tie-line eigenvalues decrease as the path is traced from the injection tie line to the initial tie line. Hence the composition wave is self-sharpening and shock is required.

The resulting intermediate shock satisfies

$$\lambda_t^b = \frac{F_1^b - F_1^c}{C_1^b - C_1^c} = \frac{F_2^b - F_2^c}{C_2^b - C_2^c} \tag{6}$$

For the initial conditions on the CH_4–C_{10} axis, $C_1^c = F_1^c = 0$. Also, for injection compositions on the CO_2–C_{10} axis, $F_2^b = C_2^b = 0$. Hence the points **b** and **c** are defined by

$$\lambda_t^b = \frac{F_1^b}{C_1^b} \tag{7}$$

and

$$\lambda_t^b = \frac{F_2^c}{C_2^c} \tag{8}$$

From point **c**, the solution route jumps to the initial composition. The velocity of that leading shock is given by

$$\Lambda_2^{cd} = \frac{F_2^c - F_2^d}{C_2^c - C_2^d} \tag{9}$$

As Fig. 3 shows, the leading shock is separated from the intermediate shock by a zone of constant state.

Comparison of Eqs. 7 and 3 indicates that the intermediate shock departs from the same point, **b**, on the injection tie line as does the leading shock for the binary solution. Furthermore, the intermediate shock in the ternary solution moves at exactly the same velocity as the leading shock in the binary case. Note that all the CH_4 that is stripped from the oil left behind the intermediate shock moves in the zone between the leading and intermediate shocks (see Fig. 3). In this simple example, where the lower viscosity of the CO_2-rich phase was ignored in the fractional flow expression (Eq. 1), little oil is left behind that shock, and hence the CH_4 bank ahead of the intermediate shock is relatively small.

Now consider how the velocity of the leading shock, Λ_2^{cd}, changes as the initial CH_4 concentration is reduced. In the limit as point **d** approaches the pure C_{10} apex, $F_2^d = C_2^d = 0$. Hence the leading shock velocity becomes

$$\Lambda_2^{cd} = \frac{F_2^c}{C_2^c} \tag{10}$$

Thus, in the limit the leading shock velocity is exactly equal to the velocity of the intermediate shock given by Eq. 8. Reduction in the initial CH_4 concentration, therefore, slows the leading shock, as a simple material balance on CH_4 indicates it should. When the CH_4 concentration reaches zero, the leading shock merges with the intermediate shock,

which has the same composition and velocity as the leading shock in the binary CO_2–C_{10} displacement. Thus the ternary solution does, in fact, reduce continuously to the simpler case. Similar behavior is observed in the four-component solutions. The proof in the four-component case follows exactly the same line of reasoning, although it is algebraically more complex, of course, because the leading and trailing pairs of shocks are coupled and must be solved for simultaneously. That proof is given in the Appendix.

Thus the addition of a component changes the dimensionality of the hodograph space in which solution routes lie, and hence routes can change discontinuously as shocks merge. That does not change recovery performance discontinuously, however. Instead, displacement efficiency varies continuously with the amount of CH_4 present.

Uniqueness

Next, a given composition in the CH_4–C_4–C_{10} plane might have more than one tie-line extension through it. In fact, the behavior predicted by the Peng–Robinson EOS is similar to that shown in Fig. 1. Consider, for example, a tie line defined by liquid and vapor compositions, (x_{CO_2}, x_{CH_4}, $x_{C_{10}}$) and (y_{CO_2}, y_{CH_4}, $y_{C_{10}}$). The projection of the tie line in the plane defined by $Z_{CH_H} = 0$ is

$$z_{CO_2} = \frac{y_{CO_2} - x_{CO_2}}{y_{C_{10}} - x_{C_{10}}}(z_{C_{10}} - x_{C_{10}}) + x_{CO_2} \qquad (11)$$

and a similar projection in the $Z_{CO_2} = 0$ plane is

$$z_{CH_4} = \frac{y_{CH_2} - x_{CH_4}}{y_{C_{10}} - x_{C_{10}}}(z_{C_{10}} - x_{C_{10}}) + x_{CH_4} \qquad (12)$$

Set $z_{CO_2} = 0$ in Eq. 11, solve for $z_{C_{10}}$, and substitute the result into Eq. 12 to find where that tie line intersects the CO_2-free plane. The definitions $y_{CO_2} = K_{CO_2}x_{CO_2}$, $y_{CH_4} = K_{CH_4}x_{CH_4}$, and $y_{C_{10}} = K_{C_{10}}x_{C_{10}}$ are inserted. The resulting expression is

$$z_{CH_4} = x_{CH_4}\left(1 - \frac{K_{CH_4} - 1}{K_{CO_2} - 1}\right) \qquad (13)$$

Equation 13 proves that, so long as $K_{CH_4} > K_{CO_2} > 1$, then the tie-line extension intercepts the CH_4–C_4–C_{10} plane at negative values of the CH_4 concentration, z_{CH_4}. Direct computation with the Peng–Robinson EOS shows that, for the CO_2–CH_4–C_4–C_{10} system, $K_{CH_4} > K_{CO_2} > 1$ throughout the two-phase region (except, of course, on the critical locus, where $K_{CH_4} = K_{CO_2} = 1$). Hence there are no tie-line extensions that intersect CH_4–C_4–C_{10} mixtures with positive CH_4 concentrations except those which lie in the CH_4–C_4–C_{10} plane itself. Thus, for the initial mixtures considered by Monroe et al., there is no possibility of nonunique paths that arise from multiple tie-line extensions through the initial composition. A similar analysis for tie lines intersecting the CO_2–C_4–C_{10} plane shows that tie lines for mixtures containing CH_4 all intersect the plane at CO_2 concentrations less than one. Therefore those tie lines cannot intersect the 100% CO_2 point. Direct computation shows that, for mixtures without CH_4, the CO_2–C_{10} axis is the only tie line in the CO_2–C_4–C_{10} plane that intersects the 100% CO_2 point.

Note that, even though nonunique tie-line extensions are not an issue in the calculations of Monroe et al., examples of such behavior are easy to find, even in ternary systems. In the phase diagram shown in Fig. 1, for example, initial compositions in the single-phase liquid region on the CO_2–C_{10} axis are intersected by the axis itself and by another tie line in the interior of the diagram. In such cases, the tie line followed in the solution route depends on the injection composition. If pure CO_2 is injected, the displacement route stays on the CO_2–C_{10} axis. If pure CH_4 is injected, the solution route enters the two-phase region along the tie line in the interior of the diagram that extends through the initial composition. The physically relevant solution in such cases is that obtained for flow with a small amount of dispersive mixing in the limit as the dispersion level goes to zero.[5]

Minimum Miscibility Pressure

In three-component systems, the required condition for development of miscibility in vaporizing gas drives is that the injection composition must lie outside the region of tie-line extensions on the ternary phase diagram. Monroe et al. argued, based on their calculated composition paths, that recovery high enough to meet experimental definitions of miscibility can easily be achieved, even though the oil composition lies in the region of tie-line extensions on the CH_4–C_4–C_{10} base, and hence the solution composition route passes through the two-phase region. Hence the contention was that use of the tie-line extension argument was inappropriate and that recovery gave a better indication of an appropriate pressure, as slim tube experimentalists have long maintained. The analysis given in the Appendix of continuity of solutions for the four-component case strengthens the conclusion of Monroe et al. In fact, the following statement is true:

> *The MMP for displacement of single-phase CH_4–C_4–C_{10} mixtures by pure CO_2 is the pressure at which the C_4–C_{10} mixture that results when the CH_4 is removed from the original oil leaves the region of tie-line extensions on the CO_2–C_4–C_{10} ternary diagram.*

The proof is based on the following reasoning. In the Appendix the limit of zero CH_4 concentration in the original oil shows that the solution route reduces continuously to the solution for displacement of C_4–C_{10} mixtures by pure CO_2. That ternary solution begins with a shock that occurs along the tie-line extension that passes

through the original oil composition. Thus, in the limiting case, there are two important tie lines. The first is the tie line in the CO_2–C_4–C_{10} face that passes through the dead oil composition, and the second is the tie line in the CH_4–C_4–C_{10} face that also extends through the same dead oil composition. As shown in the Appendix, the shock balance equations that define the leading and leading intermediate shocks in the four-component case reduce to the appropriate three-component shock balances in the limit as the CH_4 concentration goes to zero. That result implies that the tie line in the CO_2–C_4–C_{10} face that passes through the dead oil composition is the crossover tie line for the tie line in the CH_4–C_4–C_{10} face that also extends through the dead oil composition. Furthermore, if CH_4 is added along the tie-line extension in the CH_4–C_4–C_{10} face, the only change in the overall solution is the velocity of the leading shock. The composition route still jumps to the same crossover tie line.

Now, as the pressure is increased for a given dead oil composition, the crossover tie line eventually becomes the limiting tie line that is tangent to the binodal curve at the Plait point in the CO_2–C_4–C_{10} face. When that happens, the shock balance equations given in the Appendix show that there is still a leading shock in the CH_4–C_4–C_{10} face, but it has unit velocity as do all the other shocks. Thus the displacement is piston-like at that pressure, the MMP. Even at the MMP, the route passes through the two-phase region, but the shocks all merge to give a single piston-like shock. Similar behavior is observed in condensing gas drives in ternary systems. An example tie line and dilution line in the CH_2–C_4–C_{10} base are shown in Fig. 4. Point **A** is the dead oil, and point **a** is the initial composition, chosen in this case to be the saturated liquid phase. The MMP is the pressure at which the critical tie line in the CO_2–C_4–C_{10} face intersects point **B**. As Fig. 5 shows, the critical tie line in the CO_2–C_4–C_{10} face intersects point **A**, the dead oil

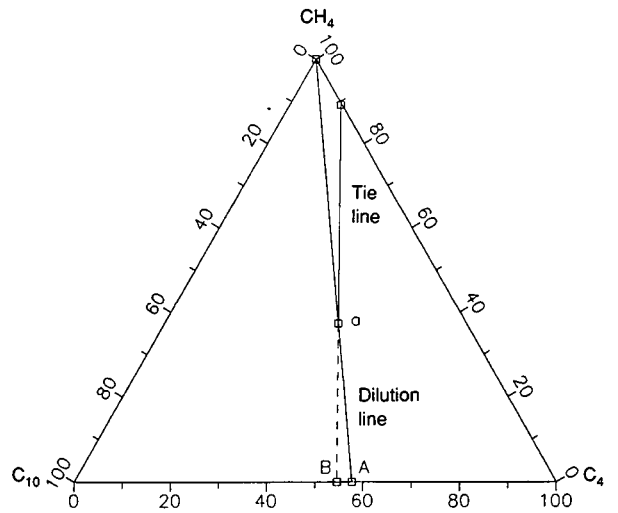

Fig. 4 Development of miscibility for CO_2 displacement of initial oil mixtures containing dissolved CO_2. The tie line shown was calculated at 160°F and 1600 psia with the Peng–Robinson EOS.

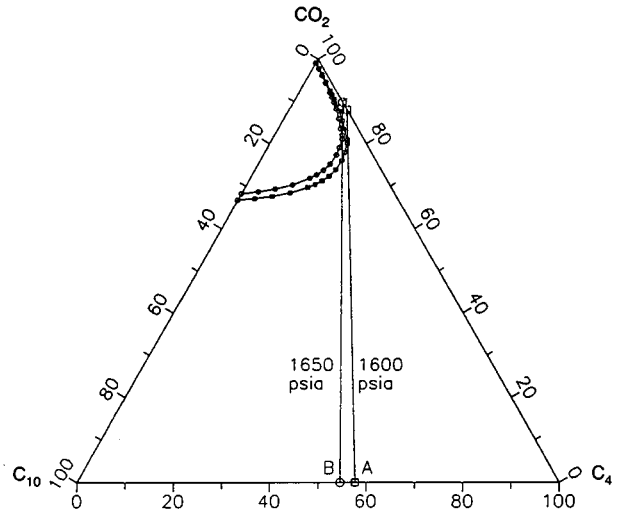

Fig. 5 Estimated critical tie lines for the mixtures A and B. The binodal curves were calculated at 1600 and 1650 psia with the Peng–Robinson EOS.

composition, at about 1600 psia. (The binodal curves in Fig. 5 are calculated with the Peng–Robinson EOS.) Figure 5 also shows that the MMP for the live oil is around 1650 psia, only about 50 psia higher than that of the dead oil, despite the fact that the live oil contains 36% CH_4.

Now, consider displacement of oil of composition **a** in Fig. 4 by CO_2 at the MMP for oil **A**. The solutions of Monroe et al. show that the path will enter the two-phase region, but the crossover tie line will be very close to the plait point on the CO_2–C_4–C_{10} face. Hence recovery will suffer only slightly, and a slight increase in pressure would restore miscibility.

This analysis, therefore, indicates that tie-line extension conditions for the MMP must be applied with understanding of the appropriate solution for the composition route when more than three components are present. Careful analysis of composition routes indicates that the MMP is much lower than the pressure required to move the original oil composition outside the region of tie-line extensions when that oil contains dissolved CH_4, for example.

The solutions presented by Monroe et al. for displacements in four-component systems have been shown to be continuous with respect to variations in initial composition data, and the uniqueness of tie lines that extend through initial compositions that contain CH_4 but no CO_2 has been demonstrated. In addition, a new criterion for the MMP has been stated for systems in which the initial oil contains dissolved CH_4.

Nomenclature

- C_i overall volume fraction of component i
- c_{ij} volume fraction of component i in phase j
- f_g fractional flow of gas

F_i overall fractional flow or overall molar flux of component i
G_i overall molar concentration of component i
K_i y_i/x_i, K-value for component i
λ_t eigenvalue for the eigenvector that points in the tie-line direction
Λ_i shock wave velocity for component i
ϕ porosity
S_g gas saturation
x_i mole fraction of component i in the liquid phase
y_i mole fraction of component i in the vapor phase
v local fluid flow velocity
z_i overall mole fraction of component i along a tie line or its extension

Appendix: Proof of Continuity of Three- and Four-Component Solutions

Consider injection of pure CO_2 into a mixture of CH_4, C_4, and C_{10}. In this analysis, effects of volume change are included. The leading shock satisfies

$$\frac{F_2^a - F_2^b}{G_2^a - G_2^b} = \frac{F_3^a - F_3^b}{G_3^a - G_3^b} \qquad \text{(A-1)}$$

where

$$G_i = \sum_{j=1}^{n_p} \rho_j x_{ij} S_j$$

$$F_i = \frac{v}{\phi} \sum_{j=1}^{n_p} \rho_j x_{ij} f_j$$

$$\frac{F_2^a - F_2^b}{G_2^a - G_2^b} = \frac{F_4^a - F_4^b}{G_4^a - G_4^b} \qquad \text{(A-2)}$$

Here component 1 is CO_2, component 2 is CH_4, component 3 is C_4, and component 4 is C_{10}. The initial composition is point **a**, so the values of F_i^a and G_i^a are all known. From point **b** in the two-phase region on the tie line in the CH_4–C_4–C_{10} face that extends through point **a**, the solution route jumps to point **c**, which is on the crossover tie line. See Fig. 6 of Monroe et al. for the locations of points **a**, **b**, and **c** on the quaternary diagram. The shock from point **b** to point **c** is an upstream intermediate discontinuity because the shock velocity equals the tie-line eigenvalue at point **c**. Hence the component material balances for that shock are

$$\lambda_t^c = \frac{F_i^b - F_i^c}{G_i^b - G_i^c} \qquad i = 1, 4 \qquad \text{(A-3)}$$

Equations A-1 to A-3 therefore define the shocks from **a** to **b** and from **b** to **c**.

If the initial mixture contains only C_4 and C_{10}, then the leading shock is from **A** to **C**, where **A** is a point on the CO_2–C_{10} axis. In that case the shock satisfies

$$\lambda_t^C = \frac{F_i^A - F_i^C}{G_i^A - G_i^C} \qquad i = 1, 3, \text{ and } 4 \qquad \text{(A-4)}$$

It is easy to show,[6] with Eq. A-4, that the point **A** must lie on the extension of the tie line in the CO_2–C_4–C_{10} face that contains point **C**.

Equations 1 to 3 reduce to Eq. 4 as **a** → **A**. Point **c** is on the CH_4-free face, so $F_2^c = G_2^c = 0$. Hence Eq. 3, written for CH_4, gives the velocity of the leading intermediate shock (**b** → **c**) as

$$\lambda_t^c = \frac{F_2^b}{G_2^b} \qquad \text{(A-5)}$$

At point **b**, no CO_2 is present, so $F_1^b = G_1^b = 0$, and Eq. A-3, written for CO_2, gives

$$\lambda_t^c = \frac{F_1^c}{G_1^c} \qquad \text{(A-6)}$$

If it can be shown that **c** → **C** as **a** → **A**, then Eq. A-6 is identical to Eq. A-4, written for CO_2, because $F_1^A = G_1^A = 0$.

The wave velocity of the leading shock is given by

$$\Lambda_2^{ab} = \frac{F_2^a - F_2^b}{G_2^a - G_2^b} \qquad \text{(A-7)}$$

In the limit as **a** → **A**, $F_2^a \to 0$ and $G_2^a \to 0$. Hence the wave velocity of the leading shock becomes

$$\Lambda_2^{ab} = \frac{F_2^b}{G_2^b} \qquad \text{(A-8)}$$

Equations A-8 and A-5 are identical. Hence, in the limit, the leading shock and the leading intermediate shock travel at the same velocity and merge into a single shock.

In the limit as **a** → **A**, substitution of Eqs. A-8 and A-5 into A-1 yields

$$\lambda_t^c = \frac{F_3^A - F_3^b}{G_3^A - G_3^b} \qquad \text{(A-9)}$$

Rearrangement of Eq. A-9 gives

$$F_3^b = F_3^A - \lambda_t^c \left(G_3^A - G_3^b\right) \qquad \text{(A-10)}$$

Similar rearrangement of Eq. A-3, written for C_4, gives

$$F_3^b = F_3^c - \lambda_t^c\left(G_3^b - G_3^c\right) \qquad \text{(A-11)}$$

Elimination of F_3^b from Eqs. A-10 and A-11 yields

$$\lambda_t^c = \frac{F_3^A - F_3^c}{G_3^A - G_3^c} \qquad \text{(A-12)}$$

Equation A-12 is exactly equivalent to Eq. A-4, written for C_4. Hence the point **c** becomes point **C** in the limit of zero CH_4 concentration in the initial mixture. Similar manipulations for the balance on C_{10} along with Eq. A-6 show that expressions identical to Eq. A-4 are obtained for all three components. Hence the leading shocks present in the four-component solution coalesce into a single shock as the initial CH_4 concentration vanishes. That shock is the corresponding three-component solution. When the point **A** lies outside the region of tie-line extensions on the CO_2–C_4–C_{10} face, then the four-component solution reduces continuously in the limit to the piston-like displacement characteristic of multicontact miscibility.

References

1. W. W. Monroe, M. K. Silva, L. L. Larsen, and F. M. Orr, Jr., Composition Paths in Four-Component Systems: Effect of Dissolved Methane on CO_2 Flood Performance in One Dimension, *SPERE*, 423-432 (August 1990).
2. K. K. Pande, *Interaction of Phase Behavior with Nonuniform Flow*, Ph.D. dissertation, Stanford University, Stanford, Calif., 1988.
3. K. K. Pande and F. M. Orr, Jr., *Composition Paths in Binary CO_2/C_{10} Displacements: Effects of Reservoir Heterogeneity and Crossflow on Displacements with Limited Solubility*, paper presented at the 2nd European Conference on Mathematics of Oil Recovery, Arles, Sept. 11–14, 1990.
4. F. G. Helfferich, General Theory of Multicomponent, Multiphase Displacement in Porous Media, *Soc. Pet. Eng. J.*, 51-62 (February 1981).
5. T. Johansen and R. Winther, *Mathematical and Numerical Analysis of Hyperbolic System Modeling Solvent Flooding*, paper presented at the 2nd European Conference on Mathematics of Oil Recovery, Arles, Sept. 11–14, 1990.
6. J. M. Dumore, J. Hagoort, and A. S. Risseeuw, An Analytical Model for One-Dimensional Three-Component Vaporizing Gas Drives, *Soc. Pet. Eng. J.*, 169-179 (April 1984).

CYCLIC CO_2 INJECTION FOR LIGHT OIL RECOVERY: PERFORMANCE OF A COST-SHARED FIELD TEST IN LOUISIANA

Contract No. DE-FG22-89BC14204

Louisiana State University
Department of Petroleum Engineering
Baton Rouge, La.

Contract Date: Nov. 21, 1988
Anticipated Completion Date: Nov. 17, 1991
Total Government Award: $499,000

Principal Investigator:
Zaki A. Bassiouni

Project Manager:
Jerry Ham
Metairie Project Office

Reporting Period: Oct. 1–Dec. 31, 1990

Objectives

The ultimate objective of this research is to provide a base of knowledge on the CO_2 huff 'n' puff process for the enhanced recovery of Louisiana crude oil. Project goals include laboratory corefloods to investigate several parameters important to the process and numerical simulation to interpret coreflood results. Additional activities include construction and analysis of a field test database to facilitate target reservoir screening and to identify sensitive operational parameters. The information from laboratory corefloods and database evaluations will be used in the design and implementation of a Department of Energy-sponsored field test. The results of all laboratory and field evaluations will be made available to the industry through workshops, periodic reports, and meetings.

Summary of Technical Progress

Laboratory Corefloods

Coreflood experiments were initiated during this reporting period to examine the influence of CO_2 injection rate on process performance. Experiments designed to determine the benefits of using a drive gas have been completed.

Previous laboratory coreflood and field test results have indicated that process performance improved when CO_2 penetrated farther into the reservoir. Deeper penetration of CO_2 may be achieved by increasing the CO_2 slug size; however, the cost of additional CO_2 may be prohibitive. Since nitrogen is a less expensive gas, a nitrogen drive might provide a cost-effective means of enhancing the reservoir penetration of CO_2.

Three sets of first- and second-cycle corefloods were performed to test this hypothesis. Corefloods were conducted with Timbalier Bay oil and the horizontal Berea core (6 ft in length; 2 in. in diameter). Experimental procedures and oil properties were described previously.[1] Injections of 16 cm^3 CO_2 or 16 cm^3 nitrogen alone were compared with injections of 16 cm^3 CO_2 followed by 16 cm^3 nitrogen. Gases were injected at 1640 psig and 78°F; the pressure of the core was slowly reduced at constant temperature to 500 psig; and the core was shut in for a soak period before production of oil commenced. Although equal volumes of CO_2 and N_2 were injected, the masses injected were quite different since the gas densities were not the same, and subsequently the gas volumes at soak conditions were different. Masses injected, volumes injected, and reservoir pore volumes of CO_2 and N_2 are compared in Table 1.

TABLE 1

Gas Volumes at Injection and Soak Conditions

	Gas	
	CO_2	N_2
Volume injected, cm^3	16	16
Density, g/cm^3		
1640 psig, 78°F	0.834	0.126
Mass injected, g	13.35	2.02
Density, g/cm^3		
500 psig, 78°F	0.079	0.04
Volume, cm^3		
500 psig, 78°F	168.7	50.4
Gas fractional pore volume		
500 psig, 78°F	0.225	0.067

Since previous studies have shown that incremental oil recovery was linearly related to the amount of CO_2 injected, the benefits of a drive gas could be evaluated by comparing the recovery achieved by injection of CO_2 followed by nitrogen ($Np_{CO_2+N_2}$) with the sum of the recoveries of the separate processes ($Np_{N_2} + Np_{CO_2}$)(Ref. 2). Coreflood results shown in Table 2 indicate that a nitrogen drive dramatically enhanced oil recovery. In the first cycle, the flood conducted with the drive gas produced 45% more oil than the combined recoveries of the first cycle floods where CO_2 or nitrogen was injected alone. The second cycle results were even more favorable, with the drive gas flood recovering 108% more oil than the combined recoveries of the CO_2 and N_2 floods. The magnitude of the benefits derived from nitrogen drive gas was unexpected, and further experiments are planned to substantiate this conclusion.

Field Tests

The past reporting period was directed toward obtaining the necessary permission from various regulatory agencies

TABLE 2

Results of Drive Fluid Investigation

Run No.	Fluid injected	Cycle	Oil recovered, cm^3	Total gas utilization,* Mscf/STB
81	CO_2	1	21	1.92
82	CO_2	2	8	5.05
107	$CO_2 + N_2$	1	50	0.99
108	$CO_2 + N_2$	2	25	1.98
111	N_2	1	13	0.71
112	N_2	2	4	2.31

*Total gas utilization, CO_2 utilization + N_2 utilization; gas utilization, Mscf gas injected/incremental bbl oil produced.

in the state of Louisiana for implementation of the planned CO_2 huff 'n' puff field test. Applications for a hearing before the Louisiana Office of Conservation and an Underground Injection Control (UIC) Permit were filed. A hearing date of March 19, 1991, has been set by the Commissioner of Conservation. Approval of the UIC Permit awaits the outcome of the hearing before the Office of Conservation. The field test should commence shortly after the hearing date.

Since the project is considered to be a pilot, a formal letter was submitted to the Department of Environmental Quality (DEQ) Air Quality Division requesting DEQ to waive the need for an emissions permit. The waiver is currently awaiting DEQ approval. Although the measurement of emissions will presumably not be required, monitoring of CO_2 and hydrocarbon emissions is planned to document emission levels and rates. A Microsensor Technology, Inc., Model P200D Double Module Gas Analyzer was purchased to facilitate monitoring of gaseous emissions. Analytical procedures for use of this instrument are currently being developed.

The following bids for Professional Engineering Services and supplies were prepared to facilitate implementation of the field test when the necessary permits are obtained.

1. Workover rig and labor to remove currently existing production tubing from test well.
2. Rental of equipment and labor for pressure testing and installation of tubing and tubing anchor in test well.
3. CO_2, CO_2 storage tanks, and pumping equipment, including labor and handling equipment.

References

1. T. G. Monger and J. M. Coma, A Laboratory and Field Evaluation of the CO_2 Huff 'n' Puff Process for Light Oil Recovery, *SPE Res. Engr.*, 1168 (November 1988).
2. J. M. Coma, *The CO_2 Huff 'n' Puff Process For Light Oil Recovery—An Initial Laboratory and Field Evaluation*, M. S. thesis, Louisiana State University, Baton Rouge, La., 1986.

FIELD VERIFICATION OF CO_2–FOAM

Contract No. DE-FG21-89MC26031

New Mexico Institute of Mining and Technology
Petroleum Recovery Research Center
Socorro, N. Mex.

Contract Date: September 1989
Anticipated Completion: September 1993

Total Project Cost:

DOE	$2,000,000
Contractor	2,000,000
Total	$4,000,000

Principal Investigators:
F. David Martin
John P. Heller
William W. Weiss

Project Manager:
Royal J. Watts
Morgantown Energy Technology Center

Reporting Period: Oct. 1–Dec. 31, 1990

Objectives

The objectives of this project are to (1) evaluate the use of foam for mobility control or fluid diversion in a New Mexico CO_2 flood and (2) prove the concept of CO_2–foam in the field by selecting a suitable reservoir where CO_2 flooding is ongoing, characterizing the reservoir, modeling the process, and verifying the effectiveness and economics. Seven tasks were identified for the successful completion of this four-year project: (1) evaluate and select a field site, (2) develop an initial site-specific plan, (3) conduct laboratory CO_2–foam mobility tests, (4) perform reservoir simulations, (5) design the foam slug, (6) implement a field test, and (7) evaluate results. This report provides results of the first year of the four-year project.

Summary of Technical Progress

A suitable field site in New Mexico, the East Vacuum Grayburg/San Andres Unit (EVGSAU), has been identified as appropriate for the proposed work through evaluation of information from candidate CO_2 floods. The initial site-specific plan was developed and submitted for Unit Working Interest Owner approval in May 1990. Details of the proposed project were discussed with the Unit Working Interest Owners at a meeting in Odessa, Tex., on May 21, 1990. The operator of the Unit, Phillips Petroleum Company, submitted ballots for project approval. A sufficient number of Unit Working Interest Owners voted in favor of the project, and the project was approved on June 25, 1990. Therefore Task 1 and most of Task 2 of the project have been completed. The first batch of representative reservoir cores was received from Phillips Petroleum Company. This core material has been assessed, plugs have been cut and prepared, and some laboratory tests have begun. These tests will consist of both CO_2–foam mobility measurements and surfactant adsorption tests. Some evaluation of the mineralogy and local heterogeneity in the cores will be sought.

A Joint Project Advisory Team was organized, and technical meetings to discuss additional details of the project were held in Odessa, Tex., on Aug. 2, 1990, and Sept. 14, 1990. A suitable pattern in EVGSAU has been selected and design considerations have been discussed. The advisory team agreed that an observation well in the pattern area would be desirable for providing cores and logs that will improve reservoir characterization as well as for monitoring foam performance. Reservoir simulation studies will begin during the next quarter.

IMPROVEMENT OF CO_2 FLOOD PERFORMANCE

Contract No. DE-FC21-84MC21136

New Mexico Institute of Mining and Technology
Petroleum Recovery Research Center
Socorro, N. Mex.

Contract Date: April 1984
Anticipated Completion: March 1991

Total Project Cost:

DOE	$1,615,000
State of New Mexico	981,000
Industry	1,366,000
Total	$3,962,000

Principal Investigators:
John P. Heller
F. David Martin

Project Manager:
Royal J. Watts
Morgantown Energy Technology Center

Reporting Period: Oct. 1–Dec. 31, 1990

Objective

The objective of this project is to produce quantitative measurements of the influence of CO_2 flood performance of the following:

1. Displacement with pure and impure CO_2.
2. Evaluation and improvement of flow uniformity.

The experimental investigations and accompanying analysis and interpretation are designed to build understanding of fundamental physical mechanisms as a basis for improved performance prediction and for optimization of process performance.

Summary of Technical Progress

All tasks of this project have been completed and the final report is being prepared.

ENHANCED OIL RECOVERY SYSTEMS ANALYSIS

Morgantown Energy Technology Center
Morgantown, W. Va.

FY91 Total Project Cost: $150,000

Principal Investigator:
James R. Ammer

Project Manager:
Royal J. Watts
Morgantown Energy Technology Center

Reporting Period: Oct. 1–Dec. 31, 1990

Objectives

The overall objective of the Systems Analysis Project is to use the results of laboratory investigations, model enhancements, and field experimental work to determine the optimum technical and economical methods for improving the recovery efficiency of the CO_2 miscible displacement process. Results from these optimization studies will be used to estimate the increase in reserves expected from the application of improved technology.

Specific Tasks for FY91

Advanced Technology Assessment Study in the Delaware Basin

This study will determine the recoverable reserves available with the CO_2 miscible flood predictive model (CO2PM) for the 49 reservoirs identified as potential candidates in the FY90 study. Sensitivity and optimization analyses will be conducted to maximize recovery efficiency and economics. The increase in reserves resulting from the application of advanced technologies will be identified.

Other assessment tasks include:

- Collect CO2PM input data and build input data sets.
- Determine maximum recoverable reserves.
- Identify the increase in reserves resulting from the application of CO_2–foam technology with the use of the updated CO2PM.

Modification and Validation of CO2PM

The model CO2PM will be modified to simulate CO_2–foam flow and associated phenomena (e.g., surfactant adsorption). The CO2PM will be tested and validated against laboratory data and simulators with the capability to model foam flow. New input requirements will be documented.

Other modification and validation tasks include:

- Incorporate the capability to simulate foam flow into the existing CO2PM code and modify the economic calculations accordingly.
- Validate against laboratory data and other simulators' predictions.
- Provide documentation of the modifications and new input requirements with suggested defaults.

Field-Scale Simulation Studies

Two field simulation studies are being conducted to investigate the potential of improved technologies to increase the recovery efficiency of the CO_2 miscible displacement process. Both studies, CO_2 foam and horizontal wells, are using two actual reservoir data sets: (1) a fairly homogeneous, nonlayered Appalachian oil reservoir (Griffithsville) and (2) a heterogeneous, layered Permian Basin oil reservoir. Economic analyses will be performed to determine the commercial application of these technologies. Tasks also include:

- Conduct the simulation on studies and perform sensitivity analyses of pertinent operation and design parameters (e.g., horizontal well length and surfactant concentration).
- Perform an economic analysis of the results.

Summary of Technical Progress

Advanced Technology Assessment Study in the Delaware Basin

The CO2PM input data sets are being completed for the 49 reservoirs identified as potential CO_2 miscible flood candidates. A literature search was conducted and several Texas and New Mexico organizations were contacted to obtain the required input data. Sensitivity runs were made to determine the effect of the number of layers used to model a given reservoir for various values of the Dykstra–Parsons coefficient, thickness, and absolute permeability. Simulation results showed little sensitivity to the number of layers (3, 4, or 5) chosen.

Modification and Validation of CO2PM

Work on the modifications of CO2PM to incorporate the capability to model foam flow was initiated. The first phase is to confirm the validity of the concept for the simplest system (i.e., no surfactant adsorption or viscous fingering). An analysis of the problem indicates that the simplest modification of the code uses saturation, a phase composition, and aqueous-phase surfactant concentration as primary variables rather than the overall concentration variables currently used. This procedure eliminates the need for a flash and allows the analytical computation of derivatives. Proof of the concept is being worked out with a stand-alone code. If this approach works properly, the stand-alone code will be used to replace several of the existing routines in CO2PM.

Field-Scale Simulation Studies

Horizontal Well Study

Simulation runs were completed for various horizontal wellbore lengths for three different scenarios: (1) horizontal injectors and vertical producers, (2) vertical injectors and horizontal producers, and (3) horizontal injectors and horizontal producers. The reservoir currently being modeled is the Permian Basin oil reservoir. Initial evaluation of the results showed that 3 to 4% more oil-in-place was recovered in Scenarios 1 and 2 than in the base case (vertical injectors and vertical producers), whereas 25% more oil-in-place was recovered in Scenario 3 than in the base case. A shale barrier that existed in the reservoir is currently being added to the model simulation to determine its effect on recovery efficiency.

CO_2–Foam Study

An input data set is being built for the Griffithsville field. Relative permeability data for water and surfactant–CO_2 are being obtained from laboratory measurements made at METC's enhanced oil recovery (EOR) laboratory. Surfactant adsorption data are being obtained from laboratory measurements made by the New Mexico Institute of Mining and Technology. A phase property package is being used to determine the vapor–liquid equilibrium data (k-values) for the reservoir oil–CO_2 system.

ENHANCED OIL RECOVERY MODEL DEVELOPMENT AND VALIDATION

Morgantown Energy Technology Center
Morgantown, W. Va.

FY91 Total Project Cost: $200,000

Principal Investigator:
Rodney A. Geisbrecht

Project Manager:
Royal J. Watts
Morgantown Energy Technology Center

Reporting Period: Oct. 1–Dec. 31, 1990

Objectives

The objectives during the current reporting period support the Morgantown Energy Technology Center (METC) FY 1990–1991 goal of assessing outstanding technical issues concerning the use of "leave-behind" lamellae in particular and surfactant-alternating-gas (SAG) injection schemes in general for mobility control and fluid diversion.

Summary of Technical Progress

During the current reporting period, three-dimensional (3-D) networks of leave-behind lamellae were generated for the prediction of realistic mass transfer rates that could be compared directly with experimental tracer data. This work is summarized under the first topical heading.

Also during the current reporting period, advancements were made in the ability to simulate and characterize unstable flows. This work is summarized under the second topical heading.

Mass Transfer Effects in Networks of Leave-Behind Lamellae

Mass transfer computations were made for networks of leave-behind lamellae generated by 3-D invasion percolation on lattices chosen to match observed relative permeability effects of leave-behind lamellae (see Fig. 1). Computed mass transfer coefficients appear consistent with recently completed tracer experiments. Mass transfer coefficients in the 0.0001 cycle/s range are low enough to adversely distort recovery curves of laboratory-scale exper-

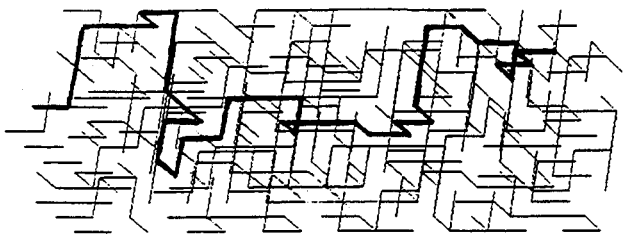

Fig. 1 Three-dimensional invasion percolation with the leave-behind flow rule (flowing channel is bold line).

iments. This appears to have been confirmed in a recently completed tertiary oil recovery experiment in the presence of leave-behind lamellae. Whether this effect will persist to the field scale is a question currently being addressed.

Simulation and Characterization of Unstable Flows

A method for obtaining a fractional flow curve from an observed saturation profile was derived and tested, since these are uniquely related for any fractional flow mechanism. Application of this method to saturation profiles generated by gradient-governed growth led to some interesting observations (Fig. 2): (1) simulated fractional flow curves were intermediate between stable and Buckley–Leverett limits for miscible displacement, (2) simulated curves converged to the Koval limit at low saturation, and (3) simulated curves converged to the Buckley–Leverett limit at high saturation. The first two observations are clearly consistent with the classic data upon which the Koval correlation is based. The validity of the third observation, which implies that the Koval correlation must overpredict incremental recovery after solvent breakthrough, is unresolved at this point.

A new parameter was devised for root-mean-moment analysis of the various flow regimes implicit in simulations of unstable flow (viscous fingering). The parameter correctly takes into account the discretized nature of the underlying lattice and allows for an unambiguous identification of unstable and quasi-stable flow regimes (Fig. 3).

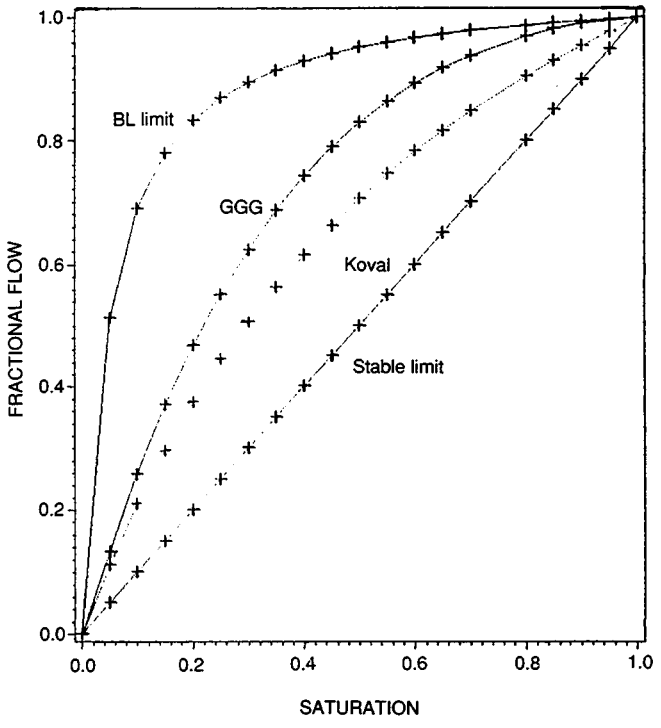

Fig. 2 Fractional flow curves for viscosity ratio = 20.

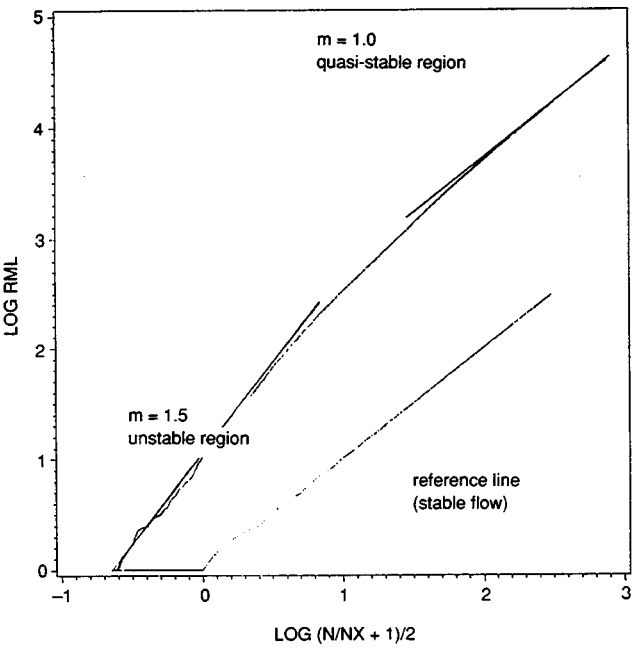

Fig. 3 Average of 10 diffusion limited aggregation runs on a 25 × 150 lattice.

A rigorous method to deal with viscous cross flow, ganglia trapping, and ganglia mobilization was devised and tested for use in the gradient-governed-growth simulator. Volume conservation is strictly enforced by stochastically following streamlines in the displaced fluid until either the system boundary or the fluid–fluid interface is reached, which eliminates artifacts of compressibility. Quasi-stable flow regimes can now be positively identified for arbitrarily long systems, and either trapping or motion of ganglia is readily accommodated.

References

1. R. A. Geisbrecht, W. N. Sams, M. L. Ferer, and D. H. Smith, Characterization of Viscous Fingering as Predicted by Stochastic Simulators, abstract accepted for the 65th Colloid and Surface Science Symposium in Norman, Okla., June 17–19, 1991.
2. R. A. Geisbrecht, D. H. Smith, W. N. Sams, Characterization of Viscous Fingering as Predicted by Stochastic Simulators, abstract accepted for the 65th Colloid and Surface Science Symposium in Norman, Okla., June 17–19, 1991.

QUANTIFICATION OF MOBILITY CONTROL IN ENHANCED RECOVERY OF LIGHT OIL BY CARBON DIOXIDE

Morgantown Energy Technology Center
Morgantown, W. Va.

FY91 Total Project Cost: $550,000

Principal Investigator:
Duane H. Smith

Project Manager:
Royal J. Watts
Morgantown Energy Technology Center

Reporting Period: Oct. 1–Dec. 31, 1990

Objectives

The current objective of the Morgantown Energy Technology Center (METC) enhanced oil recovery (EOR) research is to conduct experimental and theoretical studies to improve the recovery efficiency of the carbon dioxide (CO_2) miscible flooding process. Since reducing the mobility ratio seems to provide efficient flood performance, the research is being directed to the study and use of viscous CO_2. The technique involves the use of surfactants to generate a CO_2 dispersion that would retard the growth of viscous fingers and also act as an in situ diverting agent. The merits of CO_2 dispersion will be determined by performing linear core-flow studies on large-scale systems. This effort will be supplemented by theoretical and experimental studies of CO_2 dispersions, studies of the effects of altered wettability of rock surfaces, and determination of in situ saturation profiles as probed by X-ray computerized tomography and nuclear magnetic resonance imaging. The laboratory data will also be used to test the METC composition model, and the model will be used to plan critical experiments.

Summary of Technical Progress

The foams (or emulsions) created by capillary snap off in CO_2 mobility control commonly produce pressure gradients in excess of 500 psi/ft in steady-state relative permeability measurements. Pressure gradients of this magnitude are far too large for use in the field to modify CO_2 mobilities and could even hinder the use of CO_2 foams as blocking agents by making it difficult to inject the foaming agent.

Furthermore, three different fluid phases (gas, oil, and water) are encountered in CO_2 EOR with surfactant-based mobility control, and these phases can form many different morphologies of fluid dispersions other than "foam." Hence the study of morphologies of two-phase and three-phase ex situ and in situ dispersions is under way to develop the in-depth knowledge needed to solve these problems.

Data from literature were used to construct[1] a dispersion morphology diagram from emulsions formed by the ethanol–benzene–water system at 20°C. Equations were then developed to quantitatively describe and predict what morphology would occur and where inversions would occur as a function of parameters, such as amphiphile concentration and phase saturations. A similar study was previously done[2] with equations from catastrophe theory for cases where the temperature varied, but this approach cannot be used for ternary systems at constant temperature because the previously used equations[2] require that the tie lines be parallel. A coordinate transform was developed[1] to solve this problem for systems where extensions of the tie lines meet at a common point.[3] The method developed[1] was based on one of Hand's equations[4] and includes the transformation from a Cartesian volume–fraction coordinate system (x, y) to a new (Cartesian) coordinate system (b, a), which involves a translation and a rotation of the (x, y) coordinates. The transformation method also includes a procedure to transform from the (Cartesian) coordinate system (b, a) to a polar coordinate system (r, θ). A complete explanation of the transformation procedures is given in the paper.[1] Results showed that the transformation that converted the amphiphile concentration and phase–volume fraction into polar coordinates produced the best agreement between theory and experiment for the tie lines and for the inversion hysteresis width, but the theory did not accurately predict average inversion phase–volume fractions except at the critical point. Also included in the paper[1] is a comparison of the inversion and hysteresis in this system and in the 2-butoxyethanol/water–temperature system[2] that was previously studied.

References

1. K.-H. Lim and D. H. Smith, Experimental Test of Catastrophe Theory in Polar Coordinates: Emulsion Inversion for the Ethanol/Benzene/Water System, *J. Colloid Interface Sci.* (in press).
2. D. H. Smith and K.-H. Lim, An Experimental Test of Catastrophe and Critical-Scaling Theories of Emulsion Inversion, *Langmuir*, 1071-1077 (June 1990).
3. D. H. Smith, K.-H. Lim, and M. Ferer, Critical Theory for Systems with "Polar" Tie Lines (in preparation).
4. D. B. Hand, *J. Phys. Chem.*, 34: 1961 (1930).

THERMAL RECOVERY—SUPPORTING RESEARCH

RESEARCH ON OIL RECOVERY MECHANISMS IN HEAVY OIL RESERVOIRS

Contract No. FG22-90BC14600

Stanford University
Petroleum Research Institute
Stanford, Calif.

Contract Date: Feb. 23, 1990
Anticipated Completion: Feb. 22, 1993
Government Award: $740,000
(Current year)

Principal Investigators:
W. E. Brigham
K. Aziz
H. J. Ramey
L. M. Castanier

Project Manager:
Thomas B. Reid
Bartlesville Project Office

Reporting Period: Oct. 1–Dec. 31, 1990

Objectives

The goal of the Stanford University Petroleum Research Institute (SUPRI) is to conduct research directed toward increasing the recovery of heavy oils. Presently, SUPRI is working in five main directions:

1. Flow properties research—to assess the influence of different reservoir conditions (temperature and pressure) on the absolute and relative permeabilities to oil and water and on capillary pressure.
2. In situ combustion studies—to evaluate the effects of different reservoir parameters on the in situ combustion process. This project includes the study of the kinetics of the reactions.
3. Additives to improve steam injection—to develop and understand the mechanisms of the process with the use of commercially available surfactants for reduction of gravity override and channeling of steam.
4. Reservoir definition—to develop and improve techniques of formation evaluation, such as tracer tests and pressure transient tests.
5. Field support services—to provide technical support for design and monitoring of DOE-sponsored or industry-initiated field projects.

Summary of Technical Progress

Flow Properties Studies

A project has been initiated in collaboration with the Geophysics Department to compare saturations measured by computerized axial tomograph (CAT) scanning with results obtained on the same core by resistivity and sonic measurements. Water–gas systems will be studied first on

simple cores (Berea and Fontainebleau sandstones), and then this work will be extended to oil–water–gas systems.

A run was made to measure end effects in relative permeability flow experiments. Some difficulties were encountered because of reactions between the hexane and the rubber sleeve of the core holder. Qualitative data obtained showed that drainage is not affected by end effects. Figure 1 shows that during imbibition oil remains at the top of the core near the inlet. The four slices are taken 0.02 in. apart starting at 0.2 in. from the inlet. Oil is visible at the top of the first three slices. These scans were taken at the end of the imbibition period.

Fig. 1 Scans of four slices taken 0.02 in. apart starting at 0.2 in. from inlet. Shown are amounts of oil remaining at end of imbibition period.

In Situ Combustion

Samples of crude oils ranging from 10 to 34° API gravity have been requested from California operators. These crudes will be used in kinetics experiments, tube runs, and steamflooding displacements. The equipment is now in working order with the exception of the high-pressure liquid chromatograph (HPLC). The selection of columns suitable for accurate measurements of asphaltenes, saturates, aromatics, and polars fractions is being finalized. As soon as this task is complete kinetics experiments will begin.

A computer tape containing distillation data has been obtained from the DOE database. California crude data selected from this database will improve the correlations previously derived from a very limited number of data points. The ultimate goal of this project is to predict residual oil saturation after steamflooding and the amount of fuel burned in an in situ combustion process.

Steam with Additives

Theoretical and numerical investigations of transient foam flow in porous media were carried out further. A new theory based on a modified Buckley–Leverett method was proposed to describe the foam behavior. More experimental data are needed to validate this model. The initial matching of the experiments has been very promising. The experimental equipment was transferred to a mobile cart and is under recalibration. A longer sandpack tube was made. A computer program was written to facilitate the understanding of the theory.

A thin section of Berea sandstone was prepared for use as the model for a silicon micromodel. The lithograph of that thin section was digitized into PICT format on the Macintosh computer. A small number of pixels are removed to allow a continuous flow path through the model. The image will be moved in MEBES format for transfer on a silicon wafer by Stanford Center for Integrated Systems. The model should be ready in March 1991.

The data obtained last quarter on the one-dimensional (1-D) steam model are now being analyzed. Optimization of the amount of surfactant needed to generate high pressure gradient increases will be attempted. A first step is to decrease the slug size from 10% of the pore volume to 5%, then 1%, while keeping the surfactant concentration constant at 1% by weight.

Two runs were made in the three-dimensional (3-D) steam model. The growth of the steam zone under steam injection flow rates of 4 and 6 cm^3/min was monitored by CAT-scanning and pressure and temperature data. A run with a surfactant slug is planned for early 1991.

A study on steam injection in fractured media has started. The literature review on this topic is in progress.

Formation Evaluation

The evaluation of the UTCHEM simulator for use in tracer tests reveals the limitations of the simulator in terms of cell Peclet number. It appears that when the Peclet number is over 500, the results from UTCHEM are not valid because of numerical dispersion. The logging research on saturation determination following waterflooding is in progress. One case considered is a multilayer sandstone reservoir. The value of water saturation determined by logging is difficult to evaluate because of variations in salinity and temperature. The method sought in this study will be used to produce estimates of water saturation using logs from initial wells and wells drilled after the waterflood. It will be verified against other logging techniques and by core analysis.

Support Services

The work on screening reservoirs for enhanced oil recovery potential with the use of a simple screening model is continuing. The literature review is almost complete. Data have been sought from the DOE database to properly define the problem on the basis of available information.

MODIFICATION OF RESERVOIR CHEMICAL AND PHYSICAL FACTORS IN STEAMFLOODS TO INCREASE HEAVY OIL RECOVERY

Contract No. FG22-90BC14600

University of Southern California
Los Angeles, Calif.

Contract Date: Feb. 23, 1990
Anticipated Completion: Feb. 22, 1993
Government Award: $150,000
(Current year)

Principal Investigator:
Yanis C. Yortsos

Project Manager:
Thomas B. Reid
Bartlesville Project Office

Reporting Period: Oct. 1–Dec. 31, 1990

Objectives

The objectives of this contract are to continue previous work and to carry out new fundamental studies in the following areas of interest to thermal recovery: the displacement and flow properties of fluids involving phase change (condensation–evaporation) in porous media; the flow properties of mobility control fluids (such as foam); and the effect of reservoir heterogeneity on thermal recovery. The specific projects are motivated by and address the need to improve heavy oil recovery from typical reservoirs as well as less conventional fractured reservoirs producing from vertical or horizontal wells.

Thermal methods, particularly steam injection, are currently recognized as the most promising for the efficient recovery of heavy oil. Despite significant progress, however, important technical issues remain open. Specifically, knowledge of the complex interaction between porous media and the various fluids of thermal recovery (steam, water, heavy oil, gases, and chemicals) is inadequate. The interplay of heat transfer and fluid flow with pore-scale and macroscale heterogeneity is largely unexplored.

Summary of Technical Progress

Vapor–Liquid Flow

Work in the area of vapor–liquid flow in porous media continued. On the theoretical side, progress was made in several directions: conditions were derived for the applicability of percolation patterns of growth in the case of negligible heat conduction in the solid. For typical values, the following constraint on the heating rate was derived: $Q \ll 32.5°F/d$. This is likely to be observed in ordinary steam injection processes. Under the same conditions, the depletion of supersaturation for an adiabatic system was investigated. Here, although the bubble growth pattern remains the same, the supersaturation varies. A typical schematic of the relation between temperature and liquid pressure corresponding to a specific pore size distribution is shown in Fig. 1. These results are obtained by numerical simulation of the phase change at quasi-static conditions with nucleation included. A numerical code that simulates heat conduction in both the solid matrix and the pore space was developed to account for heat transfer. This code is to be used for the study of both concurrent and countercurrent vapor–liquid flows in the presence of temperature gradients and for the study of heat dispersion.

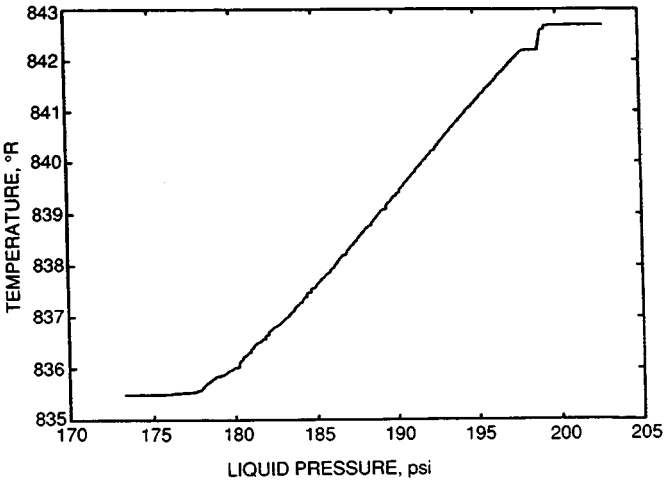

Fig. 1 Relation between temperature and liquid pressure during adiabatic change of phase simulated in a pore network.

Additional experiments were carried out in glass micromodels and in Hele–Shaw cells. In both cases the displacement of two model oils (Dutrex 739 and mineral oil) by the injection of steam at various conditions was studied. Several interesting observations were made. For the Hele–Shaw cell displacements, condensed water produced significant viscous fingering (Fig. 2). As expected, tip splitting was less intense in the mineral oil case. Steam flowed mostly along the paths of condensed water. Steam condensation occurred repeatedly, and it was followed by steam zone growth in bursts. In general, the steam front was never stationary, and repeated condensation–evaporation cycles were observed. A typical front is shown in Fig. 3. Contrary to waterfloods, injection by steam resulted in a complete displacement of residual oil from the glass plates. This mechanism, currently under investigation, appears to be a key mechanism for the improvement of oil recovery. Finally, displacement of Dutrex 739 resulted in an interesting non-Newtonian response, in which repeated

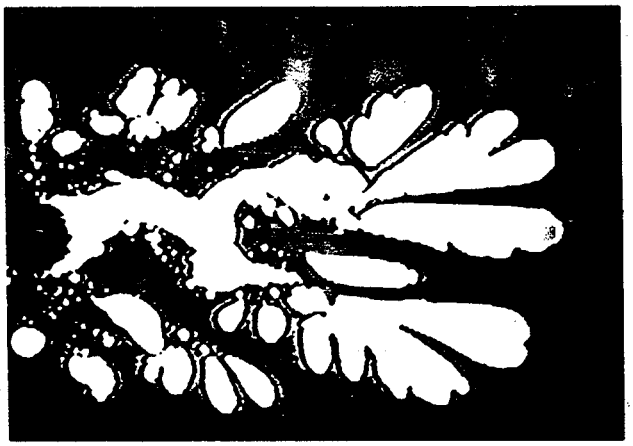

Fig. 2 Viscous fingering from condensed water during steam displacement of Dutrex 739 in a Hele–Shaw cell.

Fig. 3 Typical steam front boundary during steam injection in a Hele–Shaw cell.

cycles of finger breakup and finger reconnection were noted. This effect is also under study. Experiments in glass micromodels showed similar features. Condensation and evaporation cycles for the injected steam were commonly observed. After a period of injection, displacement of oil from dead-end pores was observed. Principal mechanisms for this process were surface roughness and film flow (Fig. 4). Ultimately, all oil trapped in dead ends was recovered. Interesting, three-phase (oil–liquid water–vapor) flow regimes were identified during this process.

Heterogeneity

Theoretical work also continued in the modeling of fractured and heterogeneous systems. During the past quarter, efforts were made to analyze the dependence of the permeability of fractal networks of fractures on the number of fracture generations and on the sample size. For this, the conductivity matrix of the network was studied. Interestingly enough, the matrix also has a self-similar structure. In addition, a numerical code was developed to study the transient response of single-phase flow in the fracture network. Both of these tasks are near completion. The numerically constructed fractal networks were also used as a prototype for glass micromodel networks of fractures. Imbibition and steam displacement experiments were conducted in these models.

Two manuscripts were prepared during the past quarter.[1,2] The first describes a new approach, based on percolation theory, for the large-scale averaging of drainage in heterogeneous systems. Since it is fundamentally proper, this approach is promising for the development of correct pseudofunctions in coarse-grid simulation. The second manuscript[2] addresses parallel flow in long and narrow Hele–Shaw cells and studies the wave behavior of fluid interfaces. The development of solitary waves and their interaction is investigated both theoretically and experimentally. In the experimental study, the investigation of the interface dynamics in a long and narrow Hele–Shaw cell continued. Experiments were conducted with pairs of silicone oil–water and mineral oil–glycerol–water solutions.

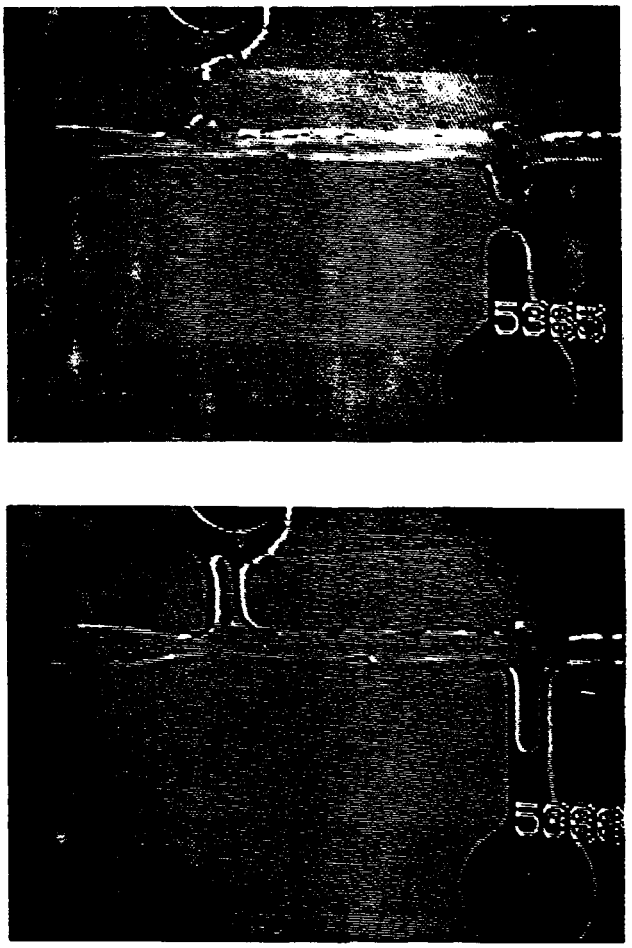

Fig. 4 Displacement of trapped oil from dead-end pores by steam injection in a glass micromodel.

Effects of rate, viscosity ratio, and geometry were analyzed in detail. Most of these were found consistent with the theoretical predictions described by Zeybek and Yortsos.[2]

Finally, significant progress was made in the analysis of flow and displacement processes in long and narrow reservoirs where Vertical Flow Equilibrium (VFE) or other parallel flow conditions apply. An asymptotic technique was developed that, for the first time, rigorously validates previous semiempirical formulations.[3,4] The asymptotic parameter in the expansion is 1/R, where $R = (L/H)(k_v/k_h)$ is assumed large (where L is length, H is thickness, and k_v and k_h are vertical and horizontal permeabilities, respectively). The technique was applied to a variety of processes, including immiscible displacement, dispersion, and gravity override.

Chemical Additives

Most of the effort in the past quarter focused on the analysis of previous experiments in foam generation and foam propagation in laboratory cores. These experiments involve the simultaneous injection at a constant rate of surfactant solution and nitrogen gas at various fractions. Two main issues previously identified, the nature of foam incubation and the importance of core length, are in need of a theoretical analysis. Current theories were found inadequate for the interpretation of the experimental results. It is possible that the dynamics of the formation of weak and strong foam are different and that the incubation period describes a transition between the two regimes. The observed effect of core length is also important, mainly because it is suspected to be an indication of end effects. An understanding of the latter is valuable, as end effects represent a limiting case of reservoir heterogeneity. Work continues in both these directions.

Finally, during the past quarter, investigations on non-Newtonian, power-law flow in porous media continued. The effects of extensional flow in the converging and diverging segments of the pore geometry and their contribution to viscous flow resistance are being studied.

References

1. Y. C. Yortsos, C. Satik, J-C. Bacri, and D. Salin, Large Scale Averaging of Drainage Under Local Capillary Control, submitted (1990).
2. M. Zeybek and Y. C. Yortsos, Long Waves in Parallel Flow in Hele–Shaw Cells, submitted (1991).
3. K. H. Coats, J. R. Dempsey, and J. H. Anderson, *Soc. Pet. Eng. J.*, 63 (1971).
4. V. J. Zapata and L. W. Lake, paper SPE 70771 presented at the 56th Annual SPE Conference, San Antonio, Tex., Oct. 5–7, 1981.

THERMAL PROCESSES FOR LIGHT OIL RECOVERY

Cooperative Agreement DE-FC22-83FE60149, Project BE11A

National Institute for Petroleum and Energy Research
Bartlesville, Okla.

Contract Date: Oct. 1, 1983
Anticipated Completion: Sept. 30, 1991
Funding for FY 1991: $300,000

Principal Investigator:
David K. Olsen

Project Manager:
Thomas B. Reid
Bartlesville Project Office

Reporting Period: Oct. 1–Dec. 31, 1990

Objectives

The objectives of this research are to (1) determine the effect of steam temperature on composition of the produced oil and residual oil saturation (hot water vs. steam at various temperatures)—determine potential override and fingering tendencies in a two-dimensional (2-D) model using oil and sand from Teapot Dome (Wyoming) field and compare steamflood performance with that from other light oil steamfloods, (2) examine the applicability of the semianalytical thermal predictive models for applicability in evaluation of light oil steamflood potential, (3) construct a new multidimensional steamflood physical model, and (4) transfer technology to others in the field of thermal oil production by participating in the Annex IV meetings between the Department of Energy (DOE) and the Venezuelan Ministry of Energy and Mines.

Summary of Technical Progress

Revision of Annual Research Plan

At the request of DOE, the FY91 Annual Research Plan[1] for both BE11A and BE11B, Thermal Processes for Oil Recovery has been modified. The new research plan will accelerate research in thermal recovery of both light and heavy oil and may help improve the economic producibility of this Nation's oil resource—the major goal of DOE's recent Oil Research Program Implementation Plan (April 1990) (Ref. 2). The construction of a new multidimensional high-pressure steamflood physical model will not be undertaken, but the current 2-D model will be upgraded.

Numerical simulation of thermal processes will be emphasized along with laboratory and simulation studies of DOE's steamflood pilots in Naval Petroleum Reserve, NPR No. 1, Elk Hills field, Calif., and NPR No. 3, Teapot Dome field, Wyo. Both projects demonstrate light oil steamflooding in different environments. The California steamflood is in a highly permeable, unconsolidated sand at a depth of 2800 ft, and the Teapot Dome pilot is in a highly fractured, consolidated, tight (63 mD) Shannon sandstone at a 325-ft depth.[3]

Research at the National Institute for Petroleum and Energy Research (NIPER) has shown that steamflooding previously waterflooded water-wet reservoirs is not economic. The 2-D physical model steamflooding studies on previously waterflooded sands that are oil-wet or of intermediate wettability indicate that these reservoirs are prime candidates for steamflooding. Oil-wet reservoirs respond poorly to waterflooding, and producing wells become stripper wells early in their productive life. Thus the more oil-wet reservoir sands have high oil saturations (after waterflood) as compared with water-wet reservoirs. Steam, in addition to supplying pressure and lowering the viscosity of the oil and altering the oil composition, changes the wettability to a more water-wet condition as part of the mechanism of steamflooding.

Steam Diversion/Mobility Control for NPR No. 3

This quarter NIPER performed a series of experiments to evaluate steam diverters for possible use in the steamflood pilot at NPR No. 3, Teapot Dome (Wyoming) field. This steamflood is being conducted in the highly fractured, tight (63 mD), shallow Shannon sandstone (325 ft) (Ref. 3). NIPER approached the evaluation of steam diverters/ mobility control agents for Teapot Dome and the evaluation of alkaline agents to reduce the amount of surfactant needed by the following:

- With one-dimensional (1-D) quartz sandpacks (oil-free and then at steamflood residual oil saturation), NIPER could evaluate the physical model and data collection system and could choose the best surfactants for diverters and evaluate the effect of added alkaline agent (knowing that the quartz sand would have little adsorption and the alkaline agent would primarily affect the foam strength and stability). These tests evaluate steam foam buildup (rate of pressure generation), maximum pressure obtainable when surfactant is injected on a continuous basis, and foam degradation (pressure decline rate when surfactant injection is stopped).
- With 1-D sandpacks composed of crushed reservoir core (as received—not cleaned), NIPER could evaluate the effect of adsorption of the surfactant and the effect of the addition of the alkaline agent. The field sand would be used only once, and mass balance on the surfactant and chemical analysis of the effluent would be conducted. These tests would be conducted at steamflood residual oil saturation.
- With the best formulation of surfactant and alkaline agent, the effect of steam diverter would be evaluated in the 2-D model to evaluate its effect on reducing the gravity override observed in the base case 2-D steamfloods with Teapot Dome oil and sand.

The first step of this screening has been completed; however, because significant difficulty has been encountered in duplicating the experiments as the result of the backpressure regulator on the system, results are not shown in this quarter. An electronic backpressure regulator is being acquired. The effect of liquid/vapor ratio (LVR), rate of steam, noncondensable gas (N_2), and the rate and concentration of surfactant all contribute to the rate of foam formation, maximum foam strength, and rate of foam degradation. The conclusions that can be drawn show the performance of surfactants (Shell LTS-18, AOS-2024, and to a lesser extent Chevron Chaser 1020) as steam foamers are dependent upon the test conditions: temperature, salinity, surfactant structure, surfactant concentration, oil composition, oil saturation, liquid/vapor ratio, and frontal advancement rate. NIPER found that surfactants which are good foamers at 315°F and experimental conditions described by Shallcross et al.[4] (AOS-2024 developing the best foam, whereas Chaser 1020 was less effective) behave quite differently when the temperature is raised to 430°F. At this higher temperature, Chaser 1020 develops pressure significantly higher and faster than LTS-18 or AOS-2024.

Analysis of Effects of Wettability on Steamflood Performance

Three papers[5–7] were prepared on the basis of recent research on the effect of wettability on steamflood performance. A series of 2-D waterfloods followed by steamfloods on sandpacks of various wettabilities was undertaken. One set of experiments was conducted on crushed Berea sandstone and another on crushed quartz sandpacks. These waterflood and subsequent steamflood experiments were conducted with 32 °API New London crude. New London field, located in south-central Arkansas, is operated by Murphy Oil Company. These experiments complement an earlier study in which waterflooding followed by steamflooding was compared with steamflooding without waterflooding using water-wet sandpacks. However, these experiments also incorporated oil-wet and intermediate or mixed wettability porous media and analyzed steamflood performance after waterflooding.

The silylation procedure used to prepare sands of various degrees of wettability has been described.[5] The thermal and hydrolytic stability of the oil-wet surface has also been discussed, and the method of determining wettability on these unconsolidated sands has been described.[6] The results of this section are being written as both a topical report and SPE paper 21769, which will be presented at the SPE Western Regional meeting in March 1991 (Ref. 7).

Participation in Annex IV Meeting

NIPER participated in an Annex IV meeting at Stanford University, Oct. 25–26, 1990. Annex IV between DOE and the Ministry of Energy and Mines (MEM), Venezuela, is designed for technology transfer between the countries in the area of thermal oil production. Each country pursues its own research, but the Annex is intended to minimize duplication of efforts and accelerate the advancement of the technology in thermal oil production The Annex promotes cooperation of the researchers and open discussion of the technical problems facing both laboratory and field development of thermal processes for oil production. The proceedings and papers presented at these meetings will be assembled during the next few months and published as a cooperative effort of DOE and MEM.

References

1. National Institute for Petroleum and Energy Research, *FY91 Annual Research Plan,* DOE Report NIPER-465, December 1990.
2. Assistant Secretary for Fossil Energy, Deputy Assistant Secretary for Oil, Gas, Shale and Special Technologies, *Department of Energy Oil Research Program Implementation Plan,* DOE Report DOE/FE-0188P, April 1990.
3. G. Moritis, Annual Production Report, Biennial EOR Survey 1990, *Oil Gas J.,* 49-83 (Apr. 23, 1990).
4. D. C. Shallcross, L. M. Castanier, and W. E. Brigham, *Characterization of Steam Foam Surfactants Through One-Dimensional Sandpack Experiments,* SUPRI Technical Report 73, DOE Report DOE/BC/14126-19, May 1990.
5. M. E. Crocker, P. S. Sarathi, J. Betancourt, and D. K. Olsen, *Evaluation of Artificially Wetted Surfaces for Use in Laboratory Steamflood Experiments,* presented at UNITAR/UNDP V International Conference on Heavy Oil and Tar Sands, Caracas, Venezuela, February 1991.
6. D. K. Olsen and M. E. Crocker, *Effects of Elevated Temperatures on Capillary Pressure and Wettability,* presented at UNITAR/UNDP V International Conference on Heavy Oil and Tar Sands, Caracas, Venezuela, February 1991.
7. D. K. Olsen, P. S. Sarathi, S. D. Roark, E. B. Ramzel, and S. M. Mahmood, Light Oil Steamflooding: A Laboratory Study of Oil Recovery from Water and Oil-Wet Porous Media in 2-D Sandpacks, SPE paper 21769, presented at Society of Petroleum Engineers Western Regional Meeting, Long Beach, Calif., Mar. 20–22, 1991.

THERMAL PROCESSES FOR HEAVY OIL RECOVERY

Cooperative Agreement DE-FC22-83FE60149, Project BE11B

National Institute for Petroleum and Energy Research
Bartlesville, Okla.

Contract Date: Oct. 1, 1983
Anticipated Completion: Sept. 30, 1991
Funding for FY 1990: $250,000

Principal Investigator:
Partha Sarathi

Project Manager:
Thomas B. Reid
Bartlesville Project Office

Reporting Period: Oct. 1–Dec. 31, 1990

Objectives

The objectives specifically for FY91 are to (1) prepare an addition to the thermal (steam) field operators' guide prepared in FY90 of the costs, sample engineered analysis, schematics, and equipment needed for implementation of a steamflood by an independent operator in a format that can be used by independent operators to help assess the economic feasibility of implementing a thermal enhanced oil recovery (EOR) process; (2) advance the current numerical laboratory thermal simulator to assist in the analysis of laboratory experiments using both vertical and horizontal steam injection; and (3) construct a new multidimensional steamflood model.

Summary of Technical Progress

Revision of Annual Research Plan

Because of recent emphasis by the Department of Energy (DOE) on short-term activities, priorities for project BE11B were reevaluated and changes to the FY91 annual research plan were made. The major change in scope of work is the deletion of the task relating to construction of a new two-dimensional (2-D) physical model, which falls into the realm of long-term research, and addition of two near-term tasks. Task 2 promotes technology transfer of a recently developed PC-based thermal predictive model by making it more user-friendly and publishing a user's manual. Task 3 calls for upgrading of the existing 2-D physical model and its utilization to calibrate the laboratory numerical thermal simulator.

Compilation of the Steamflood Operator's Guide

As part of the technology transfer work under "Thermal Processes for Heavy Oil Recovery," a primer on thermal steamflood operations is being prepared. This manual explores the concepts behind steamflooding and discusses the information required to evaluate, design, and implement steam injection processes in the field. The emphasis is on the practical aspects of steamflooding. Details of equations and calculation methods for the estimation of steamflooding performance are not discussed in this manual. The material presented is directed toward engineers and independent

operators who are familiar with routine waterflood operations but have no exposure to thermal operations. In part, it should provide a basis from which to seek help from consultants in the field who by years of experience can initiate and run a successful steam project.

This quarter two chapters, "Predictive Models for Steamflooding" and "Financing Thermal Operations," were written. The predictive models are useful for forecasting the reservoir response to heat. The chapter on the predictive models discusses the features, usefulness, and limitations of various public domain models. The accuracy and the degree of confidence that can be attached to the model results are also discussed.

Steamflood processes are capital intensive, and the profits are low. Because of the many unknown factors in the development of steam injection, the risks involved are greater, and financing must therefore be protected by a greater margin of safety than expected for primary production or waterflooding. The chapter on financing discusses the basic approach to financing steam injection processes. The importance and usefulness of a properly prepared engineering report is emphasized.

Numerical Thermal Simulator Development

The topical report, "Thermal Numerical Simulator for Laboratory Evaluation of Steamflood Oil Recovery," describing NIPER's efforts to simulate laboratory steamflood experiments was completed. The simulator is designed to run on IBM-AT compatible computers.

The developed model is a three-phase, 2-D multicomponent simulator capable of being run in one or two dimensions. Mass transfer among the phases and components is dictated by pressure- and temperature-dependent vapor–liquid equilibria. Gravity and capillary pressure phenomena are included. Energy is transferred by conduction, convection, vaporization, and condensation. The model employs a block-centered grid system with a five-point discretization scheme. Both areal and vertical cross-sectional simulations are possible. A sequential solution technique is employed to solve the finite difference equations.

The model was validated by comparing the simulator results with published data. These initial comparisons showed that the model is capable of predicting qualitatively the performance trends of the published results. Sensitivity studies were conducted with respect to rock and fluid properties, process variables, and time-step size.

The study clearly indicated the importance of heat loss, injected steam quality, and injection rate to the process. Dependence of overall recovery on oil volatility and viscosity is emphasized. The process is very sensitive to relative permeability values. Time-step sensitivity runs indicated that the current version is time-step sensitive and exhibits conditional stability.

The model stability could be enhanced by employing a fully implicit formulation. However, memory requirements and the complexity of the simulator drastically increase with the use of a fully implicit formulation and direct solution technique. The system's memory constraints precluded the coding and testing of a fully implicit formulation on an IBM-AT type personal computer.

Environmental Regulations

In recent years thermal EOR operators have been faced with increasingly stringent environmental regulations that are oriented toward preventing or ameliorating significant degradation of air and water quality and land use. These environmental laws and regulations significantly impact the design and operation of thermal EOR processes. Federal, state, and local agencies are involved in the enactment and implementation of various environmental laws and regulations. Frequently jurisdictions overlap, and confusion can occur. For example, in the state of California, both the Department of Health Services and the Regional Water Quality Control Board may be involved in determining the level of cleanup of old oilfield sumps and in improvements because the Department of Health Services regulates the hazardous wastes and the Regional Water Quality Control Board regulates any waste placed on land that may impact water quality.

Although environmental specialists within a company may be familiar with laws and regulations and aware of agencies responsible for enforcing these laws and regulations, other personnel may not have that knowledge. Technical and operating personnel responsible for reporting actions must also be aware of the essence of these regulations, so that inadvertent noncompliance with applicable environmental rules and regulations can be avoided.

Hence a paper entitled "Environmental Aspects of Heavy Oil Recovery by Thermal EOR Process" was prepared for presentation at the SPE Western Regional Meeting, Long Beach, Calif., March 1991. This paper is a condensed version of the section on "Waste Disposal and Environmental Issues" of the *Steamflood Operator's Guide*. The purpose of this paper is to familiarize thermal EOR practicing engineers and other interested personnel with applicable environmental rules and regulations. An attempt has been made to provide a summary review of many, but not all, environmental laws and regulations that could be applied to thermal EOR facilities and operations. The environmental laws that have greatest impact on thermal processes pertain to air quality, water quality, hazardous wastes, and environmental quality. In California, there are separate federal, state, and often regional or local laws and regulations pertaining to the preceding environmental subject areas. Since California's environmental standards are more stringent than those required by federal regulations, emphasis is given to California regulations. The applicable regulations of those states where thermal EOR is being implemented, or likely to be implemented, are also summarized. The material contained in this paper was assembled by consulting various federal, state, and local agencies and consultants.

FEASIBILITY STUDY OF HEAVY OIL RECOVERY IN THE MIDCONTINENT REGION (OKLAHOMA, KANSAS, MISSOURI)

Cooperative Agreement DE-FC22-83FE60149, Project SGP37

National Institute for Petroleum and Energy Research
Bartlesville, Okla.

Contract Date: Apr. 1, 1990
Anticipated Completion: June 30, 1992
Funding for FY 1991: $603,440

Principal Investigator:
David K. Olsen

Project Manager:
Thomas B. Reid
Bartlesville Project Office

Reporting Period: Oct. 1–Dec. 31, 1990

Objectives

The objectives of this feasibility study are to (1) investigate the known heavy oil resources from available informational sources in the midcontinent, (2) screen this resource for potential thermal or other enhanced oil recovery (EOR) application, and (3) evaluate various economic facets that may impact the development of this resource. If the study determines that expansion of steamflooding in the area is possible by recent advances in technology, recommendations will be made to facilitate the production of this additional resource within the next 1 to 4 yr.

Summary of Technical Progress

This quarter the scope of SGP37 was expanded to include an assessment of the recovery potential of the Nation's heavy oil reserves. This includes documentation and analysis of the resource, analysis of previous attempts to produce the heavy oil, and an assessment of the potential of producing and refining this oil. This study is being conducted on each geologic basin and contrasted with heavy oil resources in other geologic basins. Although heavy oil is defined both by gravity, >10 and <20 °API, and viscosity, >100 and <100,000 cP, the National Institute for Petroleum and Energy Research (NIPER) is including, where available, the data on the light oil reservoirs, (>25 °API) because viscosity data are seldom available and there are light oil reservoirs whose in-place viscosity would categorize the crude as light but whose gas-free viscosity would qualify it as heavy oil.

As part of the environmental analysis of heavy oil production, a Society of Petroleum Engineers (SPE) paper was prepared in cooperation with BE11B and will be presented at the Society of Petroleum Engineers Western Regional Meeting in March 1991 (Ref. 1). The first draft of the report on the Feasibility of Heavy Oil Recovery from the Midcontinent (Oklahoma, Kansas, Missouri) has been prepared for delivery in May 1991.

One task in SGP37 is to perform integrated engineering and geological analyses of heavy oil recovery processes and the reservoirs where these processes have been attempted. This task includes documentation and analysis of success or failure of various processes that have been attempted through the expanded SGP37 study area. Observations from a review of publications with applications of thermal EOR processes have been published.[2] Many of the remarks help to provide both a critical background and challenge for implementing this SGP37 project and are quoted as follows:

> By far, the most significant (and most difficult to quantify) factors are related to the reservoir definition or characterization, i.e., the single biggest unknown in enhanced oil recovery is the reservoir geology. . . . All credible EOR engineers know that the single biggest unknown in all of enhanced oil recovery is the reservoir geology. . . . Note that the reservoir appears to be systematically up to two orders of magnitude more permeable using the air data as opposed to the brine data. Also, the reservoir is less heterogeneous when using the air permeability (approximately a three-decade range) than with the brine perms (about a four-decade range). Air permeability is infinitely easier to measure and costs one-fourth as much as a brine measurement, but it can seriously overestimate the reservoir permeability and underestimate the contrast in permeability. It is this underestimation of heterogeneity contrast that causes the engineer to lose the "fidelity" of the heat and fluid flow in the reservoir. This permeability contrast leads to thermal inefficiencies, the channeling of steam, early steam breakthrough, and many operational problems. . . . It is estimated that simulation studies have been carried out on less than 3% of all domestic reservoirs (EOR and non-EOR). . . . Because of inherent uncertainties in the reservoir model and data, the nonuniqueness of solutions, and the lack of detailed mechanisms, reservoir simulation results are useful only as a probabilistic guide, not as a quantitative analytical tool. . . . Some very challenging work in reservoir engineering is just beginning to identify the proper ways to average core-measured properties into "pseudofunction" values appropriate to simulation gridblocks of several hundred feet. The pseudofunctions attempt to couple the fluid mechanics with the averaging process, but at the present time does not include their thermal effects. . . . While many (perhaps most) will describe thermal EOR as a mature technology, I see it as just emerging from its adolescent years with much still to be learned and great potential during the next few decades. Two decades had taught us a lot about thermal recovery mechanisms and operating principles, but additional improvements are necessary in the current economic environment.[2]

Normally quotations are not included in the text, but the applicability of these remarks summarizes much of the

findings in the SGP37 analysis. What is new in SGP37 is summarizing the geologic factors to increase the odds of future reservoir selection for EOR application. Geology of the reservoir dictates if the resource is recoverable and which EOR process is most applicable for economic recovery of the remaining oil in place. Geology and the engineering done during development dictate if the resource can be developed from both a technical and economic basis. Previous reservoir management of the reservoir may leave the remaining resource economically unrecoverable with current technology and the prevailing oil price. Oil production rates do not support the permeabilities that are reported. Some of the midcontinent heavy oil reservoirs have become "heavy oil" because of the practice of blowing down the reservoir pressure and flaring the gas; this leaves the higher molecular weight, more viscous oil slowly being produced from the reservoir.

As part of the expanded project, heavy oil reservoirs in California and Mississippi Embayment–Gulf Coast Basin States (Alabama, Southern Arkansas, Louisiana, Mississippi, and Texas) are being reviewed for comparison. Texas and Louisiana onshore Cenozoic Age heavy oil reservoirs (Eocene, Oligocene, Miocene, and Pliocene) are unconsolidated or very poorly consolidated with high-permeability and porosity values similar to those of heavy oil reservoirs in California of the same age. Cenozoic Age heavy oil reservoirs in Texas and Louisiana are generally unconsolidated sands deposited in a deltaic environment, whereas California heavy oil reservoirs are generally deeper marine sands deposited as turbidite in offshore canyons, but also deltaic and alluvial sands are heavy oil reservoirs. Texas and Louisiana Cenozoic Age heavy oil reservoirs are both unfaulted reservoirs and those associated with faulted salt structures. Shallow Texas and Louisiana Cenozoic Age heavy oil reservoirs should be excellent candidates for application of the thermal EOR processes being used to recover heavy oil resources from California heavy oil reservoirs.

Heavy oil resources in southern Arkansas are in Mesozoic Age sandstones and limestones. The largest heavy oil resource in southern Arkansas is in the Nacatoch sandstone, which is Upper Cretaceous in age. Nacatoch sandstone heavy oil reservoirs may be friable, poorly consolidated sandstone to well-consolidated sandstone. These sandstones were deposited in a fluvial–deltaic environmental system as tidal flat, tidal channel, tidal inlet associated, shoreface, and shelf deposits. Nacatoch sandstones may be found as reservoir rock in northern Louisiana and eastern Texas. Shallow Nacatoch sandstone heavy oil reservoirs should be excellent candidates for thermal EOR processes being applied in California because of the friable, poorly consolidated nature of reservoir rock. Some compartmentalization may be encountered in some of the deltaic deposits. Recognition of compartmentalization through reservoir characterization prior to process selection and application should offer greater, quicker success to the thermal process selected and applied.

Heavy oil resources in Mississippi and Alabama salt basins are Mesozoic Age consolidated sandstones and limestones, and Cenozoic Age unconsolidated or poorly consolidated sands. Reservoir rocks in these states are generally older and are more consolidated than those in California. The depths of these reservoirs are beyond the depth at which economic application of steam is commonly applied. Fireflooding is the thermal process that should be considered if an operator chooses to use a thermal process. Alternatively, operators may choose to use carbon dioxide for recovering heavy oil from these reservoirs. A nearby source of carbon dioxide exists on the flanks of the Jackson Dome in the Jurassic Smackover formation.

References

1. P. S. Sarathi, *Environmental Aspects of Heavy Oil Recovery*, SPE paper 21768 to be presented at the Society of Petroleum Engineers Western Regional Meeting, Long Beach, Calif., Mar. 20–22, 1991.
2. Raymond L. Schmidt, *Thermal Enhanced Oil Recovery—Current Status and Future Needs*, Chevron Oil Research Co., La Habra, Calif., Chemical Engineering Progress, January 1990.
3. Mary K. McGowen and Cynthia M. Lopez, *Depositional Systems in the Nacatoch Formation (Upper Cretaceous), Northeast Texas and Southwest Arkansas*, Bureau of Economic Geology, The University of Texas at Austin, 1983.

ENHANCED OIL RECOVERY SENSING

Lawrence Livermore National Laboratory
Livermore, Calif.

Contract Date: Oct. 1, 1984
Anticipated Completion: Oct. 1, 1991

Principal Investigator:
Mike Wilt

Project Manager:
Thomas B. Reid
Bartlesville Project Office

Reporting Period: Oct. 1–Dec. 31, 1990

Objective

The objective of this project is to monitor in situ changes in the electrical conductivity in an oil reservoir during enhanced oil recovery (EOR) operations. The goal of this project is to develop practical tools for monitoring the propagation of a steam front during an ongoing EOR operation. Cross-borehole electromagnetic (EM) induction is being used to provide an image of electrical conductivity changes associated with an encroaching steam front. This technique is being adapted to the hostile conditions in an oil field during EOR operations.

Summary of Technical Progress

During the last quarter of FY90 efforts focused on field measurements for process monitoring at the Lost Hills oil field. Steam drive for EOR begins at this field in January 1991 and will continue for at least the next several years. Some baseline EM data were collected in December 1990 with plans to remeasure in May 1991. In addition to the field work, some significant progress has occurred in numerical modeling research. An iterative inversion modeling scheme, which could significantly improve the resolution of underground images, was developed by a student at University of California, Berkeley.

Lost Hills Field Project

The Lost Hills No. 3 oil field, owned and operated by Mobil Research and Development, has been undergoing cyclic steaming (single-well steam injection followed by production) for EOR for the past several years. Beginning in 1991 the EOR process is being converted to a steam drive where separate wells are used for injection and production. In cooperation with Mobil Research and Development, the EM system has been deployed at Lost Hills to collect baseline data before the drive commences and there are plans to repeat the experiment in May 1991 to detect changes in subsurface resistivity as the result of the steamflood.

Figure 1 is a map of the Lost Hills site; the location of production, injection, and temperature observation wells is shown. As seen from the map, the production and injection wells are aligned in a northwesterly direction, which is parallel to the regional geologic strike. The oil-bearing strata will therefore be steamed in a band parallel to the strike. The steamflood is quite shallow; perforated intervals are at depths near 100 m.

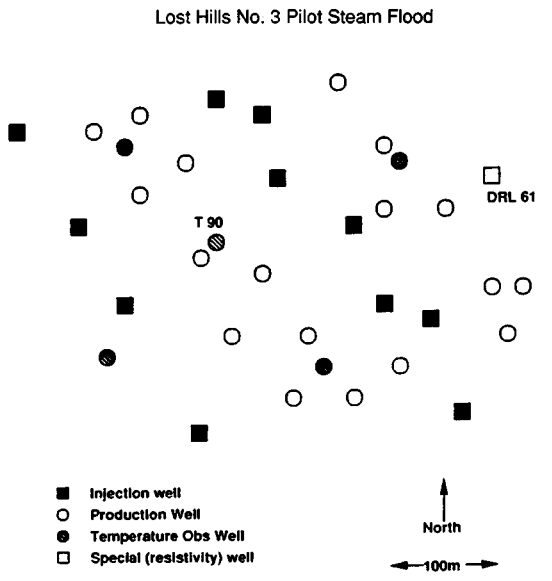

Fig. 1 Well location map for the Lost Hills No. 3 enhanced oil recovery project.

The two-dimensional nature of the flood and the shallow injection are both significant features of this project as they simplify the resistivity imaging somewhat. Another useful feature is that the oil field is located only 300 km from Livermore and is therefore easily reachable within a short time.

A problem with the project is that all available drillholes, with the exception of well DRL 61, are steel-cased. Well DRL 61 is cased with fiberglass, but it is outfitted with 2-m steel collars spaced every 10 m in the hole to transmit electrical current. The effect of steel casing on EM signals is to attenuate the field and shift the phase. This is illustrated in Fig. 2, where two surface-to-borehole EM soundings collected at the Devine, Tex., site are shown. The lower sounding lies within the steel-cased segment of the borehole, and the upper one is immediately below the casing.

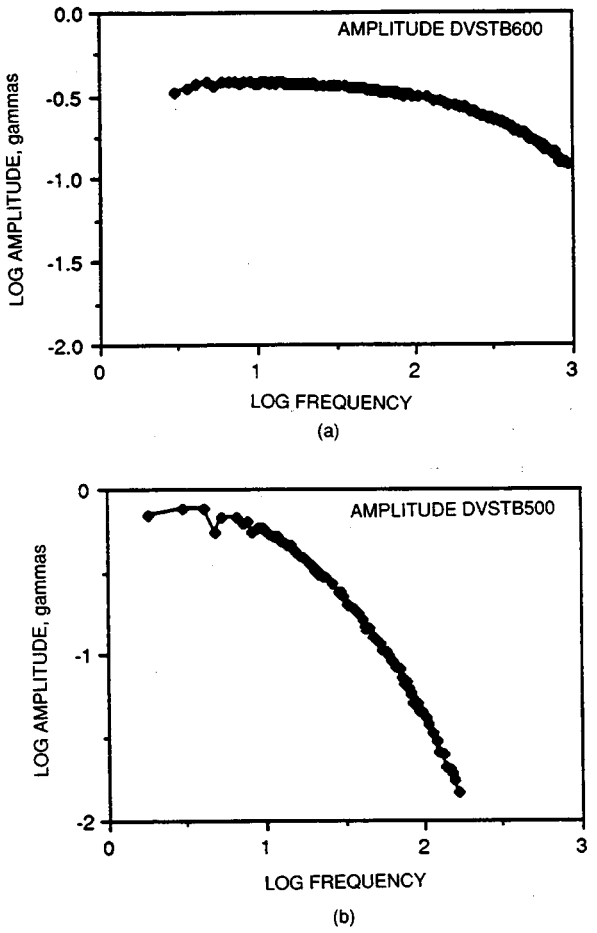

Fig. 2 Sample surface-to-borehole electromagnetic soundings through fiberglass (a) and steel (b) casings.

The figure shows that at frequencies greater than 10 Hz, the attenuation as the result of casing is significant, and at 100 Hz the fields are attenuated by a factor of 30. As demonstrated in the Devine survey, cross-borehole data can be effectively collected if one of the boreholes is steel-cased, but if both holes are cased, the attenuation is too great to recover any useful signals. Surface-to-borehole data

can be effectively collected through steel-cased wells, although, as shown above, the data are also attenuated.

Figure 3 shows some sample cross-borehole data collected during the baseline survey at Lost Hills in December 1990. The data were measured with the receiver in steel-cased borehole T90 and the transmitter moving in borehole DRL 61. The wells are separated by more than 200 m. Both of the cross-borehole profiles at 40 and 200 Hz show abrupt attenuation where the transmitter encounters the steel collars in well DRL 61; the effect is larger at 200 Hz. The figure also shows that signals are extremely small as a result of the attenuation caused by the casing as well as the great distance between holes. Repeat profiles show that these data could be reproduced at approximately the 5% level.

Model Development

Significant progress has recently been achieved in development of numerical codes for resistivity imaging using cross-borehole EM. The new development is an "iterative Brown inversion," which considerably sharpens the images as compared with the standard Born inversion. The code development is part of the research of a student at the University of California, Berkeley, who continues to work on the development of practical cross-hole imaging tools.

Devine Report

The results of the successful field experiment at the Devine, Tex., test site have been compiled into a report initially submitted to DOE and to the industrial sponsors of the research.[1] The report gives a complete description of the cross-borehole and surface-to-borehole field systems and gives cross-borehole EM profiles and the interpretation of these in terms of the known geology. Parts of this report will later be submitted to technical journals for wider dissemination.

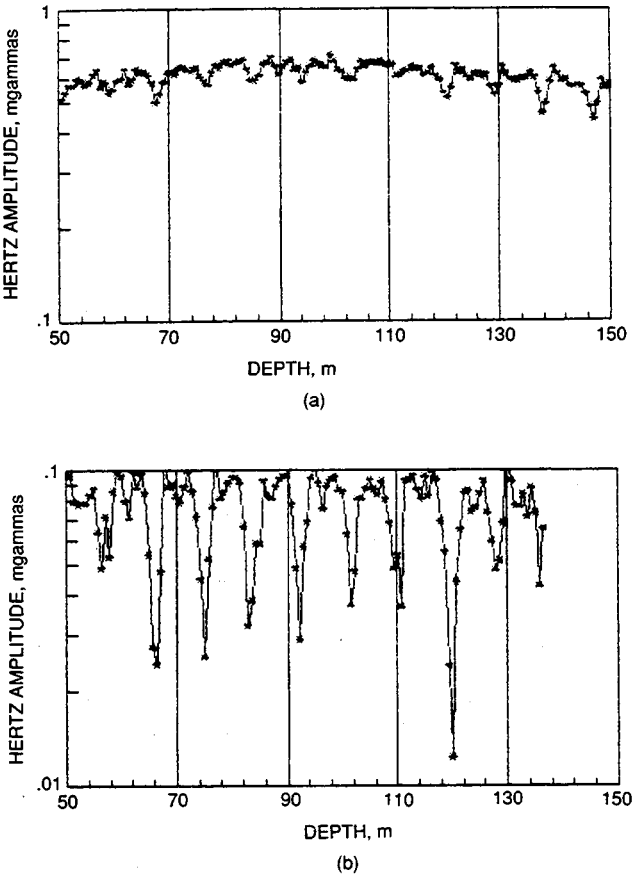

Fig. 3 Sample cross-borehole electromagnetic profiles at Lost Hills at a frequency of 40 Hz (a) and a frequency of 200 Hz (b).

References

1. M. J. Wilt, A. Becker, and H. F. Morrison, *1990 Report of a Field Test at the BP/SOHIO Test Site: Devine, Texas,* Report submitted to industrial sponsors of cross-borehole electromagnetic imaging project.

GEOSCIENCE TECHNOLOGY

RESEARCH ON IMPROVED AND ENHANCED OIL RECOVERY IN ILLINOIS THROUGH RESERVOIR CHARACTERIZATION

Contract No. FG22-89BC14250

Illinois Department of Energy and Natural Resources
Springfield, Ill.

Contract Date: June 28, 1989
Anticipated Completion: June 27, 1993
Total Project Cost:

DOE	**$2,429,000**
Contractor	**4,400,000**
Total	**$6,827,000**

Principal Investigator:
D. F. Oltz

Project Manager:
R. Michael Ray
Bartlesville Project Office

Reporting Period: Oct. 1–Dec. 31, 1990

Objective

This project will provide information that will maximize hydrocarbon production, minimize formation damage, and stimulate new production in Illinois. Such information includes definition of hydrocarbon resources, characterization of hydrocarbon reservoirs, and the implementation of methods that will improve hydrocarbon extractive technology. Increased understanding of reservoir heterogeneities that affect oil recovery can aid in identifying producible resources. The transfer of technology to industry and the general public is a significant component of the program.

The project is designed to examine selected subsurface oil reservoirs in Illinois. Scientists use advanced scientific techniques to gain a better understanding of reservoir components and behavior and address ways of potentially increasing the amount of recoverable oil. Initial production rates for wells in the Illinois Basin commonly decline quite rapidly, and as much as 60% of the oil in place cannot be recovered with standard operating procedures.

Heterogeneities (geological differences in reservoir makeup) affect the capability of a reservoir to release fluids. Bypassed mobile oil and immobile oil remain in the reservoir. To learn how to get more of the oil out of reservoirs, the Illinois State Geological Survey (ISGS) is studying the nature of reservoir rock heterogeneities and

their control on the distribution and production of bypassed, mobile oil.

Summary of Technical Progress

King Field

The King field study is complete. The report "Reservoir Heterogeneity and Improved Oil Recovery of the Aux Vases (Mississippian) Formation at King Field, Jefferson County, Illinois" resulted from this work; it will be the second publication resulting from the cooperative effort.

Old Electric Logs

The old electric log analysis study is complete and has resulted in the publication of Illinois Petroleum 134 titled "Application of Old Electric Logs in the Analysis of Aux Vases Sandstone (Mississippian) Reservoirs in Illinois."

Boyd Field

The study of Boyd field has commenced. Numerous cross sections and structure maps are complete. The sand isopach map combined with preliminary thin-section review suggests that the Aux Vases reservoir at Boyd field is similar to the depositional environment at King field.

Bartelso Field

The Bartelso field study report has been written; figures are being organized for inclusion with text. A draft for peer review will be circulated in early January 1991.

Tamaroa Field

A report on Tamaroa field, Perry County, is in final draft form. Final reservoir volumetrics are being calculated; the study will be completed by the end of the year. Minor cleanup of several data point glitches on the isopach maps will complete the mapping phase.

Very high recovery efficiencies from a waterflooded portion of the northeastern pool suggest that either high recovery potential for other portions of the pools exists and was not used or sweet spots exist in these Cypress marine bars. Drilling, completion, and stimulation methods are also suspect. Also, an expanding (secondary) gas cap associated with production and reservoir pressure depletion is a likely source for low recoveries in some portions of these pools. Pressure maintenance in the high recovery area may be the reason for the high efficiency.

Richview field, Washington County, is in the initial stage of study; the construction of a cross-section grid is in progress. Similar to Tamaroa field, this field produces from upper Cypress lenticular sand bodies.

Zeigler Field

Zeigler field produces from the Aux Vases sandstone in Franklin County, Illinois. Porosity, permeability, production, and lithology data from 43 wells in the main body of the field have been computerized. Digitized logs for these wells have been transferred from GeoQuest to Zycor format for mapping, cross-section, and fence diagram purposes. This will permit integration of engineering and geologic data for the whole field. Engineering data have been integrated with geologic work on the Mack lease at Zeigler.

Parkersburg Field

Parkersburg field produces from the Cypress Sandstone in Edwards and Richland counties, Illinois. Hand contouring of lower, middle, and upper Cypress sandstone isopachs has started. Cuttings have been used as an additional source of information for reservoir evaluation. The study of cuttings to date has shown significant changes in porosity and carbonate content over short distances, which indicates rapid facies changes that influence porosity and production.

Stewardson Field

Reservoir characterization of the Mississippian Aux Vases formation at Stewardson field in southeastern Shelby County, Illinois, is nearing completion. Tasks completed as of this date are analysis of geophysical logs, development of interval isopach maps, structure maps on both the St. Genevieve and Beech Creek formations, cross sections derived from the logs, petrographic analysis of well cuttings and core biscuits, geochemical analysis of oil and brines, clay analysis, and the determination of depositional environments and the diagenetic sequence. At this time, the final calculations of remaining recoverable reserves is the final task to be completed. A manuscript describing the Stewardson field is very near completion.

Mattoon Field

Ninety-eight impregnated thin sections were created (95% Cypress, 5% Aux Vases) on the basis of a nine-well core cross section; sixty thin sections have been examined and photographed in detail; a core-based-type log display containing selected photomicrographs, a detailed lithology column, core analyses, formation tops, and a tabulated well history was constructed; existing cross-sectional data (except for individual Cypress Sands) were submitted to the project mapping system; an initial "Top of Barlow-Structure Map" was created; Mattoon production data were compiled; and production decline/cumulative production charts were created.

Oil and Gas Development Maps

The Mt. Vernon and Roaches maps are complete except for section lines. The Xenia map was produced as a deliverable at the recent Petroleum Advisory Committee and Technical Advisory Committee (PAC/TAC) meeting.

The details of development map production at a scale of 1 : 24,000 to correspond to U.S. Geological Survey (USGS)

7.5-min topographic maps are under investigation. The USGS maps, which use the American Polyconic projection, will be used for this project.

A pay map for Boyd field was made. Pay maps show the pay zone(s) for each well, and each pay must be entered individually.

Engineering Lab

Helium porosimeter. New sleeves were machined to fill the dead space in the chamber when testing $^3/_4$-in. plugs; this reduces the amount of error involved.

Core flow unit. An experiment testing the effects of MCA (Mud Cleaning Acid) was performed on seven Aux Vases plugs cut from Energy and Zeigler field cores. Preliminary results indicate that optimum permeability may be directly proportional to the volume of MCA injected. Other factors—soak time, flow rate and fluid composition—are being evaluated.

The unit will be upgraded in January with precision relative permeability equipment.

Capillary pressure apparatus. The capillary pressure apparatus was calibrated for chamber expansion. Bulk volumes were determined with the apparatus, and they compare closely with the volumes calculated by direct measurement.

Thin-Section Preparation and Analysis

Thin-section preparation is more efficient because of the acquisition of several important pieces of equipment. Approximately 220 thin sections have been completed since the last reporting period. Thin-section analysis and improvement of photographic procedures have been greatly facilitated by the acquisition of a Zeiss Axiophot polarizing microscope.

Database Progress

An integrated/extracted oil and gas database containing header information for all known Illinois oil and gas wells was created and defined for CONQuEST, the ISGS database management system. Approximately 143,000 oil, gas, and related wells are in the current database. This database is now undergoing validation of certain data fields (i.e., location and well status).

A series of programs were written to link project top picks with the locational database to allow plotting of these data. After project picks are finalized, a piece of software will be written to back load these picks into the permanent database.

The monthly drilling report system, which currently consists of approximately 46 programs, was rewritten to run using the new oil and gas database. The new system includes oil production and well plugging input/edit/report features and is scheduled to go online as soon as the daily mail input program is complete.

Clay Minerals

A major effort has gone into the creation and use of improved analytical methods. The model X-ray-diffraction (XRD) traces for all types of clay minerals encountered were calculated. The peak intensity ratios for model traces were used to establish new relative intensity ratios for quantitative estimation of the clays. The new procedures include the weighed addition of an internal standard, fluorite or sylvite at the 5% level. The use of an internal standard makes it possible to refine the estimate of the clay mineral content. Internal standards became feasible as a result of purchase of McCrone micronizers. The error in replicate analyses was high prior to use of the new grinders; only qualitative representation was possible. In all previous field studies and in all ongoing efforts, the bulk samples have been reground and reanalyzed by XRD. The replicate error has dropped to about 10% on the intensities of non-clay peaks. Reports of results are currently being revised, and measures of precision are being calculated and reported. A computer program to rapidly collect peak areas, quantify by comparison with model XRD traces, and report the results of bulk and clay fraction analyses will be implemented. A set of ratios of K-feldspar : plagioclase and each feldspar : quartz will be calculated and reported. These ratios could further distinguish zones within a reservoir, individual reservoirs, or larger groups of reservoirs.

Chlorite in both Aux Vases and Cypress reservoirs has been shown to contain variable amounts of an interlayered serpentine-like phase. Chlorite is now being analyzed in terms of iron : magnesium and serpentine content. The aluminum content of chlorite will be analyzed to the extent possible. The varieties of illite and illite–smectite are also being determined. In part, this is an attempt to measure the compositional variation of all minerals present and to adjust the calculation factors to reflect each mineral's composition. This is also an attempt to explain the nature of anomalous scanning electron microscopic (SEM) photos of clays. Finally, a refined analysis of the types of minerals present in these reservoirs will assist other scientific and engineering aspects of the project. For example, knowledge of the association of the serpentine interlayered chlorite with high porosity and permeability, deleterious acid reactions, or other reservoir characteristics would be valuable.

A series of experiments is being designed to determine the fundamental changes that occur in the clay mineral suite during reaction with MCA-type acids. The nature of both the solid clay mineral phase and potential precipitates from the dissolved phase will be determined.

Geochemistry of Formation Fluids for Reservoir Characterization and Enhanced Oil Recovery

The main objectives of this task are to characterize and model chemistries of reservoir fluids to predict diagenetic

reactions and changes in reservoir properties in response to mixing completion, stimulation, and enhanced oil recovery fluids with formation fluids and the rock matrix.

Brine and oil samples are collected from producing wells, and pH, oxidation potential (Eh), and conductivity of the brine samples are measured in the field. The brine samples are subsequently analyzed for anions (Cl^-, Br^-, I^-, SO_4^{2-}, NO_3^-, CO_3^{2-}, HCO_3^-) and cations (Na^+, Ca^{2+}, Mg^{2+}, K^+, Sr^{2+}, NH_4^+, Al^{3+}, Si^{2+}, $Fe^{2+,3+}$, Mn^{2+}, and about 20 other trace and minor elements). The oil samples are analyzed for saturated hydrocarbons, aromatic hydrocarbons, resins, asphaltenes, pristane/C-17, and phytane/C-18. The field and laboratory data are stored in computer files.

The geochemical and mineralogical data are used as input for geochemical modeling codes (SOLMINEQ88, MINTEQA2, EQ3/EQ6) for predictive geochemistry. Whenever possible, the modeling results will be compared and adjusted with experimental data from core flow tests.

To date, 53 brine and 41 oil samples have been collected in 15 fields producing from the Aux Vases and Cypress formations. The majority of chemical analyses on these samples have been completed; however, some of the anion analyses are being repeated to ensure reliability.

Three geochemical codes (SOLMINEQ88, EQ3/EQ6, and MINTEQA2) are being investigated for the purpose of geochemical modeling. SOLMINEQ88 and MINTEQA2 have been successfully tested on a microcomputer. A preliminary modeling of brine from Energy field and its reaction with a 15% HCl solution used as an injection fluid has been carried out with SOLMINEQ88. An updated version of EQ3/EQ6 will be released soon by Lawrence Livermore National Laboratory.

Mapping of the distribution of measured geochemical parameters with ZYCOR software has been initiated; conductivity and sodium values of the brines have been mapped. Correlations between sodium and conductivity and between production depth and conductivity have also been determined.

Technology Transfer

An overview of the cooperative project that highlighted two field studies was presented at the first Archie Conference in Houston, Tex., on October 22. The presentation was entitled "An Integrated Approach to Reservoir Characterization in the Illinois Basin." This presentation was also made at the Illinois State Geological Survey and the Committee meetings.

The second 1990 PAC/TAC was held in Mt. Vernon, Ill., on December 13. Presentations on field studies, horizontal drilling technology, and database technology were given. Both PAC and TAC were involved in a roundtable discussion concerning standard operating practices in the Cypress and Aux Vases reservoirs in the state.

Thirteen other projects were highlighted in poster sessions.

Several members of the team were in the field in southern Illinois the week of November 12. Several Cypress and Aux Vases outcrops were sampled and discussed. A comparison of deposition facies in outcrop and in the subsurface is under way.

PETROLEUM GEOCHEMISTRY

Lawrence Livermore National Laboratory
Livermore, Calif.

Contract Date: Oct. 1, 1987
Anticipated Completion: Sept. 30, 1991
Government Award: $200,000

Principal Investigator:
Alan K. Burnham

Project Manager:
Thomas B. Reid
Bartlesville Project Office

Reporting Period: Oct. 1–Dec. 31, 1990

Objectives

This project will demonstrate near-term techniques for calculating kerogen maturation, overpressures, and expulsion efficiencies that can be used by industry in integrated basin analysis. The Williston Basin will be used as an example case. Estimates of thermal histories for various parts of the Williston Basin will be generated using BasinMod software from Platte River Associates. These estimates will be used in the Lawrence Livermore National Laboratory (LLNL) code PMOD, along with kinetic parameters measured for the Bakken and other possible source rocks, to calculate characteristics of hydrocarbon generation, such as expelled oil and gas, residual extractable organic matter, overpressures, and the likelihood of fractures. These calculations will be compared against field measurements. In addition, the expulsion model will be used to understand production rates and yields from fractured source-rocks reservoirs. Attempts will be made to determine areas of previously unrecognized reservoir potential.

Summary of Technical Progress

Pyrolysis kinetics were measured for a sample of the Bakken shale, and a pseudo-one-dimensional overpressuring-expulsion model was added to PMOD.

Additional literature was reviewed to establish a relationship between overpressures and rock fracturing.

Pyrolysis kinetics for the Bakken shale were measured with the Pyromat II apparatus. Problems were encountered because of the high bitumen content of the Bakken, so efforts were required to develop and test an appropriate analysis procedure. Ultimately, it was decided that the most accurate global kinetic expression was a parallel reaction model with a frequency factor of 9.8×10^{13} s^{-1} and an activation energy distribution with 2, 3, 7.5, 40.2, 20.5, 16.2, 9.1, and 2% of the reaction associated with energies of 47, 50, 51, 52, 53, 54, 56, and 59 kcal/mol, respectively. This implies that the oil generation kinetics of the Bakken are very similar to other marine source rocks examined at LLNL. For example, the midpoint of hydrocarbon generation from the Bakken is only 1 to 2°C lower at both laboratory and geological heating rates than that from the La Luna source rock of the Maracaibo Basin.

The computer code PMOD has been developed at LLNL to calculate hydrocarbon generation and expulsion for a user-specified chemical reaction network. Prior to the start of this project, the expulsion model was only a simple excess volume expulsion model not involving a pore pressure calculation. On the other hand, the LLNL code PYROL (Ref. 1) calculated hydrocarbon gas- and liquid-phase volumes as overpressures as the result of hindered leakage of pore fluids, but the code was slow and difficult to modify for routine use. Therefore an overpressuring-expulsion model that could take advantage of other PMOD features was added to PMOD. The overpressuring-expulsion model is simpler than in PYROL in that only one hydrocarbon phase is assumed. This simplification substantially decreases the required computer time. However, PMOD includes algorithms for water density and water and hydrocarbon viscosities as a function of temperature and pressure and an improved relative permeability model. Rock fracture is assumed to occur at a specified fraction of overburden pressure. Permeability is assumed to become infinite when pore pressure reaches the specified pressure and drops instantaneously to the pore permeability when pore pressure drops below the specified pressure. This assumption is currently being compared with others in the literature, including how the fracturing couples to tectonic stress.

Reference

1. R. L. Braun and A. K. Burnham, *Energy & Fuels*, 4: 132-146 (1990).

GEODIAGNOSTICS FOR RESERVOIR HETEROGENEITIES AND PROCESS MAPPING

Sandia National Laboratories
Albuquerque, N. Mex.

Contract Date: Oct. 1, 1987
Anticipated Completion: Sept. 30, 1993
Funding for FY 1989: $300,000

Principal Investigator:
David A. Northrop

Project Manager:
Robert E. Lemmon
Bartlesville Project Office

Reporting Period: Oct. 1–Dec. 31, 1990

Objective

The objective of this project is to increase the producibility of existing oil resources by better definition of reservoir heterogeneities and monitoring of oil recovery processes through the application of advanced geodiagnostics systems. This project provides a geologic and reservoir engineering perspective for the integrated Electromagnetic Geophysical Method research and development (R&D) program being coordinated by the Department of Energy (DOE) at Sandia National Laboratories (SNL), Lawrence Livermore National Laboratory (LLNL), Lawrence Berkeley Laboratory (LBL), and University of California at Berkeley (UCB). FY91 tasks are to (1) develop and apply an oil recovery/resistivity simulator system, (2) apply reservoir characterization concepts to bulk resistivity and electrical/electromagnetic (E/EM) field data interpretation, (3) acquire and characterize an industry field site, and (4) field test reservoir characterization data collection.

Summary of Technical Progress

Develop Oil Recovery/Resistivity Simulator System

For an electrical resistivity structure obtained from field EM measurements to aid in increasing the productivity of an oil reservoir, the effect of the process on the electrical properties on the reservoir must be understood and characterized. This requires an oil recovery/resistivity simulator (ORRSim) system that includes a standard oil-field simulator (such as BOAST-II) and the petrophysics to calculate electrical resistivity. Such a system can be used to provide design and validation information for the EM measurement systems, to provide conditioning information for EM inversions, and to simulate oil recovery processes conditioned to the EM measurements (use the EM measurements as "input").

During the last quarter of FY90, the petrophysics to calculate electrical resistivity were incorporated into two companion simulators, TRACK and RESIST. To summarize, TRACK models multicomponent ideal tracer flow through a time-varying aqueous flow field defined by an oil-field simulator. TRACK thus gives the ability to examine important aspects of tracer flow, such as dispersion, multiple tracers, and injected tracer concentrations. This eliminates the need to purchase an oil-field simulator with these more complex capabilities and also reduces the number of expensive oil-field simulator runs required. RESIST takes temperature and saturation data from the oil-field simulator and concentration data from TRACK to calculate the electrical resistivity as a function of space and time in the reservoir.

During the first quarter of FY91, an oil-field simulator, DOE's BOAST, was obtained. BOAST is a complex, yet capable, simulator that will allow modeling of the Richmond Field Site tests and other simple enhanced oil recovery (EOR) processes. BOAST was ported from the VAX to the CRAY and successfully ran a test problem. Attempts to generate other test problems were delayed by the complexity of BOAST and will be reported in the next quarterly report.

For the facilitation of the application of these three programs to this project, much thought has been given to the transfer of data between programs and to the graphic display of the data. For the facilitation of the eventual transfer of this system to industry, a variety of computers must be supported at minimal cost with a minimal amount of modification to the oil-field simulator to generate the data. After a brief search, the package of tools from the National Center for Supercomputer Application (NCSA) at the University of Illinois was adopted.

NCSA includes tools for image visualization and manipulation, a standard file format (HDF) for both data and images, and data translation. These tools are free from NCSA and are available on a variety of mainframe computers, workstations, and personal computers. At this point, the HDF utilities are being implemented on the CRAY X-MP (UNICOS), and the visualization tools are running on an Apple Macintosh IIfx.

Figure 1 is a schematic of the OORSim system. The three major units are oil-field process simulation, electrical resistivity simulation, and visualization. The HDF extension indicates an HDF formatted file that can be transferred between computers easily. Note that this implementation is not fixed and is designed to be flexible to accommodate future needs.

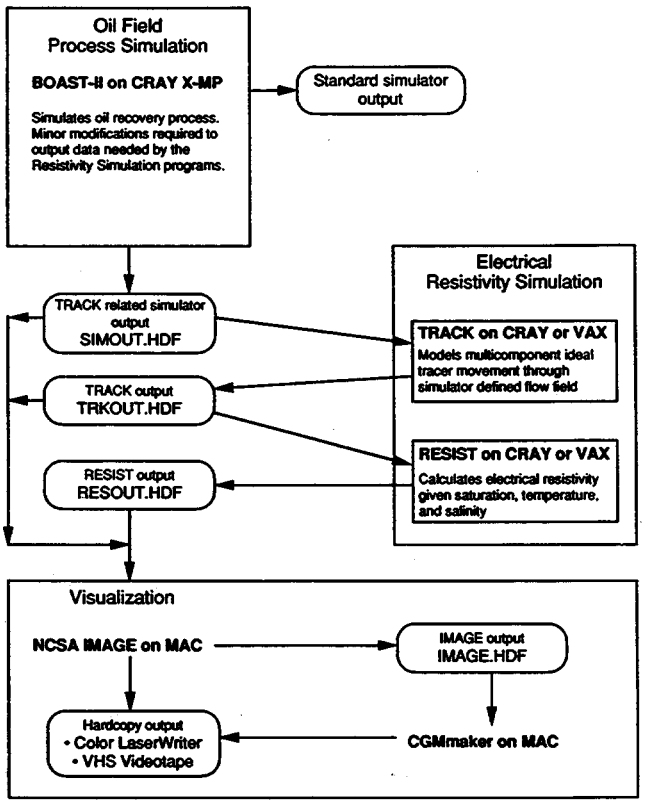

Fig. 1 Schematic diagram of the oil recovery/resistivity simulation (ORRSim) system.

Analysis of E/EM Field Data from an Oil Recovery Perspective

When an E/EM measurement uses transient or time-varying fields, the potential for dependency on frequency or on how the measurement technique samples the fields must be considered. For the investigation of these effects, conceptual experiments were investigated considering a one-dimensional medium with a change in resistivity from r to r' at z = b. At the origin (z = 0) there is a vertical current sheet (I). Two cases are considered for I, one where the magnitude of the current is sinusoidal (plane wave or PW case) and one where there is a step function change in I (θ case). At distance z = D (farther from the origin than the change in resistivity) there is an electric field meter (M). For the PW case, M records the amplitude of the electric field, and for the θ case, M records either the maximum electric field or the time of arrival of the maximum electric field.

The analytic solution for electric fields has been derived for both the PW and θ cases. An effective resistivity (r_{eff}) can be defined by equating the solutions for $r = r' = r_{eff}$ and $r \neq r'$. The meaning of r_{eff} is that, if the material on the left of z = D were replaced with a material with resistivity r_{eff}, M would report the same measurement. Thus, in some sense, r_{eff} is the average or bulk resistivity of the material between z = 0 and z = D. Figure 2 shows this r_{eff} assuming r = 1, r' = 0.5, and b = 5. Interpretations of Fig. 2 regarding how the different measurements sample the resistivity–heterogeneity and determine bulk resistivities, of course, apply to only the measurements reported here. However, the issues raised by these interpretations should give insight into whether the average or bulk resistivity determined by an experiment is a function of how the measurement technique samples the electric field.

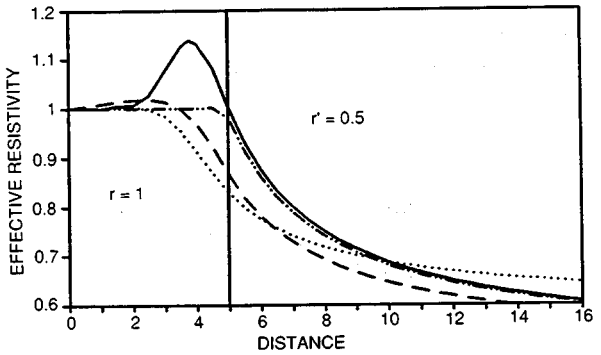

Fig. 2 Effective resistivity for plane wave (— —, w = 0.5; —· · —, w = 25) and Θ (· · · · ·, amplitude; ——, time) measurement cases.

Figure 2 shows four different curves. Two are for the θ experiment and are labeled amplitude (for the measurement of the maximum electric field) and time (for the measurement of the time of arrival of the maximum electric field). Two are for the PW experiment and are labeled w = 0.5 (angular frequency, 0.5) and w = 25 (angular frequency, 25). As a general philosophical point, r_{eff} is only an average property of the media if it is independent of the measurement technique. In surface electrical measurements (Wenner array, Schlumberger array, etc.), it is recognized that "apparent surface resistance" is a function of the array being used (each array configuration has its own type curves) and thus is not strictly a property of the media. Inversions of the apparent surface resistance are done to try to determine resistivities that are properties of the media only. Unfortunately, the nonuniqueness of the inversions obscures the question of whether the inversions are independent of the array used. For the conceptual experiments described here inversion is not required. The fact that the curves on Fig. 2 are different indicates that r_{eff} is not truly a bulk average property of the media.

The two PW curves show that measurements at different frequencies sample the media differently and thus give different r_{eff}'s, even though the resistivity of the material itself is not a function of frequency. The two θ curves show that different measurements of the same electrical excitation can give different r_{eff}'s. The deviations of r_{eff} from r = 1 when M is on the left of the material change (z = b = 5) show that the r_{eff} is influenced by material outside the region of measurement and that the wrong bulk resistivity can be reported because of heterogeneities outside the block of interest.

The previous discussion and the existence of multiple curves on Fig. 2 indicate that r_{eff} from these experiments cannot be plugged into Archie's law to determine average saturation disregarding the method of measurement. Somehow the functional dependence of r_{eff} on the measurement technique must be incorporated into the analysis before Archie's law can be used.

Oil Recovery Process Data Collection

The resistivity of the water in the reservoir must be known to interpret E/EM monitoring of an oil recovery process to determine oil saturation. When the fluid injected has a different salinity than the water originally in the formation, mixing occurs such that there is no sharp front between the injected and original fluid. The dispersivity that controls this mixing is difficult to measure and seldom known.

E/EM field tests of equipment and techniques will be conducted at the Richmond Field Site prior to application at an industry field site. A resistivity contrast is created at the Richmond Field Site by injecting saline water into an aquifer. An approach has been developed to determine the dispersivity of the aquifer by monitoring the recovery of the saline water. Figure 3 shows how the mixing zones affect the salinity of the produced fluid. To apply this approach for the determination of dispersion, the injection and recovery will be simulated with BOAST-II and TRACK with the known injected water salinity and injection and withdrawal rates. The dispersivity is determined by history matching the salinity during the recovery period.

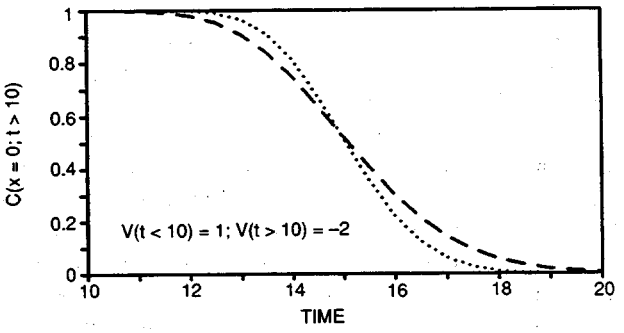

Fig. 3 Produced concentration vs. time. · · · · · · ·, D = 0.2. ——, D = 0.4.

THREE-PHASE RELATIVE PERMEABILITY

Cooperative Agreement DE-FC22-83FE60149, Project BE9

National Institute for Petroleum and Energy Research
Bartlesville, Okla.

Contract Date: Oct. 1, 1985
Anticipated Completion: Sept. 30, 1991
Funding for FY 1991: $300,000

Principal Investigator:
Dan Maloney

Project Manager:
Edith Allison
Bartlesville Project Office

Reporting Period: Oct. 1–Dec. 31, 1990

Objectives

The objectives of this project are to improve the reliability of laboratory measurements of three-phase relative permeability for steady- and unsteady-state conditions in core samples and to investigate the influence of rock, fluid, and rock–fluid properties on two- and three-phase relative permeabilities.

Summary of Technical Progress

Sample Selection and Petrographic Characterization

Routine permeability and porosity experiments were conducted on plug samples from several blocks of Berea sandstone to find a sample with gas permeability in the 100- to 300-mD range. A Berea sandstone block with a gas permeability of 270 mD and porosity of 19.6% was selected. Plugs and slabs of the Berea were cut from the block and were fired in an oven at 540°C for 24 h to stabilize clay minerals. The 540°C firing temperature was 460°C lower than that used for samples tested in FY88, 89, and 90 project years. The lower firing temperature was selected as a compromise between the need for stabilizing clay minerals and, at the same time, for preserving other rock properties. Firing at 1000°C often leaves sandstone plugs with a refractory brick-like quality and can shatter some of the sandstone grains if the temperature gradient changes abruptly during heating and cooling processes.

Samples of the fired rock were subjected to routine core analysis, X-ray-diffraction (XRD) analysis, thin-section microscopic evaluation, and mercury intrusion porosimetry. The permeability and porosity of a plug of the fired rock were 230 mD and 19.6%, respectively. XRD results indicate that the rock consists of 92% quartz, 5% feldspar, 1% dolomite, and 2% illite. Evaluations of thin sections of the rock showed that the sandstone grain and pore-size distributions by number percent for features greater in size than 10 μm are fairly well represented with lognormal distribution functions, as shown in Fig. 1. Note that the y-axis on the figure is a log scale, whereas the x-axis is a normal probability scale. Table 1 presents sizes corresponding to 84, 50, and 16 percentile values.

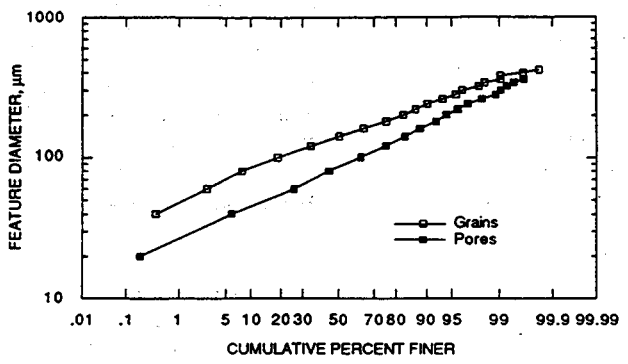

Fig. 1 Grain and pore diameter distributions from thin-section analyses, fired 230-mD Berea sandstone.

TABLE 1

Lognormal Distribution Function Characteristics for 230-mD Fired Berea Sandstone

	Size, μm			
Feature	d_{84}	d_{50}	d_{16}	σ*
Grains	205	139	93	1.485
Pores	143	84	51	1.674

*$\ln \sigma = 0.5 \ln(d_{84}/d_{16})$.

Mercury porosimetry results for the sandstone indicate that the median pore diameter by volume is 9.56 μm. Mercury intrusion results for the sample are shown in Fig. 2, which is a plot of log-specific differential intrusion volume vs. pore diameter. Figure 2 indicates that the sample contains a significant volume of pores of size less than 10 μm.

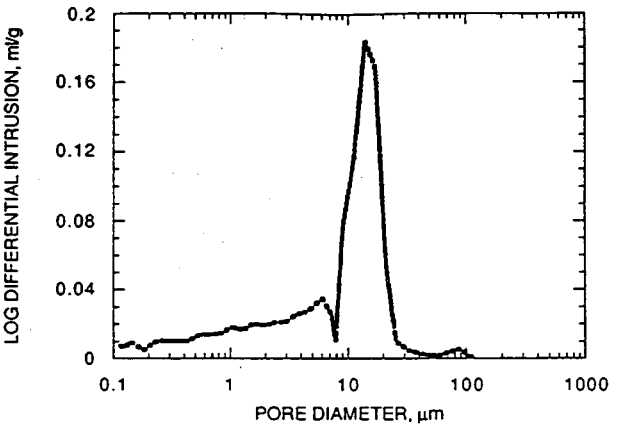

Fig. 2 Mercury intrusion porosimetry results, fired 230-mD Berea sandstone.

The porosity of the sample was 19.3% at ambient conditions, dropped to 18.7% at 2.85 MPa confining pressure, and stabilized at 18.3% when the confining pressure was increased to 21.5 MPa. The permeability of the brine-saturated sample was 261 mD. Oil and brine permeabilities were normalized with respect to the oil permeability of 116 mD when the brine saturation fraction was 0.303 at the residual brine saturation test condition. Steady-state relative permeability results are shown in Fig. 3. Little saturation-history-dependent hysteresis was seen in the data after the first drainage cycle.

Three unsteady-state oil–water relative permeability tests were conducted on a similar sample of fired Berea. The

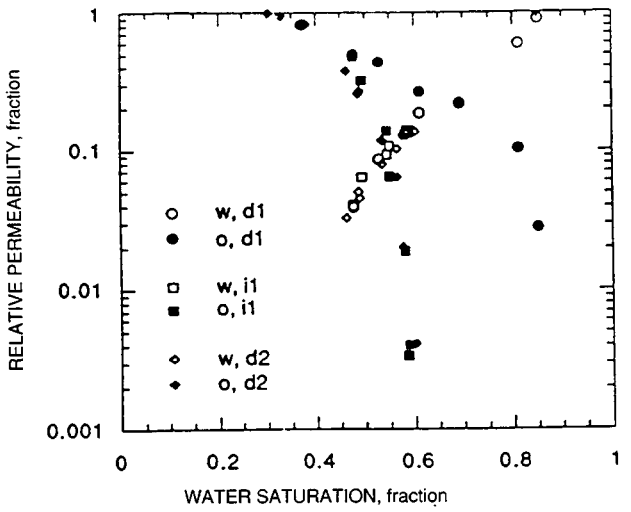

Fig. 3 Steady-state oil–water relative permeability results, Berea sandstone. Data normalized with respect to k_o = 116 mD at S_w = 0.303.

1.01-cP brine consisted of 2% NaCl by weight in deionized water. Mineral oil of 23.5 cP viscosity was used as the oil phase. The test was conducted with the core plug subjected to 2.85 MPa confining pressure. The porosity of the plug under ambient pressure conditions was 19.3% and dropped to 18.3% as the confining pressure was increased to 2.85 MPa. The brine permeability of the plug was 157 mD. After the brine permeability was measured, the sample was flooded with oil to the residual brine saturation test condition. Unsteady-state test measurements were recorded as the plug was subsequently flooded with brine (imbibition cycle for a water-wet rock). The Johnson–Bosler–Newman (JBN) method was used to calculate oil and brine permeabilities. Permeabilities were normalized with respect to the oil permeability of 110 mD at the 0.347 residual brine saturation test condition. Results for three imbibition cycles are shown in Fig. 4.

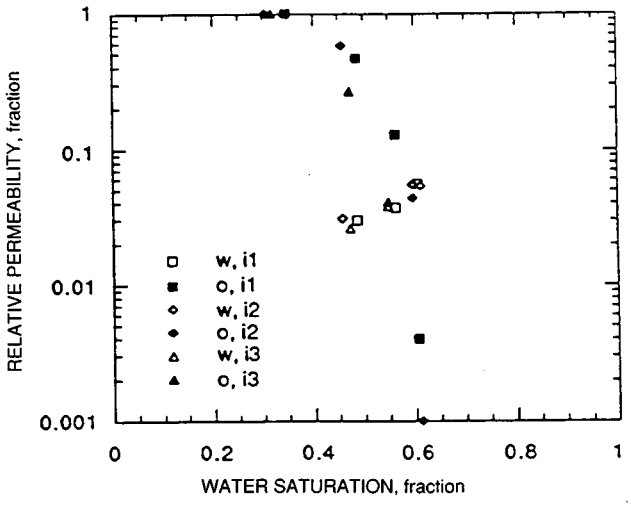

Fig. 4 Unsteady-state oil–water relative permeability results, fired Berea sandstone. Data normalized with respect to k_o = 110 mD at S_w = 0.347.

The relative permeability vs. saturation results for the three imbibition cycles followed the same trends. Hysteresis effects did not appear to be significant in the test results. The oil permeability values at residual water saturation conditions and the porosities of the two samples used for unsteady- and steady-state tests were very similar. The oil relative permeability curves from both unsteady- and steady-state tests are nearly identical, whereas the water relative permeability curve from the unsteady-state test is different from that of the steady-state test. Explanations for the discrepancy are under evaluation.

Equipment Repairs and Replacements

Two core-holder bodies were ordered during the reporting period: one of titanium and one of aluminum. The core-holder bodies are replacements for other core-holder bodies that were unsuitable for testing purposes because of length or material considerations. An experimental microwave absorption shield was constructed and is under evaluation.

IMAGING TECHNIQUES APPLIED TO THE STUDY OF FLUIDS IN POROUS MEDIA

Cooperative Agreement DE-FC22-83FE60149, Project BE12

National Institute for Petroleum and Energy Research
Bartlesville, Okla.

Contract Date: Oct. 1, 1987
Anticipated Completion: Sept. 30, 1991
Funding for FY 1991: $545,000

Principal Investigator:
Liviu Tomutsa

Project Manager:
Robert E. Lemmon
Bartlesville Project Office

Reporting Period: Oct. 1–Dec. 31, 1990

Objectives

The objectives of this research are to (1) develop a methodology to derive reservoir engineering parameters from petrographic, computerized tomography (CT) scanning and nuclear magnetic resonance (NMR) images; (2) apply state-of-the-art technology as it is developed to provide field support to characterize high-priority reservoirs; and (3) transfer the newly developed technology.

Summary of Technical Progress

The CT scanning technique and petrographic image analysis (PIA) have been used to support research in other projects (Task 1). Both private industry- and Department of Energy (DOE)-funded projects have used CT scanning for studies of core heterogeneity and for measurements of fluid distributions within cores. Core heterogeneity is defined by both the contrast of porosity and mineralogy in various regions of cores and the spatial distribution of porosity and micrology in various core regions. Computerized tomography offers rapid characterization of core heterogeneity, which allows selection of the most representative core samples for further petrophysical measurements.

During the previous fiscal year, encapsulation in CASTOLITE™ was successfully used to monitor saturation distributions at low pressure (<100 psi) and cores or slabs shorter than 6 in. The core or slab is placed within the geometry of the CT scanner with the direction of flow within the plane defined by the X-ray beam. The advantage of this approach is that, by performing scans of the dry and saturated core at a single position, the data needed to calculate the saturation distribution between the inlet and outlet ports are generated.

For higher pressure corefloods or for cores longer than 6 in., coreholders placed parallel to the axis of the scanner are needed. To obtain the saturation distributions between the inlet and outlet ports, many scans perpendicular to the core axis must be taken, all the scan data in a three-dimensional (3-D) array must be combined, and various planes parallel to the flow must be selected to reconstruct the image of saturation distribution along the core.

This approach requires (1) computer software and hardware to manipulate a large 3-D array for display in a short time, (2) a highly accurate and rapid mechanism for positioning the core in the gantry, and (3) rapid data transfer from the scanner to the computer that is doing the data manipulation.

A survey of the computer market and industrial CT applications showed that much of the software is available only on graphic workstations based on reduced instruction set chips (RISC) architecture. Such systems cost in the $30,000 to $100,000 range.

A workstation based on the Mac IIfx and a 19-in. color monitor and a 3-D reconstruction software package were purchased for considerably less than the system quoted above. This system allows viewing of any two-dimensional (2-D) object sections along planes parallel to XY, XZ, and YZ planes as well as rotation of the 3-D object around the x-, y-, and z-axes. Various color tables as well as a gray scale are available for the data display. Porosity, permeability, or saturations from CT applications or water and oil distributions at pore level from high-resolution NMRI applications can be readily displayed. This system has the advantage of compatibility with the National Institute for Petroleum and Energy Research (NIPER) network, which uses Macintosh computers for reports and presentations.

Conversion programs for the data files have been written, and both 2-D and 3-D reconstructions of CT and NMR images have been displayed. Figures 1 and 2 show some of the CT images; Fig. 3, the NMR images.

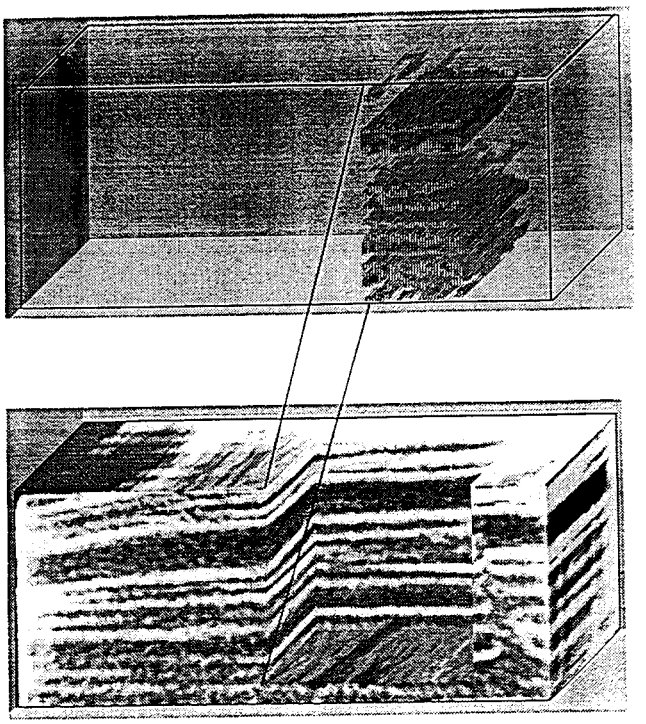

Fig. 1 Computerized tomography (CT) image of layered Shannon slab with higher porosity layers selected for enhanced viewing.

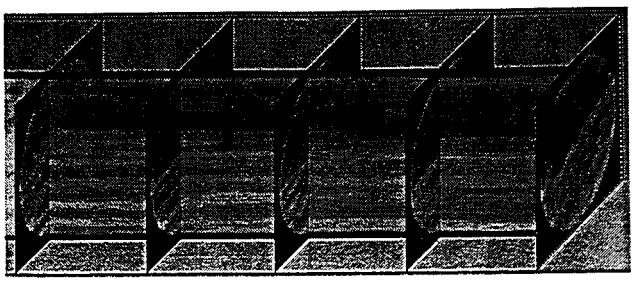

Fig. 2 Computerized tomography (CT) image of layered core.

Figure 1 shows the 3-D CT density distribution in the Shannon slab used previously for flooding experiments. The darker areas correspond to higher porosity regions. The 3-D data set was generated from 13 adjacent 2-D, 2-mm-thick slices taken in planes parallel to the largest area cross section. The cutout portion represents the higher porosity channels made visible and the remainder of the rock made transparent (background color). Figure 2 shows a 1½-in.-diameter, 6-in.-long heterogeneous Berea core placed in a magnesium alloy core holder. The 3-D array was con-

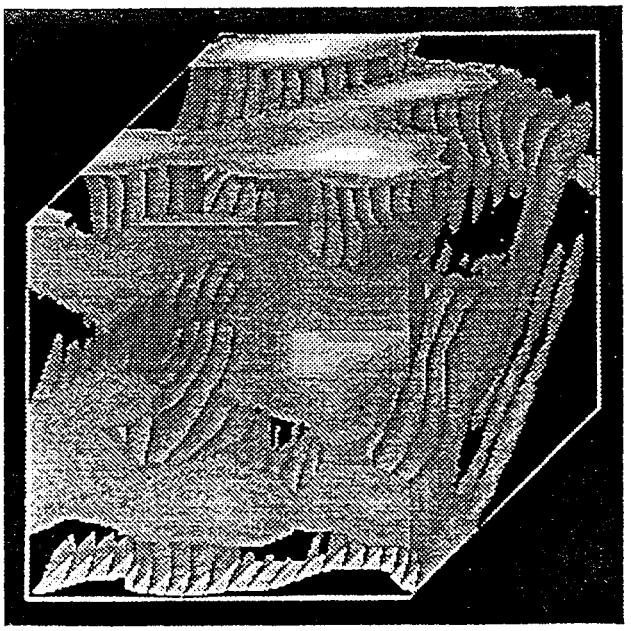

(a)

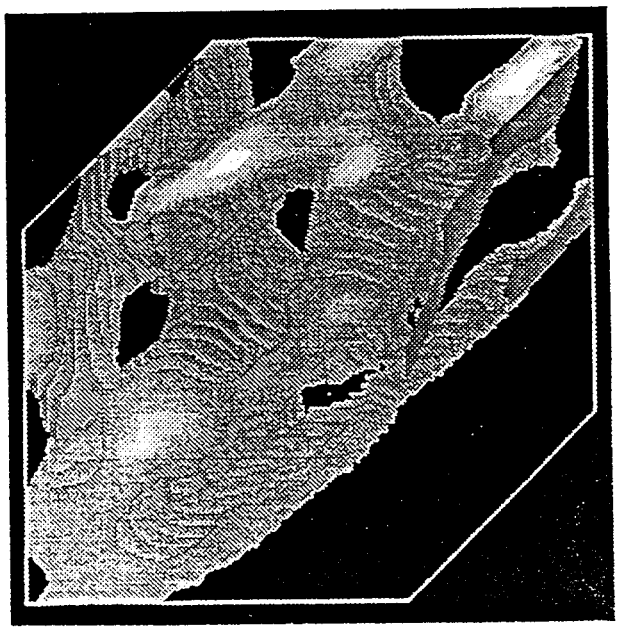

(b)

Fig. 3 Nuclear magnetic resonance imaging (NMRI) of the oil phase in a polymer beadpack showing an enlarged view of the fluid-filled pores. (a) View of the sample from the bottom. (b) View of same block rotated counterclockwise with the bottom of the beadpack to the right.

structed from 53 adjacent slices perpendicular to the axis of the core.

Various scans have to be prepared at precisely the same core locations to accurately calculate porosity and saturation distributions in a core. Because the present scanner table, even after carefully adjusting both the electronics and the mechanical systems, still has a 1- to 2-mm accuracy, the design of a new automated positioning system (to be controlled by the Mac IIfx workstation) has been initiated. This will be completed early in the following quarter.

Also early in the following quarter, a rapid data transfer system from the CT scanner to the workstation will be completed. For this purpose, a digital input/output (I/O) card and the appropriate software have been installed in the workstation and tested, and various possibilities of hardware interfacing with the CT scanner PDP 11/34 computer bus are under consideration.

Automation of core positioning, scanning, and image acquisition under the Mac IIfx workstation will greatly enhance the capability to monitor efficiency corefloods by reducing image processing time and by allowing multiple corefloods to be performed simultaneously.

Efforts this quarter toward improving NMRI resolution and data acquisition speed have been as follows.

Gradient coil designs were finalized for a gradient coil assembly that will produce imaging gradients approximately 8 times as strong as that previously attained. The X-, Y-, and Z-gradient coils are being wound on separate coil forms and then shaped and mounted in position on fiberglass forms. After each layer is completed and the separate coils connected in series, the coils are embedded in the fiberglass resin. This will create a strong and stable structure for the assembly. The gradient assembly is designed to fit over the standard NMR sample probes as well as the new sample probe described in the following paragraphs. The much stronger gradient fields produced by this coil system should permit the imaging of fluids in sandstones at resolutions below 20 μm. Construction was delayed by maintenance problems with the NMR spectrometer but should be completed in January.

Design specifications for a new multinuclear imaging probe were developed the past quarter. The radio-frequency (r-f) coils will be more efficient and generate the shorter 90° r-f pulses required for projection reconstruction NMRI at the higher gradients to be attained from the new gradient assembly described previously. The new design uses a horizontal sample orientation with solenoidal r-f coils rather than the current vertical saddle-coil arrangement found in the standard probes. Changing samples will require the probe assembly to be removed from the NMR magnet to gain access to the sample. However, because the imaging experiment for each sample will require several hours to complete, this process will not significantly extend the experiment time.

Data acquisition has been improved by the addition of a high-speed, two-channel analog-to-digital (A/D) board to the 386 computer. The A/D board can simultaneously sample the two phases of the quadrature NMRI signal at up to 1 MHz rate and store them in the computer memory, bypassing the data file transfer from the NMR spectrometer to the 386 for processing. The higher conversion rate of 1 MHz is 10 times as great as that of the built-in A/D converter in the NMR spectrometer. This will permit

digitizing the higher bandwidth signals resulting from the stronger gradients achieved with the new gradient system. Also, the direct data acquisition into the 386 computer will save considerable time for the large image files. The board came with a software package that permits the use of the computer as a two-channel storage oscilloscope. With this software, NMR signals from the spectrometer have been successfully digitized and written to disk. However, this software, although useful for testing, is not suitable for incorporation into user-written programs. A set of software drivers for operating the A/D board by incorporation into these programs was ordered and has been received. Software for translating the data file format to NMR standard data format has been written and tested.

The new workstation has been used to display the NMRI data set from the polymer beadpack. Previous image analysis software was restricted to a 2-D display of cross sections through the sample. This workstation permits the display of the 3-D structure of the fluid contained in the pore network of the sample. Software was written to reformat the NMRI data set to the format required for the workstation. Figure 3 shows this pore network structure for the polymer beadpack containing a two-phase oil and water system. The fluid used in Fig. 3 is the oil phase imaged by proton NMRI. The figure shows a cubical section of the total sample image near the top edge of the sample. The dimensions of the block are 1 mm per side. The polymer beads used to make the beadpack had diameters from 350 to 500 μm. The perspective of part a of Fig. 3 shows the sample from the bottom with the cylindrical edge of the beadpack as constrained by the wall of the sample tube shown to the bottom-right edge of the block. Part b of Fig. 3 shows the same block rotated counterclockwise 90° about the vertical axis with the bottom of the beadpack to the right. The shades of gray represent the polymer beads, whereas the fluid components of the sample have been rendered transparent to show the interior structure of the pore network. Fluids were injected into the beadpack from top to bottom with the water first followed by the oil. The pore structure defined by the beads should be generally isotropic.

The CDC Phoenix (100MB) disk drive for the NMR spectrometer is down for repairs. This is the second time the past year that this 7-yr-old drive has required maintenance. JEOL, the spectrometer manufacturer, no longer services this drive system, and newer versions of their NMR software will no longer support this drive system. JEOL, USA, offers an upgrade to a 250MB Winchester disk drive with a 2.3GB 8-mm tape cartridge backup system as a replacement for the disk drive system. This upgrade would provide much needed larger storage capacity and backup capability plus access to the newer software versions.

INFLOW PERFORMANCE RELATIONSHIPS FOR SLANTED AND HORIZONTAL WELLS PRODUCING FROM HETEROGENEOUS RESERVOIRS

Cooperative Agreement DE-FC22-83FE60149, Project SGP40

National Institute for Petroleum and Energy Research
Bartlesville, Okla.

Contract Date: July 1990
Anticipated Completion: June 1991
Funding for FY 1991: $46,500

Principal Investigator:
Aaron Cheng

Project Manager:
Thomas B. Reid
Bartlesville Project Office

Reporting Period: Oct. 1–Dec. 31, 1990

Objective

The objective of this project is to develop Vogel-type[1] inflow performance relationships (IPRs) for slanted and horizontal wells producing from heterogeneous reservoir systems under solution–gas drive. The main objectives are (1) to adapt the National Institute for Petroleum and Energy Research (NIPER) vertical–horizontal–slanted well reservoir simulator to an IBM PC/AT-type microcomputer and (2) to develop IPRs for slanted and horizontal wells producing from heterogeneous solution–gas drive reservoir systems. The NIPER reservoir simulator will be used to generate the IPR data. This project can be considered a continuation of the previously completed project, SGP27, Development of an Inflow Performance Relationship (IPR) for a Slanted/Horizontal Well Under Solution Gas Drive.[2] In the previous project, IPR data were generated for slanted and horizontal wells producing from homogeneous reservoir systems.

Summary of Technical Progress

Adaptation of NIPER's Vertical–Horizontal–Slanted Well Reservoir Simulator for an IBM PC/AT-Type Microcomputer

The dynamic redimensioning and restart features installed on the IBM PC/AT version of the vertical–horizontal–slanted well reservoir simulator were under further testing. The dynamic redimensioning was verified under working conditions and permits a maximum buffer size of 800 reservoir grid blocks. The restart feature was tested with simulation input data representing a waterflood

process in a two-dimensional homogeneous reservoir system with a horizontal injector and a vertical producer. With the use of the restart option for a 1-yr period followed by a second year using the restart data generated from the first, the result was a 0.006% elevation in the cumulative oil produced for the 2-yr period, over a run for a continuous 2-yr period without the restart option turned on. Restart after the third year in a 10-yr period created a 3.5% depression in the cumulative oil produced. The beginning time steps after restart were different, however, from those in the continuous run.

Selection of Reservoir Grid and Data for Generation of IPR Data for Heterogeneous Systems

An accurate study of the reservoir and well heterogeneities on the slanted–horizontal well IPR could not be made because the original $5 \times 5 \times 3$ grid was apparently not fine enough to appropriately incorporate these heterogeneities in a given reservoir system. Thus a much finer grid was needed to generate the IPR data of slanted and horizontal wells producing from heterogeneous systems.

After several trial runs, a $19 \times 3 \times 3$ grid was selected to study inflow performance of wells producing from heterogeneous reservoirs under solution–gas drive. However, the use of such a fine grid will significantly increase the computer central processing unit (CPU) time for executing the simulation runs. For example, a single 1000-d simulation run using the base-case data of Vogel[1] for a vertical well, with a minimum time step of 0.01 d, could take more than 24 h of turnaround time on NIPER's MicroVAX computer system. Because of the limited computing power for fine-grid simulation, a very selected number of runs will be made to study the inflow performance of slanted–horizontal wells producing from heterogeneous systems. The runs will focus on the inflow performance properties, such as oil and flow rate, gas/oil ratio (GOR), and reservoir pressure.

The grid block sizes in the x-direction of the $19 \times 3 \times 3$ grid were increased outward with a constant geometric factor from the center blocks containing the wellbore. The horizontal well was located in the center blocks and was oriented in the y-direction of the grid. This arrangement will retain more accuracy for flow computations in near-wellbore grid blocks, where rapid pressure and saturation take place, and minimize the number of grid blocks and thus computer storage and execution time.

For 20-acre well spacing as used in the base-case data of Vogel,[1] the $19 \times 3 \times 3$ grid had the following grid dimensions: constant geometric constant, 1.32; Δx_{10} (center block with wellbore), 10 ft; Δy_{1-3}, 311.13 ft; and Δz_{1-3}, 7.83 ft.

Generation of IPR Data for Base Case

With the use of the $19 \times 3 \times 3$ grid, inflow performance runs were obtained with the base-case data of Vogel[1] for a horizontal well located in the middle of the grid and draining from the middle of the pay zone. Figure 1 shows the IPR curves for a horizontal well at cumulative oil production $N_p/N = 0.1$, 4, and 8%. Figures 2 to 4 show the change of average reservoir pressure, oil flow rate, and GOR with cumulative oil production under two flowing

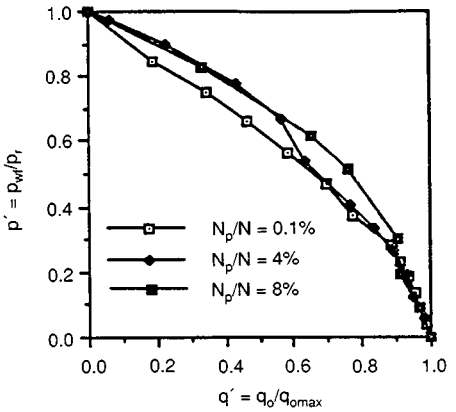

Fig. 1 Inflow performance relationship (IPR) for a horizontal well with the use of a $19 \times 3 \times 3$ grid.

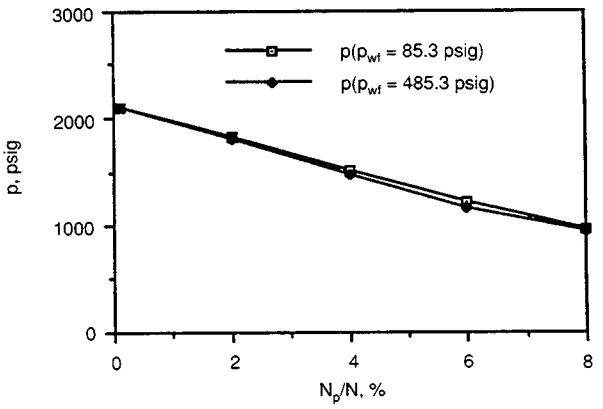

Fig. 2 Average reservoir pressure (p) vs. cumulative oil production (N_p/N) for a horizontal well.

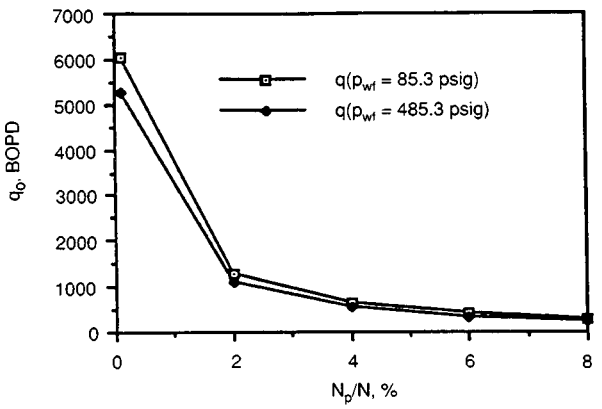

Fig. 3 Oil rate (q_o) vs. cumulative oil production (N_p/N) for a horizontal well.

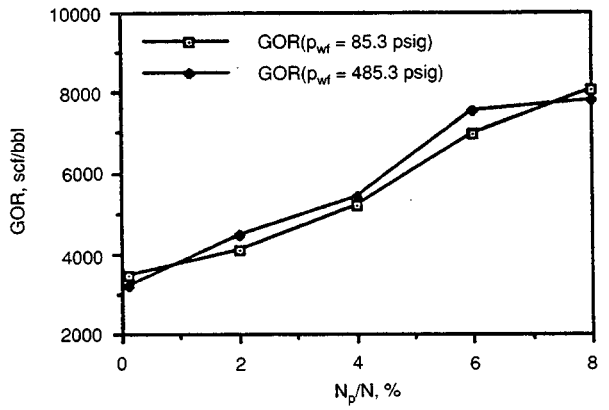

Fig. 4 Gas/oil ratio (GOR) vs. cumulative oil production (N_p/N) for a horizontal well.

bottomhole pressures p_{wf} of 85.3 and 485.3 psig, respectively. On the basis of these figures, the following was observed. As N_p/N increases, the IPR curve of a producing horizontal well shifts to the right and has more concavity or curvature (Fig. 1). The increase in curvature is probably caused by the increase of GOR as N_p/N increases (Fig. 4). The reservoir pressure depletion is independent of the flowing bottomhole pressure and is affected by the amount of oil depleted, N_p/N (Fig. 2). This would have been expected from the concept of oil material balance. Oil production rate of a horizontal well drops drastically to less than 20% of its initial rate after only 2% of the oil in place is depleted (Fig. 3). However, the oil rate will then decline at a very low rate. Figure 3 also shows that after 4% oil depletion the oil production rates for p_{wf} = 85.3 and 485.3 psig are almost identical. This implies that a lower wellbore pressure drawdown can attain the same oil flow rates as those obtained from a higher pressure drawdown.

References

1. J. V. Vogel, Inflow Performance Relationships for Solution Gas Drive Wells, *J. Pet. Technol.*, 83-93 (January 1968).
2. A. M. Cheng, *Development of an Inflow Performance Relationship (IPR) for a Slanted/Horizontal Well*, DOE Report NIPER-458, March 1990.

DEVELOPMENT OF METHODS FOR MAPPING DISTRIBUTION OF CLAYS IN PETROLEUM RESERVOIRS

Cooperative Agreement DE-FC22-83FE60149, Project SGP42

National Institute for Petroleum and Energy Research
Bartlesville, Okla.

Contract Date: July 1990
Anticipated Completion: January 1992
Funding for FY 1991: $210,000

Principal Investigator:
Bijon Sharma

Project Manager:
Edith Allison
Bartlesville Project Office

Reporting Period: Oct. 1–Dec. 31, 1990

Objective

The objective of this project is to develop techniques for mapping the types and volumes of clays in clastic reservoirs from signature analysis of log responses in clayey formations. The scope of work in this project includes identification of a few clastic reservoirs where oil production has been affected by the presence of different types and volumes of clays and mathematical processing of wireline logs from the clayey formations to identify certain mathematical properties that may be correlated with the clay characteristics. The characteristics of clays under investigation are evaluated from detailed thin-section petrography, computerized tomography (CT) scans, and geological investigations.

Summary of Technical Progress

For mathematical signature analysis of log responses in clayey formations, detailed scanning electron microscopy (SEM), energy dispersive spectroscopy (EDS), and thin-section petrographic studies were completed on core samples from the Louisiana well C Daigle No. 1. For improved accuracy and ease of handling different types of log data, the computer programs for spectral power estimates were rewritten in FORTRAN. For a more rigorous interpretation of clay characteristics, any trend present in the digitized log data should be removed before computations of the mathematical properties, therefore a subroutine was added to the main program for estimating and removing any trend that may be present in the log data that is not relevant to interpretation of clay signatures.

Petrographic Studies of Well C Daigle No. 1

Scanning electron microscope images and EDS analysis were performed on three samples from the well to augment petrographic information already available from the Louisiana well C Daigle No. 1. The samples were taken

from the producing sandstones in C Daigle No. 1 from both the comparatively cleaner upper part of the sandstone and from the much dirtier, lower part of the sandstone with much poorer reservoir quality.

A summary of the results of petrographic studies follows. The sample from the comparatively cleaner upper part of sandstone indicates that chlorite and kaolinite are the dominant clays, with chlorite slightly more abundant than kaolinite; the clays have a diagenetic origin and have been precipitated throughout the pore system; and chlorite occurs as pore lining clay, and kaolinite occurs as pore filling clay. The two samples from the much dirtier bottom part of the sandstone indicate that the sandstone is very fine grained and poorly sorted and has a much greater amount of detrital clays and that clays are mostly illite and mixed-layer illite/smectite. Earlier petrographic studies suggest this zone to be intensely bioturbated with an abundance of micropores.

Mathematical Model for Analysis of Log Signature

The estimation of spectral density as a function of frequency (cycles per foot) for different logs from clayey formations was previously discussed.[1] The computer codes were rewritten in FORTRAN to improve the accuracy of time series analysis and to obtain greater flexibility in mathematical processing. For more rigorous calculations, the presence of a linear trend in sonic transits time must be removed so that the time series is truly stationary and the mathematics of stochastic data analysis techniques can be applied to the data. This was achieved by adding a trend removal program in a subroutine that was called from the main program.

Figure 1 shows the power spectral density estimates of digitized sonic log data of the total Muddy sandstones from wells 26-4, P1, P2, and W-16 from Bell Creek (Montana) field. Prior petrographic analysis indicates that the sandstones in these wells contain various amounts and types of clays.[2] The clays are mostly diagenetic in origin and are predominantly kaolinites. The nonbarrier upper part of Muddy sandstones has some smectite, and the main barrier sandstones also have some illites and mixed-layer clays.

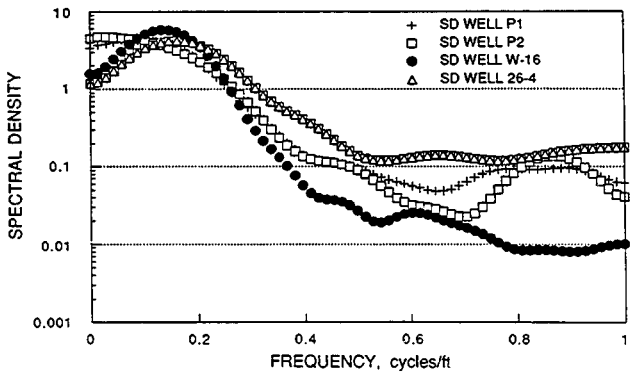

Fig. 1 Spectral density estimates of wells P1, P2, W-16, and 26-4 from Bell Creek (Montana) field.

The distribution of average porosity, geometric mean of air permeability, and clay content from four wells in the producing Muddy sandstone are shown in Table 1. The porosity and permeability values are from core measurements, and the clay content values were obtained from combined interpretation or sonic and density logs. Certain caution is required when comparing the clay values, which are averages for the entire Muddy sandstone. Within the Muddy, for example, the clay content may range from as low as 0% in the main barrier sandstone to as high as 100% in the lagoonal sandstones.[2]

TABLE 1

Distribution of Average Reservoir Properties of Muddy Sandstone from Four Wells in Bell Creek (Montana) Field

Well No.	Average porosity, %	Geometric mean of air permeability, mD	Average clay content, %	Slope of straight line through transit times*
26-4	27.2	1234	7.6	–0.207
P1	27.1	781	23.1	–0.072
P2	27.7	1538	18.3	–0.074
W-16	23.6	256	35.0	–0.025

*An indicator of formation compaction. Larger negative values are indicative of less compaction with depth.

As indicated in Table 1, well 26-4 is the cleanest of all the sandstones in the four wells. Except for a thin clayey upper zone (which has depressed the geometric mean permeability in this well), the remaining sandstone has uniformly high permeability. The sandstones from P1 and P2 have more clays than those from well 26-4. Of the four wells, well W-16 has the most clay with thick diagenetically altered and cemented layers that have practically 0% porosity and very little permeability.

The most striking feature of spectral density estimates of the total "Muddy" sandstone in the four wells (Fig. 1) is the variation in distribution of power for higher frequencies in wells that have been affected by clays. The degree of attenuation of spectral density is related to the presence of clay bands, which have contributed to higher frequencies. On closer examination of the curves, it is also apparent that other reservoir parameters (thickness of nonbarrier sandstones, for example) probably have also affected these curves. The nature of this attenuation is being investigated as this may lead to the development of a totally objective and computerized method of estimating the volume and possibly the type of clay in the reservoir.

Another noticeable feature of the spectral density curves in Fig. 1 is the presence of a "knee" in all wells that have appreciable amounts of clays. This knee occurs at around 0.35 to 0.45 cycles/ft in wells W-16, P1, and P2.

The spectral density plots for the Louisiana well C Daigle No. 1 (Fig. 2) show sharp attenuation of higher frequencies in the more clayey lower part of the producing sandstone (zones B, C, and D) compared with the relatively cleaner upper part of the sandstone (zone A). The actual cause for attenuation of this power in the clayey part of the sandstone is being investigated. Both curves have distinct knees. The clays in the upper part (zone A) are mostly chlorite and kaolinite and are of authigenic origin. In the dirty lower part (zones B, C, and D), clays are mostly illite and mixed-layer illite/smectite, and these are mostly of detrital origin.

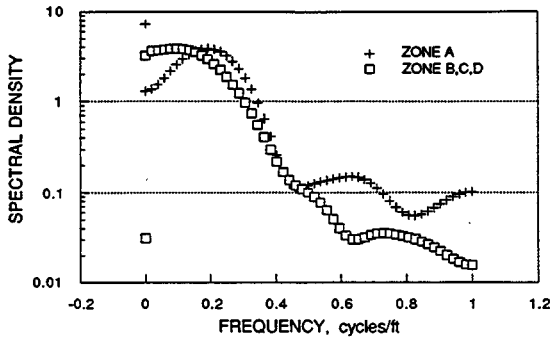

Fig. 2 Spectral density estimates of two zones from Louisiana well C Daigle No. 1.

Cross-Spectral Estimates

The power distribution with frequency in a single time series has been discussed. The mathematics of cross-spectral estimates[3] may be applied to two individual time series to find the relative change with frequency in the cross amplitude and phase spectra between two time series. The digitized sonic log data from pairs of wells have been studied to determine the cross correlation between the two time series in the frequency domain (cross spectra).

The following two parameters are first estimated from the two time series (digitized log data) under investigation:[3]

The co-spectral estimate, $\overline{L}_{12}(i)$, is given by

$$\overline{L}_{12}(i) = 2\left\{ l_{12}(0) + 2\sum_{k=1}^{L-1} l_{12}(k)\, w(k) \cos\frac{\pi i k}{F} \right\} \qquad o \le i \le F$$

The quadrature spectral estimate, $\overline{Q}_{12}(i)$, is given by

$$\overline{Q}_{12}(i) = 4\sum_{K=1}^{L-1} q_{12}(k)\, w(k) \sin\frac{\pi i k}{F} \qquad 1 \le i \le F-1$$

$$\overline{Q}_{12}(0) = \overline{Q}_{12}(F) = 0$$

where i = frequency for calculation of cross spectra

L = total number of covariance lags in estimating cross-covariance function

w(k) = smoothing window as a function of lag k

$l_{12}(k)$ = even cross-covariance estimate as a function of lag k

$q_{12}(u)$ = odd cross-covariance estimate as a function of lag k

F = 2 to 3 times L

The smoothed spectral estimates are computed at frequencies 0, 1/2F, . . . 1/2Δ, where Δ is the sampling interval. The following three different estimates have been made from the cross spectra.

I. Cross amplitude spectra, $\overline{A}_{12}(i)$, given by

$$\overline{A}_{12}(i) = \left(L_{12}^2(i) + Q_{12}^2(i)\right)^{1/2} \qquad o \le i \le F$$

II. The phase spectral estimate, $\overline{F}_{12}(i)$, given by

$$\overline{F}_{12}(i) = \text{Arctan}\left(-\frac{\overline{Q}_{12}(i)}{\overline{L}_{12}(i)}\right) \qquad o \le i \le F$$

III. The smoothed coherency spectra, $\overline{k_{12}^2}(i)$, given by

$$\overline{k_{12}^2}(i) = \frac{\overline{A_{12}^2(i)}}{\overline{C}_{11}(i)\,\overline{C}_{22}(i)}$$

where $\overline{C}_{11}(i)$ is the smoothed spectral estimate of series 1 and $\overline{C}_{22}(i)$ is the smoothed spectral estimate of series 2.

A computer program that first removes any trend present in the digitized sonic log data by calling a subroutine was written in FORTRAN. From the trend-corrected digitized data, autocovariances and cross covariances and autocorrelations and cross correlations are estimated. Then spectral estimates of individual series and the cross-spectral estimates of the two series are made.

The coherence estimates of wells P1 and P2 (Fig. 3) show that, until a frequency of 0.7 cycle/ft is reached, the

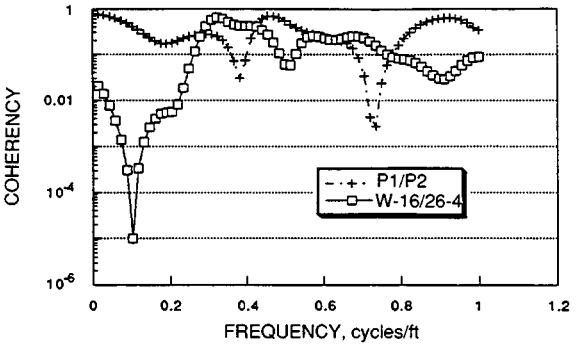

Fig. 3 Coherency spectra of wells P1, P2, W-16, and 26-4.

coherency is high, but then it drops sharply for higher frequencies. The coherency for wells W-16 and 26-4 is very low until a frequency of 0.3 cycle/ft is reached, then it shows sharp increase. The amplitude cross spectra (Fig. 4) show almost a gradual decrease of amplitude with frequency for wells P1 and P2, but for wells W-16 and 26-4, low values are obtained at lower frequencies. As expected, the phase cross spectra for relatively clean sandstones in wells P1 and P2 have small values compared with those for wells W-16 and 26-4. The effects on coherency, amplitude, and phase as a result of lithology and possibly other geological factors are being studied.

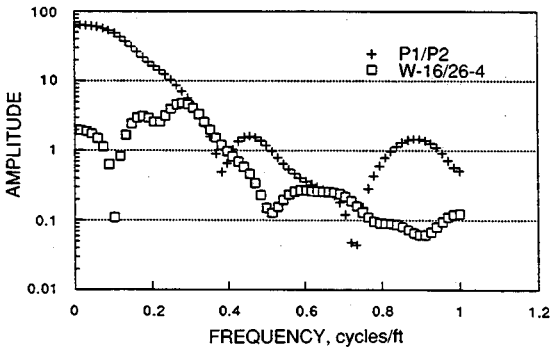

Fig. 4 Amplitude spectra of wells P1, P2, W-16, and 26-4.

References

1. National Institute for Petroleum and Energy Research, *Quarterly Technical Report for July 1–September 30, 1990,* Vol. II, Energy Production Research, DOE Report NIPER-501, pp. 92-100, October 1990.
2. B. Sharma, M. M. Honarpour, M. J. Szpakiewicz, and R. A. Schatzinger, Critical Heterogeneities in a Barrier Island Deposit and Their Influence on Various Recovery Processes, *SPE Formation Evaluation,* 5(1) (March 1990).
3. G. Jenkins and D. Watts, *Spectral Analysis and Its Applications,* Holden-Day, Inc., Oakland, Calif., 1968.

IDENTIFICATION OF CROSS-FORMATIONAL FLOW IN MULTIRESERVOIR SYSTEMS USING ISOTOPIC TECHNIQUES (PHASE I)

Cooperative Agreement DE-FC22-83FE60149, Project SGP43

National Institute for Petroleum and Energy Research
Bartlesville, Okla.

Contract Date: August 1990
Anticipated Completion: March 1991
Funding for FY 1990: $42,500

Principal Investigator:
Michael Szpakiewicz

Project Manager:
Robert E. Lemmon
Bartlesville Project Office

Reporting Period: Oct. 1–Dec. 31, 1990

Objective

The objective of this project is to substantiate fluid migration patterns into, within, and out of a reservoir by adapting natural isotopic geochemical techniques to the requirements of quantitative hydrodynamic reservoir modeling.

Summary of Technical Progress

The project was initiated in mid-August 1990. The study has been designed to add quantitative, and sometimes unique, solutions to the problem of undesirable hydraulic intercommunication conventionally detected by analysis of anomalous well production and costly pressure buildup tests, interference tests, and tracer tests. The emphasis this quarter has been on review of (1) further evidence of dynamic conditions and cross flow in multireservoir systems, (2) successful field applications of geochemical stable isotopic techniques to identify cross-formational flow, and (3) preselection of candidate hydrocarbon (HC) reservoirs for isotopic study.

For the substantiation of a need for adapting geochemical methods for identification of cross-formational flow in HC reservoirs, several reported field cases were reviewed to demonstrate commonality of such phenomena in the subsurface. Interreservoir migration and mingling of formation fluids in the area of discontinuity or breakage were normally caused by erosional channel cuttings, deep fluid discharge through open faults, or a rupture of the confining layer caused by a buildup of formation pressure in hydrodynamically closed systems.

Numerous applications of isotopic technique in hydrogeology and those recently reported in the petroleum literature indicate that the relative isotopic differences between fluid samples can be used to identify cross-formational flow in larger scales. Decameter and hectometer scales are best applied in the interwell (horizontally) and interreservoir (vertically) areas. Hectometer and kilometer scales are best applied to fieldwide and interfield interpretations.

Recently reported applications of carbon-13 isotopic composition of wet gas components (mostly propane, isobutane, and *n*-butane) by Exxon Production Research Company, Esso Resources Canada, Exxon Company USA, Esso Norge a.s. Statoil, and Norsk Hydro for correlation of reservoir gases in their North American (Canada and United States) and Norwegian (North Sea) fields,[1] as well as the isotopic study performed by Chevron, Amoco, and other majors, indicate strong interest in the emerging geochemical techniques. In most reviewed cases, however, the emphasis is on the genetic aspects of reservoir fluids and their source rock–reservoir correlation rather than on the identification of current active flow paths in the interconnected systems by correlating one reservoir gas with another.

Further Evidence of Hydrodynamic Conditions and Cross Flow as the Rationale for the Project

The reviewed cases of cross-formational fluid migration highlight the importance of fluid leakage for hydrodynamic characterization of reservoirs. Hydrocarbon leakage through ruptured overburden clearly indicates a necessity of quantification at the advanced stages of reservoir development. In some cases, the actual vertical distribution of hydrocarbons has been explained by their migration through ruptures in confining layers toward carrier horizons of lower pressure potential. If the generative potential of a source rock vastly exceeds the storage capacity of the traps in the area, as in the Haltenbanken provinces of the North Sea,[2] the generated liquids and gases must break toward carrier horizons of lower pressure potential or even to the surface. The constant flow keeps conduits open or rupture will reoccur in geochemically healed areas if thermodynamic conditions in the system favor mineral-scale precipitation.

Natural gas has great tendency to migrate vertically because it has a lower specific gravity than oil and water. The migration will generally result in a spatial separation of oil and gas.

Seismic sections, such as those running across Gullfaks field, North Sea,[3] reveal strong faulting of the pre-Cretaceous formations and seismic evidence for gas escape structures in the Tertiary–Quaternary system. Disturbed reflectors overflying Gullfaks field were observed on the seismogram, which indicated a mechanism such as natural hydrofracturing for gas escape. This may explain why the fields shallower than Brent field do not have a gas cap. Seismic reflection profiles across mud or shale diapirs in petroliferous areas have been demonstrated by Hedberg.[4] Some fluid escape forms in the Gulf of Mexico area may extend vertically for thousands of feet and later for tens of thousands of feet (compare Figs. 6, 7, 8, 10, 11, and 12 in Hedberg[4]). An actual dynamic flow, however, cannot be demonstrated by a seismic tool. A spatial homogenization of isotopic composition of methane molecules in a vertical profile would indicate active flow through randomly distributed leakage spots, such as gas escape structures (mud diapirs). A linear homogenization in the vicinity of distinctive linear features would indicate a gas leakage through conductive faults.

Selected Applications of Isotopic Technique for Solving Problem of Fluid Leakage Between Horizons

A recent study in Germany concerning the distribution of stable isotopes and trace elements helped enormously to improve a previous hypothesis on the origin and hydraulic connections between different groups of oils in the German Molasse sediments. Triassic oils are isotopically lighter than those in the Jurassic and Tertiary sediments. All the oil groups are clearly separated because of their distinct stable carbon isotope composition.

Prosolov et al.[5] provided stable isotope data for about 40 gas fields of West Siberia, including such supergiants as the Urengoy and Yamburg gas fields. They documented two isotopically distinctive groups of natural gases, those in the Upper Cretaceous and those in the Lower Cretaceous, which appear to have formed in two separate gas kitchens. These groups are not in vertical hydrodynamic contact because the carbon of the methane of the Upper Cretaceous Cenomanian gas is isotopically light: the average value of $\delta^{13}C$ is $-47.2 \pm 5.9‰$. Most pools have values between –45 and –50‰. The methane of the Lower Cretaceous Neocomian gas is heavier at $-39.7 \pm 4.6‰$ cm^3.

Distribution of isotopic ratios of carbon in gases from the Lower and Upper Cretaceous reservoirs indicates horizontal hydraulic communication between some of the reservoirs. For example, the Upper Cretaceous horizons of the Urengoy, Zapolyar, Medvezh, and Sever (North) Urengoy are characterized by similar isotopic composition ($\delta^{13}C = -47.5$ to $-50‰$) and seem to be horizontally in hydraulic contact. The gas in the adjacent Urengoy field is significantly lighter, which indicates impairment of horizontal hydraulic communication with other gas reservoirs in the region.

Another example of successful practical application of the environmental isotopic techniques to identification of cross-formational flow has been provided by Coleman et al.[6] The underground storage of pipeline gas was attempted in the Middle Ordovician St. Peter formation in three storage areas at depths of about 2000 ft. The integrity of the confining layer had been in question, and the system was sampled for chemical and isotopic analysis (Table 1). Isotopically light biogenic methane ($\delta^{13}C = -64$ to $-90‰$) has been naturally generated near the surface in glacial drift deposits in the area, and the gas commonly appeared in the shallow aquifers tapped by numerous water wells. The injected pipeline gas had $\delta^{13}C$ values in the range of –40 to –46‰. A distribution of isotopic composition of methane in samples collected from the aquifers and from gas storage

TABLE 1

Chemical and Isotopic Composition of Pipeline Gas Injected into St. Peter, Galesville, and Mt. Simon Sandstones in Illinois and the Composition of Methane from Shallow Aquifers*

Sample number	Type of well	Depth, ft	Material	CH_4, %	C_2H_6, %	C_3H_8, %	C_4H_{10}, %	$\Sigma C_{n>4}$, %	δC^{13}, ‰
Crescent City Reservoir Area									
21-75	Water	225	Silurian ls	100	nd†	nd	nd	nd	–75.2
22-75	Water	193	Silurian ls	100	nd	nd	nd	nd	–75.8
20-74	Gas	1399	St. Peter SS	94.7	2.6	0.4	0.1	2.2	–46.1
Manlove Reservoir Area									
2-75	Water	162	Glacial drift	100	nd	nd	nd	nd	–77.9
12-76	Water	284	Glacial drift	100	nd	nd	nd	nd	–76.0
96-75	Water	286	Glacial drift	100	nd	nd	nd	nd	–55.4
5-75	Water	205	Glacial drift	100	nd	nd	nd	nd	–41.1
28-75	Gas	1554	St. Peter SS	94.9	3.9	0.9	0.3	nd	–40.9
10-76	Gas	‡	Mt. Simon SS	95.1	2.2	0.4	0.2	2.1	–44.8
11-76	Gas	4142	Mt. Simon SS	94.1	2.9	0.5	0.2	2.3	–41.1
Herscher Reservoir Area									
19-76	Water	112	Ft. Atkinson (Divine) LS	99.2	0.7	0.1	nd	nd	–60.1
18-76	Gas	705	St. Peter SS	94.4	2.9	0.5	0.2	2.1	–40.7
17-76	Gas	905	Prairie du Chien Group	95.2	2.6	0.4	0.1	1.7	–41.6
16-76	Gas	1774	Galesville SS	93.2	2.5	0.4	0.1	3.8	–42.8
15-76	Gas	2568	Mt. Simon SS	94.2	2.8	0.5	0.2	2.3	–41.8
14-76	Gas	2665	Mt. Simon SS	92.8	3.3	0.5	0.2	3.2	–42.2
13-76	Gas	§	Galena (Trenton) Group	94.1	3.0	0.5	0.2	2.2	–41.9

*Chemical composition is not necessarily diagnostic in distinguishing between gases from different sources, whereas the isotopic composition clearly identifies the pipeline and biogenic gases as well as their mixtures as the result of leakage (after Colemen et al. 1977).[6]

†Not detectable (that is, <.05%).

‡This sample was from a pipeline feeding injection gas to several wells.

§This sample was from a collection line servicing several wells in the Galena (Trenton) Group.

reservoirs in the three underground storage locations clearly indicates (1) no cross-formational gas leakage in the first area; (2) the obvious leakage of the stored gas upward to the shallow aquifer in the second area, with the highest concentration of leaking gas located directly over the injection area; and (3) a partial leakage, estimated for 15 to 65% of the injected gas in the aquifer gas in the third area.

The isotopic data cast new light on the safety and economics of the project, and the storage of natural gas in the St. Peter formation was discontinued. The gas was withdrawn from units overlying the Galesville Sandstone and was safely reinjected to the deeper and nonleaking Mt. Simon formation.

On the basis of the chemical data alone (Table 1), it would normally be concluded that the gas in the water wells is of bacteriogenic origin and is unrelated to the storage reservoir because the heavier hydrocarbons were obviously removed as the gas migrated upward from the St. Peter Sandstone to the surface.[6]

The isotopic analyses of natural gases in Po Basin, Northern Italy, provided evidence for hydraulic isolation and a different source of gas in three gas fields located less than 4 miles apart.[7] Collecchiano field produces isotopically light bacterial gas ($\delta^{13}C$ = –76.3‰) from a depth of 560 ft, whereas a dry thermogenic gas is being produced in Vigatto field ($\delta^{13}C$ = –42.3‰) from a depth of 1942 ft and in Medesano field ($\delta^{13}C$ = –44.1‰) from a depth of only 460 ft. Chemically, the Medesano gas resembles almost exactly the shallow gas from the adjacent Collecchiano field, and a bacterial origin for both gases is clearly assumed. The authors[7] relate the vertical migration of thermogenic Medesano gas from a greater depth to strong faulting in the area close to the Apennine overthrust frontier. The tectonic related migration paths must remain open for active flow to keep the shallow gas isotopically heavy.

Quantitative hydrodynamic reservoir modeling based on geochemical/isotopic and other evidence of fluid migration in a system require, however, more systematic methodological study. Such a methodological study, involving interdisciplinary effort and based on specific field results, is being planned as Phase II of this project, in addition to a

field demonstration of the method in a selected oil–gas reservoir.

Preselection of Candidate Reservoirs for Field Demonstration of the Isotopic Method in Phase II

Field application of the stable isotope techniques for solving specific reservoir problems in the decameter and hectometer scales is being considered for Patrick Draw, Big Muddy, and Elk Basin oil and gas fields in Wyoming. Study of fluid intercommunication in hectometer and kilometer scales also is considered for major oil-bearing horizons in the Powder River Basin, namely, the Fall River-Lakota, Muddy, Frontier, Shannon, Sussex, and Teapot formations. Tectonic discontinuities and large breccia pipes may provide conduits for extensive fluid exchange between these productive horizons in the Powder River Basin.

A possibility of horizontal compartmentalization and vertical leakage of fluids through open conduits in the multireservoir system of Patrick Draw field is strongly indicated by the anomalous original pattern of fluid distribution revealed by the analysis of the initial production data and by geochemical information.[8,9] Further study is needed to substantiate these observations with additional geologic and engineering data and to design sampling programs for fluids from different productive horizons located several hundred feet apart for examination of their stable isotope composition. Better understanding of hydrodynamic conditions in this area is of vital importance before implementation of an enhanced oil recovery (EOR) process.

In Big Muddy field, an extensive leak between the Dakota and the oil-productive Second Wall Creek formations was documented by chemical, geochemical, and radioactive tracer methods.[10] The Second Wali Creek Sandstone may be in hydraulic communication with the Niobrara, Shannon, and other formations located nearly 2000 ft apart. Application of a stable isotope technique is strongly recommended for identification of hydrodynamic intercommunication in Big Muddy field.

Lateral continuity of pay zones and vertical communication between horizons were serious concerns in the multireservoir Elk Basin field since an early period in its development. After 10 yr of development of the Madison formation reservoir, the operational plan had to be changed because of fundamental reinterpretation of continuity and integrity of a confining layer (solution breccia) separating major productive horizons.

Patrick Draw field and the other preselected reservoirs will be more specifically addressed as candidates for field demonstration of the isotopic method in the final report on Phase I of the project.

References

1. A. T. James, Correlation of Reservoir Gases Using the Carbon Isotopic Composition of Wet Gas Components, *AAPG Bull.*, 74(9): 1441-1458 (1990).
2. O. R. Heum, A. Dalland, and K. K. Meisingset, Habitat of Hydrocarbons at Haltebanken (PVT-Modeling as a Predictive Tool in Hydrocarbon Exploration), in *Habitat of Hydrocarbons on the Norwegian Continental Shelf*, A. M. Spencer et al. (Eds.), published by Graham and Trotman for the Norwegian Petroleum Society, 1986.
3. J. A. Milles, Secondary Migration Routes in the Brent Sandstone of the Viking Graben and East Shethland Basin: Evidence from Oil Residues and Subsurface Pressure Data, *AAPG Bull.*, 74(11): 1718-1735 (1990).
4. H. D. Hedberg, Methane Generation and Petroleum Migration, *AAPG Stud. Geol.*, 10: 179-207 (1980).
5. E. M. Prosolov, I. L. Kamenskiy, A. P. Meshik, Y. S. Subbotin, L. N. Surovtseva, and O. N. Yakovlev, Formation of Gas Fields of the North of West Siberia from Isotopic Data, in *Proiskhozhdeniye i Formirovaniye Sostava Prirodnych Gazov Po Dannym Isotopnoy Geokhimii*, pp. 64-82, VNIGRI, Leningrad, 1981.
6. D. D. Coleman, W. F. Meents, Chao-Li Liu, and R. A. Keogh, Isotopic Identification of Leakage Gas from Underground Storage Reservoirs—A Progress Report, *Illinois Petroleum III*, pp. 1-10, Illinois State Geological Survey, Urbana, Ill., 1977.
7. L. Mattavelli, T. Ricchuto, D. Grignani, and M. Shoell, Geochemistry and Habitat of Natural Gases in Po Basin, Northern Italy, *AAPG Bull.* 67(12): 2239-2254 (1983).
8. M. Szpakiewicz, Analysis of the Initial Production in Patrick Draw Field, Wyoming, in *Quarterly Technical Report—Reservoir Assessment and Characterization, Project BE1, October 1–December 31, 1990*, National Institute for Petroleum and Energy Research, DOE Report NIPER-522, in press.
9. M. Szpakiewicz and A. G. Collins, *Hydrochemical Study of the Upper Cretaceous and Lower Tertiary Formation in the Uinta, Piceance and Greater Green River Basins; Implications for Oil and Gas Related Problems*, Topical Report NIPER-95, August 1985.
10. Conoco, Inc., Interoffice Communication, Big Muddy DOE Project Engineering Committee Meeting, File: PES-414-CF, July 16, 1985.

SUMMARY OF GEOLOGICAL AND PRODUCTION CHARACTERISTICS OF CLASS I, UNSTRUCTURED, DELTAIC RESERVOIRS

Cooperative Agreement DE-FC22-83FE60149, Project SGP46

National Institute for Petroleum and Energy Research
Bartlesville, Okla.

Contract Date: Nov. 1, 1990
Anticipated Completion: Mar. 31, 1991
Funding for FY 1991: $200,000

Principal Investigator:
Susan Jackson

Project Manager:
Edith Allison
Bartlesville Project Office

Reporting Period: Oct. 1–Dec. 31, 1990

Objective

The objective of this project is to summarize the geological and production characteristics of Class I, fluviodeltaic system reservoirs. This work is not intended as an exhaustive study; rather, it is a summary of what is generally known about clastic deltaic reservoirs and what areas have the greatest potential for further investigation to preserve economic access to the resource.

Summary of Technical Progress

The purpose of the document prepared for the Class 1 Symposium in Dallas, Tex., Jan. 29–30, 1991, is to provide a brief summary of the general characteristics and reservoir properties within deltaic deposits. It is not an exhaustive treatise; rather, it is intended to provide some basic information to stimulate discussions about recovery characteristics and problems within deltaic reservoirs. A more complete document that contains the findings from the Class 1 Symposium will be published in mid-1991.

The following topics are addressed and summarized in this report: (1) a general review of the sedimentological aspects of deltaic systems; (2) average reservoir properties and production characteristics derived from data from 359 Class 1, unstructured, deltaic reservoirs in the Tertiary Oil Recovery Information System (TORIS) database; and (3) a summary of commonly encountered problems in 26 enhanced oil recovery (EOR) projects which result from depositionally related heterogeneities.

General Sedimentological Characteristics of Deltaic Deposystems

An important aspect of recovering more oil from Class 1 reservoirs is improving the geological characterization as a basis for implementation of appropriate secondary and tertiary production processes. Improved, often more detailed, knowledge about the depositional framework and the scale and frequency of reservoir heterogeneities may be required, but it offers the best opportunity to anticipate and alleviate problems commonly encountered by infill drilling, waterflood, or other enhanced oil recovery processes.

Interwell continuity is often the direct result of the geometry of depositional facies. These facies are produced by the interplay of depositional processes that are characteristic of particular depositional environments. Thus the recognition of facies (the distinguishable rock units) can be tied to genetically related types of deltas (fluvial, wave, or tide dominated), which define the distribution of potential high-quality reservoir sandstones.

The general area where an active stream enters the ocean or other body of water is called the delta front. Each of the three major types of deltas affects the distribution of the delta-front sands, often the best reservoirs, in different ways. Fluvial-dominated deltas tend to build elongate "fingers" of delta-front sands, and the general distribution of major sands tends to be parallel to the depositional slope. The delta-front sands on wave-dominated deltas tend to be reworked into numerous coastal barriers that parallel depositional strike. Tide-dominated deltas tend to have sand-choked channels and build tidal sand ridges in the delta-front area which are oriented parallel to the depositional slope.

Deltas can be defined as stream-fed depositional systems depositing sediments in lakes, bays, lagoons, or oceans and creating an irregularity on that shoreline. There must be some preserved constructional or progradational aspect for the system to be deltaic. The scale of deltas can be small; for example, the bayhead delta of the Colorado Delta of Texas discussed by Kanes[1] was only 1300 ft wide at the turn of the century. The scale of deltas can be large; for example, the Nile Delta is about 170 miles wide along the shoreline and nearly 100 miles from its apex to the shoreline.

Deltas can be subdivided into three general physiographic settings: (1) upper delta plain, the subaerial part of the delta plain dominated by fluvial processes; (2) lower delta plain, the part that lies between the lowest tide level and the most updip influence of the tides; and (3) subaqueous delta plain, the part that is dominated by marine processes.[2]

Geometry and Dimensions of Deltaic Facies

The geometry of channel deposits is a function primarily of (1) the size of the delta, (2) the position of the channel in the delta, (3) the type of material being cut into, and (4) to a lesser degree, the forces at the mouth of the channel distributing the sediments.[3] Channels can be filled with up to 90% sand or clay/silt material depending on whether it migrates laterally or becomes abandoned. The geometry of the delta front is typically attributed to (1) the rate of sediment supply and (2) the relative strengths of the wave, tide, and fluvial processes acting on the sandbody. However, synsedimentary faulting, slumping, clay diapirism, and gravity sliding can drastically affect the geometry and structure of delta front and mouth bar deposits.[4]

Table 1 includes data on the dimensions and geometry of deltaic facies of distributary channel, distributary mouth bars, distal bar sandstones, and crevasse splay channels. The data include information from nine studies that represent a variety of ancient and modern deltaic settings.[5] Note that the distributary mouth bar deposits tend to be twice as thick and 10 times as wide as distributary channel deposits. The width/thickness ratio for distributary mouth bars is 7 times as great as that for distributary channels.

Shale Lengths

Dimensions of shale layers tend to vary as a function of depositional setting.[6] Shales associated with deltaic barrier sand deposits are usually quite continuous and are generally

TABLE 1

Facies Dimensions for Primary Reservoir Facies in Deltaic Deposits*

Facies	90% less than:	50% less than:	20% less than:
Distributary channels			
Width, ft	2,805	1,073	248
Thickness, ft	60	30	12
Width/thickness	130:1	40:1	10:1
Distributary mouth bars			
Width, dip, ft	21,120	10,560	3,696
Thickness, ft	99	60	23
Length, strike, ft	31,680	21,120	10,560
Width/thickness	820:1	280:1	50:1
Length/thickness	1,240:1	360:1	42:1
Length/width	2.7:1	2.1	1.2:1
Distal bar sandstones			
Thickness, ft	2		
Crevasse splay channel			
Width, ft	838	244	36
Thickness, ft	33	13	1
Width/thickness	76:1	34:1	10:1

*Modified from P. Lowry, *Establishment of a Geologic Database for Improved Reservoir Characterization, Part I: Geometry of Delta Front Sandstones,* Report No. IFE/KR/F-89/056, Institute for Energiteknikk, Kjeller, Norway, 1989.

concentrated in the lower half of the sandy interval. Delta-front and delta plain sediments, however, contain shale breaks that are usually less extensive because of erosion by migrating and nonmigrating rivers and tidal channels. Shale breaks are often less than 30 ft in lateral extent in distributary channel fill deposits. The most common occurrence of laterally discontinuous shale layers is related to trough crossbedding, where the shale layers often merge and thus cause barriers to horizontal as well as vertical fluid flow.[6]

General Reservoir Characteristics from TORIS Database

The TORIS database was screened for unstructured, deltaic reservoirs containing oil with gravity greater than 20°API. The reservoirs contained in the database are only the larger reservoirs screened by volume. The mean, median, and standard deviation of reservoir fluid properties for the 359 reservoirs analyzed are listed in Table 2.

Visual analysis of cross plots of data from 359 TORIS reservoirs indicates that primary production is most strongly correlated with permeability and that the primary recovery factor increases with the increase of the average permeability value for that field. The rate of increase of the primary recovery factor is related to the degree of permeability heterogeneity. In reservoirs with pseudo Dykstra–Parsons coefficients (PDP) ranging from 0.75 to 0.90, the primary recovery is about 20% when reservoir permeability is less than 100 mD and increases to approximately 40% when the permeability value increases to 1000 mD. In relatively homogeneous reservoirs (PDP less than 0.75), the primary recovery factor can be well over 50% in contrast to heterogeneous reservoirs (PDP greater than 0.90) where the primary recovery factor will probably be less than 30% even at high permeability values, such as 1000 mD.

Effects of Geologic Features on Enhanced Oil Recovery Processes

Twenty-seven EOR projects conducted in unstructured, deltaic reservoirs were reviewed to document the effects of reservoir heterogeneity on the efficiency of EOR. The most commonly reported fluid-flow problems caused by geologic features were channeling, compartmentalization, directional trends, high-salinity regions, and formation parting (Table 3).

Channeling was reported when a disproportionate volume of injected fluid was accepted by a high-permeability zone. As discussed previously, high-permeability zones may occur at the top of a sequence as in the distributary mouth bar and delta-front facies or on the bottom as in the distributary channel facies. This phenomenon was reported in 20 of the 27 EOR projects reviewed.

Compartmentalization was documented when geologic studies of the EOR projects reported the presence of compartments or barriers to fluid flow. Compartmentalization was observed in 13 of the EOR projects reviewed and is perceived to be the reason for the lower-than-expected recovery efficiencies for projects with well spacing greater than 0.8 acre.

Directional trends of permeability may be caused by the orientation of crossbeds, shale baffles, or higher permeability channel deposits; are typically oriented parallel to depositional dip; and generate a preferential direction of flow. This feature was observed in six of the projects reviewed.

Contact of high-salinity regions was reported only in chemical flooding projects, where high salinity affected the injected chemicals. The high-salinity regions are partly a result of poor waterflood sweep efficiency as a result of either compartmentalization or the presence of a high-permeability channel.

Formation parting is not directly related to the depositional environment; however, it is included because it occurred quite frequently in the projects reviewed. Formation parting was reported in many of the chemical flood projects where high-viscosity fluids were injected for mobility control.

TABLE 2

General Statistics of Class 1 Reservoir Properties from TORIS Database

Variable	No. of fields	Minimum	Maximum	Mean	Median	Standard deviation
Net pay, ft	359	2.0	272.0	23.3	15	27.44
Gross pay, ft	359	2.4	5,500.0	60.0	20.4	323.8
Porosity, %	359	6	40	20.2	19	6
S_{oi}, %	359	28	90	67	69	9
S_{wi}, %	359	10	72	33	31	9
Initial form, vol. factor	359	0.97	2.02	1.22	1.20	0.15
Current form, vol. factor	359	0.96	1.63	1.13	1.11	0.10
Depth, ft	357	400	10,246	4,476	4,650	2,138
Form temperature, °F	359	65	250	136	136	39
Pressure, psi	359	100	4,233	1,237	1,201	718
Permeability, mD	359	0	3,100	282	111	445
Oil gravity, °API	359	17	50	38	39	5
Viscosity, cP	359	0.1	100.0	3.3	1.1	9.3
Initial oil-in-place, bbl	359	30,744	7,558,000,100	122,736,420	26,060,000	475,587,350
Primary recovery factor	358	0.01	0.84	0.29	0.25	0.17
Cumulative recovery, bbl	359	12,318	5,004,040,200	41,731,693	6,271,000	272,142,220
Primary recovery, bbl/acre-ft	358	6.4	1,447.0	267	202.6	230.1
Primary recovery, bbl	358	12,318	4,938,630,100	38,695,463	5,544,595	266,697,580
Initial GOR, scf/bbl	359	0.0	10,000.0	602.4	569.4	613.3
Reservoir, acres	359	3	140,000	4,818	1,907	9,624
Initial form pressure, psi	359	200	6,047	1,931	1,885	966
S_o(Swept)	359	6	59	26	25	6
Dykstra–Parsons coefficient	359	0.50	0.98	0.78	0.84	0.17

TABLE 3

Geologic Factors Affecting Enhanced Oil Recovery (EOR)

Field name	EOR type*	Well spacing, acres	Recovery efficiency, %	Channeling	Compartmentalization	Contact high salinity	Formation parting (pressure)	Directional trend	Facies†
Benton, Ill.	S/P	1	27	yes	yes	yes			
Big Muddy 1, Wyo.	S/P	1	36				yes (0.42 psi/ft)		dc, dfg
Big Muddy 2, Wyo.	S/P	10	14	yes			yes		
Delaware–Childers, Okla.	S/P	2.5	7	yes		yes		yes	
El Dorado, Kans.	S/P	6.4	0			yes			
Glennpool, Okla.	S/P			yes	yes		yes	yes	
Loudon 1, Ill.	S/P	0.625	15.3			yes			
Loudon 2, Ill.	S/P	0.68	60	yes		yes		yes	dmb, mb, df
Loudon 3, Ill.	S/P	0.71	68	yes	yes				
Loudon 4, Ill.	S/P	2.5/5	27/33	yes	yes				
Main Consolid.1, Ill.	S/P	0.75	63	yes			yes		dc, pb
Main Consolid.2, Ill.	S/P	10	39	yes					
Main Consolid.3, Ill.	S/P	3	27 to 33						
Main Consolid.4, Ill.	S/P	2.5/5	20/17	yes	yes	yes	yes		
Manvel, Tex.	S/P								
North Burbank, Okla.	S/P	10	25	yes	yes	yes	yes (0.5 psi/ft)	yes	fc, mmtl
North Burbank, Okla.	P	20		yes			yes	yes	fc, mmtl
North Stanley, Okla.	P		1.4	yes					
Ranger, Tex.	S/P	40	25		yes				dc
Salem 1, Ill.	S/P	5	14	yes	yes	yes			df
Salem 2, Ill.	S/P	5	47	yes		yes			
Sloss, Neb.	S/P	9	yes	yes					
Bay St. Elaine, La.	CO_2M								obs
Garber, Okla.	CO_2M	10.4	14	yes	yes				dc, df
Rock Creek 1, W.Va.	CO_2M	10.3	yes	yes					
Rock Creek 2, W.Va.	CO_2M	1.55	11	yes	yes				
Grann. Creek, W.Va.	CO_2M	0.85/6.7	37/6	yes	yes				

*S/P, surfactant (including microemulsion, low tension, and soluble oil-polymer); P, polymer; CO_2M, carbon dioxide miscible.

†dc, distributary channel; df, delta front; dfg, delta fringe; dmb, distal mouth bar; fc, fluvial channel; mb, mouth bar; mmtl, marginal marine tidal or lagoonal deposit; obs, overbank splay; pb, point bar.

References

1. W. H. Kanes, Facies and Development of the Colorado River Delta in Texas, *Spec. Pub.—Soc. Econ. Paleontol. Mineral.*, 15: 78-106 (1970).
2. J. M. Coleman and D. B. Prior, Deltaic Environments, in Sandstone Depositional Environments, P. A. Scholle and D. Spearing (Eds.), *Mem.—Am. Assoc. Pet. Geol.*, 31: 139-178 (1982).
3. R. M. Sneider, C. N. Tinker, and L. D. Meckel, Deltaic Environment Reservoir Types and Their Characteristics, *J. Pet. Technol.*, 1538-1546 (November 1978).
4. A. J. Pulham, Controls on Internal Structure and Architecture of Sandstone Bodies Within Upper Carboniferous Fluvial-Dominated Deltas, County Clare, Western Ireland, in *Deltas: Sites and Traps for Fossil Fuels*, M. K. G. Whateley and K. T. Pickering (Eds.), Geological Society Special Publication No. 41, pp. 3-10, 1989.
5. P. Lowry, *Establishment of a Geologic Database for Improved Reservoir Characterization, Part 1: Geometry of Delta Front Sandstones*, Report IFE/KR/F-89/056, Institute for Energiteknikk, Kjeller, Norway, 1989.
6. K. J. Weber, Influence of Common Sedimentary Structures on Fluid Flow in Reservoir Models, *J. Pet. Technol.*, 665-672 (March 1982).

AN EXPERIMENTAL AND THEORETICAL STUDY TO RELATE UNCOMMON ROCK–FLUID PROPERTIES TO OIL RECOVERY

Contract No. AC22-89BC14477

Pennsylvania State University
University Park, Pa.

Contract Date: Sept. 21, 1989
Anticipated Completion: Aug. 31, 1992
Government Award: $260,221

Principal Investigators:
Turgay Ertekin
Robert W. Watson

Project Manager:
Robert E. Lemmon
Bartlesville Project Office

Reporting Period: Oct. 1–Dec. 31, 1990

Objectives

The overall objectives of the project are to develop a better understanding of some important, but not well-investigated, rock properties, such as tortuosity, pore-size distribution, surface area, wettability, and neck–throat average rock size; develop a better insight on capillary pressure variation with respect to wettability and pore geometry of Berea sandstone, limestone, and dolomite; develop a relationship between oil recovery at breakthrough and wettability and surface area of the rocks; develop correlations between ultimate oil recovery and wettability and surface area of these different porous media; investigate variations of average residual water saturation (S_{wr}) and average residual oil saturation (S_{or}) with respect to wettability; and improve the understanding of fluid flow in porous media under conditions of secondary and tertiary recovery through the laboratory study of the performance of enhanced recovery methods, such as waterflooding.

Summary of Technical Progress

A total of 20 radial limestone cores were waterflooded. Displacement studies were conducted at injection rates equivalent to a field drainage rate of 1 ft/d to model a field situation where water advance is moderated. The containment pressure on the limestone cores was maintained at 200 psig. The containment pressure for the limestone was 300 psi lower than that used to contain the sandstone cores. Experience indicated that the limestone cores failed at pressures equal to or greater than 300 psig. The containment pressure of 200 psig was adequate in that it permitted water injection without the inducement of fractures in the limestone cores and prevented water channeling. Temperature was maintained at 35°C throughout the experimental runs. The wetting phase was a brine consisting of 1.5 wt % sodium chloride, distilled water. Formalin was used to preserve the brine and prevent bacterial growth. The nonwetting phase is a binary system containing 70 vol % of Blandol and 30 vol % of Soltrol. This combination was selected to yield a viscosity of 10 cP. This viscosity was chosen to simulate the viscosity of common reservoir oil. Before mixing and before each experimental run, the wetting and nonwetting phases were filtered through a 0.45-μm filter. Waterflooding experiments were performed with a fully automatic coreflooding station. Radial cores of limestone, 5 in. × 2 in., were used as the porous media during the first stage of the waterflooding process study. An injection well was drilled into the middle of each limestone core. The internal diameter of the core holder was 5 in. The radial waterflooding experiments were used to obtain the tortuosity of each radial core, the average residual water saturation, the average residual oil saturation, oil recovery at breakthrough, and ultimate oil recovery.

Results and Discussion

Statistical descriptions of the different variables studied are shown in Tables 1 and 2.

Correlation matrices (Tables 3 and 4) were used to correlate the ultimate oil recovery to porosity, residual water saturation, and residual oil saturation for the two porosity ranges used. The correlation coefficients indicated that the ultimate oil recovery was proportional to residual water

TABLE 1

Statistical Description of Variables of Waterflood Experiments for Less Porous Limestone Cores

Variable	Dimension of variable						Standard deviation, %
	Mean	Median	Minimum	Maximum	Q_1	Q_3	
Ultimate oil recovery	0.4487	0.4374	0.3933	0.5270	0.4155	0.4791	4.650
Oil recovery @ BT	0.2217	0.2079	0.1805	0.2741	0.2004	0.2479	3.130
S_{oi}	0.5153	0.5173	0.4677	0.5508	0.4992	0.5329	2.508
S_{wi}	0.4847	0.4827	0.4492	0.5328	0.4671	0.5008	2.508
S_{or}	0.2842	0.2932	0.2349	0.3155	0.2562	0.3088	2.900
ϕ	0.1134	0.1147	0.1009	0.1185	0.1115	0.1166	0.498

Note: oil recovery @ BT, oil recovery at breakthrough, fraction; S_{oi}, initial oil saturation; S_{wi}, initial water saturation; S_{or}, residual oil saturation; ϕ, porosity, fraction; Q_1, lower quartile of the frequency distribution; and Q_3, upper quartile of the frequency distribution.

TABLE 2

Statistical Description of Variables of Waterflood Experiments for More Porous Limestone Cores

Variable	Dimension of variable						Standard deviation, %
	Mean	Median	Minimum	Maximum	Q_1	Q_3	
Ultimate oil recovery	0.3872	0.3848	0.3015	0.4664	0.3719	0.4083	4.210
Oil recovery @ BT	0.2532	0.2579	0.1825	0.3018	0.2197	0.2884	4.020
S_{oi}	0.4154	0.4135	0.3655	0.5062	0.3786	0.4375	4.150
S_{wi}	0.5846	0.5865	0.4937	0.6345	0.5625	0.6214	4.150
S_{or}	0.2549	0.2463	0.2135	0.3159	0.2265	0.2794	3.450
ϕ	0.1612	0.1637	0.1444	0.1705	0.1560	0.1666	0.818

Note: oil recovery @ BT, oil recovery at breakthrough, fraction; S_{oi}, initial oil saturation; S_{wi}, initial water saturation; S_{or}, residual oil saturation; ϕ, porosity, fraction; Q_1, lower quartile of the frequency distribution; and Q_3, upper quartile of the frequency distribution.

TABLE 3

Correlation Matrix for More Porous Limestone

	Ultimate oil recovery	S_{or}	S_{wr}	S_{oi}
S_{or}	–0.701			
S_{wr}	0.248	–0.865		
S_{oi}	–0.248	0.865	–1.000	
ϕ	–0.43	–0.264	0.666	–0.666

Note: S_{or}, residual oil saturation; S_{wr}, residual water saturation; S_{oi}, initial oil saturation; and ϕ, porosity, fraction.

TABLE 4

Correlation Matrix for Less Porous Limestone

	Ultimate oil recovery	S_{or}	S_{wr}	S_{oi}
S_{or}	–0.878			
S_{wr}	0.119	–0.579		
S_{oi}	–0.119	0.579	–1.000	
ϕ	–0.411	0.602	–0.568	0.568

Note: S_{or}, residual oil saturation; S_{wr}, residual water saturation; S_{oi}, initial oil saturation; and ϕ, porosity, fraction.

saturation and inversely proportional to porosity and residual oil saturation. These results are, in part, atypical for water-wet reservoirs where capillary forces are predominant. These results may be an indication of experimental artifacts.

Futhermore, in Berea sandstone cores, which are relatively homogeneous and strongly water wet, little oil production was realized after water breakthrough. By contrast, in the tight limestone cores, significant oil production occurred after water breakthrough and continued after the displacement of several pore volumes of water. The more porous limestone cores, however, performed similarly to the sandstone in that little oil production was realized after water breakthrough. The explanations for these observations have not been formulated. Additional experiments, such as mercury porosimetry, are necessary to reach any definitive conclusions.

Figures 1 and 2 contain plots of residual oil saturation and residual water saturation vs. porosity, respectively.

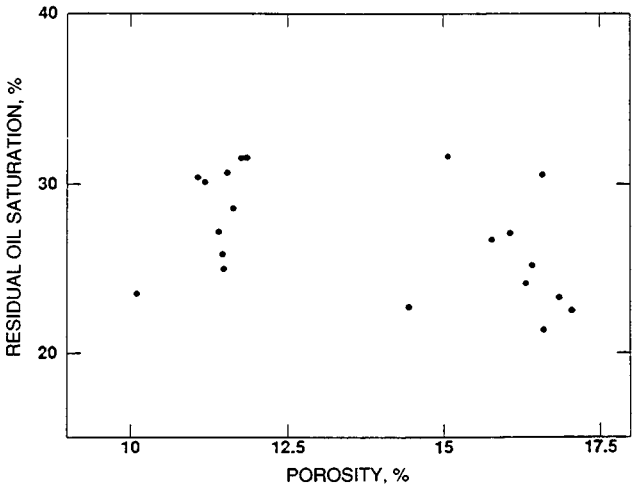

Fig. 1 Residual oil saturation vs. porosity.

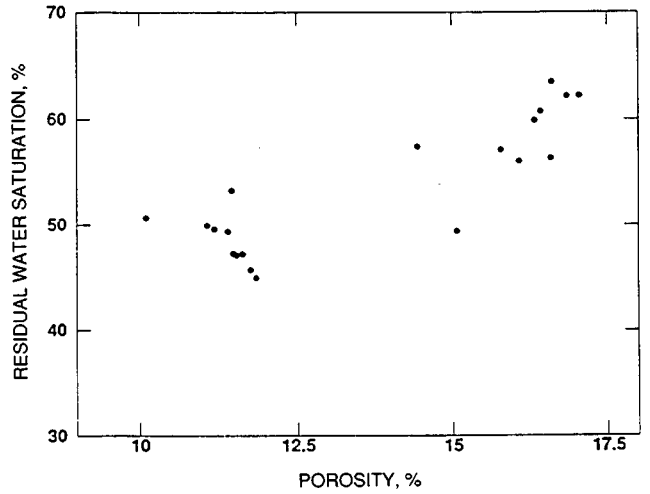

Fig. 2 Residual water saturation vs. porosity.

Figure 1 indicates that residual oil saturation is proportional to porosity for the low porosity range cores and inversely proportional to porosity in the high porosity range cores. Figure 2 indicates that residual water saturation is inversely proportional to porosity for the low porosity range cores and directly proportional to porosity for the high porosity range cores. As previously noted, additional experiments are required to reach any definitive conclusions concerning these observations.

Major Achievements

The major portion of a survey of relevant literature concerning the analysis of oil recovery from limestone and dolomite rocks has been completed.

Waterfloods were conducted on radial limestone cores with a fully automatic coreflooding station. Statistical analyses of measured parameters, such as average residual water saturation, average residual oil saturation, porosity, tortuosity, average initial oil saturation, oil recovery at breakthrough, and ultimate oil recovery, were begun. Preliminary results suggest a high degree of randomness with respect to these variables.

Conclusions

Waterflooding experiments in the radial limestone cores have provided data that will require additional experiments to adequately interpret.

Bibliography

Bell, A., F. Squires, and G. V. Cohee, 1942, *Secondary Oil Recovery in Illinois, Secondary Recovery of Oil in the U.S.*, Vol. 157, American Petroleum Institute, New York.

Cuiec, L., D. Longeron, and J. Pacsirszky, 1979, On the Necessity of Respecting Reservoir Conditions in Laboratory Displacement Studies, SPE paper 7785 presented at the Middle East Oil Technical Conference of the Society of Petroleum Engineers in Manama, Bahrain, March 25-29.

Salathiel, R. A., 1973, Oil Recovery by Surface Film Drainage in Mixed-Wettability Rocks, *J. Pet. Technol.*, 1216-1224 (October).

Smith, W. O., P. D. Foote, and P. F. Busang, 1930, *Phys. Rev.*, 36: 524-530.

Spencer, O. F. and R. W. Harding, 1959, *Secondary Recovery of Oil*, 2nd ed., Pennsylvania State University, University Park, Pa.

Treiber, L. E., D. L. Archer, and W. W. Owens, 1972, A Laboratory Evaluation of the Wettability of Fifty Oil-Producing Reservoirs, SPE paper 3526 presented at the SPE 46th Annual Fall Meeting held in New Orleans, Oct. 3–6; *Trans. Am. Inst. Min Metall. Pet. Eng.*, 253: 535.

Wardlaw, N. C., 1982, The Effects of Geometry, of Wettability, Viscous and Interfacial Tension on Trapping in Single Pore-throat Pairs, *J. Can. Pet. Technol.*, 21(3): 7 (May-June).

IN SITU STRESS AND FRACTURE PERMEABILITY: A COOPERATIVE DOE–INDUSTRY RESEARCH PROGRAM

Sandia National Laboratories
Albuquerque, N. Mex.

Contract Date: Oct. 1, 1986
Anticipated Completion: Sept. 30, 1991
Funding for FY 1989: $200,000

Principal Investigators:
David A. Northrop
Lawrence W. Teufel

Project Manager:
Edith Allison
Bartlesville Project Office

Reporting Period: Oct. 1–Dec. 31, 1990

Objectives

This is a cooperative U.S. Department of Energy (DOE)–Industry Research Program between Sandia National Laboratories and Phillips Petroleum Company to study and understand the interrelationships between in situ stresses, natural fractures, and reservoir permeabilities. There are three different but coupled tasks: (1) measurements of in situ stresses in the reservoir and adjacent formations, (2) laboratory deformation and permeability measurements in fractured and intact reservoir rock, and (3) characterization of the natural fracture system in the reservoir. The primary focus is the Ekofisk oil field in the Norwegian sector of the North Sea.

Summary of Technical Progress

Knowledge of in situ stress and how stress changes with reservoir depletion and pore pressure drawdown is important in a multidisciplinary approach to reservoir characterization, reservoir management, and enhanced oil recovery projects. Over 20 yr of petroleum production from the Ekofisk field has resulted in a 21- to 24-MPa reduction in reservoir pore pressure. The decline in pore pressure has led to an increase in the fraction of the overburden load that must be supported by the structurally weak chalk matrix, which, in turn, has caused significant reservoir compaction and seafloor subsidence.

An important objective of this cooperative program is to determine the effect of production and pore pressure drawdown on the in situ stress state across the reservoir. As the pore pressure is drawn down, the effective stresses in the reservoir will increase, but at different rates depending upon the loading path and boundary conditions on the reservoir. Measurements of the minimum horizontal in situ stress have been determined from closure stresses derived from analysis of shut-in pressure data of hydraulic fractures conducted in 32 wells in the Ekofisk field during the past 15 yr.

The effect of pore pressure drawdown on the total minimum in situ stress is shown in Fig. 1. The data are separated into three groups on the basis of well location with respect to position on the structural dome that forms the Ekofisk reservoir: crest, flank, and outer flank. Total minimum stress has decreased linearly with pore pressure drawdown. The change in minimum horizontal stress is about 80% of the net change in pore pressure.

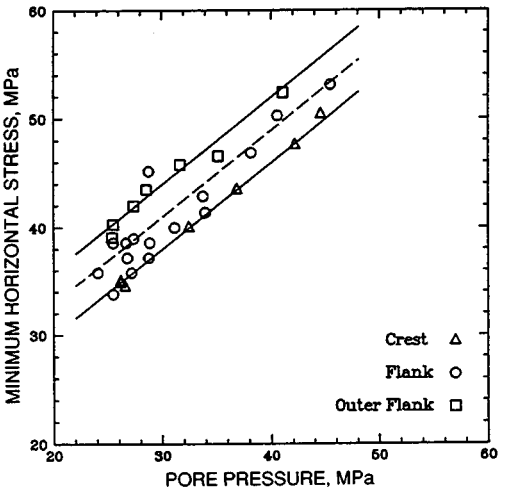

Fig. 1 Plot of minimum horizontal stress vs. pore pressure in the Ekofisk field, North Sea. $\Delta S_{Hmin}/\Delta P = 0.80$.

In general, the change in total minimum horizontal stress with pore pressure drawdown is the same across the field. However, magnitudes of minimum horizontal stresses vary spatially across the field as a function of position on the structure. The lowest magnitudes of minimum stress are on the crest of the structure, and the highest magnitudes are on the outer north and south flanks. As the pore pressure was drawn down over the crestal area of the field from 46 MPa in 1975 to 25 MPa in 1990, the minimum horizontal stresses decreased from about 51 to 34–36 MPa, respectively. In wells on the outer north and south flanks, which have pore pressures of about 25 MPa, the minimum horizontal stress ranges from 39 to 41 MPa.

Initial minimum horizontal stresses before the start of production are estimated, from linear regression extrapolation, to have ranged from about 52 MPa on the crest to 58 MPa on the outer flanks of the structure. Total overburden stress ranged from 61 MPa on the crest to 65 MPa on the outer flanks.

Measurements of the total minimum horizontal stress as a function of pore pressure drawdown can be used to provide an understanding of the boundary conditions on the reservoir and the stress path that has been followed by

reservoir rock during the production history of the Ekofisk field. With pore pressure drawdown, the effective stresses in the reservoir increase but at different rates. Following Rice and Cleary,[1] effective stress is defined by

$$\sigma = S - \alpha P$$

where σ = effective stress
S = total stress
P = pore pressure
α = poroelastic constant

Laboratory poroelastic-deformation experiments of Ekofisk chalk have shown that α is unity for high-porosity chalks.[2]

Figure 2 is a plot of effective minimum horizontal stress vs. effective vertical stress during primary production from the Ekofisk field. For this plot, the total vertical stress in the reservoir is assumed to be constant during the production history of the reservoir and equal to the total stress exerted by the weight of the overburden. Accordingly an incremental reduction in pore pressure corresponds directly to an incremental increase in effective vertical stress of the same magnitude.

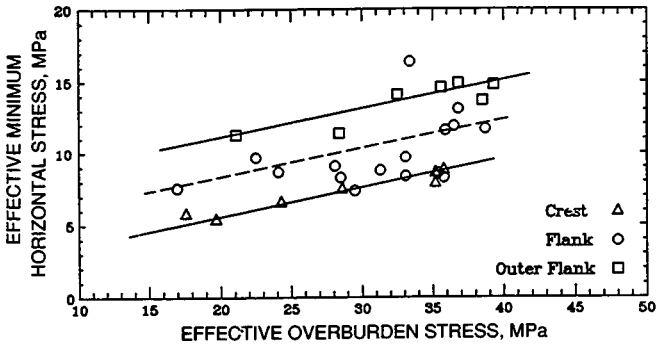

Fig. 2 Plot of effective minimum horizontal stress vs. effective overburden (vertical) stress in the Ekofisk field, North Sea. Change in effective stress is caused by pore pressure drawdown. $K = \Delta\sigma_{Hmin}/\Delta\sigma_V = 0.20$.

The ratio of effective minimum horizontal stress to effective overburden stress varies spatially across the field with the lowest ratios on the crest and the highest ratios on the outer flanks of the structure. In general, the incremental change in effective minimum horizontal stress with an incremental increase in effective overburden stress is nearly constant over the entire reservoir. The ratio of change in effective minimum horizontal stress to change in effective overburden stress, K, is approximately 0.20 with the use of a linear regression. Hence, with pore pressure drawdown, the effective minimum horizontal stress has increased at a much slower rate than the effective vertical stress.

The stress path measured in the Ekofisk reservoir during pore pressure drawdown clearly indicates that the boundary condition on the reservoir is not a strict stress boundary condition where an incremental increase in effective overburden stress is matched by an identical increase in effective horizontal stress (i.e., K equals 1.0). Rather, the boundary condition is a displacement boundary condition or a combined displacement–stress boundary condition in which an incremental reduction in pore pressure produces a greater incremental increase in effective overburden stress than in effective horizontal stress (i.e., K is less than 1.0).

Laboratory experiments that simulate the stress path that has been followed by reservoir rock during the production history of the Ekofisk field indicate that shear failure has occurred during compaction of high-porosity chalk as the shear stress progressively increased with pore pressure drawdown. Figure 3 is a shear stress vs. normal stress diagram showing failure envelopes with end caps for 39 and 34% porosity Ekofisk chalk and a series of Mohr circles illustrating how the effective stress state on the flank of the Ekofisk reservoir has evolved along a stress path of 0.20 during pore pressure drawdown. The first Mohr circle represents the initial effective stress state prior to production when the pore pressure was 48.1 MPa, and the last Mohr circle represents the effective stress state in 1990 when the pore pressure was 24 MPa. The deviatoric or shear stress is more than sufficient to cause shear failure of chalk with porosities of 34% or more. Accordingly, in the Ekofisk reservoir shear failure likely occurred in high-porosity chalks as the in situ shear stress progressively increased with pore pressure drawdown.

Permeability and productivity of a reservoir are assumed to decrease with reservoir compaction and porosity reduction. Shear failure during depletion can have a positive effect on production, however, because it can increase fracture density and reduce matrix block dimensions and thereby maintain reservoir permeability. Pore pressure increases associated with water injection may lead to additional shear failure,[3,4] which would further increase fracture

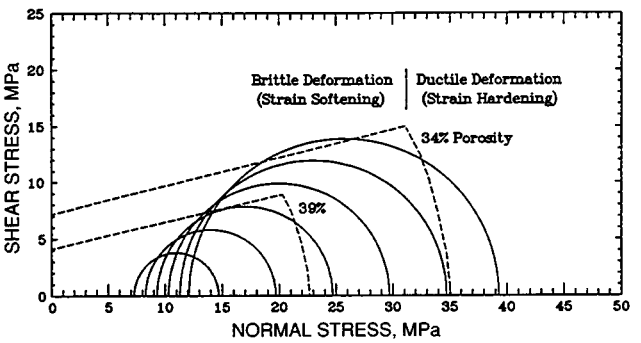

Fig. 3 Plot of shear stress vs. normal stress showing failure envelopes with end caps for 39 and 34% porosity chalk and a series of Mohr circles representing the stress path in the Ekofisk reservoir during pore pressure drawdown. Ekofisk flank, 1970 to 1990; pore pressure drawdown, 48.1 to 24 MPa; stress path, K = 0.20.

density and fracture surface area and therefore improve imbibition rates and waterflood sweep efficiency. Accordingly, the shear failure process may account for the continued good producibility of the Ekofisk field, in spite of compaction, as well as the very good performance of the Ekofisk waterflood. The influence of shear failure on reservoir compaction and subsidence is currently being evaluated.

References

1. J. Rice and M. Cleary, Some Basic Stress Diffusion Solutions for Fluid-Saturated Elastic Porous Media with Compressible Constituents, *Rev. Geophys. Space Phys.*, 14:227-241 (1976).
2. L. W. Teufel and N. R. Warpinski, Laboratory Determination of Effective Stress Laws for Deformation and Permeability of Chalk, in *Proceedings of the Third North Sea Chalk Symposium,* Copenhagen, Denmark, June 11–12, 1990.
3. D. W. Rhett and L. W. Teufel, Water Injection-Induced Shear Fracturing in the Ekofisk Field, in *Proceedings of the 32nd U.S. Symposium on Rock Mechanics,* Norman, Okla., July 10–12, 1990.
4. L. W. Teufel and H. E. Farrell, Distribution of In Situ Stress and Natural Fractures in the Ekofisk Field, North Sea, in *Proceedings of the Third North Sea Chalk Symposium,* Copenhagen, Denmark, June 11–12, 1990.

ANALYSIS OF RESERVOIR HETEROGENEITIES DUE TO SHALLOWING-UPWARD CYCLES IN CARBONATE ROCKS OF THE PENNSYLVANIAN WAHOO LIMESTONE OF NORTHEASTERN ALASKA

Contract No. AC22-89BC14471

University of Alaska
Fairbanks, Alaska

Contract Date: Sept. 29, 1989
Anticipated Completion: Dec. 31, 1992
Government Award: $149,935

Principal Investigator:
Keith F. Watts

Project Manager:
Robert E. Lemmon
Bartlesville Project Office

Reporting Period: Oct. 1–Dec. 31, 1990

Objectives

The primary objective of this project is to develop an integrated database to characterize reservoir heterogeneities resulting from numerous small-scale shallowing-upward cycles comprising the Pennsylvanian Wahoo Limestone of northeastern Alaska. The Wahoo Limestone is the upper part of the extensive carbonate platform sequence of the Carboniferous Lisburne Group that is widely exposed in the Brooks Range and is a widespread potential reservoir unit in the subsurface of the North Slope of Alaska.

The project involves a number of carbonate researchers from four institutions. A computerized database system is being developed to accommodate information on carbonate petrology, diagenesis, and biostratigraphy derived from analyses of thousands of samples systematically collected from over 25 stratigraphic sections in the Arctic National Wildlife Refuge (ANWR). The objective is to determine lateral and vertical variations in the complex mosaic of carbonate facies comprising the Wahoo Limestone.

The correlation scheme, with distinct marker beds and cyclic stratigraphy, allows interpretation of the depositional history and paleogeographic evolution of the region and development of predictive facies models and paleogeographic maps. Biostratigraphic data, provided by the University of Montreal (algae and foraminifera) and the U.S. Geological Survey (conodonts), are serving as independent means of correlation. Exposure surfaces and associated variations in cement stratigraphy analyzed by the University of Kansas figure importantly in refining these correlations.

The ultimate goal is to construct sea-level curves modeling the carbonate cycles and to evaluate the use of cyclic stratigraphy as a means of correlation. In the later stages of the project, the relationship between cyclic stratigraphy and reservoir properties in correlative rocks at the Lisburne oil field will be examined, in addition to testing the use of cyclic stratigraphy for regional correlations. The detailed analysis of the Wahoo Limestone will provide a basis for interpreting correlative rocks in the adjacent subsurface of the coastal plain of ANWR, a potential hydrocarbon lease–sale area. In a broader sense, this work will provide an excellent example of carbonate shallowing-upward cycles that are ubiquitous in shallow-marine carbonate sediments. If the cyclicity resulted from global (eustatic) sea-level fluctuations, the sea-level curves may be applicable to Pennsylvanian rocks elsewhere.

Summary of Technical Progress

Following field work conducted in the summer of 1990, work in the fall of 1990 involved processing samples for later petrographic and conodont analyses. Geochemical analyses of stable isotopes ($\delta^{13}C$ and $\delta^{18}O$) of selected cements yielded interesting results that are apparently related to previously recognized subaerial exposure surfaces.

Computerized Database

A report form was developed to summarize some of the most important petrographic information contained in the

Wahoo database (Table 1). The symbols used to indicate the different grain types allow much information to be presented in petrographic reports. With this format (Table 1), data entered into the Wahoo database during the September 1989–1990 fiscal year were reported in the first annual report.[1] These tables provide a detailed record of compositional changes in different carbonate lithologies and interpretations of depositional environments.

TABLE 1

Example of a Report Compiling Some of the Data Contained in the Wahoo Computerized Database

Sample Number *	Grains > 10%	Grains < 10%	Carb Lithology †	Paleoenvironment ‡
AK10M0			Packstone	open platform
AK10M0.5			Packstone	open platform
AK10M1			Grainstone	open platform
AK10M1.5			Packstone	restricted platform
AK10M2			Grainstone	open platform
AK10M2.5			Packstone, Wackeston	restricted platform
AK10M3			Packstone	restricted platform
AK10M3.5			Packstone	restricted platform
AK10M4			Packstone	open platform
AK10M4.5			Packstone	restricted platform
AK10M5			Wackestone	restricted platform
AK10M6			Wackestone	restricted platform
AK10M6.5			Packstone	open platform
AK10M7			Packstone	open platform
AK10M7.5			Wackestone	restricted platform
AK10M8			Packstone, Wackeston	restricted platform
AK10M8.5			Wackestone	restricted platform
AK10M9			Packstone	restricted platform
AK10M9.5			Packstone, Wackeston	restricted platform
AK10M10			Grainstone	open platform
AK10M11			Grainstone	open platform
AK10M11.5			Boundstone	open platform
AK10M12			Packstone	restricted platform
AK10M12.5			Packstone	open platform
AK10M13			Packstone	restricted platform
AK10M13.5			Packstone	restricted platform

LEGEND

SKELETAL GRAINS

- Pelmatozoan
- Bryozoan (full-frond fenestrate)
- Bryozoan (undifferentiated)
- Brachiopod
- Bivalve
- Gastropod
- Foraminifera
- Trilobite
- Ostracod
- Sponge Spicule
- Colonial Coral
- Solitary Coral
- Coral (undifferentiated)
- *Asphaltina sp.*
- *Donezella sp.*
- *Calcisphaera sp.*
- Algae (undifferentiated)
- Bioclast (undifferentiated)

NON - SKELETAL GRAINS

- Ooid
- Superficial Ooid
- Peloid
- Intraclast
- Grapestone
- qtz Detrital Quartz

*The sample number is in two parts: AK10M refers to the Shublik Mountains stratigraphic section; the subsequent number is in meters above the base of the section.

†The carbonate lithology column provides textural information using the Dunham limestone classification.

‡Paleoenvironmental interpretations are based on grain types and lithology together with position within a parasequence and relationship to adjacent lithologies.

Diagenetic Studies

Samples collected during the 1990 field season were processed to make doubly polished thin sections for detailed studies of diagenesis. Microsamples of selected calcite cements in the Wahoo Formation from the northern Sadlerochit Mountains (Marsh Creek section; see Fig. 3 in Ref. 1) were analyzed to determine stable isotope ratios. Stable isotopic ratios of carbon ($\delta^{13}C$) and oxygen ($\delta^{18}O$) contained in calcite cements are commonly used as indicators of the diagenetic environment in which the cements formed.

Two types of cements in the Wahoo Limestone were analyzed. Nonferroan calcite forms syntaxial overgrowths on echinoderm grains, and ferroan calcite occurs as the outer growth zones on syntaxial overgrowths or as medium to coarsely crystalline, equant, void-filling spar. Earlier studies of petrographic fabrics, with the use of cathodoluminescence zonation and the distribution of distinct cements within the stratigraphic sequence, led to the following hypotheses: (1) the nonferroan calcite formed in shallow, freshwater diagenetic environments during intermittent periods of subaerial exposure within the Wahoo Limestone, and (2) the ferroan calcite formed after significant burial in a reducing environment.

Nonferroan Calcite Cements

A plot of $\delta^{13}C$ and $\delta^{18}O$ of nonferroan calcite vs. position in the stratigraphic sequence shows five groups of related measurements with consistent trends (part a of Fig. 1). As shown in a $\delta^{13}C$–$\delta^{18}O$ cross plot (part b of Fig. 1), these groups also have distinct but partially overlapping fields. The three lower groups (Groups 1 to 3 in Fig. 1) show depletion (decreasing values) of $\delta^{13}C$ upsection toward subaerial exposure surfaces previously recognized in field studies. Groups 1 and 2 both show upward enrichment (increasing values) in $\delta^{18}O$. Data points in Group 3 are too widely spaced to distinguish the effects of the two subaerial exposure surfaces associated with this part of the section. The fourth group of data points has the most positive $\delta^{13}C$ values. The nearest subaerial exposure surface is 40 m above Group 4, and no trends are evident within this tightly grouped cluster of points. Group 5 has lower values for both $\delta^{13}C$ and $\delta^{18}O$, but no trends are evident over the stratigraphic interval sampled. No isotopic data are available for the uppermost Wahoo at this time. However, the lower isotopic values toward the top of the Wahoo may be related to major unconformity that truncates the top of the Lisburne Group beneath the Permian Echooka Formation.

The separate groups of isotopic data for the nonferroan calcite cements indicate that pore waters had variable isotopic compositions that resulted in the precipitation of the different cements throughout the stratigraphic sequence. The apparent relationship between subaerial exposure surfaces and trends in isotope composition suggests that these cements formed because of freshwater influx during these exposure events. Most compelling are the abrupt depletion in $\delta^{13}C$ across the exposure surfaces and gradual upward depletion in $\delta^{13}C$ and upward enrichment in $\delta^{18}O$ toward exposure surfaces in the lower two groups of isotopic data.

Ferroan Calcite Cements

In general, the ferroan calcite cements in the Wahoo Limestone have slightly more positive $\delta^{13}C$ and much more negative $\delta^{18}O$ compared with average values for the nonferroan calcite cements (Fig. 2). These values support the hypothesis that the ferroan calcite formed in a deep burial setting. Theoretically, mature fluids, such as brines, may have a more positive $\delta^{13}C$, whereas higher temperature during burial cementation would cause fractionation of the oxygen isotopes and thus result in more negative $\delta^{18}O$ values. This hypothesis may not account for all the ferroan calcite in the Wahoo Limestone. Because of considerable overlap in the nonferroan and ferroan calcite data, much of the ferroan calcite may have formed under reducing conditions imposed by progressive occlusion of porosity and permeability. With stagnation resulting from cementation and reduced flow of pore fluids, the nonferroan calcite may have precipitated while still within a freshwater diagenetic environment. The ferroan calcite filling fractures typically have more negative values, which may indicate burial cementation.

Biostratigraphic Studies

Conodont samples collected during the 1990 field season were shipped for processing (Table 2). Results are expected in March 1991.

Regional Stratigraphic Framework

Samples collected from fifteen stratigraphic sections measured during the 1990 field season were processed, and chips were sent to a petrographic lab for thin sections to be made. Studies of down-dip changes in the nature of shallowing-upward cycles (parasequences) on a carbonate ramp are nearing completion. In September, a research project on cyclicity in the Lisburne Group was begun. Regional variations in the nature of shallowing-upward cycles will be analyzed and the type of detailed analyses mentioned in previous studies will be extended farther down depositional dip to examine basinal facies at Wahoo Lake and updip to examine shallower-marine deposits in the eastern Sadlerochit Mountains. The work may also include analysis of core from the subsurface of Prudhoe Bay (see Fig. 3 Ref. 1). Various DOE reports were written for the DOE peer review, and progress was made on a paper on the stratigraphic framework of the Lisburne Group to be submitted to the American Association of Petroleum Geologists Bulletin.

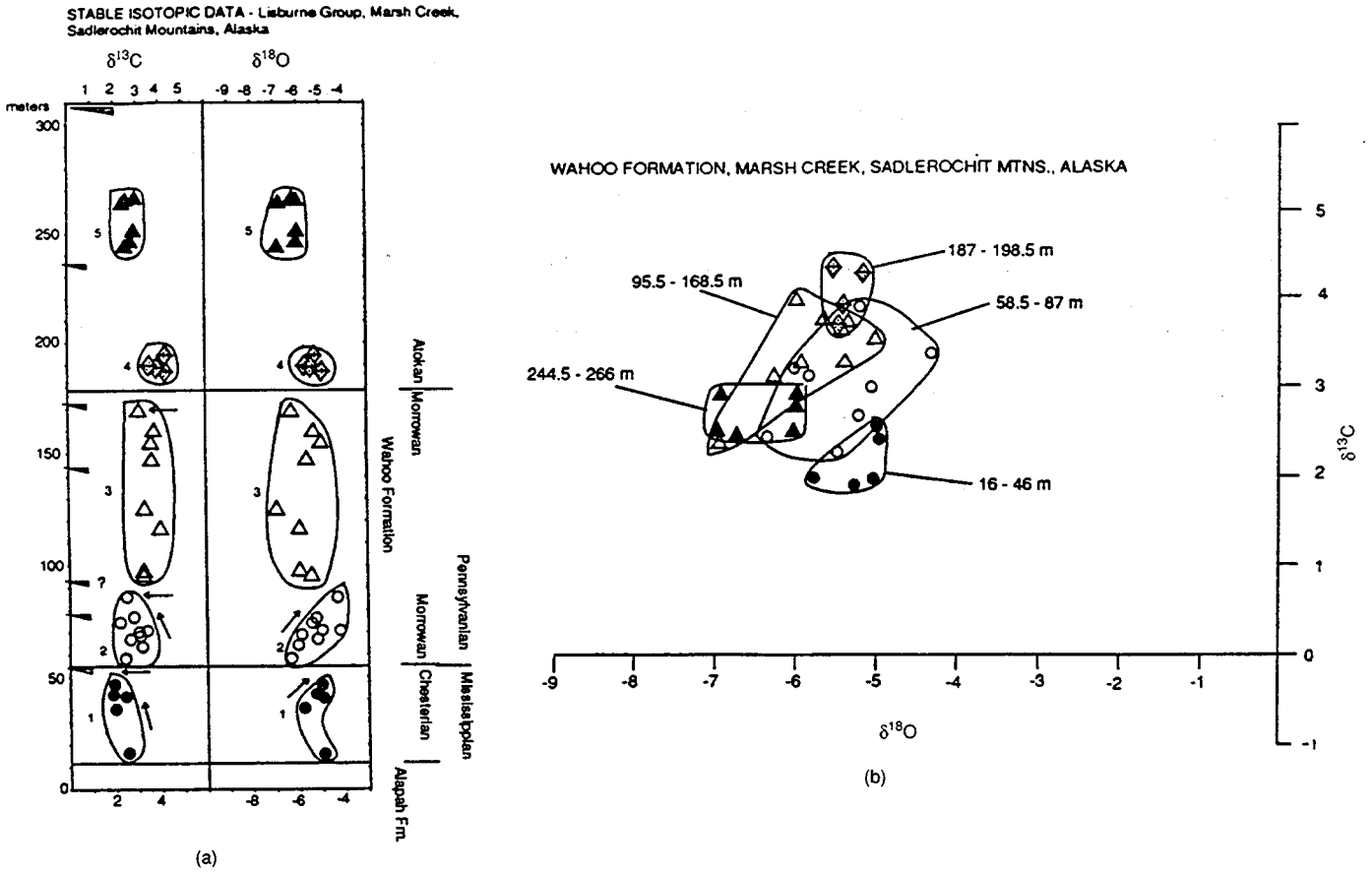

EXPLANATION OF SYMBOLS FOR CARBON AND OXYGEN STABLE ISOTOPES

nonferroan calcite cements
- 16 - 46 m
- 58.5 - 87.0 m
- 95.5 - 168.5 m
- 187 - 198.5 m
- 244.5 - 266 m

ferroan calcite cements
- intergranular pores
- fractures

Trends in isotope data
- more negative upward
- more positive upward
- negative shift downward

surface of subaerial exposure identified from outcrop and petrographic evidence.

Fig. 1 Stable isotopes in nonferroan calcite cements in the Wahoo Limestone. (a) Isotopic values of $\delta^{13}C$ and $\delta^{18}O$ are plotted against position in stratigraphic section in the northern Sadlerochit Mountains. Groups of circled data points are discussed in the report. (b) Cross plot of $\delta^{13}C$ and $\delta^{18}O$ showing the same groups of data points outlined in part a.

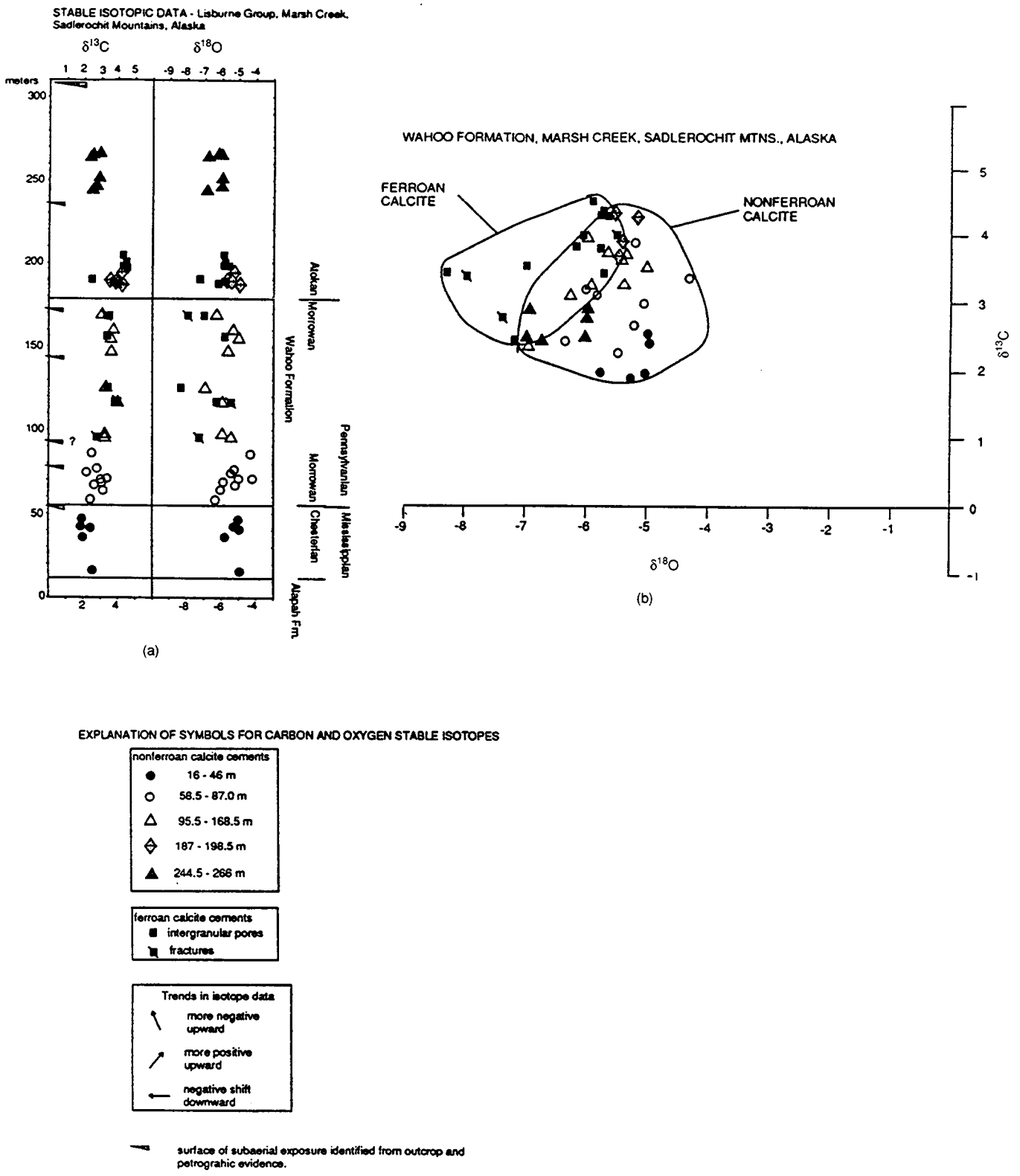

Fig. 2 Stable isotopes in calcite cements in the Wahoo Limestone. (a) Isotopic values of $\delta^{13}C$ and $\delta^{18}O$ are plotted against position in stratigraphic section in the northern Sadlerochit Mountains and includes data from ferroan cements (small squares). (b) Cross plot of $\delta^{13}C$ and $\delta^{18}O$ compares ferroan and nonferroan calcite cements.

TABLE 2

List of Conodont Samples Collected During the 1990 Field Season and the Number of Thin Sections Being Made from Samples Collected from Each Stratigraphic Section Measured by Watts*

Conodont Samples collected by Keith Watts, Julie Dumoulin, and Sue Morgan in 1990, University of Alaska

Sample	Museum Number	Location	Stratigraphic Section	Latitude - Longitude	Thin sections
90KW38		Echooka anticline	uppermost Wahoo, <5m below Echooka	69° 09.4'N 146° 57.9'W	
990A- 0.2	AK80M	Echooka anticline	upper Wahoo,132 m below Echooka contact	69° 09.5'N 146° 56.9'W	126
90A- 26.0	AK80M	Echooka anticline	upper Wahoo,132 m below Echooka contact	69° 09.5'N 146° 56.9'W	
90A- 68.0	AK80M	Echooka anticline	upper Wahoo,132 m below Echooka contact	69° 09.5'N 146° 56.9'W	
90A- 105.3	AK80M	Echooka anticline	upper Wahoo,132 m below Echooka contact	69° 09.5'N 146° 56.9'W	
90KW42	AK80M	Echooka anticline	uppermost Wahoo, below Echooka contact	69° 09.5'N 146° 56.9'W	
90B-4.5	AK81M	Wahoo Lake	upper Wahoo, just below Echooka	69° 02.0'N 147° 03.5'W	18
90D-0.5	AK83M	Wahoo Lake	within Wahoo Limestone, incomplete section	69° 01.0'N 147° 00.8'W	8
90E-0.5	AK84M	Wahoo Lake	lowest well-exposed Alapah Fm	69° 01.6'N 147° 03.5'W	35
90E-32	AK84M	Wahoo Lake	Alapah Fm., coralline dolo, 156 m below Wahoo	69° 01.6'N 147° 03.5'W	
90E-43.3	AK84M	Wahoo Lake	upper Alapah Fm., 145 m below Wahoo	69° 01.6'N 147° 03.5'W	
90E-137.5	AK84M	Wahoo Lake	Alapah, top of exposure, above speleothems	69° 01.6'N 147° 03.5'W	
90F-0.3	AK85M	Atigun Gorge	upper part of Wahoo Formation,	68° 29.3'N 149° 09.7'W	20
90F-7.5	AK85M	Atigun Gorge	upper part of Wahoo Formation,	68° 29.3'N 149° 09.7'W	
90F2-5.5	AK86M	Atigun Gorge	upper part of Wahoo Formation,	68° 29.3'N 149° 09.7'W	24
90F3-12.3	AK87M	Atigun Gorge	Wahoo just below silicified zone and Siksikpuk	68° 29.3'N 149° 09.7'W	16
90G-0.5	AK89M	Atigun Gorge	limestone marker in Kayak	68° 26.7'N 149° 15.8'W	62
90G-156.0	AK89M	Atigun Gorge	limestone marker in Kayak , thrust repeat?	68° 26.7'N 149° 15.8'W	
90G-210.5	AK89M	Atigun Gorge	lowest exposed Lisburne above Kayak	68° 26.7'N 149° 15.8'W	
90G-439.5	AK89M	Atigun Gorge	base of cliff-forming unit in lower Lisburne	68° 26.7'N 149° 15.8'W	
90G-474.0	AK89M	Atigun Gorge	Lisburne, ~260 m above base	68° 26.7'N 149° 15.8'W	
90G-532.0	AK89M	Atigun Gorge	Lisburne, ~322 m above base	68° 26.7'N 149° 15.8'W	
90G-545.5	AK89M	Atigun Gorge	Lisburne, top of small peak on ridge	68° 26.7'N 149° 15.8'W	
90G2-10.8	AK90M	Atigun Gorge	Lisburne, ~345 m above base, grainstone	68° 26.3'N 149° 15.3'W	23
90G2-44.5	AK90M	Atigun Gorge	Lisburne, ~380 m above base	68° 26.3'N 149° 15.3'W	
90G2-54.0	AK90M	Atigun Gorge	Lisburne, ~355 m above base, top of section	68° 26.3'N 149° 15.3'W	
90H-0.0	AK91M	Itikmalak Creek	Wahoo Formation, Siksikpuk contact at 8m	68° 22.9'N 149° 41.7'W	10
90KW50	AK91M	Itikmalak Creek	uppermost Wahoo Formation below Siksikpuk	68° 22.9'N 149° 41.7'W	
90I-1.0	AK92M	Shainin Lake	limestone in Kayak, 34 m below Wachsmuth	68° 19.5'N 150° 59.0'W	14
90I-34.5	AK92M	Shainin Lake	lowermost Wachsmuth, contact at 35m	68° 19.5'N 150° 59.0'W	
90J-61.5	AK93M	Shainin Lake	Wachsmuth Formation, >61.5 m above Kayak	68° 19.4'N 151° 00.5'W	32
90J-108.0	AK93M	Shainin Lake	Wachsmuth Formation, > 108.0 m above Kayak	68° 19.4'N 151° 00.5'W	
90K-24.0	AK94M	Shainin Lake	Wachsmuth Formation, ~ 350 m below Alapah	68° 19.5'N 151° 01.2'W	89
90K-159.0	AK94M	Shainin Lake	Wachsmuth Formation, ~ 214 m below Alapah	68° 19.5'N 151° 01.2'W	
90K-215.5	AK94M	Shainin Lake	Wachsmuth Formation, ~ 158 m below Alapah	68° 19.5'N 151° 01.2'W	
90K-305.0	AK94M	Shainin Lake	Wachsmuth Formation, ~ 68 m below Alapah	68° 19.5'N 151° 01.2'W	

Systematic conodont sampling of Andrea Krumhardt in 1990, University of Alaska

Sample	Museum Number	Location	Stratigraphic Section	Latitude - Longitude	Conodont Samples
87B-	AK11M	Shublik Mountains	Alapah	69° 30.8'N 145° 39.7'W	20
87C-	AK12M	Shublik Mountains	lower Wahoo	69° 31.0'N 145° 41.4'W	2
87D-	AK13M	Fourth Range	Alapah, lower Wahoo, and upper Wahoo	69° 21.0'N 145° 38.5'W	70
88A-	AK22M	eastern Sadlerochit	lower and upper Wahoo	69° 38.6'N 144° 34.7'W	12
AK90C	AK78M	eastern Sadlerochit	lower Wahoo, Miss.-Penn. boundary	69° 38.6'N 144° 34.7"W	3
AK90D	AK79M	eastern Sadlerochit	upper Alapah below section 88A	69° 38.6'N 144° 34.7"W	13
86A1	AK1M	eastern Sadlerochit	Wahoo, Carlson's Ridge	69° 37.9'N 144° 36.8'W	3
86A2	AK2M	eastern Sadlerochit	Alapah	69° 38.2'N 144° 37.4'W	6

*Krumhardt systematically collected conodont samples from stratigraphic sections previously measured and sampled for petrographic studies (microfacies and diagenesis); thin sections prepared for each sample will allow comparison of lithofacies/microfacies data with conodont biofacies analyses.

References

1. K. F. Watts, Analysis of Reservoir Heterogeneities Due To Shallowing-Upward Cycles in Carbonate Rocks of the Pennsylvanian Wahoo Limestone of Northeastern Alaska, *First Annual Progress Report,* Bartlesville Project Office, 1991.
2. K. F. Watts, R. C. Carlson, P. Gruzlovic, T. A. Imm, A. P. Krumhardt, A. G. Harris, B. Mamet, and J. D. Dumoulin, Stratigraphic Framework and Depositional History of the Lisburne Group, Northeastern Alaska, to be submitted to the American Association of Petroleum Geologists Bulletin.

CHARACTERIZATION OF OIL AND GAS RESERVOIR HETEROGENEITY

Contract No. FG22-89BC14403

University of Texas
Austin, Tex.

Contract Date: September 1988
Anticipated Completion: September 1991
Government Award: $235,000
(Current year)

Principal Investigator:
William Fisher

Project Manager:
Chandra Nautiyal
Bartlesville Project Office

Reporting Period: Oct. 1–Dec. 31, 1990

Objectives

Progress in the seventh quarter of research funded under the auspices of Memorandum of Understanding (MOU) Annex I is summarized with respect to seven main subtask areas. These are: (1) definition of the distribution of carbonate sandbar facies for Grayburg reservoirs, (2) definition of three-dimensional (3-D) geometry of carbonate sand bodies, (3) analysis of engineering and petrophysical attributes of reservoir flow units, (4) development and testing of extended conventional oil recovery strategies, (5) characterization of gas reservoirs, (6) geologic and engineering characterization of generic gas reservoir types, and (7) refinement of exploitation strategies. Key areas of progress for the seventh quarter concern subtasks 1, 2, 3, and 6.

Summary of Technical Progress

Subtask 1

The regional reservoir framework of the Grayburg in the Guadalupe Mountains and in the North Foster Grayburg area, eastern Central Basin Platform, has been completed, and synthesis of these data is nearly complete. An upcoming publication of the outcrop Grayburg stratigraphy/reservoir framework will be published initially as a Permian Basin Society of Economic Paleontologists and Mineralogists (SEPM) field trip guidebook (April 1991). Write-up of the subsurface stratigraphic/reservoir framework studies is ongoing and nearing completion.

Detailed mapping of high-porosity/permeability packstones/grainstones in both outcrop and subsurface and mapping of production data from the North Foster Grayburg Unit both indicate that higher quality reservoir facies are concentrated seaward of the underlying San Andres shelf margin. For better characterization of this relationship, additional outcrop data were collected during the seventh quarter from the Last Chance Canyon in the Central Guadalupe Mountains. Here Grayburg outcrops span the underlying San Andres shelf margin and display thickening of grainstone complexes crossing from landward to seaward across the underlying margin. Some additional outcrop data will be collected during the eighth quarter to finalize these critical reservoir-framework–scale relationships.

Subtask 2

Data from 16 measured sections at 1000 to 2000 ft lateral spacing have enabled subdivision of the Grayburg outcrop into 34 upward-shallowing, upward-coarsening parasequences that define the reservoir framework scale of the outcrop analog study. During the seventh quarter, a detailed window study area in a ramp-crest setting (Stone Canyon window) was developed to help quantify variability of geological facies and petrophysical parameters on an interwell scale. Nine detailed sections at 100 to 300 ft lateral spacing covering mainly the highstand systems tract portion of the Grayburg (200 ft vertical by 2000 ft lateral) form the framework. Within this framework individual carbonate grainstone bodies were selected for petrophyscial quantification.

More than 270 plug samples for porosity and permeability analysis were collected with a portable core-plug drill from one of the highstand grainstone bars at Stone Canyon. Sampling strategy was directed at establishing characteristic porosity and permeability parameters for the various Grayburg facies that compose the grainstone-dominated strata at Stone Canyon, mapping laterally porosity and permeability on a single depositional interval (parasequence), and mapping porosity and permeability on several foot-scale grids to assess inch-scale variability for scaling up analysis.

The lateral sampling exercise included geologic description and sampling at 6-in. vertical spacings of the interval at five locations spaced 350 to 700 ft apart and supplementary sampling at 6-in. vertical spacing of three additional sections spaced 90 ft apart between two of the five geologically described sections. Additionally, two

grids with 2-in. sample spacing were located at opposite ends of the outcrop-sampling area, a distance of 2000 ft.

The condition of the samples was very good, and initial test results suggest that data quality will be excellent for mapping and petrophysical analysis.

Subtask 3

Subtask 3 is a parallel study of a subsurface Grayburg reservoir to allow evaluation of outcrop data/modeling as applied to an active reservoir in a similar depositional setting. The reservoir selected was the ARCO North Foster Unit. A detailed examination of cores and logs from the North Foster Unit and the surrounding area is now complete, and results are being compiled for a final report on the subsurface portion of this project. This reservoir study concentrated on the ARCO North Foster Unit, from which the operator made available logs from 127 wells; continuous cores from 7 wells; and production, well-history, and test data for all wells. Cores from the adjoining leases were also examined to provide insight as to the lateral extent of the facies recognized in the North Foster Unit. ARCO provided logs and cores from eight wells from their J. L. Johnson AB and D leases. Conoco provided logs and cores from two wells in their J. L. Johnson Unit and one from their Gist Unit, and cores and logs were also obtained from six wells in the Cities Service Johnson Grayburg/San Andres Unit.

All cores in the study area were correlated on the basis of early recognition of nine major correlation markers. After these correlations were established, the cross sections were examined in more detail for identification of smaller scale features recognized from the Grayburg outcrop study. The basal Grayburg consists of 20 ft of coarse-grained grainstone followed by 60 ft of fusulinid wackestone, which represents the maximum flooding event of the Grayburg over the San Andres tidal flat. The overlying highstand section consists of 19 upward-coarsening cycles that range in thickness from 4 to 20 ft.

As a general rule, each cycle contains more mud in the lower part and more grains in the upper part. Silty mudstone or siltstone occurs at the base of many cycles. Laterally, three facies belts have been identified: tidal-flat birdseye and coated-grain grainstone of the ramp crest, coarse-grained grainstone of the ramp crest, and diagenetically altered fine-grained grainstone of the outer ramp. The ramp-crest facies occur on the western side of the field in north-south-oriented bands approximately 1 mile wide, but the west limit of these facies has not been delineated; the outer-ramp facies tract occurs as a northwest-trending 2-mile-wide band on the east side of the field. To the east, the outer-ramp facies grades into the fusulinid wackestone facies.

Subtask 6

In this subtask, which is cofunded by the Gas Research Institute, the aim is to document the spatial variation in geometric and petrophysical attributes in a deltaic reservoir with the Cretaceous Ferron Sandstone of central Utah as an analog for Gulf Coast deltaic reservoirs. During this quarter field data obtained from three outcrop windows—the Teardrop Hill window in north Muddy Creek, the south Muddy Creek window, and the Pictured Flats window—were processed. Delta-front and distributary-channel complexes along Muddy Creek and Pictured Flats were selected for detailed study on the basis of their exposure, accessibility, and permeability characteristics. The Muddy Creek windows were selected to contrast heterogeneity on the proximal delta platform, where distributary channels are dominant, with that in locations farther seaward, where the increased influence of marine processes is manifested. In the Pictured Flats window, less than 2 miles seaward of Muddy Creek, marine reworking of the delta platform results in sand-body geometries that are markedly different from those in Muddy Creek.

In the Pictured Flats and Muddy Creek windows located in the updip parts of the delta platform, Ferron Deltaic Unit 5 consists of basal delta-front sandstones that are erosionally overlain by distributary-channel and associated sandstones. Thickness and geometries of the delta-front sandstones have therefore been influenced by both depositional and erosional processes. Thicknesses of the delta-front sands range from 0 (where erosionally removed) to 35 ft.

The delta-front sandstone interval is a composite of at least four subintervals. In each of the subintervals, grain size is very fine and does not appreciably increase vertically. The maximum flooding surface at the base of the deltaic succession contains relict, locally preserved, hummocky cross-stratification; however, intense bioturbation is the dominant characteristic of this sandstone. Overlying the bioturbated zone are three discrete subintervals containing hummocky, planar, trough, and ripple cross-stratification. Lateral facies variation in the subintervals is subtle, and no well-defined facies boundaries have been detected.

Vertical variation, in contrast, is pronounced. The lower bounding surface of each delta-front subinterval is erosional; upper bounding surfaces are composed of laterally continuous interbedded siltstone and mudstone layers. The uppermost of the subintervals is the thickest. Its basal surface is strongly erosional into the underlying subinterval.

The external geometry of the fluvially dominated, wave-modified delta-front sandstones is lobate. Internally, however, individual sandstone subunits display a tabular geometry. Each of the tabular subintervals extends downdip for at least 1 mile. Thus the dominant style of heterogeneity in the delta-front sandstones is vertical stratification with subintervals ranging from 3 to more than 10 ft thick. Lateral heterogeneity resulting from depositional processes in the subintervals is minimal, and component lateral variability of the delta-front sandstones is more a product of the erosive processes associated with the deposition of the superposed distributary sandstones.

Sandstones deposited in the distributary system are characterized by a high degree of both lateral and vertical heterogeneity. Three stages of channel formation are recognized in the distributary system: (1) early tidally influenced channels, (2) channel sedimentation dominated by lateral accretion, and (3) channel sedimentation characterized by deep, relatively narrow channels. Each stage of channel sedimentation is characterized by distinctive internal and external geometries.

Tidally influenced channels: At the base of the distributary complex and erosive into the underlying, tabular delta-front sandstones is a series of relatively narrow and laterally isolated channel sandstones. The channels are mostly small features characterized by remarkably consistent width/thickness ratios (average of 9.5). Bedding in the tidally influenced channels is varied. Large avalanche foresets are locally present in the main axis of the channel. Herringbone crossbedding may be present on the shallower flanks of the channels. Paleocurrent directions are bimodal.

Early meandering distributary channels: Early-stage meandering distributary-channel sandstones are much more laterally extensive than the subjacent tidally modified channel sandstones. The two distributary-channel complexes exposed in Muddy Creek are 1200 and 1320 ft wide, respectively. The channels are strongly erosional into the underlying channels and into the delta-front sands and locally erode completely through the delta-front sandstones. The channel complexes shale out laterally into overbank muds and silts or are truncated by superjacent distributary-channel sandstones.

A typical vertical sequence contains three stratal types beginning with a basal zone of clay-clast-bearing trough crossbeds that overlie a sharp erosional base. These mud clasts typically deform into pseudomatrix during compaction. These mud-clast-rich zones display substantially lower permeabilities than the mid-to-upper distributary sediments and may provide effective baffles to fluid flow. Grain size decreases upward, ranging from very coarse to medium fine. Planar crossbeds with minor amounts of horizontal stratification abruptly overlie trough crossbeds and also display an upward-decreasing trend in stratification and grain size, from medium to small scale and medium- to fine-grained, respectively. The sequence is capped by fine- to very fine-grained, moderately to highly contorted strata or less commonly by very fine-grained ripple laminated sandstones.

The dominant characteristic of this lithofacies is well-defined lateral accretion surfaces that dip gently toward the channel thalweg. Angles of dip of the accretion surfaces are between 4 and 8°. There is considerable variability in the dimensions of the point-bar packages bounded by the accretion surfaces. Updip in the distributary system (in Muddy Creek) widths of the sigmoid-shaped point-bar bodies averages 360 ft but ranges from 75 to almost 700 ft. Individual lenses are 3 to 15 ft thick and erosionally overlap to form multilateral sand bodies with cumulative thicknesses of 15 to 40 ft. Individual sand lenses are 100 to 400 ft wide; belt width is up to 1200 ft. There are also substantial differences between the lateral-accretion-bounded point-bar sandstones in Muddy Creek and those farther seaward in Pictured Flats canyon, where the sigmoidal bodies have narrowed slightly (average of 308 ft) but are twice as thick as the equivalent units in Muddy Creek. These assemblages compose two distinct populations. Width/thickness ratios decrease seaward from 48:1 in Muddy Creek to 21:1 in Pictured Flats canyon.

Bounding elements are subhorizontal to inclined discontinuities that divide stratal types into subsets as well as separate genetic facies. Bounding elements considered in this investigation include contacts among different stratal types, channel scours, and lateral accretion surfaces. In the lower part of the complex, bounding elements separating individual sand bodies consist dominantly of a scoured surface overlain by poorly sorted, mud-clast-rich sandstone. In the middle-to-upper part of the complex, the bounding elements consist of scoured sand on sand contacts and lateral accretion surfaces. Clay drapes are not a common feature in this channel type.

Late-stage distributary channels: Channel deposits that formed during the final stage of distributary-channel sedimentation are narrower than those in the underlying, highly meandering distributary complex but are considerably thicker. Typically, these late-stage point bars are perched above and erode deeply into the subjacent sandstones. The basal point-bar contacts are typically rich in intraformational mud clasts.

Because lateral accretion surfaces in the late-stage distributaries are not accentuated by abundant mudchips, they are less well defined than those of the early meandering distributaries. In the Teardrop Hill window, remnant accretion surfaces are mainly preserved at the base of the channel sandstones, the upper part of the point bar being characterized by intense contortion of the fine-grained sandstones.

RESERVOIR CHARACTERIZATION OF PENNSYLVANIAN SANDSTONE RESERVOIRS

Contract No. DE-AC22-90BC14651

University of Tulsa
Tulsa, Okla.

Contract Date: Aug. 9, 1990
Anticipated Completion: Aug. 8, 1993
Government Award: $100,316

Principal Investigator:
Balmohan G. Kelkar

Project Manager:
Rhonda Patterson
Metairie Site Office

Reporting Period: Oct. 1–Dec. 31, 1990

Objectives

The overall objectives of this work are to (1) investigate the importance of various qualities and quantities of data on the optimization of waterflooding performance and (2) study the application of newly developed, geostatistical techniques to analyze available production data to predict future prospects of infill drilling.

Specifically, for the first objective, the feasibility of applying fractal geometry concepts to characterize individual formations will be studied; a three-dimensional conditional simulation program to define reservoir properties at various scales will be developed; a method to integrate the data collected at various scales, including the well test and the core data, will be established; and the utility of outcrop data for describing subsurface reservoir details will be investigated. For the second objective, various techniques to utilize the production data, including initial potential and the production decline, in proposing a possible location for a future infill well will be investigated. The techniques investigated will include geostatistical and time-series analyses. The study will be restricted to Pennsylvanian sandstone reservoirs commonly found in Oklahoma.

Summary of Technical Progress

Collection of Data

After preliminary analysis of the available information, two fields were selected for further investigation. These two fields are Burbanks field operated by Phillips Petroleum Company and Glenpool field operated by various companies. The data collection from the Burbanks field has already begun. Log data, core data, well test data, and geological information have already been collected for that field. For the Glenpool field, the possibility of getting the data from two operators has been discussed, and the data collection should begin shortly.

Waterflooding Optimization

Characterization with Fractals

The primary goal of this work is to study the feasibility of applying a fractal geometry technique to characterize producing formations. The characteristics dimension to be investigated is called an intermittency exponent, H (Ref. 1). Several techniques are available to estimate the value of H on the basis of the available data. These techniques include R/S analysis, spectral analysis, box counting method, and the variogram analysis. A computer program that incorporates all these techniques to analyze trace data has been developed. In addition, a new technique, an integral of variogram method, has been incorporated in the program.

The reliability of these various techniques needs to be tested with synthetic data having known properties. A program that uses a spectral analysis method has been written to generate synthetic fractional Gaussian noise (fGn) and fractional Brownian motion (fBm). Primary results indicate that for fGn traces the R/S analysis method and the box counting method are reliable when the H values are between 0.7 and 0.9 (values commonly observed for the wellbore data). For fBm traces, the variogram method seems to be a reliable estimator of the H value.

The next step includes further testing of synthetic traces over a wide range of H values. Once the reliability of the methods is established, the analysis will continue with the mixture of traces before applying it to the actual field data.

Three-Dimensional Conditional Simulation

Once the spatial variability of reservoir properties is established, a method is needed to generate the reservoir properties to describe the reservoir. A method of annealing has been selected for this purpose. Originally proposed by Farmer,[2] the method is based on the principle of swapping randomly generated values with a predefined probability function until a desired level of spatial relationships is established. The method is fast, flexible, and allows incorporation of various constraints in the generation of the reservoir properties.

A three-dimensional (3-D), conditional simulation program has been developed. The program allows two constraints: histogram of input data and the spatial relationships (defined by variograms) in several discrete directions. The type of variograms allowed include the conventional variograms, such as spherical and exponential variograms, and fGn and fBm functions, which can be used to describe the fractal behavior.

The annealing program is currently being tested. Synthetic data sets have been generated with known histogram and spatial structure. The generated values were compared with the input constraints. The match between the two is excellent. A preliminary study has also been

conducted where a cross section between two wells is generated with the information from those two wells. Log data from a third well, which is drilled between the two wells, is then compared with the simulated log data at the same location. The match between the two is quite good.

Future work includes optimization of the computer program, incorporation of other types of constraints, and investigation of additional data from some horizontal wells so that the structure in the areal direction can be predicted more reliably.

Effective Properties for a Grid Block

Reservoir properties are measured on various scales. Core data are collected on a 2-in. size, whereas the well test data are collected on a reservoir size of thousands of cubic feet. From the simulation point of view, determination of the grid block properties is of interest. A typical grid block size may vary between ten feet and one thousand feet in size.

So that the effective property of a grid block can be estimated, a two-dimensional system with a size of typical grid blocks will be simulated. It will be assumed that the grid blocks contain small-scale heterogeneities and that the structure of the heterogeneities is known. For simplicity, miscible, unit mobility ratio displacement will be assumed. A finite-element simulator with negligible numerical dispersion will be used for this study.

Simulation for the grid block will be carried out in two directions. These two directions will be normal to each other. Knowledge of the superficial velocities and the pressure gradients in x and y directions will allow the effective permeability tensor for the grid block to be solved. Definition of the same grid block with the effective tensor permeability will allow the results of the simulation to be compared with the results in the presence of small-scale heterogeneities.

The testing of the simulator is complete. Preliminary simulations indicate that the use of effective grid-block property gives reliable results. Additional testing is needed before any final conclusions.

Outcrop Studies

An outcrop has been selected for further studies. This outcrop is called a Blue Jacket sandstone and is located approximately 45 miles northeast of Tulsa. This outcrop contains the same Red Fork sand as the sand from which Glenpool field is producing. Coring of the outcrop will begin as soon as all the requisite permissions are gathered.

Infill Drilling

A synthetic reservoir is being used to develop a procedure to locate infill drilling prospects. The main advantage of using a synthetic reservoir is that there is no need to be concerned with production and operational constraints imposed upon the actual production. Further, drilling and location of the wells can be controlled.

The data from the Burbanks field will be used to generate a synthetic, but realistic, reservoir. Part of the Burbanks field was selected that is approximately 1900 acres in size. After the log and the core data were collected from all the wells located in that part, the facies present at each well location were identified. A total of five facies could be identified.

First a reservoir facies model will be constructed with the facies description and the help of indicator algorithm.[3] After this model is complete, grid block properties based on the facies description will be assigned. Once the properties are assigned, simulation of the reservoir performance by a black oil simulator will begin. So that the effect of time is minimized, it will be assumed that all the original wells are drilled at the same time. After these wells have produced for a fixed period, available geostatistical and time series techniques will be used to propose an optimum location of a new well. The actual performance will be compared with the predicted performance to test the applicability of these methods.

References

1. T. A. Hewett, *Fractal Distributions of Reservoir Heterogeneity and Their Influence on Fluid Transport*, paper SPE 15386 presented at the 1986 SPE Annual Technical Conference and Exhibition, New Orleans, La., Oct. 5–8, 1986.
2. C. L. Farmer, *Numerical Rocks*, paper presented at the joint IMA/SPE European Conference on the Mathematics of Oil Recovery, Robinson College, Cambridge University, July 25–27, 1989.
3. V. Suro-Perez and A. G. Journel, Stochastic Simulation of Lithofacies for Reservoir Characterization, paper presented in IMA Meeting, Airles, France, Sept. 4–9, 1990.

ANALYSIS AND EVALUATION OF INTERWELL SEISMIC LOGGING TECHNIQUES FOR RESERVOIR CHARACTERIZATION

Contract No. DE-AC22-90BC14649

Southwest Research Institute
San Antonio, Tex.

Contract Date: June 29, 1990
Anticipated Completion: June 1993
Government Award: $272,600
(Current year)

Principal Investigator:
Jorge O. Parra

Project Manager:
Chandra Nautiyal
Bartlesville Project Office

Reporting Period: Oct. 1–Dec. 31, 1990

Objective

The objective of this 3-yr research program is to investigate interwell seismic logging techniques for indirectly interpreting oil and gas reservoir geology and pore fluid permeability. This work involves a balanced study of advanced theoretical and numerical modeling of seismic waves transmitted between pairs of reservoir wells combined with experimental data acquisition and processing of measurements at controlled sites as well as in full-scale reservoirs. This reservoir probing concept is aimed at demonstrating unprecedented high-resolution measurements and detailed interpretation of heterogeneous hydrocarbon-bearing formations.

Summary of Technical Progress

Task 1

A computer program to calculate or predict seismic full waveforms associated with a point source in a layered elastic medium is being developed. This program will include numerical integration algorithms for solving irregularly oscillatory kernels. This numerical algorithm was tested with the use of simple models.

Task 2

The theory of seismic wave propagation for a point force in a stratified isotropic saturated porous medium was developed. A technical paper describing this theoretical analysis was submitted for publication to the *Journal of the Acoustical Society of America*. This paper is entitled "Analysis of Seismic Wave Propagation in Stratified Saturated Porous Media for Interwell Logging Applications."

Seismic data contain large amounts of information, including first-time-of-arrival, attenuation, and the diffraction patterns of the full waveforms. Analysis of the actual waveform requires solutions of the seismic wave equations in the unknown medium. The first-time-of-arrival and attenuation can be investigated with tomographic techniques. Computer programs have been developed for tomographic analysis with a number of numerical methods. For illustrative purposes, this discussion will be restricted to the use of first-time-of-arrival data but with the use of several data scans with various offset distances between the transmitter and receiver.

For a given pair of transmitter and receiver positions, the first-time-of-arrival depends upon the path that the seismic wave takes when traveling from the transmitter to the receiver. In general, the wave propagation can be determined by solving the wave equations. In the high-frequency (short-wavelength) regime, however, the propagation can be considered as rays. This approximation requires that all lengths of interest, including feature size and borehole separation, be much larger than the wavelength. In such an approximation, the measured travel time is actually an average of time intervals along the path. Mathematically, this can be represented as a line integral

$$T = \int_A^B \frac{d\ell}{v(x)} \tag{1}$$

where v(x) is the seismic velocity at a point x along the path from point A to point B. This is a nonlinear integral, however, because the actual path taken depends upon the velocity distribution of the medium, which is unknown.

The most obvious way to use Eq. 1 is to assume that the path is straight, which would be the case in a homogeneous medium. With this assumption, Eq. 1 becomes linear. The solution is to divide the region between the boreholes into rectangular cells. The velocity is assumed to be constant within each cell. Now the problem to be solved is to find the velocity in each cell. If many raypath measurements, with paths that cross throughout the region, are taken, sufficient information can be obtained to determine the velocity distribution. If there are M paths (measurements) and N cells (unknowns), then Eq. 1 can be written as a matrix equation:

$$[T_i] = [D_{ij}][S_j] \quad \begin{matrix} i = 1,\ldots M \\ j = 1,\ldots N \end{matrix} \tag{2}$$

Here, T_i is the measured travel times of the M paths and S_j is the inverse velocities (called "slowness" in the literature) of the N cells. Often N, the number of unknowns, is chosen to be less than M, the number of measurements. Because of this, as well as the ever-present measurement errors, Eq. 2 is a linear system that must be solved as a least-squares problem.

A number of techniques can be used to solve this linear least-squares problem. Currently three techniques are being used: (1) The Back-Projection Technique (BPT), which is a noniterative method; (2) the Simultaneous Iterative Reconstruction Technique (SIRT), which is an iterative method; and (3) a variant of the iterative conjugate-gradients method. Facilities are being incorporated in the method to allow the inclusion of any other known information about the problem, such as borehole logging data and velocity constraints, as well as smoothing, if desired.

The linear problem shown in Eq. 2 is usually somewhat ill-conditioned; that is, it has no unique solution. This is particularly true if there is any noise in either the distance matrix or the vector of travel times. Smoothing and variance conditions are introduced to stabilize and adhere to desired characteristics of the problem. These could be constraints or smoothing parameters. These additional conditions are coupled with the linear problem of Eq. 2 to make a larger linear system for solving with the aforementioned methods.

Synthetic data are being used to test the various methods to find the best methods to use under different circumstances. An example of a simple test model is shown in the

contour plot of Fig. 1. This model has a low velocity layer located in a higher velocity medium. The boreholes are 30 m deep with a separation of 10 m. There were 20 equally spaced source positions in the left borehole and 20 equally spaced detector positions in the right borehole for a total of 400 paths. The region was divided into a grid of 15 by 15 cells for a total of 225 cells. The slowness is plotted so that the middle layer had a slowness of 8.33 ns/m and the outer layers, 7.41 ns/m. The closely spaced contour lines of Fig. 1 show the sharp boundary.

Figure 2 shows the tomographic inversion with the use of the BPT method. Although not identical to the model, it does show the same basic nature, with the largest slowness being in a middle layer and the slowness tapering off slowly from there. The slowly varying nature of the solution is expected with this technique because it relies heavily on averaging methods.

Figure 3 shows an inversion of the synthetic model with the use of the SIRT method. This figure is in quite close agreement with the model; it shows clearly a flat low velocity layer between two high velocity layers. The actual values are also quite close; the values on the middle plateau range from 8.29 to 8.47 ns/m. The actual figure shown used some constraining (setting the values at the boreholes to the values in the original model), but when no constraints were used, only a small amount of undesired structure was shown. In more complicated geometries and situations, constraining is expected to make much more difference, especially with the introduction of measurement noise.

These calculations were done on a Hewlett-Packard 9000 Series 520 computer. The programs were written in FORTRAN. The BPT method took approximately 10 s to compute the inversion, whereas the SIRT method took approximately 10 min (the stopping criteria were not set

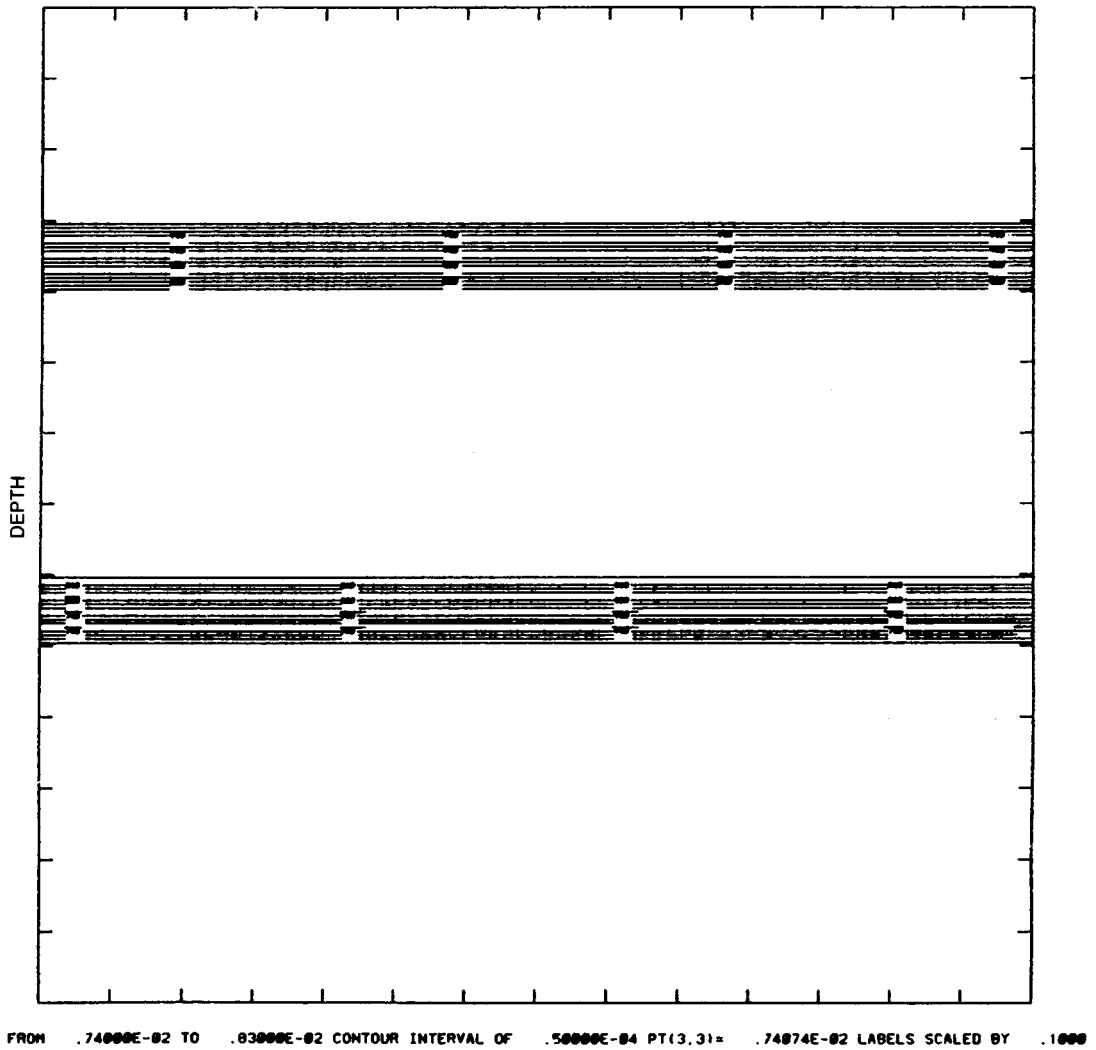

Fig. 1 Contour plot showing the velocity distribution of the model used to test the tomographic analysis. The horizontal axis is the lateral distance, with the boreholes at the left and right edges.

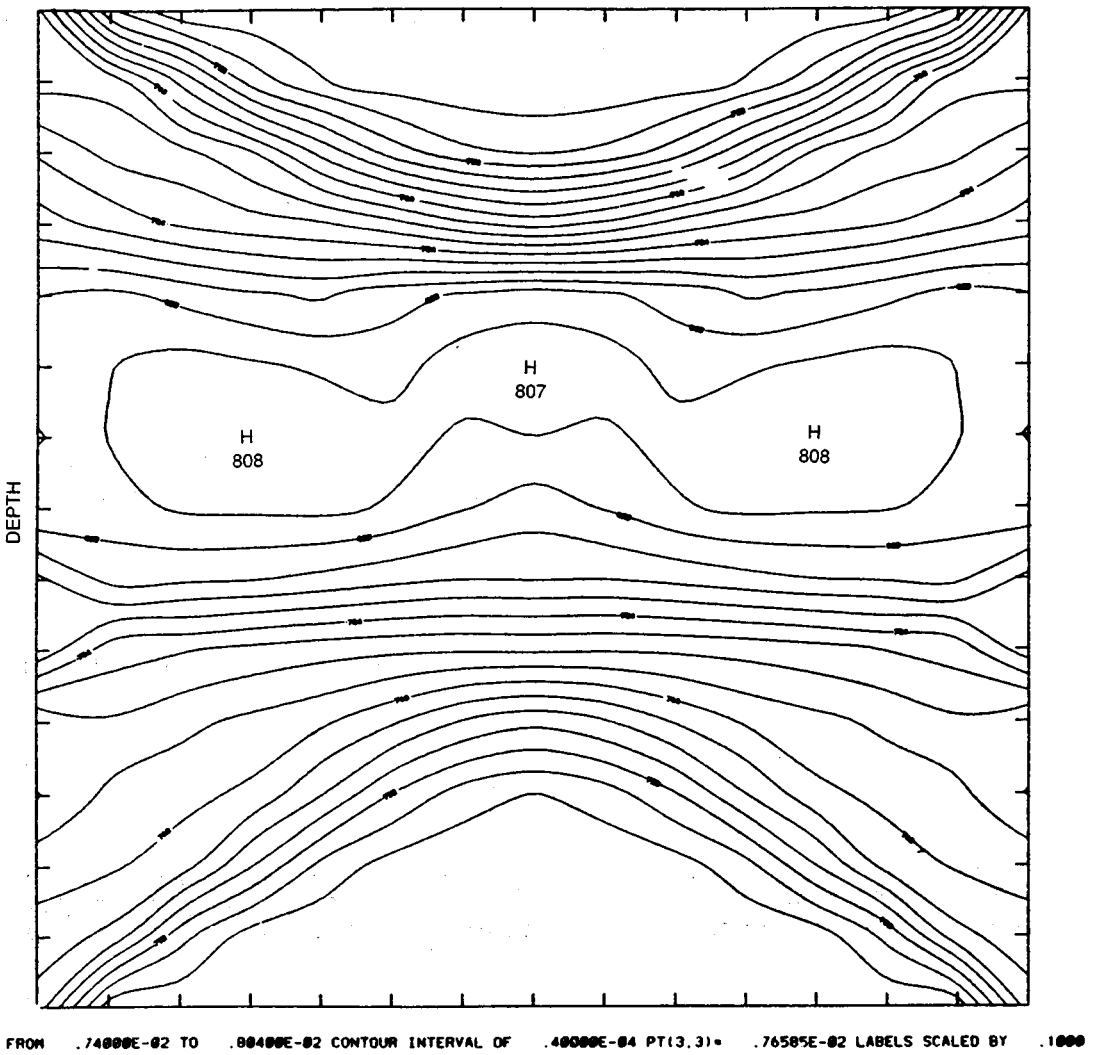

Fig. 2 Contour plot showing the velocity distribution found by using the back-projection technique. The input data were generated from the test model of Fig. 2.

properly, as it ran for the maximum allowed number of 100 iterations).

The agreement with the single model shown is quite encouraging, but more testing is needed. Other promising methods have appeared in the literature that should be incorporated. A number of tomographic methods should be ready by the time field data are ready for analysis.

All the methods discussed here depend on the straight ray approximation. This approximation is not valid, however, if the variations in the slowness distribution are too large, more than 10%, for instance (which is about the variation that was present in the simple layered synthetic model that was used). Further refinement of the computed velocity distribution requires a more sophisticated method of determining the arrival times. For example, modeling based on the currently computed velocity distribution could be used to determine the actual ray paths used. A revised distance matrix corresponding to these computed rays can then be used to solve for the distribution again. Note that such an iterative method relies upon developing efficient methods of modeling seismic wave propagation in the ground.

Current Progress

Synthetic data are currently being used to test the tomographic inversion. This will help determine the best methods and parameters to use under different circumstances. Noise-free data can be inverted to provide a very faithful reconstruction of the velocity model. Noise levels up to a few percent can be tolerated with the results being recognizable reconstructions of the original model. Success in the case of noise is still somewhat dependent on proper setting of smoothing parameters because the algorithms are willing to converge to a noisy reconstruction, which is not a likely model geologically. The calculations are being done on a Hewlett-Packard 9000 Series 520 computer. The programs are written in FORTRAN and take approximately 1 min to run.

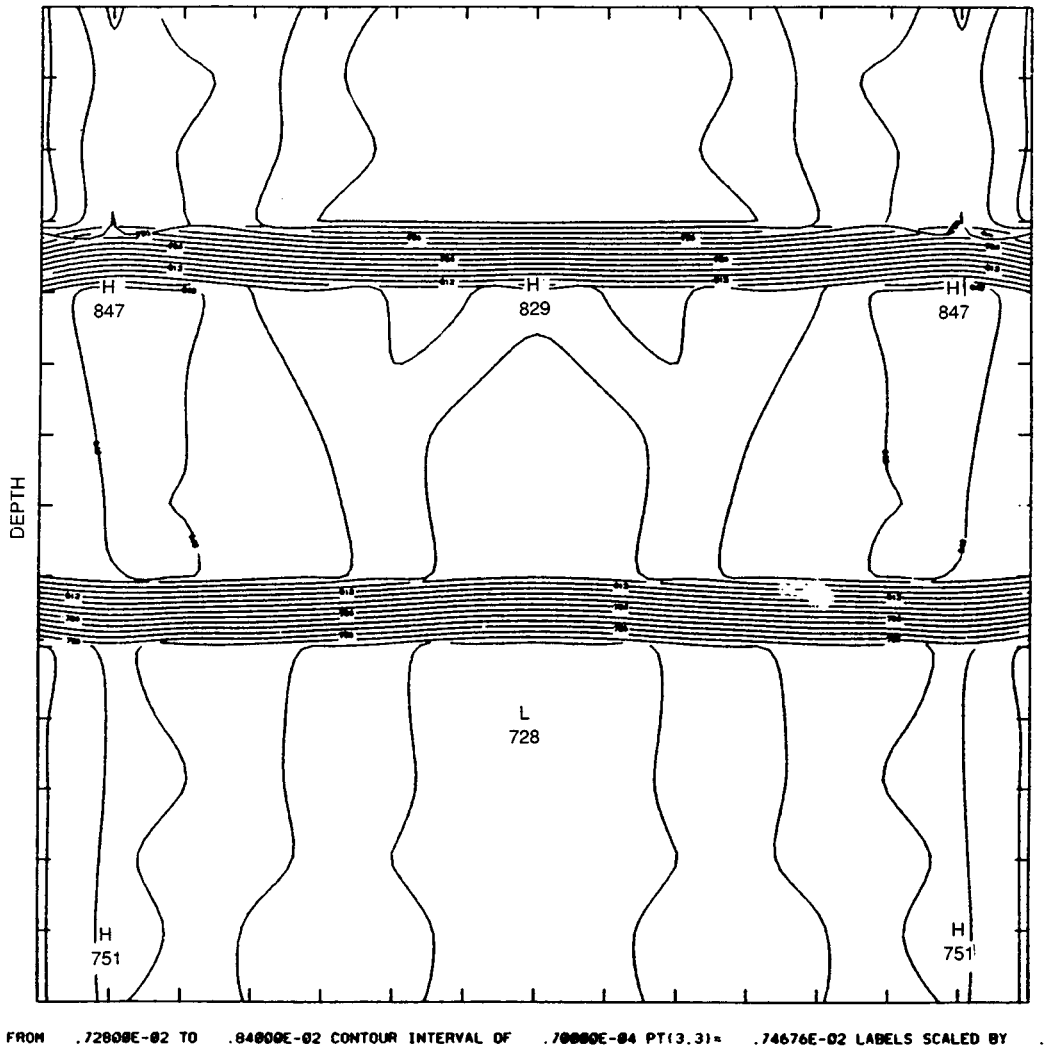

Fig. 3 Contour plot showing the velocity distribution found by using Simultaneous Iterative Reconstruction Technique. After every iteration, the cells along the borehole were forced to their values in the test model as if borehole logging information was used.

An automatic time-picker is being developed. Previously the seismic wave arrival times had to be chosen by hand, a tedious task at best. Filtering and envelope averaging are being used to enable the computer to choose its best guess at the first arrivals. It will then display its choices along the waveforms and allow a user to adjust them if necessary; as more refined methods of automatic picking are developed, fewer time adjustments will be needed. This hybrid automation will still ease the task of choosing the first arrival times on the hundreds of waveforms that are often used.

Task 4

The mechanical modifications of the piezoelectric cylindrical bender borehole source transducer were completed during this reporting period, and preliminary tests were performed on the resulting two-element transducer operating as a monopole (P-wave) source. The changes in the source probe assembly conform with the planned design modifications reported in the first quarterly report. The method for remotely controlling the downhole transformer polarity required for changing the source operation from monopole (P-wave) to vertical dipole (S-wave) was revised in design to operate using a-c control signals instead of d-c control as reported previously. The a-c control signals are to be generated by the source power amplifier at a frequency well above the normal frequency spectrum used for seismic measurements. The switching circuit will employ a tuned stepping relay that requires only momentary switching power so as to be efficient in operation and immune to interference switching errors. This remote switch will reverse the polarity of one of the two downhole power transformers so that they are in phase for monopole operation and out of phase for dipole operation. For testing of the two-element source probe prior to

completion of the remote-control switching, the downhole transformer polarities can be changed manually by means of terminal connections on the transformer primary windings. Laboratory tests of the source probe have demonstrated successful operation as a two-element monopole and as a dipole.

Preliminary borehole operation tests were performed to check the mechanical modifications of the cylindrical bender source transducer. Figure 4 illustrates typical interwell P-wave pulse waveform responses observed in the Anacacho Limestone at the Institute's Borehole Test Facility with boreholes spaced 18 m apart. The detector probe used in these tests was a broadband hydrophone with a uniform frequency response over the range of 200 to 4000 Hz. The five-cycle pulses appearing in the first 3 msec of the detector output traces are artifacts caused by inductive coupling between the source and detector cables and equipment. Although these feedover signals do not affect the propagated pulses and are normally suppressed in the field data records, they serve a useful purpose here as approximate replicas of the source signals for reference comparison with the radiated and detected pulses. One horizontal path and two offset propagation paths are shown in which the source was located at 5.6 and 10.6 m above the hydrophone detector depth. For waveforms with the source located at 45- and 50-m depths, the transmitted pulses are very accurately reproduced for the three different frequencies used in the tests. With the source located at a depth of 40 m, the 46-in. length of the two transducer elements of the cylindrical bender source extended across an interface between a clean fine-grained limestone and a softer overlying marl, which resulted in a weaker radiated source signal as well as distortions caused by the proximity of the interface between the contrasting rock layers. The secondary pulses arriving later in waveform traces shown in Fig. 4 are interpreted to be reflections from the overlying interface at 40 m and/or from a thin underlying marl layer at a depth of 55 m. More extensive tests are scheduled to be performed in other deeper formations (e.g., the Austin chalk) in these boreholes to further test the monopole and dipole operation of the source and as preparation for larger scale interwell field measurements at other borehole test sites.

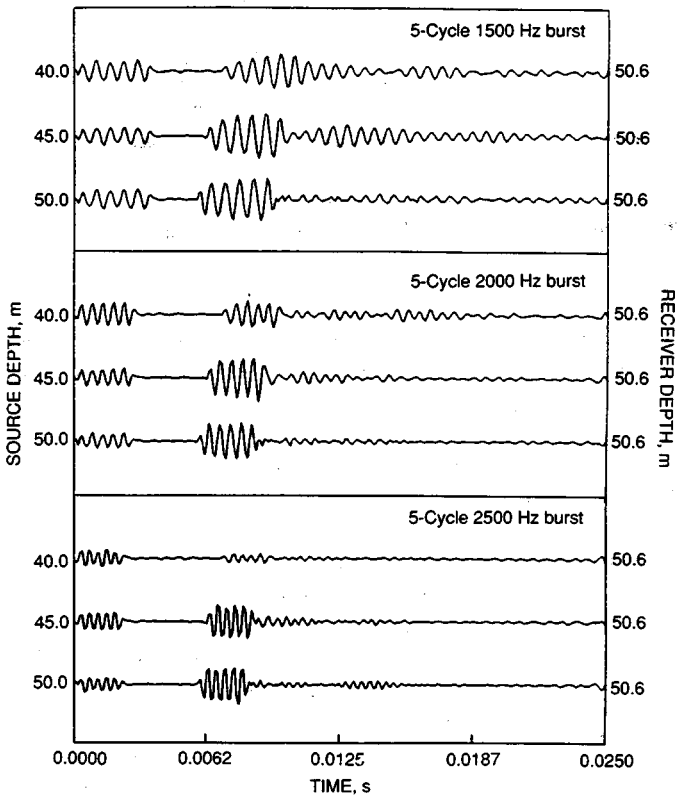

Fig. 4 Sinewave pulse waveforms generated by the two-element monopole (P-wave) piezoelectric cylindrical bender source (borehole separation distance, 18 m; 200 to 4000 Hz Hydrophone detector).

Work to be performed during the next reporting period will include completion of laboratory tests and installation of the downhole remote-controlled switching circuits for controlling monopole and dipole operation of the cylindrical bender source. The two-element cylindrical bender source will be tested further to evaluate its performance in interwell P-wave and S-wave measurements in limestone layers in boreholes located on the Institute grounds. Arrangements with BP Exploration, Inc., are in progress to test the two-element interwell seismic measurement system in boreholes to 3000 ft deep by the end of the next reporting period. Responses of monopole and dipole source operation will also be recorded with a three-component wall-lock detector probe capable of resolving the particle motions and polarizations of the detected seismic waves.

SIMULATION STUDIES TO EVALUATE THE EFFECT OF FRACTURE CLOSURE ON THE PERFORMANCE OF NATURALLY FRACTURED RESERVOIRS

Contract No. DE-AC22-90BC14654

K&A Energy Consultants, Inc.
Tulsa, Okla.

Contract Date: Sept. 18, 1990
Anticipated Completion: Sept. 30, 1993
Government Award: $582,269

Principal Investigator:
Dwight L. Dauben

Project Manager:
Rhonda Patterson
Metairie Site Office

Reporting Period: Oct. 1–Dec. 31, 1990

Objectives

The two principal objectives of this study are to (1) evaluate the effects of fracture closure on the recovery of oil and gas reserves from naturally fractured petroleum or natural gas reservoirs and (2) evaluate procedures for improving the recovery of these reserves with the use of innovative fluid injection techniques to maintain reservoir pressure and mitigate the impact of fracture closure.

The scope of the study has been divided into three main tasks:

1. Baseline studies (non-pressure-sensitive fractures).
2. Studies with pressure-sensitive fractures.
3. Innovative approaches for improving oil recovery.

The Baseline Studies task will be performed in the current contract year and is comprised of the following subtasks:

- Development of representative reservoir conditions.
- Prediction of primary recovery from vertical wells.
- Prediction of primary recovery from horizontal wells.
- Prediction of secondary recovery from vertical wells.
- Sensitivity analyses.

Summary of Technical Progress

The TRIAD general-purpose dual-porosity simulator was modified to accommodate dual-permeability reservoir systems with provision for matrix and fracture permeabilities as functions of pressure and the treatment of horizontal wells. The revised simulator will be used for the subject study.

The TRIAD program was installed on an enhanced personal computer suitable for simulator execution. This new machine has an 80386 central processing unit (CPU) operating at 33 MHz, 16 MB of 70-ns RAM, a Cyrix 80387-compatible coprocessor, a caching hard drive controller with 4 MB of 28-ns cache memory, a 660-MB ESDI hard drive, an enhanced VGA video controller, and a 16-in. VGA multi-synch monitor.

The technical work has focused on the development of a set of representative reservoir conditions. To this end, a review of the pertinent literature was undertaken. This work was nearing completion at the end of the reporting period. A bibliography of technical papers dealing with some aspect of fractured reservoir analysis and production forecasting is being compiled for inclusion in a subsequent report.

The goal is to identify a reservoir with sufficient data that have demonstrated fracture closure characteristics as reservoir pressures decline. Such a reservoir may be difficult to identify because other factors can influence flow behavior, including two-phase flow behavior. If such a reservoir is not identified, the approach will be to use laboratory-derived data that evaluate the conductivity of fractures as related to the net confining pressure. This laboratory-derived model will be built into the simulator to predict the performance of a reservoir that shows the effects of the pressure-sensitive fracture. It is very important to incorporate physically derived data so that the simulated behavior is as realistic as possible.

MINOR AND TRACE AUTHIGENIC COMPONENTS AS INDICATORS OF PORE FLUID CHEMISTRY DURING MATURATION AND MIGRATION OF HYDROCARBONS

Contract No. DE-AC22-90BC14656

Texas A&M University
College Station, Tex.

Contract Date: May 22, 1990
Anticipated Completion: May 21, 1992
Government Award: $36,773

Principal Investigator:
Thomas T. Tieh

Project Manager:
Rhonda Patterson
Metairie Site Office

Reporting Period: Oct. 1–Dec. 31, 1990

Objectives

The primary objectives of the proposed study are to (1) determine the petrological, mineralogical, minor element, and isotopic chemistry of late authigenic sulfides in the Smackover formation of the North Louisiana Salt Basin; (2) determine the abundance, distribution, and nature of occurrence of uranium and thorium in these rocks; (3) assess whether spatial and temporal variations in sulfide mineralogy, as well as in the abundance and nature of occurrence of uranium and thorium, are reflective of pore fluid evolution during hydrocarbon maturation and migration in the Smackover of the North Louisiana Salt Basin; and (4) integrate this information with that obtained by conventional studies of diagenesis to gain further insight into the processes operative during late-stage diagenesis of the Upper Smackover formation of the North Louisiana Salt Basin.

Summary of Technical Progress

Eleven cores of the Upper Smackover were sampled at Louisiana State University's core repository in November.

This is in addition to the six cores sampled at Texas A&M University. These seventeen cores lie along a linear trend stretching across the North Louisiana Salt Basin from the northeast to the southwest. The various facies in the Upper Smackover are well represented in this suite of samples. Additional samples may be sought, at a later date, if it is thought they would enhance the conclusions of this study.

Three thin sections were made from samples of the Tenneco Fee 1 core from the North Haynesville field. This was done to test the hypothesis proposed in the previous quarterly report to explain variations in sulfide chemistry and mineralogy between the Tenneco Seeger–Waller 1 and Tenneco Lowe 1 cores. As previously reported, the Tenneco Lowe 1 core contains the sulfide assemblage sphalerite–pyrite–galena, whereas the Tenneco Seeger–Waller 1 core contains the assemblage sphalerite–galena–marcasite. The sphalerites of the Tenneco Seeger–Waller 1 core also contain more cadmium than those of the Tenneco Lowe 1 core. As proposed, this may reflect a siliciclastic source of mineralizing fluids to the east of the North Haynesville field. The Tenneco Fee 1 well is to the east of the other two wells and contains the sulfide mineral assemblage marcasite–galena–chalcopyrite. This supports the hypothesis that a siliciclastic source of mineralizing fluids lies to the east of the North Haynesville field. This is an important preliminary conclusion because it shows that sulfide minerals do record the chemical evolution of pore fluids in the Upper Smackover.

In the past quarter electron microprobe analyses of the sulfides were continued in the Tenneco Lowe 1, Tenneco Seeger–Waller 1, and Tenneco Fee 1 cores. The sulfate minerals in these cores are being analyzed. Preliminary analyses show that some anhydrites have minor compositional zoning of strontium. In addition, two distinct phases in the barite–celestite series have been recognized with the electron microprobe. One phase contains 27 wt % strontium, whereas the other contains 10 wt % strontium. The necessary electron microprobe analyses will be completed by the end of the next quarter.

Separation of sulfur-bearing minerals for sulfur isotope measurements was begun in the past quarter. The least contaminated samples of each mineral species are being obtained by hand picking mineral grains from polished slabs with dental picks. These samples will be sent to a commercial laboratory for sulfur isotope analyses. In the past quarter Dr. John Valley at the University of Wisconsin at Madison was contacted to discuss possible use of his laser probe mass spectrometry system for sulfur isotope determinations. This has the great advantage of allowing sulfur isotope ratios to be determined on individual mineral grains rather than in bulk. If an authigenic phase has multiple generations, the sulfur isotope ratios for each generation may well be different. Measurement of bulk mineral separates results in average sulfur isotope ratios that obscure the true values for each generation and can lead to erroneous conclusions. Analyzing individual grains negates this problem and enhances the usefulness of sulfur isotope ratios.

In the past quarter another batch of ten Upper Smackover thin sections was irradiated for fission track analysis. The total neutron dose was reduced in the samples received by about one third to ensure that fission track densities corresponding to stylolites were low enough to be counted accurately. This appears to have been successful; however, the tracks have not been counted yet. In the next quarter samples will be processed for fission track analysis of uranium behavior in the Upper Smackover.

Because of delays at the Nuclear Science Center at Texas A&M, the results of instrumental neutron activation and neutron counting analyses of samples submitted this past October are not complete. The analyses should be completed by the end of January. These results are important because they pertain directly to whether stylolites are fluid conduits in the Upper Smackover.

In the past quarter two abstracts have been accepted for presentation at the annual meeting of the American Association of Petroleum Geologists in April. A third abstract has been submitted for presentation at the annual convention of the Gulf Coast Association of Geological Societies in October 1991.

DEMONSTRATION OF HIGH-RESOLUTION INVERSE VSP FOR RESERVOIR CHARACTERIZATION APPLICATIONS

Contract No. DE-AC22-89BC14473

Southwest Research Institute
San Antonio, Tex.

Contract Date: Oct. 1, 1989
Anticipated Completion: Sept. 30, 1991
Government Award: $147,702
(Current year)

Principal Investigator:
Jorge O. Parra

Project Manager:
Chandra M. Nautiyal
Bartlesville Project Office

Reporting Period: Oct. 1–Dec. 31, 1990

Objective

The objective of this project is to demonstrate inverse vertical seismic profiling measurements with new experimental field instrumentation capable of providing at least

an order of magnitude improvement in the resolution of structural details in comparison with conventional seismic images. This two-year project will entail instrumentation tests under controlled field conditions during the first year followed by full-scale field demonstration tests in a representative oil-bearing reservoir formation during the second year.

Summary of Technical Progress

The design for the conversion of the pneumatically clamped three-component accelerometer borehole seismic detector to hydraulic operation was completed, and the detector is being assembled for testing during this reporting period. Laboratory tests of the hydraulic actuator functions, the pressure seals, and the magnetic compass orientation sensor indicate that the revised probe will be appropriate for extended field use in shallow boreholes. The new probe weighs 9 lb and is configured to operate in boreholes drilled to 50 ft deep. A wall-lock clamping force up to 200 lb is produced by a small hydraulic hand pump at the surface. The probe is designed to operate in either water- or air-filled boreholes to a practical immersion depth of 100 to 200 ft as limited by the ability to handle the hydraulic hose downhole from the surface.

The assembled hydraulically clamped detector probe will be tested in boreholes on the Institute grounds during the next reporting period. These tests will involve the use of the piezoelectric cylindrical bender source at depths ranging from 30 to 140 m in one borehole and the hydraulically clamped detector at a depth of 15 m in a separate borehole spaced 18 m away from the source borehole. Other detector transducers, including the pneumatically clamped probe, will be tested in the same borehole stations for comparative evaluation.

Bibliography

Balogh, W. T., T. E. Owen, and J. M. Harris, A New Piezoelectric Transducer for Hole-to-Hole Seismic Applications, *Technical Program Abstracts*, pp. 155-157, 58th Annual International Meeting of the Society of Exploration Geophysicists, Anaheim, Calif., 1988.

Montmollin, V. de, Shaker Tests on Downhole Seismic Tools, *Geophysics*, 53: 1160-1168 (1988).

Owen, T. E. and E. P. Karisch, Design Improvements to the Piezoelectric Cylindrical Bender Seismic Source, in *Proceedings of the Third International Symposium on Borehole Geophysics*, Las Vegas, Nev., October 1989.

——, W. T. Balogh, and W. R. Peters, An Arc Discharge Pulse Source for Borehole Seismic Measurements, *Technical Program Abstracts*, pp. 151-154, 58th Annual International Meeting of the Society of Exploration Geophysicists, Anaheim, Calif., 1988.

Parra, J. O. and T. E. Owen, *Demonstration of High-Resolution Inverse VSP for Reservoir Characterization Applications: Task I—Development and Evaluation of Detector Planting Techniques*, Annual Report, DOE Contract No. DE-AC22-89BC14473, SWRI Project 15-3200, October 1990.

Wuenschel, P. C., The Vertical Array in Reflection Seismology—Some Experimental Studies, *Geophysics*, 41: 219-232, 1976.

INNOVATIVE TECHNIQUES FOR THE DESCRIPTION OF RESERVOIR HETEROGENEITY USING TRACERS

Contract No. DE-AC22-90BC14653

University of Texas
Austin, Tex.

Contract Date: Aug. 2, 1990
Anticipated Completion: Aug. 1, 1993
Government Award: $224,456
(Current year)

Principal Investigators:
Gary A. Pope
Kamy A. Sepehrnoori

Project Manager:
Edith Allison
Bartlesville Project Office

Reporting Period: Oct. 1–Dec. 31, 1990

Objectives

The objectives of this study are to present the results of a simulated single-well tracer test in a reservoir composed of three layers and describe the test procedure used in the simulations.

The theory of a single-well backflow tracer test to estimate permeability contrast of a layered reservoir has been described in an earlier report.[1] Some simulated results for a reservoir consisting of two layers of identical properties except permeability were initially used to test this theory.

The development of the test used the fact that in some formations there exists linear fluid movement in some part of the reservoir. This fluid drift adds an irreversibility to the single-well backflow tracer test in such a way that it is possible to get multiple peaks, one for each layer, in the produced tracer concentration history.

Summary of Technical Progress

The test procedure has been modified to become more robust. The test consists of

1. An injection period to introduce the tracers into the reservoir.

2. A shut-in period to allow fluid drift to move the tracer slugs away from the well.

3. An injection of a tracer-free water buffer to help increase the distance of the slugs (mainly in the least permeable layers) from the test well.

4. A production period (phase I) still under the influence of fluid drift to help keep the slugs apart.

5. A production period (phase II) without fluid drift to recover the slugs in the most permeable layers earlier.

Results

Single-well tracer tests have been simulated with reservoirs composed of three layers of identical properties except permeability. These simulated layers had permeability ratios of 16:4:1, 9:3:1, and 4:2:1. The results of one of the simulations for the first permeability ratio are shown. The reservoir, test, and simulation data are given in Table 1.

TABLE 1

Reservoir, Test, and Simulation Data

	Layer 1	Layer 2	Layer 3
Thickness, ft	6.67	6.67	6.67
Permeability, mD	1600	400	100
Porosity	0.34	0.34	0.34
Water saturation	0.70	0.70	0.70
Residual oil saturation	0.30	0.30	0.30
Longitudinal dispersivity, ft	0.6	0.6	0.6
Transverse dispersivity	0	0	0
Drift velocity, ft/d	6.86	1.71	0.43
Injection and production rate, bbl/d		1000	
Slug sizes used, bbl		80, 40, and 20	
Shut-in time, d		20	
Chase water slug, bbl		75	
Phase I production time, d		4	
Phase II production time, d		26	
Δx, ft		2.989	
Δy, ft		2.989	
Grid		90 × 10	

Figure 1 shows the tracer concentration profile in a cross section passing through the well for each of the three layers. Figure 2 shows the concentration history for each layer separately. The distance between peaks is a function of the test parameters, such as drift velocities, shut-in time, and production time of phase I. The composite production of tracer from all three layers is shown in Fig. 3. There are three distinct peaks corresponding to the three permeability layers.

Conclusions

From the results obtained in this and many other simulations with the use of different test parameters and permeability ratios, the following is inferred:

1. It is possible, under certain conditions, to get multiple peaks in the tracer concentration history from a single-well tracer test.

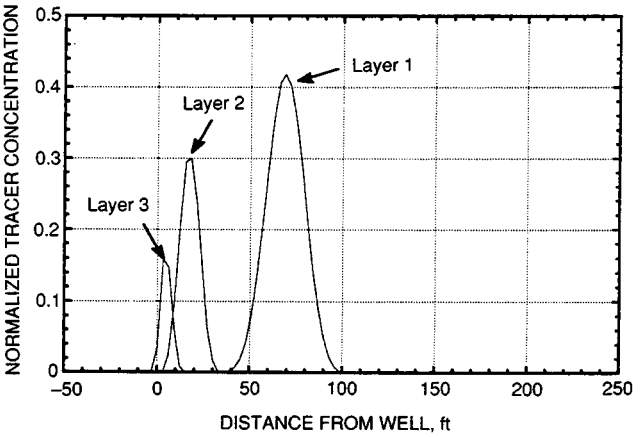

Fig. 1 Profiles of Run P3L034.

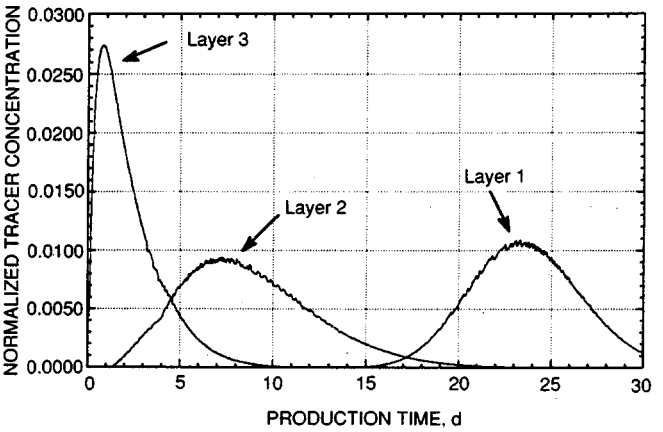

Fig. 2 Concentration histories of Run P3L034.

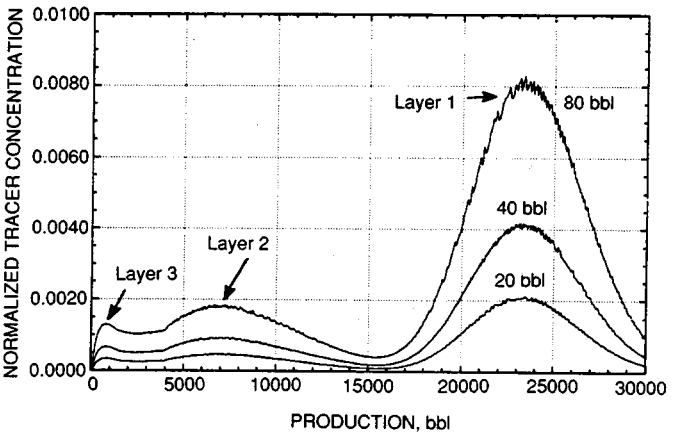

Fig. 3 Concentration histories of Run P3L034.

2. For the cases used in these simulations, the greater the slug size, the better the distinction between peaks.

3. The injection of a chase water slug is necessary when the permeability contrast is high and the drift velocity and/or the shut-in time is small.

4. The variation in the drift velocity is of great importance for the results of the test.

5. The greater the shut-in period and/or the higher the drift velocity, the better the results.

Reference

1. G. A. Pope, L. W. Lake, and R. S. Schechter, *Quarterly Report for the Period September 1989–December 1989: Reservoir Characterization in Enhanced Oil Recovery Research*, prepared for the U.S. Department of Energy under Contract No. DE-FG22-89BC14251.

DISPERSION MEASUREMENT AS A METHOD OF QUANTIFYING GEOLOGIC CHARACTERIZATION AND DEFINING RESERVOIR HETEROGENEITY

Contract No. DE-AC22-90BC14652

University of Oklahoma
Norman, Okla.

Contract Date: July 12, 1990
Anticipated Completion: July 1, 1993
Government Award: $218,033

Principal Investigator:
Donald E. Menzie

Project Manager:
Jerry Ham
Metairie Site Office

Reporting Period: Oct. 1–Dec. 31, 1990

Objective

The objective of this research is to characterize and define reservoir heterogeneities by a measure of dispersion in a porous medium. Various laboratory methods of measuring and interpreting the dispersivity of a rock will be applied to identify the flow system. New dispersivity measuring methods will be investigated and evaluated, including the use of X-ray imaging, special tracers, electrical conductivity, and well log analysis. A standard method of measuring dispersion in an oil field between wells will also be investigated.

Summary of Technical Progress

The literature search on dispersion and dispersivity is continuing in order to cover a very diverse range of disciplines, such as chemical engineering, civil engineering, chemistry, physics, environmental engineering, and groundwater and petroleum engineering. Results of this effort will be reported later for both longitudinal and transverse dispersion measurement methods and reported results.

Dispersivity and Heterogeneity

The X-ray scanner was used to determine the small-scale heterogeneities of 29 clean dry cores that may be used in future dispersion experiments. The cores were x-rayed after being coated with J-B Weld and plastic and then x-rayed again after being saturated with liquid. The results of the X-ray tracings indicate porosity and permeability variations from inlet to outlet of the core. These Berea, Brown, and limestone cores will be used to investigate the effect of length on dispersivity. The variation of the X-ray intensity along the core shows the nonuniformity or nonhomogeneity of the rock sample (Table 1 and Figs. 1 to 6).

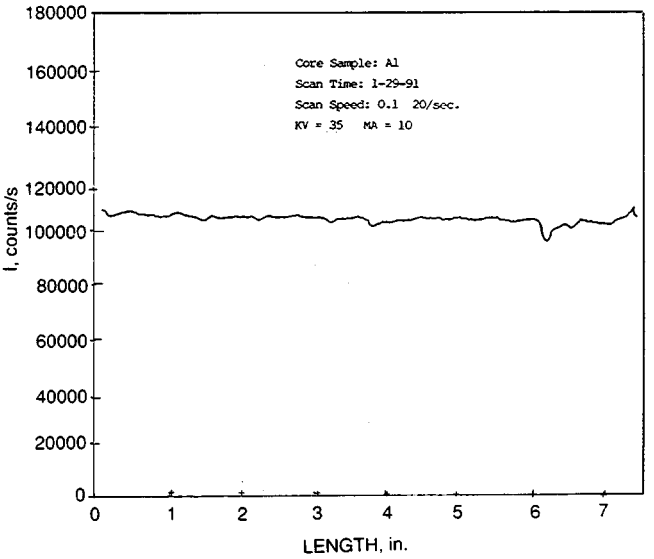

Fig. 1 X-ray scanning curve of the dry core A1.

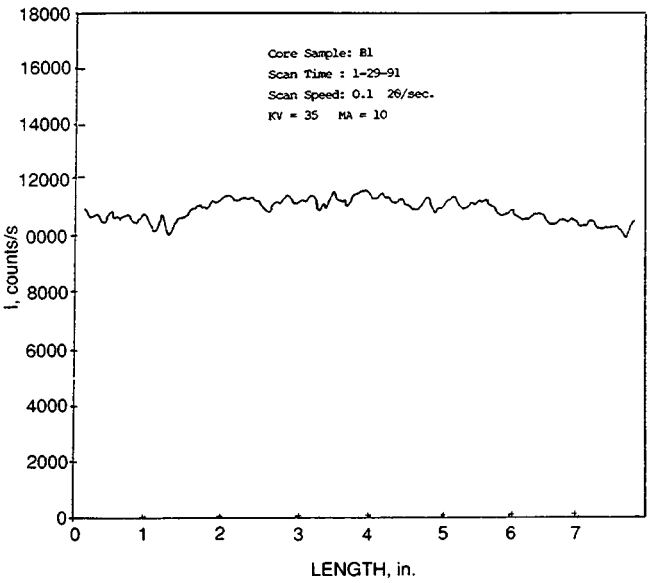

Fig. 2 X-ray scanning curve of the dry core B1.

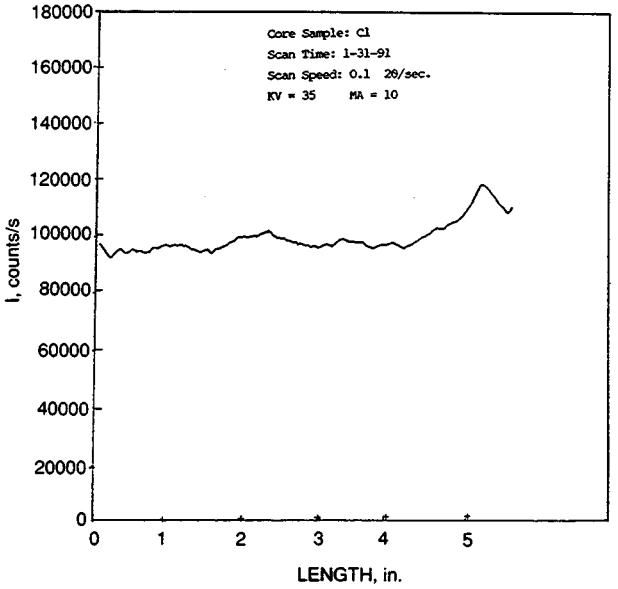

Fig. 3 X-ray scanning curve of the dry core C1.

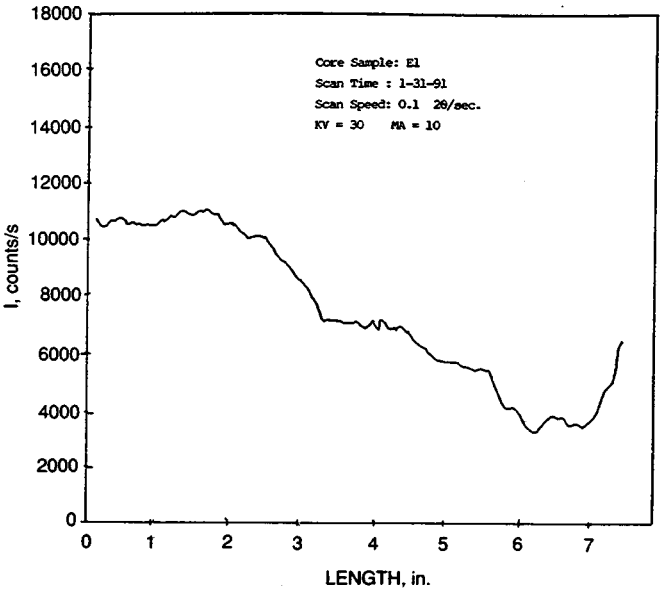

Fig. 5 X-ray scanning curve of the dry core E1.

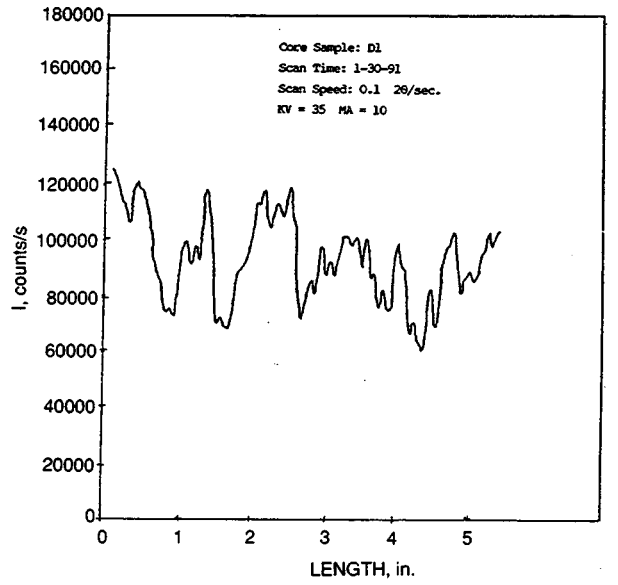

Fig. 4 X-ray scanning curve of the dry core D1.

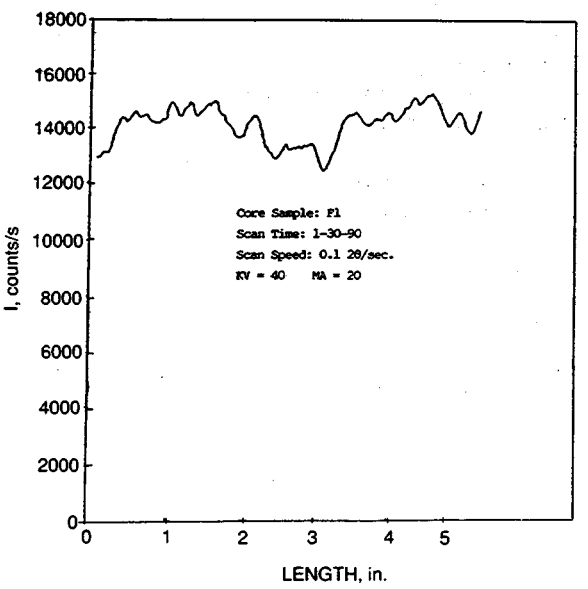

Fig. 6 X-ray scanning curve of the dry core F1.

A series of miscible experiments were designed. The experiments were selected to investigate the effects of system scale and spatial porosity and permeability variations on miscible displacement. The role of dispersivity in heterogeneous systems will be evaluated after these experiments are performed.

Dispersivity from Well Logs

The preliminary study on the correlation of dispersivity and log-derived parameters was started. Cores were cut, Soxhlet extracted, oven-dried, and saturated with brine. The heterogeneity of the core was then evaluated by an X-ray scan. Porosity was determined by weight of the dry and saturated cores. Electrical resistances were measured with a conductivity bridge. Data are shown in Tables 2 to 4 and Fig. 7. Data analysis is in progress.

Dispersivity in a Homogeneous Core

A homogeneous, synthetic core was purchased to investigate the effect of flow rate on the measured dispersion in a porous media. This fundamental work is in progress.

TABLE 1

Summary of Core Samples

No.	Length, cm	Diameter, cm	K, mD	Type	No.	Length, cm	Diameter, cm	K, mD	Type
A1	18.6	3.8	About 100	Berea	C1	14.25	3.78	Unknown	Berea
A2	18.6	3.8	About 100	Berea	C2	14.25	3.78	Unknown	Berea
A3	18.6	3.83	About 100	Berea	C3	14.25	3.8	Unknown	Berea
A4	18.6	3.8	About 100	Berea	C4	14.25	3.8	Unknown	Berea
A5	18.6	3.8	About 100	Berea	C5	14.25	3.77	Unknown	Berea
B1	18.8	3.73	About 500	Berea	D1	14.25	3.8	Unknown	Berea
B2	18.8	3.73	About 500	Berea	D2	14.25	3.8	Unknown	Berea
B3	18.6	3.73	About 500	Berea	D3	14.25	3.77	Unknown	Berea
B4	18.6	3.72	About 500	Berea	D4	14.25	3.78	Unknown	Berea
B5	18.9	3.72	About 500	Berea	D5	14.25	3.79	Unknown	Berea
E1	18.6	3.8	About 800	Brown	F1	14.25	3.8	Unknown	Limestone
E2	18.6	3.8	About 800	Brown	F2	14.25	3.8	Unknown	Limestone
E3	18.6	3.79	About 800	Brown	F3	14.25	3.8	Unknown	Limestone
E4	18.6	3.79	About 800	Brown	F4	14.25	3.8	Unknown	Limestone
E5	18.6	3.79	About 800	Brown					

TABLE 2

Basic Data of Berea and Brown Sandstone Samples

Core No.	Diameter, cm	Length, cm	Area, cm^2	Dry weight, g	Wet weight, g	Pore volume, cm^3	Porosity, %
B1	2.50	9.65	4.91	101.67	111.70	9.64	20.36
B2	2.50	9.50	4.91	99.61	109.92	9.91	21.26
B3	2.50	9.20	4.91	96.87	106.58	9.34	20.67
B4	2.50	9.45	4.91	98.62	108.77	9.76	21.04
B5	2.50	9.33	4.91	98.49	108.24	9.38	20.47
B6	2.50	7.23	4.91	76.20	83.77	7.28	20.51
B10	2.50	9.36	4.91	94.11	105.26	10.72	23.33
B11	2.50	9.38	4.91	94.47	105.64	10.74	23.33
B12	2.50	7.18	4.91	71.71	80.16	8.13	23.05
BN1	2.50	9.40	4.91	95.31	106.25	10.52	22.80
BN2	2.50	9.60	4.91	97.37	108.47	10.67	22.65
BN3	2.50	9.52	4.91	96.57	107.68	10.68	22.86
BN4	2.50	6.40	4.91	64.91	72.45	7.25	23.08
LB1	3.80	14.70	11.34	360.90	393.90	31.73	19.03
LB2	3.80	14.65	11.34	360.40	392.70	31.06	18.69
LB3	3.80	14.50	11.34	358.08	391.00	31.65	19.25
LB4	3.80	14.10	11.34	347.41	378.90	30.28	18.93
LB5	3.80	14.05	11.34	344.47	376.10	30.41	19.09
LB6	3.70	14.80	10.75	347.25	379.40	30.91	19.43
LB7	3.80	14.65	11.34	358.07	391.50	32.14	19.35
LB8	3.80	14.30	11.34	345.42	378.80	32.10	19.79

TABLE 3

Brine Solution Data

Components, %	3% MaCl, 1% $CaCl_2$
Salinity, ppm	About 40,000
Density	1.04
Viscosity, cP	1.00 at 70°F
Resistivity, ohm-m	0.19 at 70°F

TABLE 4

Electrical Formation Factors of Core Samples of Berea and Brown Sandstones

Core No.	Diameter, cm	Length, cm	Area, cm^2	ro, ohm	Ro, ohm-m	F*
B1	2.50	9.65	4.91	495	2.52	13.25
B2	2.50	9.50	4.91	475	2.45	12.92
B3	2.50	9.20	4.91	475	2.53	13.34
B4	2.50	9.45	4.91	465	2.42	12.71
B5	2.50	9.33	4.91	485	2.55	13.43
B6	2.50	7.23	4.91	376	2.55	13.44
B10	2.50	9.36	4.91	378	1.98	10.43
B11	2.50	9.38	4.91	385	2.01	10.60
B12	2.50	7.18	4.91	300	2.05	10.79
BN1	2.50	9.40	4.91	395	2.06	10.86
BN2	2.50	9.60	4.91	420	2.15	11.30
BN3	2.50	9.52	4.91	418	2.16	11.34
BN4	2.50	6.40	4.91	280	2.15	11.30
LB1	3.80	14.70	11.34	381	2.94	18.37
LB2	3.80	14.65	11.34	379	2.93	18.34
LB3	3.80	14.50	11.34	376	2.94	18.38
LB4	3.80	14.10	11.34	367	2.95	18.45
LB5	3.80	14.05	11.34	357	2.88	18.01
LB6	3.70	14.80	10.75	362	2.63	16.44
LB7	3.80	14.65	11.34	357	2.76	17.27
LB8	3.80	14.30	11.34	327	2.59	16.21

*F, formation factor.

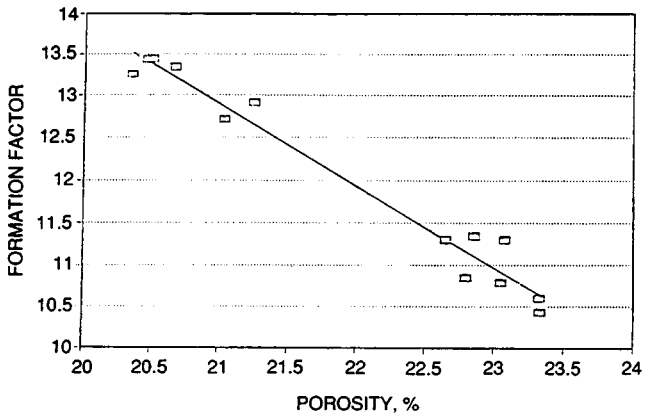

Fig. 7 Formation factor vs. porosity for Berea and Brown sandstones.

PREDICTABILITY OF FORMATION DAMAGE—AN ASSESSMENT STUDY AND GENERALIZED MODELS

Contract No. DE-AC22-90BC14658

University of Oklahoma
Norman, Okla.

Contract Date: Apr. 5, 1990
Anticipated Completion: Apr. 4, 1992
Government Award: $193,017

Principal Investigator:
Faruk Civan

Project Manager:
Gene Pauling
Metairie Site Office

Reporting Period: Oct. 1–Dec. 31, 1990

Objectives

The project objective is to develop improved generalized predictive models to be used for investigation of reservoir formation damage and control for various fluid and rock conditions and to account for these effects in reservoir simulation.

This objective can be accomplished by critically studying and evaluating the previous modeling efforts and the experimental studies reported in the literature. Then generalized predictive models will be formulated by combining the previous attempts and by improving and generalizing the modeling approaches to accommodate a variety of conditions encountered in actual field applications.

A critical review of the previous work addressing its theoretical basis, assumptions and limitations, and the generalized and improved model developed in this study will be presented in a systematic manner in terms of a standardized definition and nomenclature for direct comparison. Case studies with the generalized model will be presented to demonstrate its capacity and validity. User-friendly computer programs implementing the improved modeling approaches will also be supplied.

From this study an assessment of the available models and methods for evaluating and predicting formation damage and improved models will be formed. Therefore it will be an important reference for the petroleum industry.

Summary of Technical Progress

As a result of this work, the following papers were prepared:

• "Identification of Relative Effects of Particulate Processes in Petroleum Bearing Formations," E. M. Arcia

and F. Civan, presented at the 1990 Annual Meeting of the American Institute of Chemical Engineers, Chicago, Ill., Nov. 11–16, 1990. This work was funded by Maraven S. A., Venezuela, and the School of Petroleum and Geological Engineering at the University of Oklahoma.

• "Predicting Skin Effects Due to Formation Damage by Fines Migration," H. A. Ohen and F. Civan (partially funded by the previous DOE project), SPE 21675 paper to be presented at the 1991 Society of Petroleum Engineers Production Operations Symposium, Oklahoma City, Okla., April 7–9, 1991.

The Ohen and Civan formation damage model has been extended to include the chemical dissolution and precipitation effects. The extended model is being validated with experimental data. Simultaneously, for the generation of original core data, laboratory tests are being prepared under controlled conditions.

The preparation and documentation of the state-of-the-art modeling approaches on rock–fluid interactions are continuing.

Dr. Civan organized four sessions for the 1990 Annual Meeting of the American Institute of Chemical Engineers on Rock–Fluid Interactions and Particulate Processes in Petroleum Reservoirs and Porous Media, which was held in Chicago, Ill., on Nov. 11–16, 1990.

Significance to Enhanced Oil Recovery Plan

Controlling formation damage and efficient selective plugging of heterogeneous reservoir formation are among the important issues for improving the sweep efficiency of enhanced oil recovery (EOR). For the most part, the methods proposed for controlling the formation characteristics to achieve good sweep efficiency have not been satisfactory. In many cases the efforts for the improvement of sweep efficiency resulted in adverse effects.

The present study critically analyzes the various processes influencing the sweep efficiency during EOR. The relevant studies and results reported in the literature are reviewed and incorporated into the analysis. The effects of various factors are discussed and illustrated by means of typical case studies. Finally, an overall assessment of the processes controlling the sweep efficiency is presented in a systematic manner for reference.

Future Research Plans

The overall objective is to develop a working generalized model that can be used for characterizing, evaluating, and preventing formation damage in oil and gas reservoirs. Hence this model will be a useful tool for development of strategies to maximize the performance of oil and gas production from in situ reservoirs. Future research efforts to accomplish this objective will include experimental and theoretical studies.

Bibliography

Civan, F., A Generalized Model for Formation Damage by Rock–Fluid Interactions and Particulate Processes, paper SPE 21183 in *Proceedings of SPE 1990 Latin American Petroleum Engineering Conference,* Rio de Janeiro, Brazil, Oct. 14–19, 1990.

——, R. M. Knapp, and H. A. Ohen, Alteration of Permeability by Fine Particle Processes, *J. Pet. Sci. Eng.*, 3(1/2): 65-79 (October 1989).

Millan-Arcia, E., and F. Civan, Experimental Characterization of Formation Damage in Petroleum Reservoirs, paper submitted to *Journal of Canadian Petroleum Technology,* June 1990 (in review).

Ohen, H. A., and F. Civan, Simulation of Formation Damage in Petroleum Reservoirs, paper SPE 19420 in *Proceedings of the 1990 SPE Symposium on Formation Damage Control,* Lafayette, La., Feb. 22–23, 1990, pp. 185-200.

——, and F. Civan, Predicting Fines Generation, Migration and Deposition Near Injection and Production Wells, in *Proceedings of the First Regional Meeting, American Filtration Society,* Houston, Tex., Oct. 30–Nov. 1, 1989, pp. 161-164.

——, and F. Civan, Formation Damage in Petroleum Reservoirs I: Modeling, paper SPE 19380 submitted to Society of Petroleum Engineers July 1989 (in review).

——, and F. Civan, Formation Damage in Petroleum Reservoirs II: Parameters Estimation and Simulation Studies, paper SPE 19381 submitted to Society of Petroleum Engineers July 1989 (in review).

MEASURING AND PREDICTING RESERVOIR HETEROGENEITY IN COMPLEX DEPOSYSTEMS

Contract No. DE-AC22-90BC14657

Appalachian Oil and Natural Gas Research Consortium
Morgantown, W. Va.

Contract Date: Sept. 20, 1990
Anticipated Completion: Sept. 20, 1993
Government Award: $1,915,000

Principal Investigators:
Alan C. Donaldson
Robert Shumaker
Christopher Laughrey
Kashy Aminian
Michael Ed. Hohn

Project Manager:
Edith Allison
Bartlesville Project Office

Reporting Period: Oct. 1–Dec. 31, 1990

Objectives

The recovery of additional oil from existing fields in the Appalachian basin is hampered by poorly known permeability barriers within the reservoirs. Vertical barriers,

caused by stacking of sandstones separated by shale breaks, are relatively easy to recognize in a given well but difficult to project laterally. Lateral barriers caused by facies changes are more difficult to predict, and subtle changes within the reservoir caused by diagenetic changes are the most difficult of all. Thus several scales of heterogeneity exist, from those imposed by shifts in depositional environments to the pore throat barriers developed during diagenesis. The result is that the oil reservoirs consist of a complex series of flow systems dependent on lithology, sandstone genesis, and structural and thermal history.

The proposed research is designed to use a multidisciplinary approach to measure and map heterogeneity at various scales and ultimately to develop tools and techniques to predict heterogeneity, both in existing fields and in undrilled areas. Two stratigraphic units have been chosen for this research. The Big Injun sandstone (Mississippian) in West Virginia and the Rose Run Sandstone (Ordovician) in Ohio and Pennsylvania. The main objectives of this research are to:

1. Map the geometry of sandstone bodies within a regional depositional system and classify these bodies in a scheme of relative heterogeneity, which will determine the heterogeneity across the depositional systems.
2. Map facies changes within the given reservoirs, interpret environments for each facies, predict the inherent relative heterogeneity of each facies, and share these results with petrologists and petroleum engineers.
3. Correlate structural variations with hydrocarbon production and variations in geologic and engineering parameters that affect production in Big Injun reservoirs in West Virginia.
4. Develop a reliable seismic model of the reservoir expressed in terms of impedance variation such that physical heterogeneity within the reservoir can be interpreted.
5. Describe the pore types and relate them to permeability, fluid flow, and diagenesis and by integrating petrographic studies with facies and depositional environments derived from stratigraphic work develop a technique to use diagenesis as a predictive tool in future reservoir development.
6. Study the effects of heterogeneities on fluid flow and efficient hydrocarbon recovery in order to improve reservoir management and future development.
7. Apply graphical methods to production data and develop new geostatistical methods to detect regional trends in heterogeneity.
8. Use the geologic and engineering data on Big Injun reservoirs in West Virginia to construct facies maps and compute the local probability that new, in-fill wells will intersect rock with favorable reservoir characteristics.

The main goal of this research project is to understand reservoir heterogeneity sufficiently to predict optimum drilling locations vs. high-risk locations in a given field so that the most cost-effective infill-drilling programs can be recommended.

Summary of Technical Progress

Stratigraphy

In the regional-scale study of Big Injun sandstones, a base map (which includes 24 counties of West Virginia) showing the location of wells with geophysical log data through the reservoir unit has been completed. In the initial phase of data collection, geophysical logs (gamma-ray, density, and neutron) of 1432 wells from the regional area were copied. Twenty stratigraphic cross sections were constructed for the interval of the Berea/Sunbury–Big Lime (Mississippian Age), and the sandstones were correlated as the upper and lower Big Injun; Squaw; and upper, middle, and lower Weir units. Thickness maps of the intervals for the upper Big Injun, lower Big Injun, Squaw, and upper Weir sandstones were drawn for Kanawha, Roane, Calhoun, and part of Clay counties. Within this four-county area, the Big Injun sandstones change laterally into shale and in places are missing as a result of the regional pre-Greenbrier unconformity.

For the more detailed phase of the study, a 17-mile seismic profile from the southern part of the Granny Creek oil field of Clay County was analyzed for the stratigraphic interpretation of the Berea–Big Lime interval as well as for recognition of the local relief of the regional pre-Greenbrier (Big Lime) erosional surface (unconformity) and the ability to determine where some pinch-outs of Big Injun sandstones occur. In the same general area, a base map that shows well locations at approximately 500-ft spacing was donated by a gas company, and arrangements were made to obtain geophysical logs of the study interval from about 40 wells. A stratigraphic cross section from the well data is being constructed for comparison with the cross section of the seismic profile.

For the regional stratigraphic study of the Rose Run Sandstone in Ohio, approximately 15 additional geophysical logs from the adjacent states of Pennsylvania, West Virginia, Kentucky, Indiana, and Michigan were digitized, along with the 20 geophysical logs from Ohio, and used to construct a network of preliminary cross sections. Stratigraphic cross sections were hung on the base of the Black River Limestone (Ordovician), and units were correlated from the top of the Trenton (Ordovician) to the Precambrian. These computer-generated cross sections were printed at a scale of 1 in. equals 100 ft. The computer database of information from 600 completion cards was updated with all wells that penetrated the Rose Run.

In Pennsylvania, during the first quarter work focused on the preliminary tasks of learning the subject. All wells in western and north-central Pennsylvania that penetrated to the Cambrian and Ordovician carbonates were identified and plotted on a base map. In addition, logs were collected from certain wells outside Pennsylvania to aid in regional correlations. Logs of specific wells within and outside the boundaries of the Commonwealth were selected to construct stratigraphic cross sections that will be used to

identify formation tops and stratigraphic sequences. They will ultimately be used to correlate the remaining logs.

Construction of seven cross sections of the interval from the base of the Upper Ordovician Utica Shale to the top of the Precambrian basement rocks has begun (see Fig. 1 for locations of the cross sections). At the end of the quarter, five of the seven sections, showing geophysical logs (gamma-ray and neutron, in most cases) and generalized lithology, had been completed. Preliminary corrections have been made on three of these sections, but they will not be finalized on the original copies until further study, including comments from geologists in the Ohio Division of Geologic Survey and any other geologists familiar with the Cambrian and Ordovician sequence in the Appalachians, has been completed. The preliminary cross sections will be displayed at the I. C. White Symposium in Morgantown, W. Va., in March 1991, and symposium participants will be invited to comment on their preliminary status.

A literature search was begun, and most of the volumes dealing with the section in question have been identified and entered into a preliminary bibliography. This bibliography is expected to grow as the project continues and knowledge of the section expands.

Structural Geology

Regional studies of the Big Injun were initiated to establish the structural settings and structural histories of the smaller field areas being studied. The initial phase of data collection to build regional structural maps and cross sections has started. Data are being provided from university, state survey, and private industry fields. No serious problems have been encountered thus far.

Detailed structural maps and cross sections of the fields being studied will be constructed to determine interrelationships between oil production and structural parameters that affect production. The initial phase of data collection has started. Logs and base maps of the Granny Creek field are being accumulated from public and private sources.

The primary objective of the reflection seismic work to be undertaken in this contract is to reconcile differences between surface seismic, synthetic seismograms derived from borehole sonic and density data and the vertical seismic profile. The results of this research will improve the resolution of acoustic properties in surface seismic data, particularly from the reservoir interval. This information may be useful to other tasks.

A quarterly milestone was to complete an examination of specification data from the study areas. Information on available specification data was provided by two companies. The only potentially useful data are several miles of single-fold dynamite data shot by Exxon in the early 1970s. During a meeting with Columbia Natural Resources (CNR) this quarter, CNR agreed to allow inspection of the Exxon data over the study areas. Hence there is no plan to purchase these older data, but the money will be used to collect additional new data during the second field season (summer and fall 1991).

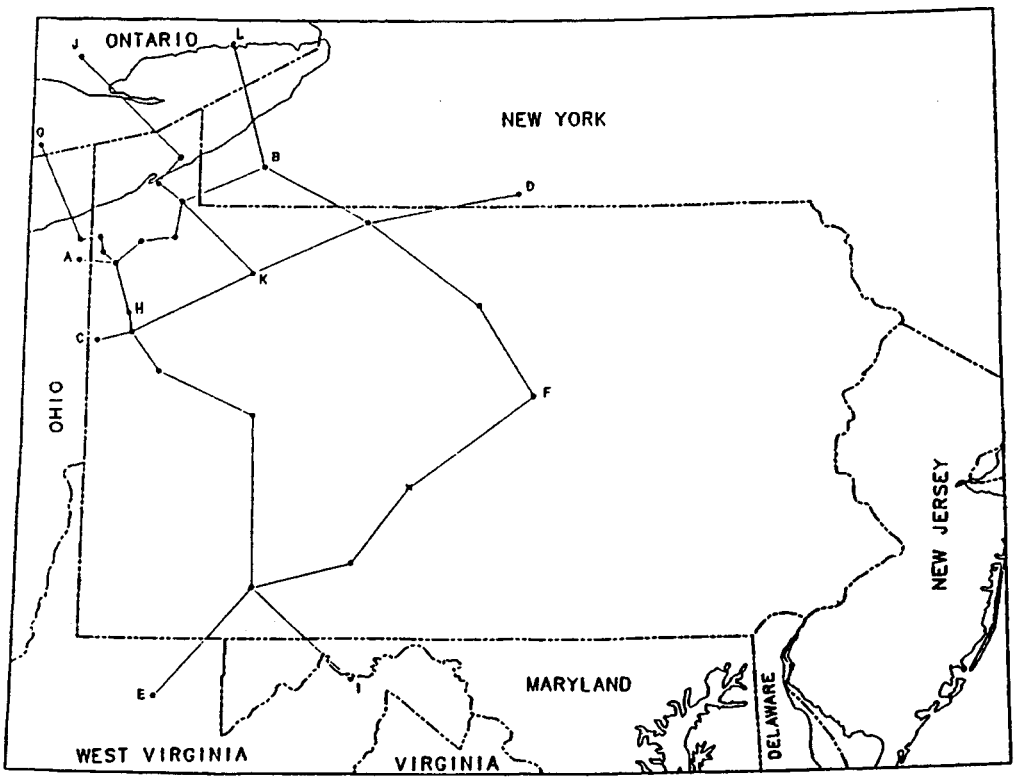

Fig. 1 Location of regional cross sections of the interval between the Utica Shale and the Precambrian basement.

As part of the structural geology study of the Rose Run Sandstone in Ohio, a computer database containing geophysical logtops interpreted by project geologists and based on correlations from regional cross sections was begun. Geophysical logs from approximately 400 wells penetrating the Rose Run Sandstone have been interpreted within the area of investigation. Logtops were picked on selected units and include the following: Precambrian; Mt. Simon Sandstone (Cambrian); Rome Formation (Cambrian); Conasauga Formation (Cambrian); Kerbel Formation (Cambrian); Knox Dolomite, including the "Copper Ridge" dolomite; the Rose Run Sandstone; the "Beekmantown" dolomite (Cambro-Ordovician); Wells Creek Formation (Ordovician); Black River Limestone (Ordovician); Trenton Limestone (Ordovician); "Packer Shell" limestone (Silurian); Salina Group (Silurian), Onondaga Limestone (Devonian); and Berea Sandstone (Mississippian).

Approximately 30 companies were contacted regarding the availability of seismic data to be used in this investigation. Six of these companies committed to donate the use of their data to assist in the Rose Run Sandstone investigation.

Work to be completed in the second quarter will consist of completing the logtop picks for all wells penetrating the Rose Run Sandstone within the area of investigation. All completion card and logtop information that has been input into an Enable database will be uploaded to the VAX where it can be used on the Intergraph Computer Mapping System. A well location map showing productive areas in the Rose Run and a Rose Run subcrop map will be generated with these data. If time permits, structure and isopach maps will be initiated on selected units. All available seismic data that have been collected will be examined for their usefulness in the project.

In Pennsylvania, most of the research performed during the initial quarter of this contract was concentrated on the stratigraphic task, not the structural task. However, logtops interpreted for the stratigraphic task will be used in the preparation of structural maps and cross sections. Structural mapping will begin when all the available logs have been correlated.

A search and review of available literature pertaining to the Cambrian-Ordovician ("Knox") unconformity, the Rome trough, and other structural influences was initiated. In addition, a few companies were contacted regarding the availability of seismic information.

Petrology

The work of Task III this quarter included start-up and orientation, sample and data inventories, and preliminary sample preparation and interpretation. All available cores of Big Injun reservoir sandstones at both federal and state facilities were identified, located, and had access arranged. An extensive literature review of previous Big Injun studies and careful examination of numerous Big Injun thin sections were done to explore the Mississippian reservoir's petrography.

In Ohio, all the available Rose Run cores stored at the Ohio Geological Survey's core repository were inventoried. This inventory included the preparation of a computer-generated map of the well locations from which the cores were recovered. Three additional available Rose Run cores at academic and private industry facilities were also identified. Two of the cores were cut and slabbed for megascopic examination. Twenty-five samples were taken from these two cores for thin-section preparation. Table 1 is a list of the Ohio Rose Run cores; this table also shows the status of each particular core's sampling and thin-sectioning history.

TABLE 1

Rose Run Cores Available in Ohio

Core No.	County	Comment
2958	Scioto	
2898	Jackson	
2923	Morgan	
2852	Coshocton	Slabbed for analysis in 11/90
2853	Coshocton	Sampled for thin sections in 12/90
2963	Tuscawaras	
0867	Guernsey	
2850	Columbiana	
Univ. of Akron	Ashtabula	
Stone Cont. Corp.	Coshocton	

In Pennsylvania, the cores available for this study were inventoried at the Pennsylvania Geological Survey's core repository. Splits of the core samples were made for thin-section preparation. All available well samples for the investigation were catalogued, and a preliminary description of one of the cores was completed. Thin-section, geophysical, petrophysical, lithologic, and X-ray-diffraction data were compiled from the Gatesburg Formation cores recovered from the Hammermill well in Erie County. The thin-section data were graphed to estimate the relative contribution of compaction and cementation in the rocks to porosity reduction during geologic time (Fig. 2). Pore throat sorting and relative pore throat size were calculated from capillary pressure curve data (Fig. 3), and this information was related to petrographic observations.

Development of Reservoir Models (Subtask IV-A). The objective of this subtask is to develop a systematic reservoir model for heterogeneous reservoirs. During the past quarter the development of a composite model for heterogeneous reservoir studies was initiated and progressed satisfactorily. The model will be used to study the effect of transmissibility and mobility variations on fluid distribution in the reservoir. In addition, a probabilistic model for residual oil saturation distribution in heterogeneous reservoirs was formulated. Attempts to collect data also were initiated.

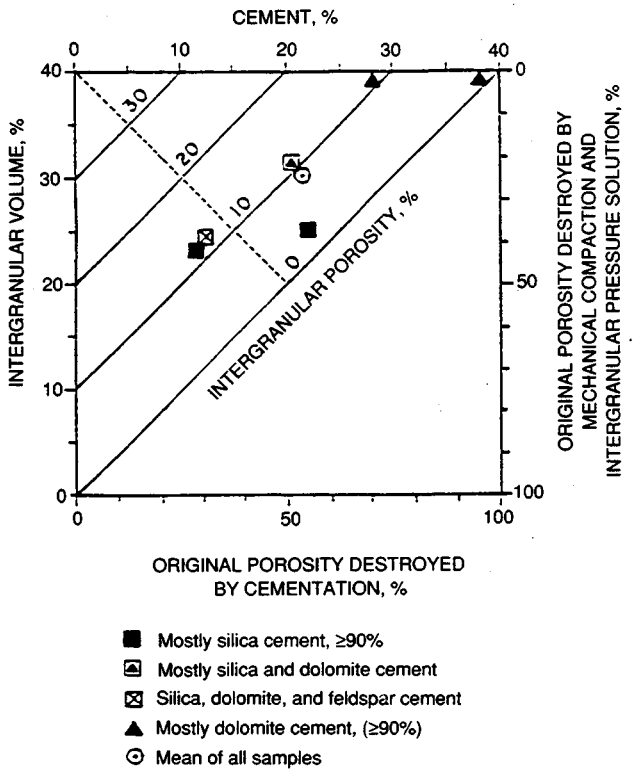

Fig. 2 Plot of intergranular volume vs. amount of cement in samples of the Gatesburg Formation sandstones. The plot is a technique developed by Houseknecht[1] for determining the relative importance of compaction and cementation as porosity-reducing processes in sandstones. Most data points fall in the upper right portion of the diagram and are spread out in that region. This indicates that cementation was a significant process in porosity reduction in these sandstones.

Contacts were made with Pennzoil and CNR to obtain necessary data on Rock Creek and Granny Creek oil fields.

Oil Recovery and Reservoir Management (Subtask IV-B). The objective of this task is to study and understand the influence of heterogeneity on hydrocarbon recovery. During the past quarter the PC version of BOAST was obtained and used for preliminary simulation studies. The PC version of BOAST is a recent release by the Department of Energy that was designed to overcome the limitations of the original BOAST with size necessary to fit on a personal computer. Preliminary simulation runs were focused on the effect of reservoir heterogeneity on oil saturation distribution during production as well as oil movement and redistribution after a long shut-in period. An extensive literature review relative to capillary effects on fluid movement in porous media was also initiated. The results of this review will be used in characterizing heterogeneity in the reservoir models.

Predicting Porosity and Permeability (Subtask IV-C). The objective of this subtask is to determine the effect of shape on porosity and permeability and its influence on fluid movement in porous media. The permeability of rocks is not a well-understood phenomenon. An understanding of the mechanisms and flow path of multiphasic fluids in a permeable solid is important if effective recovery is to be realized. During the past quarter a model of the porous media with a regular matrix of connected pores with two sizes of connections or ostioles between pores was developed. The model was used to gain insight into flow characteristics through a complex network and to determine features that need to be studied in greater detail.

Geological Modeling and Statistics

A program was located in the literature to perform conditional indicator simulation; it may be used to compute risk-qualified estimates of geological and economic variables (e.g., probability of obtaining production above a given value or probability of encountering a given thickness of favorable reservoir rock). The program will have to be modified and tested before it can be accepted.

The oil and gas database at the West Virginia Geological Survey will be used for storage and retrieval of information as the project progresses. Some changes to be made to the structure of the database to allow more efficient retrieval by field and reservoir have been designed. A new table was added to the database, and data entry programs were modified.

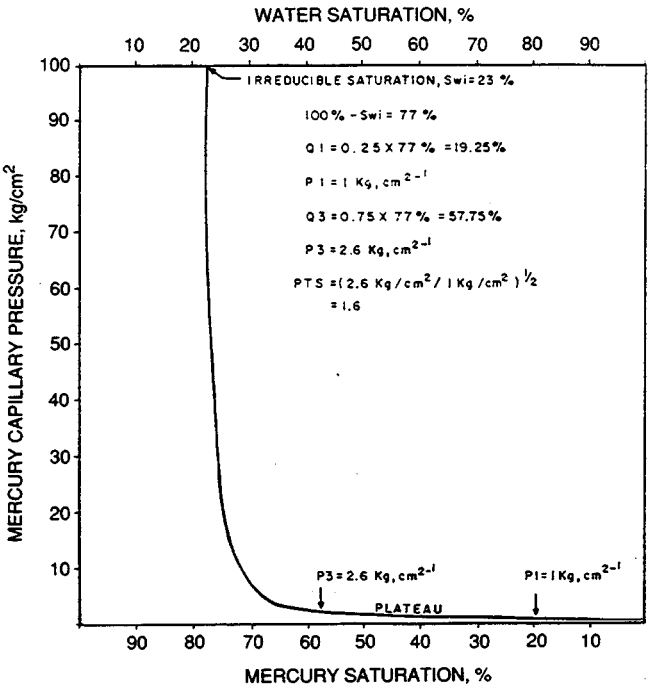

Fig. 3 Capillary pressure curve of a Gatesburg Formation sandstone (Rose Run Sandstone, Hammermill well, Erie Co., Pa.). This sample has a porosity of 13.9%, horizontal permeability of 192 mD, and vertical permeability of 11.1 mD. The sample is a fine-grained, silica-cemented subarkose. The calculations next to the curve show the determination of pore throat sorting (PTS). The value of 1.6 is in Ref. 2.

References

1. D. W. Houseknecht, Assessing the Relative Importance of Compaction Processes and Cementation to Reduction of Porosity in Sandstones, *Am. Assoc. Pet. Geol., Bull.*, 71: 633-642 (1987).
2. J. B. Jennings, Capillary Pressure Techniques; Application to Exploration and Development Geology, *Am. Assoc. Pet. Geol., Bull.*, 71: 1196-1209 (1987).

OIL RECOVERY ENHANCEMENT FROM FRACTURED, LOW PERMEABILITY RESERVOIRS

Texas A&M University
College Station, Tex.

Contract No. DE-FG07-89BC14444

Contract Date: June 13, 1989
Anticipated Completion: Sept. 1, 1992
Government Award: $256,000

Principal Investigator:
S. W. Poston

Project Manager:
Rhonda Patterson
Metairie Site Office

Reporting Period: Oct. 1–Dec. 31, 1990

Objective

The objective of this project is to develop and advance new concepts and technology to increase oil and possibly gas recovery from fractured, low-matrix permeability reservoirs. The overall study is to encompass geological, geophysical, laboratory, and imaging flow studies and analytical and computer modeling as well as field trials.

Summary of Technical Progress

Interpreting and Predicting Natural Fractures

Geological Studies. Detailed maps of the fractures in the Austin Chalk mapped at six field locations were redrafted and copied to permit a statistical analysis of the fracture development.

Figure 1 shows the fracture spacing data from four locations that have been incorporated into a single plot. More than 90% of all fractures in the database are spaced closer than 39 cm. These data need to be calibrated against fracture spacing data in the subsurface.

Exxon Production Company donated access to compressive strength (C_o) data determined at 17 and 34 MPa confining pressures on a total of 40 specimens from two horizontal wells in the Pearsall field. Exxon donated cores from those same two wells for the study.

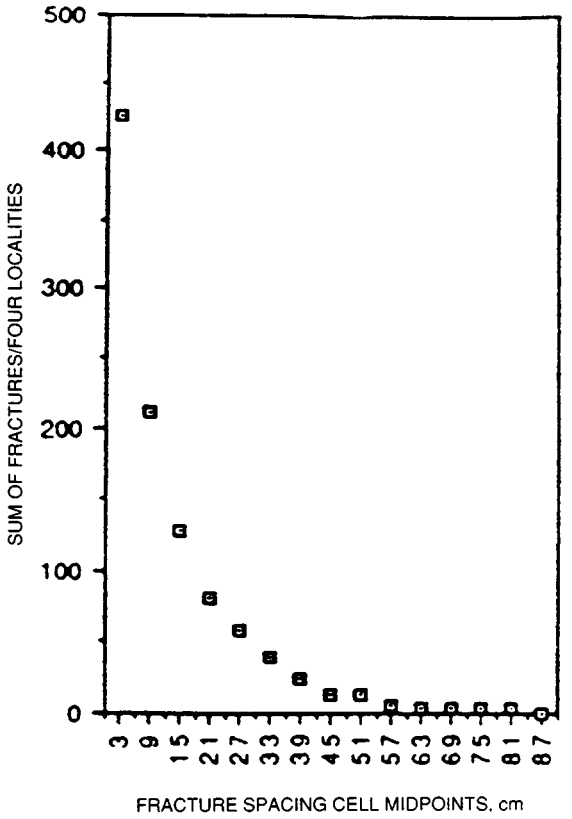

Fig. 1 Fracture spacing in the Austin Chalk.

Point loading tests were performed on machined disks of the Austin Chalk specimens sampled adjacent to the Exxon specimens for the compressive strength tests. The tensile strength (T_o) of the rocks is determined from these point loading tests and will be correlated with the compressive strength (C_o). The purpose of this work is to determine if the correlation between the T_o and C_o is sufficient to enable the T_o term to be used for the compressive strength analysis.

A good correlation between C_o and T_o with a correlation coefficient of 0.81 was observed in one of the Exxon wells. However, the initial analysis of the data from the second well is disappointing. The correlation coefficient is 0.20. These data are currently being analyzed.

A day-long seminar on fractures in reservoirs with special emphasis on the Austin Chalk was conducted at a meeting of the Corpus Christi Geological Society. As a result of this seminar it was agreed that formation microscanner data (and corresponding software packages) from segments of Austin Chalk horizontal wells would be provided for study. These data will allow the fracture spacing data measured on outcrops to be calibrated with subsurface fractures.

References 1 and 2 are papers to be presented. Additionally, a guidebook for a projected field trip to Austin Chalk outcrops immediately prior to the Spring

Annual Meeting of the American Association of Petroleum Geologists (AAPG) in Dallas, April 6 and 7, is being prepared.

Geophysical Studies. Nine-component Vertical Seismic Profile (VSP) data have been analyzed with programs recently developed for the project. These programs (1) generate SV, SH, and vertical source components from arbitrarily oriented vector sources; (2) reorient geophone components (using gyro data) to obtain vertical, in-line, and cross-line orientations for the resulting geophone components; and (3) generate hodograms of these geophone components to determine the principal directions for the anisotropy at the VSP well. The anisotropy is the result of the orientation of vertical fractures, and these orientations are deducible from the directions of the principal axes.

The directions of the principal axes have been determined for the four horizontal components of the data. These are the most important components for determining the orientation of the in situ fractures. The fracture orientations have been determined to be oriented approximately North 55° East. The cross-axis data have small amplitudes when the geophone orientations are set equal to the principal directions. Theoretically, the cross-axis data should go to zero for orthogonal principal axes if the anisotropy is orthorhombic. The study indicates anisotropy is not orthorhombic but is most likely monoclinic because the cross-axis data do not vanish.

The data are currently being analyzed to determine the actual type of existing anisotropy and how to modify the processing to accommodate the more complex anisotropy. The study is trying to determine if there are nonorthogonal principal axes. Preliminary results with nonorthogonal fast and slow principal axes have given a decrease in the amplitudes of the cross-axis data, but these amplitudes still have not been reduced to zero.

Relating Recovery to Well-Log Signatures

Geological Studies. The second phase of the study involves relating well performance to log signatures. An area comprising approximately 50 wells has been selected. Data include resistivity logs for nearly all wells, density–neutron logs for about half the wells, and all available completion records (i.e., perforated zones, tests, and initial potentials). Data collection and digitization will continue during the next period.

Petroleum Engineering. Monthly production records for the candidate wells have been collected for analysis. Weekly well tests taken over an 8-yr period were obtained from an Austin Chalk well. At least five sections within the producing history have been identified as displaying individual decline curve characteristics. These declines are currently being evaluated.

Work continues to formulate an understanding of the correlation parameters for the Chen-type curves.

A paper[1] concerning the relationship between the model derived from the outcrop studies, pertinent flow equations, generation of a set of type curves, and Austin Chalk well production decline curves was written and submitted for presentation at the Society of Petroleum Engineers (SPE) Production Operations Symposium to be held in Oklahoma City in April.

Laboratory Studies of the Imbibition Process

Laboratory Displacement Studies. Imbibition runs were conducted on limestone core samples to study the effects of carbonated water on permeability and recovery efficiency. Carbonated water increased the limestone permeability about 10% (minimum) and yielded an additional average 10.14% of oil. The results of the experiments are shown in Table 1.

Another limestone core sample showed zero recovery when imbibed in brine but yielded 10% of oil in place when imbibed in carbonated water. The acidic nature of the carbonated water was assumed to affect the wettability of the rock sample. Figure 2 is an example of a typical experimental imbibition test. Recovery was increased when the core was imbibed with CO_2-enriched water and when the core was evacuated to cause the CO_2 to evolve at the end of the run.

TABLE 1

Average Recovery from Limestone Cores

Air permeability, mD	Porosity, %	Pore volume cm^3	N_p* brine, %	N_p brine + CO_2, %	Permeability @ S_{or}† brine, mD	Permeability @ S_{or} brine + CO_2, mD
29	27.0	6.9	10	24	9	15
7	19.5	5.2	16	32	1	5
30	22.0	6.7	25	35	3	10
10.6	25.4	6.2	18	28	6	9
12.3	26.3	5.8	13	21	7	11

*N_p,
†S_{or}, residual oil saturation.

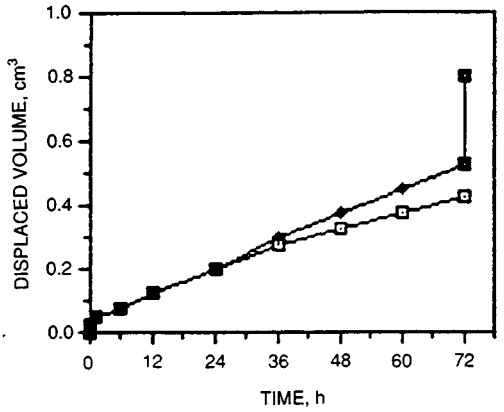

Fig. 2 Cumulative oil displaced during imbibition. –❑–, brine; –◆–, CO_2 + brine; –■–, evacuated.

Various minor equipment problems with conducting imbibition displacement at higher temperatures and pressures precluded significant progress. Modifications to the apparatus were accomplished. Tests at higher temperatures and pressures are currently under way.

Magnetic Resonance Imaging (MRI) Studies. CO_2-enriched water was used in an attempt to accelerate oil production from core plugs. Normally, the CO_2 moves into the carbonate rock and thus changes fluid properties and possibly increases rock permeability by dissolving the rock matrix. After the imbibition process is complete, some CO_2 remains in place.

A significant increase in oil production is observed when the pressure is dropped below the bubble point, which causes the remaining dissolved CO_2 inside the sample to evolve. This localized gas drive forces the oil out of the face of the core sample. Figure 3 is an example of a laboratory experimental run. The bubble point pressure was 500 psi and the test was conducted at 2000 psi. Oil recovery was increased from 17.5% at the end of the imbibition run to 34% when the run pressure was decreased to atmospheric pressure.

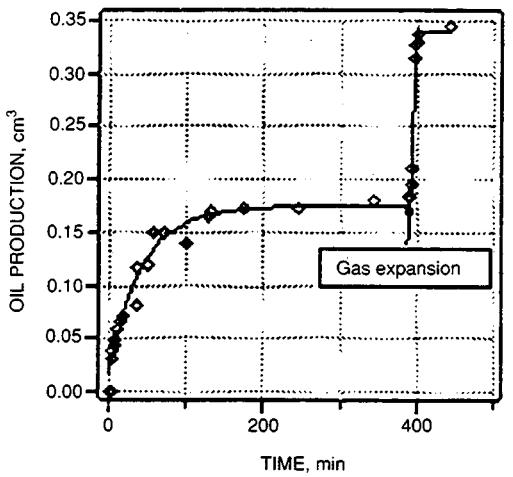

Fig. 3 The effect of imbibition and solution gas drive on recovery.

A new combination of imbibition and CO_2-solution gas drive experiments was designed and implemented. Figure 4 shows that the cumulative production time required to produce a given amount of oil was reduced to near one third when compared with the normal imbibition process.

The method uses the beneficiating properties of CO_2 in two different ways: (1) Changing fluid and rock properties accelerate and improve the water imbibition recovery process; and (2) the expansive properties of the dissolved gas remaining inside the rock sample create a localized gas drive, and incremental oil production may be accelerated in a cyclic manner.

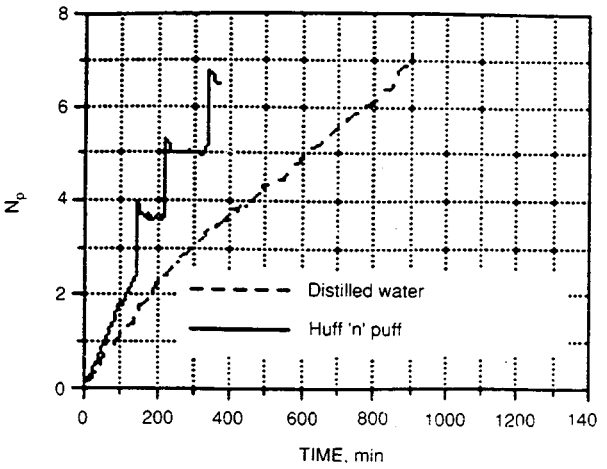

Fig. 4 Cyclic CO_2 evolution and oil recovery.

CT Imaging Studies. No definitive results were achieved this quarter. However, the experimental apparatus was assembled and tested and several experiments in a related area of research were conducted which helped to refine the experimental techniques.

Image Analysis. The magnetic resonance imaging (MRI) binary conversion program has been modified to handle 256×256 and 256×128 image sizes. A 256×256 NMR image was used to scan longitudinal and vertical sections in the core. Cross sections were scanned with a 256×128 resolution. The user can choose the image size from the menu option, and the program will perform the transformation in about 8 s.

The program is now running on a Macintosh IIfX and is used to produce images from the MRI data obtained from research experiments.

Mathematical Modeling

The quasi-linear differential-integral equation is difficult to solve analytically or numerically because the solution may not always exist or may be smooth. De Swaan[4] linearized and solved the equation using the limiting

assumption that the oil–water viscosity ratio is equal to 1. The semi-analytical technique was used to solve a nonlinear equation for varying viscosity ratios. The nonlinear solution matched the cited laboratory imbibition waterflood performance with a greater accuracy.

The compositional mathematical model is continuing to be modified for fractured systems. The compositional model was compared with the SPE Comparative Case.[5] The compositional model provided comparable results to the other models in the SPE paper.

The following differential-integral equation developed by De Swaan is solved with the use of a semi-analytical approach:

$$-u_f \frac{\partial f_{wf}}{\partial x} = \frac{\partial S_{wf}}{\partial t} + \frac{\lambda R_\infty}{\phi_f} \int_o^t e^{-\lambda(t-\tau)} \frac{\partial S_{wf}}{\partial \tau} d\tau$$

The Laplace transformation and nonlinear iteration method were used to solve the equation. The new solution technique eliminated the simplifying assumption of unit oil–water viscosity ratio. Analysis of the computation and laboratory results indicated that:

1. The imbibition waterflood performance, such as phase saturation distribution in the fracture, is greatly influenced by the viscosity ratio.

2. When the viscosity ratio is greater than 1, the saturation distribution in the fracture showed a continuous single-valued function of distance and time.

3. When viscosity ratio is less than 1, the phase saturation distribution, in general, will approach a discontinuous, piston-like feature.

4. The nonlinear solutions matched the laboratory imbibition waterflood performance with a greater accuracy.

Field Trials

A field trial of the CO_2-enhanced oil recovery imbibition technique is to be attempted by Oryx Energy Company this year. The well candidates are currently being selected.

References

1. K. P. Corbett, M. Friedman, D. V. Wiltschko, and J. Hung, Characteristics of Natural Fractures in the Austin Chalk Outcrop Trend in *Proceedings of the Symposium on the Austin Chalk*, South Texas Geological Society, San Antonio, February 1991.
2. D. V. Wiltschko, K. P. Corbett, M. Friedman, and J. Hung, *Strategies for Measuring Fracture Length, Spacing, and Connectivity in the Austin Chalk*, Texas, to be presented at the Gulf Coast Association of Geological Societies, October 1991.
3. S. W. Poston and H. Y. Chen, *Fitting Type Curves to Austin Chalk Wells*, paper SPE 21653, to be presented at the SPE Production Operations Symposium in Oklahoma City, Okla., Apr. 7–9, 1991.
4. A. De Swaan, Theory of Waterflooding in Fractured Reservoirs, *Soc. Pet. Eng. J.*, 117-122 (April 1978).
5. J. E. Killough and C. A. Kossack, *Fifth Comparative Solution Project: Evaluation of Miscible Flood Simulators*, paper SPE 16000, presented at the Ninth SPE Symposium on Reservoir Simulation, San Antonio, Tex., Feb. 1–4, 1987.

RESOURCE ASSESSMENT TECHNOLOGY

ESTABLISHMENT OF AN OIL AND GAS DATABASE FOR INCREASED RECOVERY AND CHARACTERIZATION OF OIL AND GAS CARBONATE RESERVOIR HETEROGENEITY

Contract No. FG22-89BC14425

Geological Survey of Alabama
Tuscaloosa, Ala.

Contract Date: Apr. 19, 1989
Anticipated Completion: Apr. 18, 1992
Government Award: $240,000
(Current year)

Principal Investigator:
Ernest A. Mancini

Project Manager:
R. Michael Ray
Bartlesville Project Office

Reporting Period: Oct. 1–Dec. 31, 1990

Objectives

The objectives of this project are to augment the national reservoir database, Tertiary Oil Recovery Information System (TORIS), to increase the understanding of geologic heterogeneities that affect the recoveries of oil and gas from carbonate reservoirs in Alabama, and to identify those resources that are producible at moderate cost. These objectives will be achieved through detailed geological, geostatistical, and engineering characterization of typical Jurassic Smackover Formation hydrocarbon reservoirs in selected productive fields in Alabama. These studies will be used to develop and test mathematical models for the prediction of the effects of reservoir heterogeneities in hydrocarbon production.

Summary of Technical Progress

Work to date has focused on completion of Subtasks 1, 2, and 3 of this project as stated in Annex 1 to the Memorandum of Understanding between the U.S. Department of Energy (DOE) and Alabama, through the Geological Survey of Alabama (GSA) and attachments to said Annex. Work on Subtask 4 began in this quarter, and substantial additional work has been accomplished on Subtask 2.

Subtask 1

Subtask 1 is complete and a topical report detailing this subtask has been submitted to DOE. Subtask 1 included the survey and tabulation of available reservoir engineering and geological data relevant to the Smackover reservoir in southwestern Alabama. These data were submitted to DOE via magnetic computer tape in a format compatible with the national reservoir database, TORIS. Data are being added and/or updated into the database periodically, and this will continue throughout the project.

Subtask 2

Subtask 2 comprises the geologic and engineering characterization of Smackover reservoir lithofacies. This was accomplished through detailed examination and analysis of geophysical well logs, core material, well cuttings, and well-test data from wells penetrating Smackover reservoirs in southwestern Alabama. From these data, parameters relating to reservoir heterogeneity, such as lateral and vertical changes in lithology, porosity, permeability, and diagenetic overprint, were recognized and used to produce maps, cross sections, graphs, and other graphic representations to aid in interpretation of the geologic parameters that affect these reservoirs. Geological and engineering research pursuant to this subtask has focused on descriptions of core material and petrographic thin sections and computer entry of pertinent data (including available core analyses), as well as digitization of geophysical well logs. The ultimate goal of this research is a comprehensive characterization of all Smackover fields in the state.

Cores from four Smackover fields (Uriah, Silas, Blacksher, and Zion Chapel fields) were described this quarter (cores from 23 fields have been described since the start of the project), and graphic summaries of the core descriptions were integrated with other data to generate reservoir characterizations for these fields. Depositional and diagenetic sequences were interpreted and summarized for each core. Petrographic thin-section studies have been made on 10 of the 23 fields described to supplement and extend interpretations made from core descriptions. Three hundred fifty-two thin sections have been described (53 this quarter); 299 have been made but not yet described; and 66 have been selected but not yet made. This is a total of 717 thin sections. A comprehensive record, in the form of an annotated file of 35-mm color slides, is being compiled from all thin sections examined. Paragenetic sequences have been reconstructed for most of the 23 fields described. Eighty-nine thin sections have been point counted (63 this quarter) to estimate the relative proportions of particle and pore types making up the reservoirs.

Capillary pressure data are being collected on samples taken from selected cores from Smackover fields. These data will supplement the petrographic and geophysical data. To date, 47 capillary pressure analyses have been run on samples from four fields, and 106 other samples have been prepared for analysis. Preliminary capillary-pressure analyses of Smackover reservoir rocks suggest, as expected, that lithologically similar samples yield similar capillary-pressure curves. Samples from North Choctaw Ridge field and Silas field, predominantly oomoldic and pelmoldic dolostone reservoirs with substantial amounts of relict primary interparticle porosity, exhibit leptokurtic unimodal throat-size distributions. This means that nearly all pores are accessed through throats of a very restricted size range. These pore throats appear to result from a combination of (1) incomplete cement coatings on the ooids (now moldic porosity), (2) open primary pores that originally formed a highly permeable network, and (3) interconnection of neighboring particle molds resulting from partial crushing of the rigid cement framework. Further details on the origin and distribution of the all-important pore throats connecting the large moldic pores will be investigated by fluorescence microscopy. The core log of the North Choctaw Ridge field is shown in Fig. 1.

Point counting of more than 80 thin sections from 10 Smackover fields, as well as examination of cores and thin

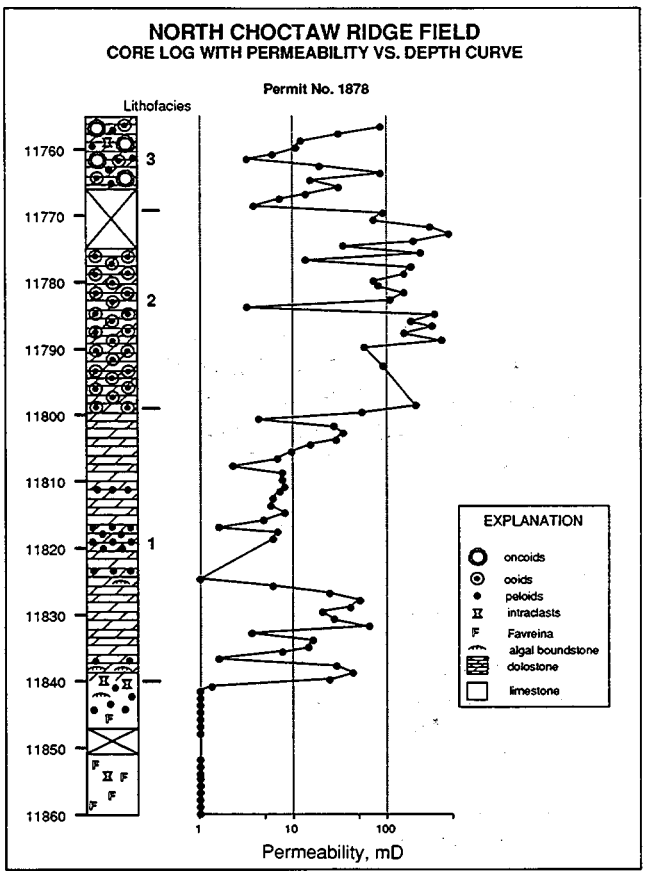

Fig. 1 Variation in permeability values for three lithofacies distinguished by lithology and by pore types, North Choctaw Ridge field, Choctaw Co., Ala. Lithofacies 1 is dominated by intercrystalline pores, lithofacies 3 is dominated by moldic pores, and lithofacies 2 is characterized by a combination of these two pore types plus interparticle pores.

sections from a total of 23 Smackover fields, has revealed that Smackover pore systems in Alabama are dominated by only a few pore types. Particle moldic pores (primarily oomolds and pelmolds), including secondary intraparticle pores (partial molds), and intercrystalline pores in dolostones, account for 85% of all porosity in Smackover carbonate reservoirs examined to date in Alabama. Interparticle pores, fractures, vugs, and fenestral pores are locally common, but only interparticle and fracture pores materially enhance reservoir permeability. Particle molds dominate reservoirs that are not fully dolomitized or in which dolomitization was fabric selective. More highly altered reservoirs strongly affected by nonselective dolomitization are dominated by intercrystalline pores. Although these two "end-member" reservoir types can be defined, intermediates are common, and most intermediate reservoirs more closely resemble intercrystalline reservoirs. The pore systems of intermediate reservoirs consist of "isolated" moldic pores, or clusters of secondary intraparticle pores within former particles, connected by networks of intercrystalline pores that lie between dolomite crystals in dolomitized calcium-carbonate cements. Consequently the intercrystalline pore systems are the conduits through which the hydrocarbons in the isolated molds must drain. Because the characteristics of a conduit control the rate at which a storage space can fill or empty, these intermediate reservoirs tend to behave like intercrystalline reservoirs.

Subtask 3

Subtask 3 includes the geologic modeling of reservoir heterogeneities for Smackover reservoirs. This research was completed before this quarter began.

Subtask 3 also requires that GSA host an annual public conference targeted at Alabama oil and gas operators for the purpose of transferring data and results of the project. The first of these conferences was held Sept. 18–19, 1990, at the University of Alabama in Tuscaloosa, Ala. The second technology transfer conference is planned for sometime in the coming year (precise date and location not yet decided).

Detailed topical reports of Subtasks 1, 2, and 3 have been completed.

Subtask 4

Subtask 4 includes the development of reservoir exploitation methodologies for strategic infill drilling, based on the results of subtasks 2 and 3, for typical Smackover reservoirs. These strategies are to be verified by geostatistical modeling. The Smackover field to be examined as part of Subtask 4 is Chunchula field. The three components of this study are (1) geological and petrophysical reservoir characterization of the Chunchula reservoir, (2) geologic flow modeling, and (3) geostatistical modeling of Chunchula field.

Geological and Petrophysical Reservoir Characterization

So that the spatial variation of and controls on reservoir characteristics within Chunchula field can be elucidated, 12 general maps and 14 cross sections have been constructed for Chunchula field. These maps provide information on the three-dimensional (3-D) configuration of the Smackover reservoir, general variation in porosity and permeability within the field, and factors (depositional and structural) that control reservoir quality and distribution.

The cross sections were hung on a stratigraphic datum (top of Buckner Anhydrite Member). For each well on the cross sections, Smackover lithologies (dolomite vs. limestone), distribution of reservoir within the Smackover, and porosity and permeability values are indicated. These cross sections suggest that Chunchula field may contain a highly compartmentalized reservoir and that the porosity lenses in the reservoir have irregular shapes.

In addition to the cross sections, a series of "slice maps" were prepared to depict variation in porosity and permeability within the field. These maps are isopach maps of the 5-ft average porosity and permeability at selected structural and stratigraphic horizons within the field. A series of 13 maps were generated for porosity and permeability on both structural and stratigraphic datums. These maps indicate that the Chunchula reservoir is very complex.

A tentative interpretation of the distribution of reservoir-grade rock within Chunchula field has been made. An initial model that defines individual reservoir compartments has been developed. Efforts during the remainder of the project will concentrate on testing and refining this model. The reservoir-distribution model will be tested against more detailed lithologic data now being collected from Chunchula field as described later. The model will be revised as needed to incorporate the new lithologic data. In addition, interpretations that are now being made of drainage areas for individual wells and of interconnectedness of well pairs will be compared with the model and necessary modifications made. The ultimate goal will be to accurately define the 3-D geometry and other characteristics of the reservoir that makes up Chunchula field and to identify the geologic factors that control this geometry.

Four Chunchula cores were described in detail this quarter, and three detailed core logs were produced. One hundred fourteen thin sections were made.

Three of the four Chunchula cores described contain the upper part of the Norphlet Formation. High- and low-angle cross-laminae interpreted to be eolian dune and interdune deposits and structureless sandstone suggesting partial marine reworking occur at the top of the Norphlet in these cores. This indicates that transgressing Smackover seas only partially reworked Norphlet dunes. The resulting uneven topography may have influenced the distribution of Smackover depositional facies.

The lowest Smackover facies is an algal boundstone. This facies varies in thickness from 2 ft in the north-central

part of the field to 20 ft in the southernmost part of the field. Intertidal flat laminated algal boundstone with a predominantly muddy matrix grades upward into mottled algal boundstone with a peloid oncoid packstone–grainstone matrix in the southern part of the field. In the northern part of the field, thin algal boundstone is overlain by lower energy peloid oncoid wackestone, probably deposited in deeper water than equivalent rocks to the south. In the central part of the field, the algal boundstone is overlain by shoal-to-shoal margin deposits. These dramatic facies variations indicate (1) significant topographic variation in early Smackover time, possibly influenced by Norphlet dune–interdune paleotopography, and (2) that the Chunchula reservoir is heterogeneous both vertically and laterally.

Smackover rocks in Chunchula field show an overall stratigraphic progression (although there is considerable geographic variation) from predominantly grainy strata to muddy strata in the middle Smackover and back to grainier strata in the upper Smackover, forming a transgressive–regressive cycle. Even though all the lower Smackover and most of the upper Smackover was thoroughly dolomitized, the best porosity commonly occurs in grain-supported strata. The most common pore types are particle-moldic and intercrystalline, with less secondary intraparticle and minor vuggy porosity. Dolomite in reservoir lithofacies is predominantly medium to coarsely crystalline. Where a significant amount of calcium carbonate occurs, porosity is commonly poor.

Geologic Flow Modeling

The purpose of this project is to evaluate the effects of reservoir heterogeneity and reservoir continuity on the production performance of Chunchula field. Engineering analysis forms a part of the overall study of Chunchula field aimed at developing a program for enhanced oil recovery (EOR) by means of strategic infill drilling and injection. A program of data acquisition and reservoir-engineering analysis was undertaken to accomplish the immediate goal of evaluating the effects of reservoir heterogeneity and reservoir continuity on production performance of Chunchula field. These data will be used as input to a suite of reservoir-engineering analyses. The primary method of reservoir-engineering analysis will be the application of a black-oil simulator. Initial qualitative analysis of the data indicates that the reservoir is heterogeneous but appears to be continuous throughout the field with at least one exception. Simulation studies will begin during the next quarter, and more definitive information on reservoir dynamics should be available.

Fluid composition in Chunchula field is complex, including gas, condensate, and oil. For long-term management, a compositional simulator would be favored over a black-oil simulator. However, evaluation of the long-term behavior of the reservoir is not a primary goal of this study. Rather, an analysis of the continuity and heterogeneity of the reservoir is the objective. The black-oil simulator can be used with sufficient accuracy to achieve this objective because the reservoir-fluid pressure does not drop below the dew-point pressure and therefore the reservoir behaves as a single-phase system. As long as the reservoir fluid is single phase, a black-oil simulator can be adjusted to provide results comparable to those which could be derived from the more complex and computationally more intensive compositional simulation.

Geostatistical Modeling

During this quarter the geostatistics group refined and continued development of the hierarchical simulation algorithm described in the last quarterly report. Further two-well tests of this algorithm have been run on the Cray computer. In addition, parameterization of spatial correlation of permeability values in Chunchula field was completed.

Significant progress has been made in the development of the hierarchical fractal simulation program. This hierarchical approach is used because it requires significantly less computer time and memory than alternate methods and therefore permits the simulation of larger systems. Recent simulations contain 64×66 (4,224) cells and are larger than would be possible with conventional methods (or at least represent the upper limit of such methods). The present version of the simulation algorithm reproduces the input well data exactly while estimating values for the vertical two-dimensional panel between the two wells. The present limitation on the size of the model system is set by the amount of memory available on the computer. In January there will be a more than twofold upgrade of the Cray, which will permit simulation of a system roughly four times larger ($128 \times 128 = 16{,}384$ cells); this will be undeniably larger than anything that can be done with other methods. Being able to handle systems of this size is significant, for it makes possible for the first time meaningful 3-D simulations (e.g., $32 \times 32 \times 16$ cell matrices).

The following tasks are contemplated for the remainder of the project period: (1) completion of geostatistical modeling, (2) indicator kriging (involving conversion of continuous permeability data to two-stage variables with various reservoir cutoffs), and (3) further development of the simulation algorithm and its application to the whole of Chunchula field.

In any discussion of the impact of reservoir heterogeneity or fluid movement within a formation, the issue of scale is a vital consideration. The data for reservoir description are commonly derived from cores and logs that examine relatively small quantities of rock. Thus a fundamental problem exists in scaling up the detailed reservoir description data to something representative of typical reservoir model grid-block sizes. Conditional simulation is a geostatistical technique that can be used to generate outcomes of a spatial random function, such as permeability. The generation of equiprobable maps with a given

spatial structure is termed stochastic simulation. Conditional stochastic indicator simulations will be performed with core-derived permeability data. The future plan is to apply the hierarchical algorithm to simulation of porosity and permeability distributions of selected cross sections bounded by two wells. After simulation of some cross sections, contour plots of the variation of various quantities such as the probability of having a porosity in excess of 9 or 12%, will be produced.

Significant Accomplishments

Significant accomplishments include completion of Subtasks 1, 2, and 3 and completion of comprehensive topical reports of the results of these subtasks. In addition, significant progress has been made toward development of detailed predictive geostatistical and geologic reservoir models for the Smackover reservoir at Chunchula field.

Significance to EOR Research Plan

The results of Subtasks 1 and 2 research provide the basic data necessary for an understanding of the Smackover reservoirs in southwestern Alabama. The results of Subtask 3 allow reservoirs to be placed into a hierarchical ranking scheme of reservoir heterogeneity. This ranking scheme gives a relative means by which to rate reservoirs in terms of those most likely to contain unswept or uncontacted mobile oil and therefore most likely to be candidates for infill drilling or EOR.

Progress in geostatistical and geologic reservoir modeling is significant to the EOR research plan because these models will provide stochastic and deterministic predictions, respectively, of reservoir geometry, compartmentalization, and fluid-flow pathways. These data are important to the design of EOR methodologies and to the infill drilling strategy within a field.

CHARACTERIZATION OF SANDSTONE HETEROGENEITY IN CARBONIFEROUS RESERVOIRS FOR INCREASED RECOVERY OF OIL AND GAS FROM FORELAND BASINS

Contract No. FG07-90BC14448

Geological Survey of Alabama
Tuscaloosa, Ala.

Contract Date: Feb. 20, 1990
Anticipated Completion: May 30, 1993
Government Award: $175,000
(Current year)

Principal Investigator:
Ernest A. Mancini

Project Manager:
Chandra M. Nautiyal
Bartlesville Project Office

Reporting Period: Oct. 1–Dec. 31, 1990

Objectives

The objectives of this project are to augment the National Reservoir Database Tertiary Oil Recovery Information System (TORIS), to develop models of reservoir heterogeneity, and to identify resources that are producible at reasonable cost; this will increase recovery of hydrocarbons from Carboniferous siliclastic reservoirs in the Black Warrior Basin. The objectives will be achieved through detailed geological, engineering, and geostatistical investigations of Carboniferous sandstone reservoirs in the basin. These investigations will be used to develop and to test geological and mathematical models for predicting the effect of reservoir heterogeneity on the recovery of hydrocarbons.

Summary of Technical Progress

Outcrop Investigation of Sandstone Heterogeneity

Outcrop investigation of sandstone heterogeneity is nearly complete, and a topical report will be submitted during the next quarter. Outcrop investigations focused on characterization of vertical variations, changes, and sequences in Carboniferous strata of the Black Warrior Basin through stratigraphic analysis. Most attention has focused on three sandstone units in northern Alabama that provide critical evidence regarding variation in Carboniferous sandstone reservoirs. These units include the Lewis sandstone, the Hartselle Sandstone, and the Mary Lee cycle of the Pottsville Formation, which includes the upper Nason sandstone. The Lewis sandstone is one of the major oil-producing reservoirs in the Black Warrior Basin. Each of these units was deposited in a variety of settings, including beach-barrier and open-shelf systems. The Lewis sandstone and the Hartselle Sandstone are of particular significance because these units contain asphalt. Thus hydrocarbon distribution in heterogeneous reservoirs can be directly observed. Additionally, excellent lateral exposure of a distance of approximately 1 mile in quarry walls permits determination of heterogeneity at an interwell scale.

A three-part model was developed for the Lewis sandstone and associated carbonate units (Fig. 1). The beds

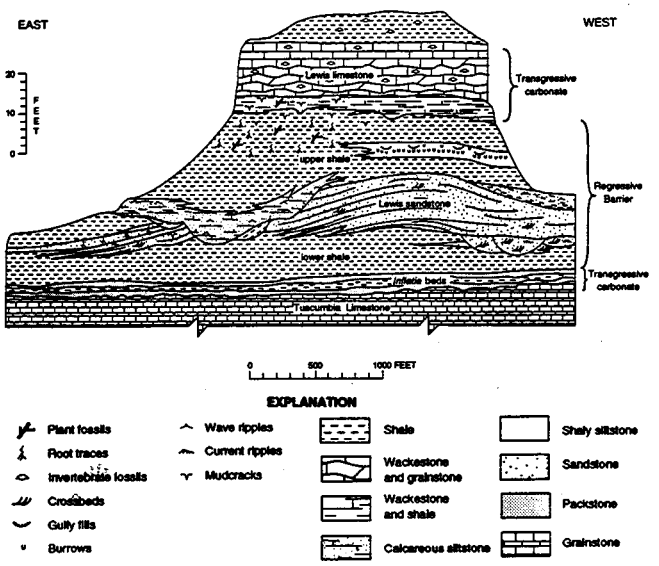

Fig. 1 Lewis sequence in a wall of the Tuscumbia Quarry.

at the base of the Lewis sandstone are interpreted to overlie the Tuscumbia Limestone and apparently represent transgressive oolite-shoal and storm deposits. The Lewis sandstone evidently represents a major regressive episode and is interpreted to include storm-dominated-shelf and beach-barrier deposits. Lewis sandstone deposition may have culminated in the development of a system in which sediment was supplied by drift from deltaic sources and reworking of shelf sandstone bodies. The final episode in Lewis deposition apparently was transgressive carbonate sedimentation. Facies relationships between sandstone and limestone suggest that topography from barrier formation may have been a key factor in determining the distribution of transgressive carbonate units.

The Hartselle Sandstone is characterized by extreme facies heterogeneity and is interpreted to represent a series of prograding beach systems that were subsequently reworked during a marine transgression. Complex facies patterns evidently resulted from that reworking, but internal facies patterns are difficult to distinguish in the sandstone. Even so, beach facies, which contain the most homogeneous sandstone, are most abundant near the base of the sandstone, and shelf, lagoonal, intertidal marsh, and swamp facies appear to be most common in the upper part. Additionally, plant fossils are most common in the lower part of the sandstone, whereas marine fossils are most common in the upper part. Wavy-bedded shelf, back-barrier, and intertidal sandstone deposits are lithologically similar, but results of ichnologic analyses demonstrate that these deposits may be separated on the basis of trace fossils. In the Appalachian fold-and-thrust belt, synsedimentary activity of Appalachian structures apparently had a pronounced effect on paleocurrent distribution in the sandstone.

The Mary Lee cycle of the Pottsville Formation, which includes the upper Nason sandstone, represents a diverse assemblage of rocks that reflect progressive coastal-plain evolution in response to regional marine regression and transgression. The first episode of Mary Lee deposition apparently included progradation of a fluvially dominated deltaic complex. The extent of deltaic progradation was limited, and the upper Nason sandstone subsequently accumulated beyond the inactive delta front. The upper Nason evidently represents an open-shelf and sand-ridge system that was reworked into shoreface systems and was possibly dissected by fluvial systems in response to a relative lowering of sea level. Exposed delta platforms apparently provided ideal conditions for alluvial peat (coal) accumulation, and synsedimentary activity of Appalachian structural precursors may have influenced the distribution of tributary deposits and peat. West of the delta platforms, marine transgression predominated, and accumulation of peat and siliclastic sediment in a tidally dominated delta complex gave way to estuary formation and thereby set the stage for the next cycle of deposition.

In conjunction with the field investigations, a set of subsurface cross sections was constructed to extend outcrop information into the subsurface. This subsurface cross-section network demonstrates the correlation of units from the Devonian Chattanooga Shale through the Pennsylvanian Mary Lee cycle of the Pottsville Formation in the Black Warrior Basin. This network defines a series of regionally traceable, marker-bound units and defines the extent and traceability of Carboniferous reservoir sandstone bodies, including the Lewis, Carter, and *Millerella* sandstones. These cross sections also provide a basis for subsurface correlation and identification of stratigraphic units on the basis of well-log signature. Subsurface mapping and construction of cross sections will continue in the next quarter to provide a regional framework for reservoir characterization.

The cross sections demonstrate that Mississippian carbonate platform-ramp systems (Fort Payne, Bangor, and *Millerella*) dipped southwest and that episodes of carbonate sedimentation were episodically interrupted by clastic sedimentation and deposition of reservoir sandstone bodies (Lewis, Evans, and Carter). Progradation of the upper Parkwood clastic sequence marked the end of regional carbonate sedimentation. Additionally, the coal-bearing Pottsville Formation appears to overlie unconformably the Parkwood Formation and apparently truncates Mississippian carbonate units along the northeast margin of the Black Warrior Basin. Potential reservoirs are most widespread at the base of the formation and systematically migrate northwestward and decrease in areal extent.

Geologic and Engineering Characterization of Carboniferous Reservoirs

Twenty-six oil fields containing 33 pools in the Lewis, Carter, and *Millerella* sandstones of Alabama have been prioritized for reservoir characterization on the basis of production and availability of data. Oil fields in the

Mississippi part of the Black Warrior Basin currently are being identified and prioritized with similar criteria. Characterization of oil fields is being accomplished through detailed examination and analysis of geophysical well logs, petrophysical data, and core material. Field-type logs, base maps, isopach maps, structural contour maps, and cross sections are being constructed for inclusion in reservoir characterization packets for each field. For fields where cores are available, these packets will include a lithologic core log for a type well, including description and diagenetic character and porosity and permeability profiles. Porosity–permeability cross plots will also be included in the field packets. Tabulation and insertion of all available geologic and engineering data into computerized reservoir characterization forms are near completion for Alabama oil fields. All available commercial porosity and permeability data for oil fields in Alabama have been entered into a spreadsheet and plotted with the use of standard software. Reservoir units have been picked for all logs in 11 fields.

Cubes and plugs for permeability determination have been prepared for 316 samples of Carter sandstone from the North Blowhorn Creek oil unit, which will serve as a model area during subsequent tasks. From these samples, 48 horizontal and vertical air-permeability measurements were made during the reporting period. Capillary-pressure data were collected for 83 of 267 samples cut from cores from the North Blowhorn Creek oil unit. Thin-section blanks were cut from the ends of 153 samples used for porosity determination; 115 new blue-epoxy impregnated thin sections were prepared from these blanks to supplement 210 existing thin sections prepared for previous studies of Black Warrior Basin sandstones at the Geological Survey of Alabama. Preparation of porosity and permeability samples and thin sections will continue into the next quarter. All thin sections made thus far have been qualitatively examined to determine diagenetic character. A modal analysis scheme geared toward quantifying pore types and the distribution of authigenic minerals was devised on the basis of this examination. Selected samples were polished and surface stained with a fluorescent dye to examine pore systems by ultraviolet and blue light-induced fluorescence microscopy. Backscattered electron imaging with a scanning electron microscope (SEM) and an electron microprobe of five carbon-coated, polished thin sections from North Blowhorn Creek oil unit also was used to examine pore systems and to qualitatively assess chemical variation in authigenic carbonate minerals. Five high-resolution energy-dispersive X-ray maps were also made of carbonate-mineral cements to document chemical variation and to assist in the formulation of a strategy for quantitative chemical analyses to be performed with the electron microprobe during the next quarter. Cement-stratigraphic relationships and pore geometry were examined with an SEM for 25 gold–palladium-coated, broken-surface samples from North Blowhorn Creek oil unit and Tuscumbia Quarry. Stratigraphic relationships between authigenic minerals and hydrocarbons were noted to determine the timing of hydrocarbon migration in Carter and Lewis sandstone reservoirs. A photographic atlas of secondary and backscattered electron images and X-ray maps documenting pore geometry and cement–hydrocarbon relationships is being compiled.

Criteria for Recognition of Reservoir Heterogeneity

Progress on this task during the reporting period concerns field investigations associated with Task 1 and detailed petrographic studies of samples from cores from the North Blowhorn Creek oil unit and outcrop localities. Because cores are scarce in the Black Warrior Basin, criteria for recognition of reservoir heterogeneity throughout the basin ultimately must be based on interpretation of geophysical well logs. Thus far, efforts have been directed toward identification of key types of heterogeneity on the basis of direct observation of rock in outcrop and core. In addition to the outcrop areas described previously, the North Blowhorn Creek oil unit has been chosen as a model study area because cores are available from 12 of the 50 wells in the oil unit.

Five levels of heterogeneity have been identified in Carboniferous reservoirs of the Black Warrior Basin. The first level is the reservoir body itself—a body of reservoir rock surrounded by nonreservoir rock. Level-2 heterogeneity includes large-scale features that restrict fluid flow in an area that contains several wells in a single oil reservoir. Level-3 heterogeneity consists of features that have areal extent less than the average well spacing. Level-4 heterogeneity includes features at the scale of a wellbore or core, whereas level-5 heterogeneity occurs at the scale of hundreds of pores and pore throats to a single pore.

Synthesis of variation observed in outcrop with heterogeneity models indicates that considerable heterogeneity exists in Carboniferous reservoir sandstone of the Black Warrior Basin. Differing styles of heterogeneity may necessitate using a number of recovery strategies to optimize production of liquid hydrocarbons. The relative intensity of heterogeneity at the various levels outlined previously varies among the three units examined in outcrop (Table 1). For example, Lewis sandstone bodies are isolated and are confined vertically and laterally by impermeable shale, whereas upper sandstone bodies may extend continuously for tens of miles. Sandstone bodies represent an example of level-1 heterogeneity that is intermediate between Lewis and the upper Nason. Although regional subsurface isopach and isolith patterns suggest that the sandstone body has greater lateral extent than the upper Nason, outcrop investigations suggest that the Hartselle is internally the most heterogeneous sandstone unit examined. Lewis sandstone in outcrop is most similar to the oil-producing fields in Fayette and Lamar counties that have been examined thus far.

TABLE 1

Heterogeneity in Carboniferous Sandstone, Black Warrior Basin*

Level	Unit		
	Lewis sandstone	Hartselle Sandstone	Upper Nason sandstone
1	Isolated, lensoid sandstone bodies in shale	Regionally extensive sandstone body composed of sandstone lenses and shale partings	Regionally extensive sandstone body lacking major shale units
2	Carbonate cement at margins of sandstone body; asphaltic sandstone in axis	Lensoid sandstone bodies; asphalt accumulations localized	Quartz-cemented sandstone along upper contact
3	Inlet facies poorly connected with sandstone axis; lagoonal channel facies causes reservoir discontinuity that is difficult to predict	Anastomosing, clay-rich permeability barriers; asphalt preserved mainly in wavy flaser, and lenticular beds, scarce in crossbedded sandstone	Pinch and swell of sandstone bodies; clay drapes on major sandstone foresets
4	Interlaminated carbonate-cemented and asphaltic sandstone; coarsest laminae cemented; finest laminae asphaltic; clay laminae	Anastomosing clay laminae; carbonate cement; mudstone clasts, bioclasts, bioturbation	Clay drapes; grain-size variation
5	Carbonate cement; authigenic and detrital clay; asphalt?	Carbonate cement, authigenic and detrital clay asphalt?	Quartz cement

*Determined from outcrop.

Petrologic studies reveal that diagenetic overprinting introduced heterogeneity at levels 2 to 5. Some types of diagenetically induced heterogeneity show clear relationships to texture and sedimentary structures, whereas other types are products of burial diagenesis, unrelated to these features. Carbonate minerals, quartz, and kaolinite are the most abundant authigenic minerals, both in outcrop and in the subsurface. The authigenic carbonate mineral assemblage is complex; it consists of calcite, ferroan calcite, nonferroan dolomite, ferroan dolomite or ankerite, and siderite. The presence of calcite clearly is associated with concentrations of shell debris in channels or washover deposits, which served as a source of components for the cement. Calcite formed early in the diagnetic sequence and disrupts the continuity of the reservoir. Siderite occurs as early-formed isopachous rims on detrital grains, dispersed "wheat seed" crystals, and concretionary patches. Ferroan dolomite or ankerite is the most abundant late-stage authigenic carbonate mineral and pervasively fills pores near the margins of Lewis and Carter beach-barrier sandstone bodies and thus forms an important level-2 heterogeneity. In reservoir sandstone, ferroan dolomite occurs as isolated, rhombic crystals. Backscattered-electron imaging and fluorescence microscopy reveal complex chemical zonation in both early- and late-stage carbonate-mineral cements, which suggests complex evolution of formation water during burial. It is not clear at present if the concentration of ferroan dolomite cement near the margins of the sandstone bodies is related to the proximity of shale as a source of components for the cement. If, after further evaluation, this proves to be the case, then the volume of isolated Lewis and Carter sandstone bodies and sandstone/shale ratios would become important criteria for predicting heterogeneity in these reservoirs.

Kaolinite fills grain-size volumes and may be both detrital and authigenic in origin. Kaolinite is most common in nonreservoir sandstone that was deposited under low-energy conditions and also contains abundant mud clasts. These sandstones disrupt the continuity of the reservoir in the North Blowhorn Creek oil unit. In reservoir sandstone, authigenic kaolinite fills scattered pores and framework-grain size patches. This type of sandstone has a bimodal pore-size distribution consisting of micropores and macropores. Because kaolinite contains micropores, typically filled with irreducible water, care should be taken to avoid misinterpretation of effective porosity and water saturation based on well log evaluation. The presence of kaolinite should also be considered during field development because of the potential for formation damage.

Authigenic quartz is locally pervasive in Carter sandstone in the North Blowhorn Creek oil unit, but in reservoir sandstone it most typically occurs as syntaxial overgrowths on detrital quartz grains. Etching or pitting of smooth overgrowth surfaces was not detected by SEM observation. This suggests that pores surrounded by these quartz overgrowths are modified primary pores rather than secondary pores formed through dissolution of intergranular carbonate-mineral cement. Some secondary pores formed during burial diagenesis through dissolution

of mud clasts and, perhaps, feldspars. However, the chemically stable nature of the detrital framework precludes significant enhancement of the interconnected pore system through framework grain dissolution. Although pores exist in carbonate-cemented zones as a result of partial dissolution of fossil fragments, they are isolated and not part of an effective pore system.

Pressure-solution features include seams along shale interbeds and clay drapes, wispy microstylolites, and areas of intergranular pressure solution. Pressure-solution seams are effective barriers to vertical fluid flow, whereas wispy microstylolites and areas of intergranular pressure solution are smaller features that increase the tortuosity of fluid flow.

Future Work

Identification of heterogeneity in outcrop sections is essentially complete. In the next quarter outcrop observations will be synthesized with petrologic, geochemical, and petrophysical data from producing oil fields in the Black Warrior Basin to begin to develop predictive geological models for recognition of reservoir heterogeneity at the levels outlined in Task 3. Detailed subsurface maps will be made for individual oil units in several of the fields and regional maps and cross sections of sandstone thickness will be compiled for each reservoir unit on the basis of well-log data. Cores will continue to be described lithologically. Petrologic and petrophysical analyses will include determination of sandstone fabric and composition from thin-section, back-scattered electron and fluorescence imaging of pore distribution and type, chemical and isotopic analyses of authigenic minerals, and determination of porosity, permeability, and pore-throat size distribution. Samples of shale-surrounded reservoir sandstone bodies will be selected for organic geochemical analysis.

DEPOSITIONAL SEQUENCE ANALYSIS AND SEDIMENTOLOGIC MODELING FOR IMPROVED PREDICTION OF PENNSYLVANIA RESERVOIRS

Contract No. DE-FG07-90BC14434

Kansas Geological Survey
Lawrence, Kans.

Contract Date: Feb. 1, 1990
Anticipated Completion: Apr. 30, 1993
Government Award: $173,479
(Current year)

Principal Investigator:
W. Lynn Watney

Project Manager:
Chandra Nautiyal
Bartlesville Project Office

Reporting Period: Oct. 1–Dec. 31, 1990

Objectives

The objectives of this research are to (1) assist operators in the location and production of petroleum not currently under development because of technological problems or the inability to identify details of reservoir compartmentalization, (2) decrease risk in field development, and (3) accelerate the retrieval and analysis of baseline geoscience information for initial reservoir description. The interdisciplinary data sought in this research will be used to resolve specific problems in correlation of strata and to establish the mechanisms responsible for the Upper Pennsylvanian stratigraphic architecture in the midcontinent. The data will better constrain ancillary problems related to the validation of depositional sequence and subsequence correlation, subsidence patterns, sedimentation rates, sea-level changes, and the relationship of sedimentary sequences to basement terrains. The geoscientific information, including data from field studies, surface and near-surface reservoir analogs, and regional database development, will also be used for development of geologic computer process-based simulation models tailored to specific depositional sequences for use in improving prediction of reservoir characteristics.

Summary of Technical Progress

Depositional Sequence Characterization

Drum Limestone study, Montgomery County, Kansas. An objective of this activity is the characterization of an oolitic grainstone called the Drum Limestone. The database thus far consists of a long exposure in a quarry wall in Independence, Kans., other surface exposures in the Independence area, coreholes and oil and gas tests with accompanying wireline logs, and seismic profiles. The present focus is directed to characterizing the three-dimensional (3-D) distribution of a shallow oolite bank and associated strata using cores, logs, and seismic surveys.

Another high-resolution seismic line (some 300 shot points) was shot in December along a 0.3-mile transect near Independence, Kans., with closer-spaced geophones than previously used (2.5-m vs. 5-m spacing). A new seismograph was also used in this second profile. This line was

shot to (a) better determine the limits of resolution by tracing a bed that either pinches out or is truncated, (b) enhance understanding of the geometric configuration of the main Drum oolite and the surrounding strata, and (c) better determine locations for coring.

Figure 1 is the uninterpreted processed seismic reflection profile of this second attempt. The traverse crosses the Drum oolite where it thins from 60 ft thick on the left to 0 ft thick over a distance of 300 ft. The results from this seismic line will be written up by the end of February 1991 for submission to a journal for publication (e.g., *AAPG Bulletin*).

One core and half of another cored interval were drilled during this quarter. Coring operations were postponed because of bad weather and holidays. Coring will continue in January. Well-log data and isopach maps continue to be generated. Correlations and tie-ins to data to the north and west are complete. Thin-section preparation and petrographic studies continue.

Plans include additional field work in January to increase data on outcrop details and for preparation of the AAPG guidebook for a field trip on the Drum to be held in October 1991 in the Independence area.

Hertha, Swope, and Dennis Limestones, southeastern Kansas. The objective of this activity is to understand the impact of depositional slope and relative sea-level change on the geometry and depositional facies of stratal sequences and reservoir development. The dominant reservoir type encountered is oolitic grainstone. The work done this quarter has been focused on coring and logging in Bourbon County, Kansas.

Five cores ranging up to 350 ft in length were acquired over a 34-d field operation during this quarter. Cores were placed at strategic locations to examine oolite tracts situated along a prominent paleo-depositional slope. Wells were logged with gamma-ray, neutron-density, and induction resistivity. This geologic setting is similar to sites of reservoir development in western Kansas.[1] A total of 3600 ft of core has been taken.

Preliminary core descriptions were completed, and new cross sections that include these cores were prepared; this begins a refined stage of interpreting characteristics of depositional sequence and reservoir development.

Plans are being made to have core plugs taken for porosity and permeability analysis. Additional coring is also now being considered. Thin sectioning and isotopic analyses of the cores are planned for the next quarter. Plans were also under way to prepare aspects of this work for publication.

Regional sequence mapping in Kansas City Group linking near-surface sites with western Kansas. This activity will provide the sequence stratigraphic framework to establish the configuration of the shelf and to assess regional controls on sedimentation between contrasting shelf locations over a distance of 400 miles. The shelf setting varies from the distal edge of the Arkoma basin in eastern Kansas to a similar setting above the Anadarko basin on the west. The database will facilitate correlation of results from reservoir analogs in eastern Kansas with reservoirs in the west and provide parameters for geologic simulation modeling.

During this quarter, detailed gamma and neutron-density porosity logs were copied for several hundred wells in central and western Kansas. A database was designed and programming begun to enter sequence and reservoir data for the Kansas City section from these wells.

Plans are to complete the database acquisition during the next quarter and begin to input the data. Data will be merged with existing databases.

Correlation Methods

This activity began with the study of gamma-ray spectrologs from wells in western Kansas for use in correlating and interpreting depositional sequences. This form of chemical stratigraphy may provide signatures to verify physical correlations in the absence of biostratigraphic data. The method also holds promise in recognizing subtle signals in the depositional record to aid in interpreting processes that affect sedimentation.

New software that digitizes scanned log images is being examined on a trial basis. An assessment of the use of this software to digitize wireline logs for this study is under

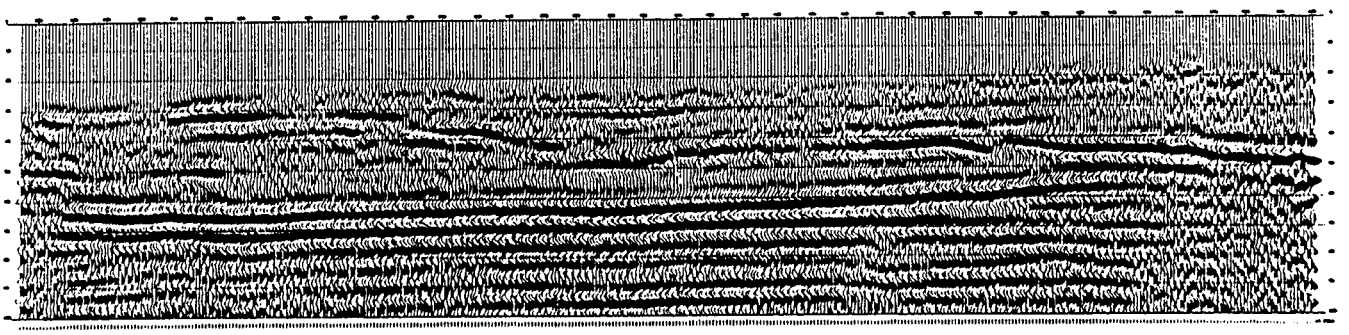

Fig. 1 Uninterrupted, processed, high-resolution reflection seismic profile crossing a pinch-out of the Drum oolite. Line was acquired near Independence, Kans. Approximate thickness shown here is 500 ft; horizontal thickness is 1300 ft.

way. Test sets of logs were provided for digitizing. Steps were taken to acquire a scanning system. Plans are to analyze the digitized spectral gamma-ray data using Fourier analysis and discriminant analysis.

Subsidence Patterns/Rates

The basic framework for structural and stratigraphic analysis is being accomplished in this activity linking eastern and western Kansas. The pulling and correlating of wireline logs and scout tickets were completed during this quarter for southwestern Kansas. The database includes stratigraphic picks from basement through the Pennsylvanian. Detailed Pennsylvanian datums will provide the basis for assessing subsidence history and evolving shelf configuration. Completed cross sections with detailed correlations now extend from border to border across Kansas.

Biostratigraphic sampling and analysis were initiated during this quarter and continue at present. Preliminary results confirm the physical correlation of individual markers and depositional sequences in the long Amoco Rebecca Bounds core from Greeley County in extreme western Kansas.

A set of maps that will be used to compare relationships of Pennsylvanian stratigraphy and petroleum production from Pennsylvanian reservoirs to predecessor structural elements that have undergone recurrent movement is in preparation. This framework will be the basis for selecting strategic wells from the database for more detailed basin (shelf) history analysis.

Plans are to extend the well database to areas of the Central Kansas uplift, the locus of Lansing–Kansas City production. Biostratigraphic analysis will continue into the next quarter. A custom backstripping program is being developed for use in interpreting subsidence history, rates, and patterns.

Computer Modeling

The two parts of the modeling efforts are database programming and simulation model development. The database programs are under final development. They will facilitate integrating and exchanging data among different projects and transfer of data to different hardware, including mainframes, PCs, and workstations. A large amount of varied data are being collected. Such programs are essential in making efficient use and access to the data. These programs will be used beginning in the next quarter to build, edit, and map data from regional, field, and near-surface reservoir analog projects.

Computer simulation development continues on the 386-based personal computer. An improved user interface is being developed for the present two-dimensional (2-D) model, including multiple windows for selecting parameters for modeling runs and conducting up to four simultaneous runs. The new additions also include providing for real-time adjustment of sea-level, variable duration of runs and design of Milankovitch orbitally influenced sea-level curves.

Work began on converting the Pascal code to the C-language. This will facilitate porting the existing 2-D program to the graphics workstation. This is essential to proceed to the next phase of three-dimensional (3-D) modeling. Plans are to begin implementation and testing of various approaches to 3-D modeling on the workstation during the next quarter.

Reservoir Development, Prediction, and Play Potential

Development of the reservoir database is proceeding slowly. Wireline logs and completion data have been pulled on Cahoj field. The Pen field thesis is being defended. Well and completion data from Victory field are being gathered. The thesis on Collier Flats field is in the second quarter. A set of Lansing–Kansas City cores from Thomas County in western Kansas has been located, and these cores are to be acquired for examination during the next quarter. These cores are from oolitic reservoirs that may be similar to those targeted in the near-surface analog projects.

Reference

1. W. L. Watney and J. A. French, Characterization of Carbonate Reservoirs in the Lansing–Kansas City groups (Upper Pennsylvanian) in Victory Field, Haskell County, Kansas, in *Occurrence and Petrophysical Properties of Carbonate Reservoirs in the Rocky Mountain Region: 1988 Carbonate Symposium,* S. M. Goolsby and M. W. Longman (Eds.), Rocky Mountain Association of Geologists, Denver, Colo., pp. 27-46, 1988.

RESERVOIR ASSESSMENT AND CHARACTERIZATION

Cooperative Agreement DE-FC22-83FE60149, Project BE1

National Institute for Petroleum and Energy Research
Bartlesville, Okla.

Contract Date: Oct. 1, 1985
Anticipated Completion: Sept. 30, 1991
Funding for FY 1991: $800,000

Principal Investigator:
Min K. Tham

Project Manager:
Edith Allison
Bartlesville Project Office

Reporting Period: Oct. 1–Dec. 31, 1990

Objective

The objective of this project is to develop an improved methodology for effective characterization of barrier island reservoirs to predict oil saturations at interwell scales and flow patterns of injected and produced fluids.

Summary of Technical Progress

Distribution of Stratigraphic Intervals UA 6 and UA 5

Production from the Arch Unit of the Patrick Draw (Wyoming) field is dominantly from the upper stratigraphic interval called UA 5, but some production is from UA 6, the lower interval. Permeable sand isolith maps for each unit were constructed by Irwin,[1] and the successive distribution of subunits UA 5A and B is shown (Figs. 1 and 2).

The upper stratigraphic interval near the top of the Almond formation is called UA 5 and can be divided vertically into A (upper) and B (lower) intervals. UA 5B (Fig. 2) is the source of most of the oil production from the Arch Unit. An uppermost oyster-bearing high-resistivity marker is present at the top of UA 5B in part of the Arch Unit, as shown in the cross sections (Figs. 3 and 4), and a shale marker separates UA 5A from UA 5B. Generally north–south-oriented thins in the permeable sandstone isolith map for UA 5B define the boundary between the eastern and western sand accumulations within UA 5B and have previously been interpreted as distinct reservoirs.[2,3] The sandstone isolith map (Fig. 2) also indicates that UA 5B extends well east of the Patrick Draw field to the Table Rock Unit. The western extent of UA 5B is not well defined but extends beyond the western limits of Patrick Draw field. The large areal coverage by this unit and the

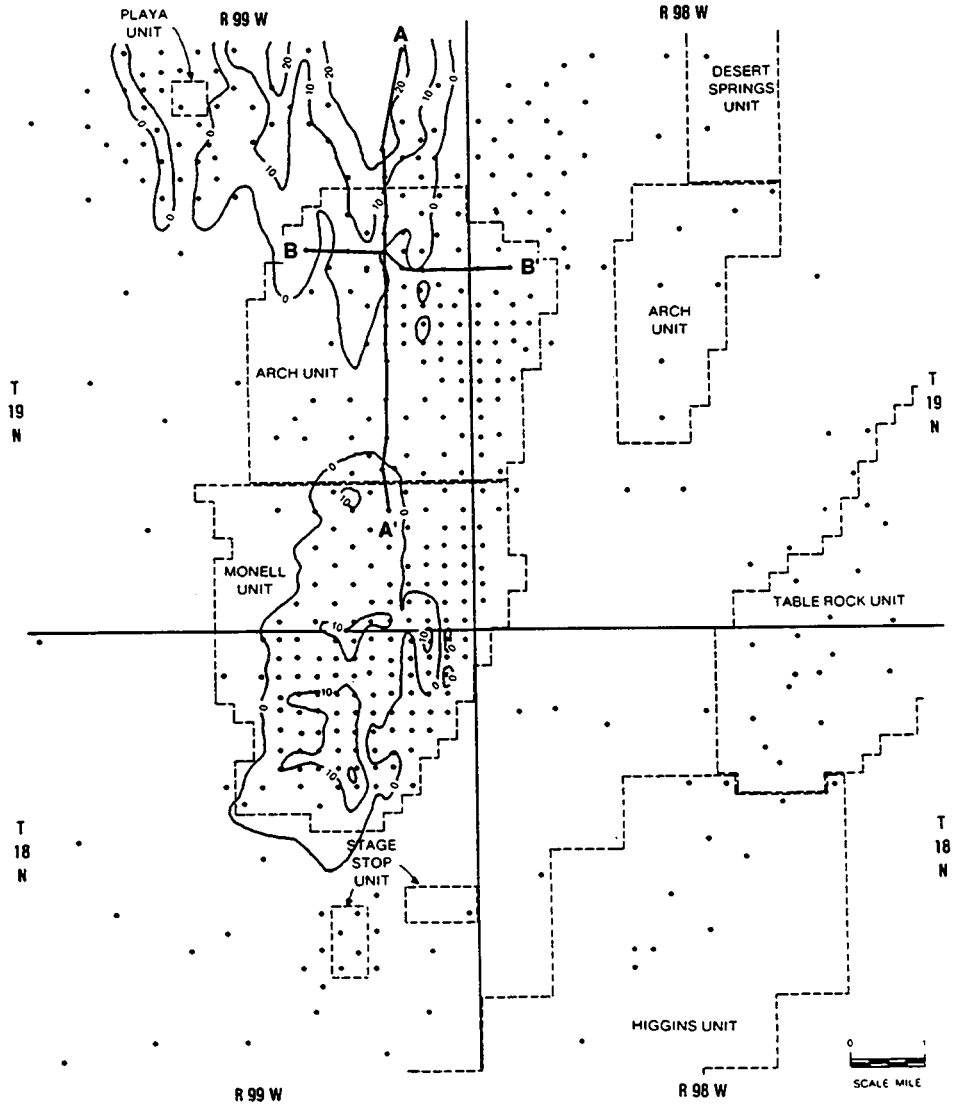

Fig. 1 UA 5A permeable sandstone isolith map. (After Irwin.[1]) The locations of stratigraphic cross sections A-A' and B-B' are also shown.

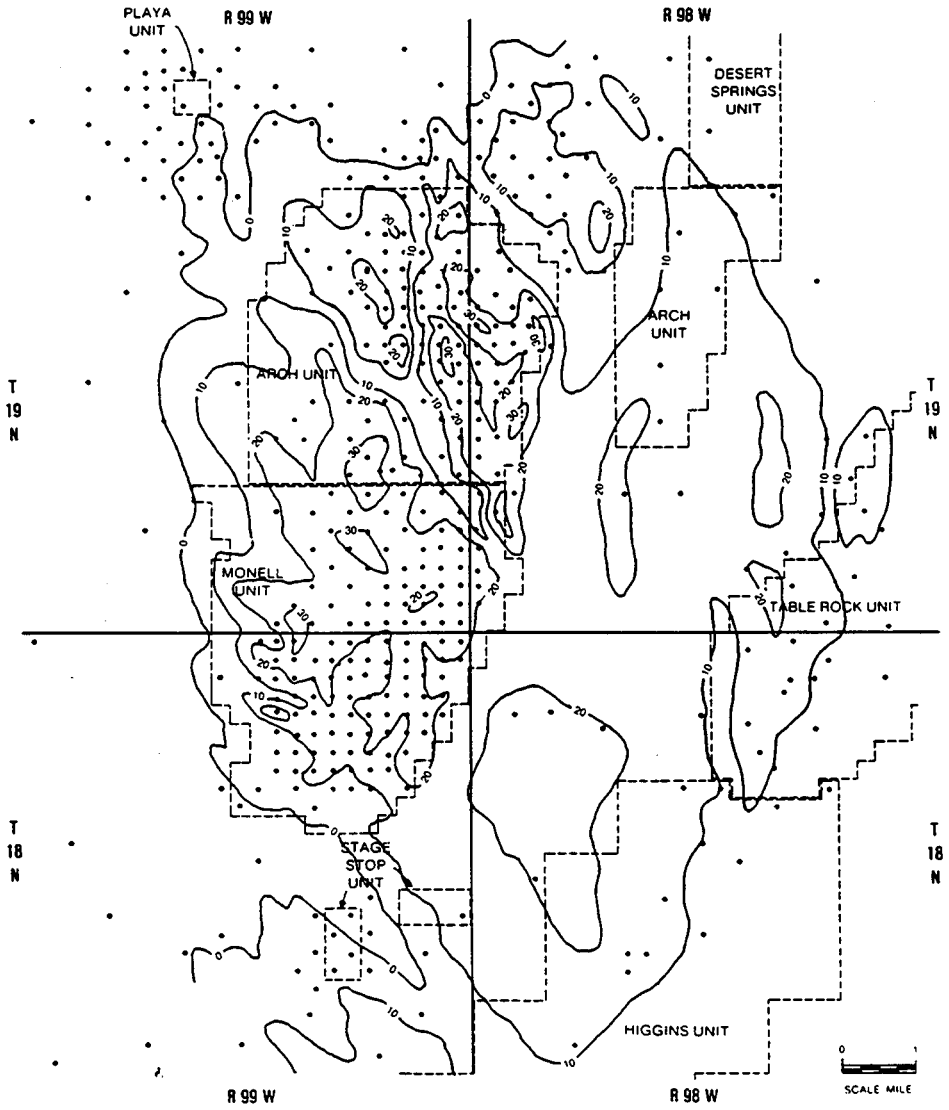

Fig. 2 UA 5B permeable sandstone isolith map. (After Irwin.[1])

presence of sand thicks between Patrick Draw and Table Rock indicate that an overall understanding of UA 5 deposition cannot be fully comprehended by interpretation only within the oil-bearing section at Patrick Draw field.

UA 5A, the uppermost interval, is shown by the sandstone isolith map (Fig. 1) and cross sections (Figs. 3 and 4) to have a discontinuous distribution. It is poorly developed within the Arch Unit but is greater than 25 ft thick north of the production unit. UA 5A sandstones in the Monell Unit are clearly not hydraulically connected to the UA 5A sandstone developed within the Arch Unit, where it is wet and nonproductive. Within the Monell Unit, the north–south-oriented UA 5A interval tends to overlie UA 5B sandstone thicks in the northern part of the unit, but UA 5A contains thicks that extend farther south than do the UA 5B sandstone thicks.

Comparison of Initial Oil Production in Bell Creek (Montana) and Patrick Draw (Wyoming) Fields

Comparison of initial oil production from the Lower Cretaceous Muddy formation marine shoreline barrier sandstones deposited in a microtidal environment at Bell Creek field[4] with the Upper Cretaceous Almond formation, mostly mesotidal back barrier sandstones at Patrick Draw field (Fig. 5), reveals a somewhat similar productivity potential for the two systems. Geological characteristics of the two reservoirs, such as stratigraphy and depositional architecture of reservoir and nonreservoir units (facies assemblages and their continuity), are, however, very different.[5,6] Permeability contrasts also are very high (hundreds and thousands of millidarcys in Bell Creek vs.

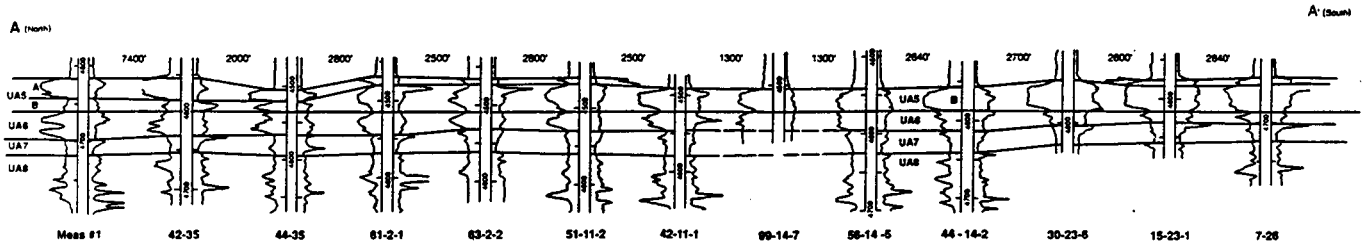

Fig. 3 Stratigraphic cross section A-A'. (After Irwin.[1]) Datum is top of stratigraphic interval UA 6A. Location is indicated in Fig. 1.

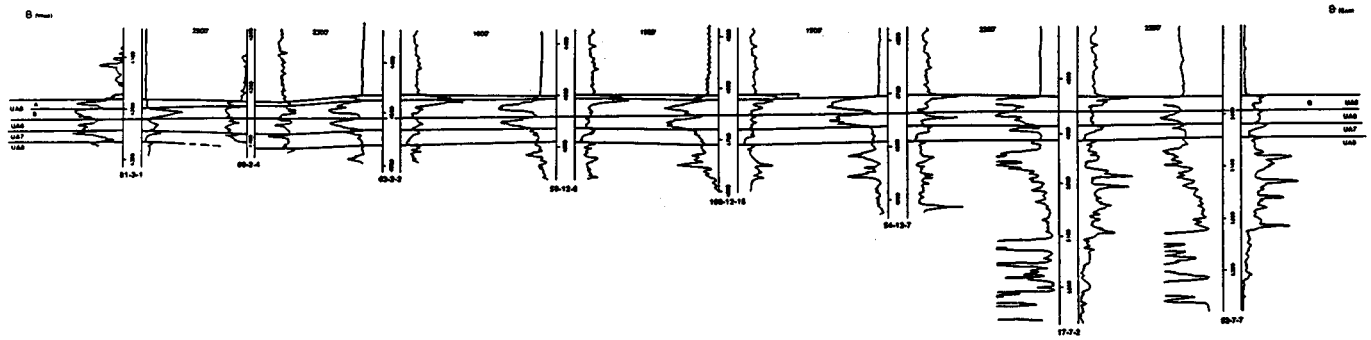

(Art was reproduced from the best available copy.)

Fig. 4 Stratigraphic cross section B-B'. (After Irwin.[1]) Datum is top of stratigraphic interval UA 6A. Location is indicated in Fig. 1.

tens of millidarcys in Patrick Draw), mostly as a result of opposite diagenetic effects. A reason for such high initial production in the Patrick Draw field [greater than 1500 barrels of oil per day (BOPD) from a few wells and greater than 700 BOPD in numerous wells] despite the rather unfavorable geological and petrophysical properties needs to be clarified.

The two reservoirs appeared to be underpressured at the initial stage of hydrocarbon production. They also differ in hydrocarbon gas content. Little gas has been produced from the Bell Creek field, and gas caps were virtually nonexistent except in Unit C. Patrick Draw field, however, has an extensive gas cap above the major oil-producing horizons (UA 5 and UA 6 sandstones). Some wells produce oil and gas, whereas others produce only a single hydrocarbon phase. This may indicate horizontal compartmentalization of fluids. Little water is being produced in the Patrick Draw field, and its salinity and ionic composition vary greatly across the field; this once again indicates poor horizontal communication between updip and downdip portions of the reservoir. These and other features differ between the Bell Creek and Patrick Draw reservoir systems. It is unclear which features are common (inherited from the environment of deposition) and which are unique as the result of unrelated postdepositional processes.

A closer analysis of initial oil production, "specific production," and cumulative oil production in Patrick Draw field has been performed to initiate a comparative study. Ongoing analyses of major geologic and engineering factors will substantiate the initial and cumulative productivity of the Patrick Draw reservoir, and differences as well as similarities in performance of both studied shoreline barrier deposystems will be compared.

Analysis of Initial Production in Patrick Draw Field

The overall productivity of a microtidal (Bell Creek) and a mesotidal (Patrick Draw) shoreline barrier oil reservoir has been analyzed by comparison of the productivity of different sections of each field. In Patrick Draw field, the initial production (IP) from the Upper Cretaceous Almond formation varied broadly, as illustrated in Fig. 5. In the northern and northeastern sections of the field, which comprise about two-thirds of Arch Unit, the IP varied greatly between adjacent wells and created a highly nonuniform "mosaic" pattern. A similar mosaic pattern was found in the southern and southeastern sections of Patrick Draw field, which comprises more than half of the Monell Unit. In extreme cases, the IP of adjacent wells differed by 40 times; for example, in wells 95 and 17 (section 18 of the Arch Unit, 8 and 324 BOPD, respectively) or even by 60 times, such as between wells 95 and 26 (8 and 504 BOPD, respectively). Gross sandstone thickness, lengths of perforated intervals, and number of shots per foot of perforation could all affect IP but were essentially the same in these wells.

In the west-central updip portion of the field, however, uniformly high (above 700 BOPD) initial production prevailed (Fig. 5). Three wells clustered in section 23 of

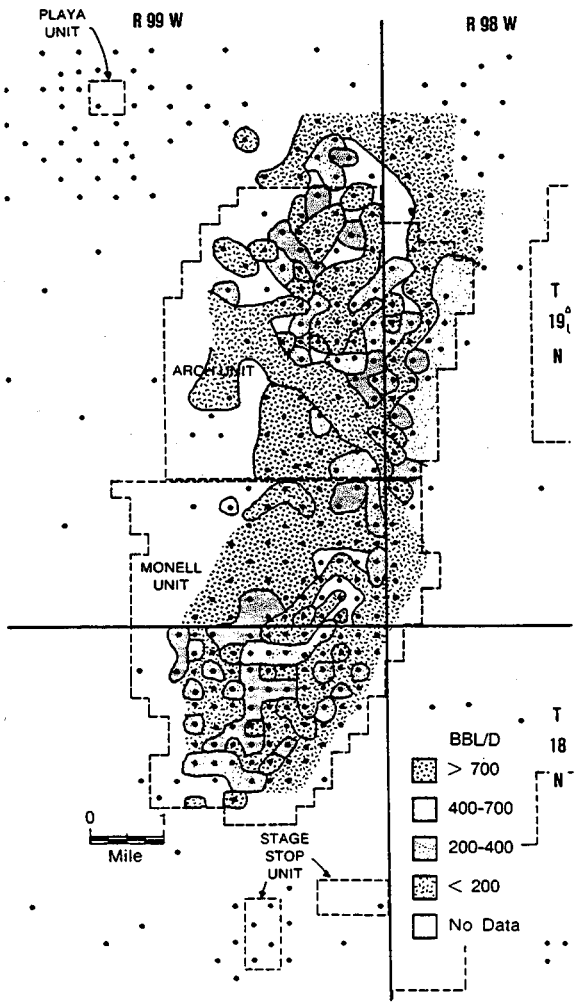

Fig. 5 Distribution of initial oil production (bbl/d) for Patrick Draw field.

Arch Unit (15, 19, and 20) initially produced the record high volume of oil in the entire field: 1800, 1680, and 1578 BOPD, respectively.

Figure 6 illustrates the distribution of wells producing a single hydrocarbon (oil or gas) compared with wells producing the two hydrocarbon phases simultaneously. The relationship between the mostly mosaic pattern of initial production and simultaneous production of oil and gas is quite clear. A more uniform ("patchy") pattern of high productivity prevails in the area where only oil is being produced.

The relationship is much more pronounced, however, in the southeastern portion of Monell Unit than in the northeastern portion of Arch Unit. Areas of simultaneous oil and gas production in Arch Unit within the primarily oil-producing unit suggest compartmentalization of fluids or vertical rather than horizontal hydrodynamic communication. In Monell Unit, the initial simultaneous production of oil and gas dominates in the downdip portion of the reservoir (close to the oil–water contact), whereas the exclusively oil-producing wells dominate in a broad area updip (below the oil and gas contact) (Fig. 6).

Such an arrangement of fluids within productive UA 5 and UA 6 Almond sandstones at the initial stage of production may suggest horizontal isolation between the downdip and updip portions of the reservoir and possible vertical leakage of gas into the southeastern (downdip) portion of Monell Unit from a deeper horizon. Gas production (1226 Mcf) from the much deeper UA 8 Almond horizon in this area was obtained in 1988 from well 178 (Sec. 15-T18N-R99W) located near the southern tip of Monell Unit.

A strong anomaly in the Almond formation water salinity and composition across the Monell Unit was reported.[7] An increased total salinity of 70,000 ppm was recorded in the updip portion of Monell Unit compared with 20,000 ppm (and less) in the downdip portion. This anomaly corresponds with the observed change in pattern of hydrocarbon production and strongly indicates a lack of horizontal communication between the downdip and updip sections of the reservoir.

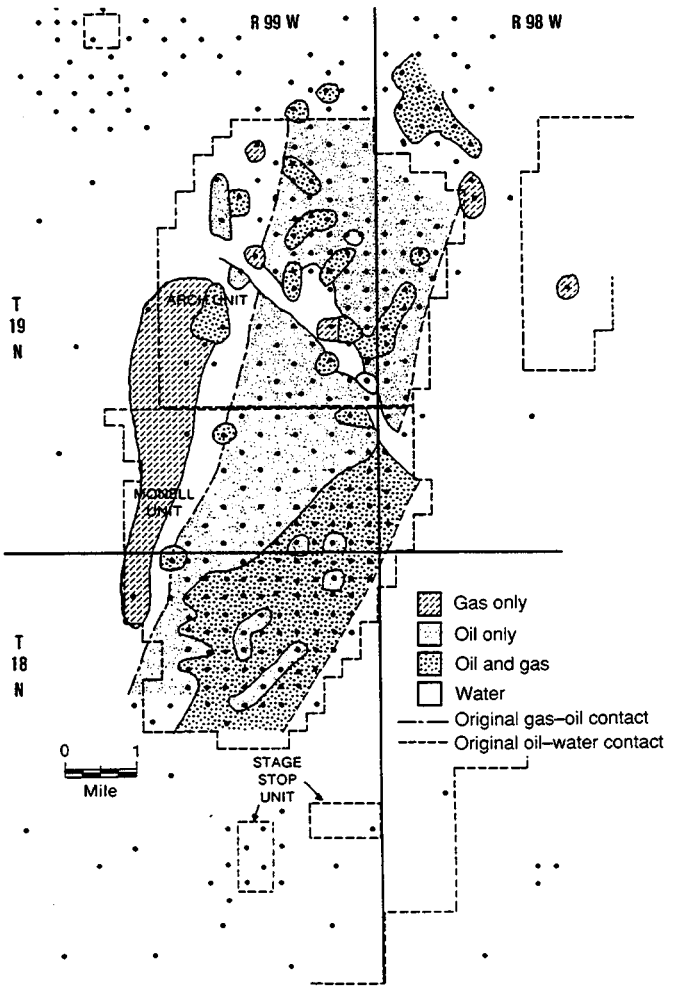

Fig. 6 Distribution of wells producing a single hydrocarbon compared with those producing oil and gas.

High gas production (9500 Mcf from well 1 in Sec. 8 and 2264 Mcf from well 1 in Sec. 5-T19N-R98W) from the Fox Hills formation, which overlies the Almond formation, may suggest that gas migrated through the Lewis Shale formation to horizons above the Almond formation. There are no other known hydrocarbon accumulations above the Almond formation in the Patrick Draw area.[8] However, a distinct soil gas anomaly has been recorded above Patrick Draw field.[9]

The possibility of horizontal isolation and vertical leakage of fluids through open conduits in the system indicated by the initial production and geochemical information is important for planned enhanced oil production by CO_2 injection into Monell Unit. Further analysis is needed to substantiate this observation with geologic and engineering data to provide a sound explanation of reservoir performance and to optimize design of enhanced oil recovery (EOR) process.

One powerful tool that can provide valuable data to substantiate the hypothesis of vertical cross-formational flow is isotopic analysis. Geochemical isotopic analyses of hydrocarbon gas produced from different horizons (UA 8, UA 6, UA 5, and Fox Hills) and in different areas of Patrick Draw field could cast new light on the connectivity of the system and help in the design of a more effective method of stimulated oil production. Most wells produce from individual well-defined horizons, and (as indicated by field reconnaissance) the gas samples for stable isotopes can be taken at selected wellheads. A good opportunity now exists for sampling the formation fluids. A new gas well was completed in early October 1990 in Sec. 34-T19N-R99W. The UA 5 interval was perforated at 4180 to 4200 ft in this well. Other new wells are planned to better define the gas cap in the UA 5 horizon.[10]

UA 5 and UA 6 horizons are not in communication according to the present knowledge at Union Pacific Resources Corporation (UPRC).[10] Most wells were hydraulically fractured, and these fractures definitely lessened the success of the waterflooding process. In a number of cases, circulation was lost, and the injected water was never relocated.[10] This contradictory information must be verified before implementation of an EOR process. Isotopic techniques seem to be well suited for this purpose and should work well for EOR by defining the migration paths and the origin of gaseous hydrocarbons in Patrick Draw field.

Analysis of "Specific Production" in Patrick Draw Field

The productivity index and the specific productivity index cannot be calculated at this point because the pressure drawdown data are not available. However, the calculated ratio of initial production (IP) to the length of perforated interval, called "specific production," provides a more reliable indication of contrasts in formation productivity between adjacent wells as well as the larger areas of the field than does the initial production alone.

The specific production values have been checked for wells within and around sections 18 and 23 (T19N-R99W), which are located on opposite sides of the northeast–southeast trending permeability barrier that has been identified on the UPRC Patrick Draw field map as a "tidal inlet zone" in the Almond formation. The fill of the semipermeable zone in the Almond formation consists mostly of poorly productive or nonproductive facies and is considered to be a lateral barrier or baffle for fluid communication between northeastern and southwestern oil and gas productive areas of Arch Unit. There is a considerable shift in position of the original oil–water and gas–oil contacts (175 and 50 ft, respectively) across the inlet zone. Examination of core from well 39-13-7 in Sec. 13 (USGS B176), which produced 2479 Mcf of gas, and core photographs from the recently drilled well Arch 121 in Sec. 11, indicate that the lithostratigraphy is highly unfavorable for fluid flow in that area. Gas production from well 39, however, may indicate the role of fractures or faults (vertical rather than horizontal matrix permeability) in local migration of fluids in this multireservoir system.

There was originally an oil column of about 1025 ft between the oil–water and gas–water contacts within the eastward dipping UA 5 shoreline barrier front and back barrier Almond sandstones in the Arch Unit on both sides of the permeability barrier (inlet zone). However, contrasts in the initial production and the specific productivity of wells located within and around sections 18 and 23 are very large. Thus the presence of hydraulic compartments is highly possible there. In section 23 the specific production varies between 7.6-28.0 and 56.7-72.0 BOPD per foot of perforation (the outside numbers indicate extreme cases and the inside numbers represent the most common range). These values indicate that commonly the volume of produced oil varies by a factor of 2 but may vary by as great as a factor of 10 in extreme cases. In section 18 the specific production varies between 0.4-10.0 and 36.7-86.7 BOPD per foot of perforation, and the variation is much larger than that in section 23 (more than 200 times in extreme case). Analysis of well performance in the Arch Unit of Patrick Draw field is ongoing, and a geological and/or engineering justification for such drastic differences in initial productivity is being sought.

Petrophysical Investigations in Patrick Draw Field

Correlation of core and log analysis on a number of wells with complete suites of log and core data is required to provide calibration for wells where only log data are available. The first well to be analyzed was well Arch 120.

Porosity data computed from density logs are in good agreement with core analysis data, whereas those computed from neutron and density + neutron methods would need

some type of correction to match the core analysis values (Fig. 7).

Water saturation calculated by both the Simandoux' and Fertles' methods is in good agreement with core-derived data if allowances were made for the usually higher values for the latter method as a result of drilling mud infiltration. Archie's and Waxman and Smit's (calculated by a service company) methods give values that differ significantly from core-derived values.

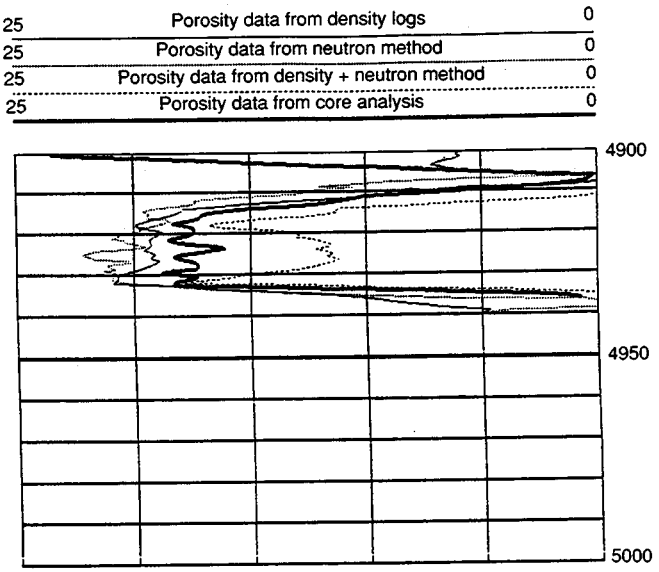

Fig. 7 Log-derived porosity determined by different methods compared with core measurements.

Plots of core-derived porosity (ø) and permeability (k) (natural log of permeability) data showed that the relationship [ø – ln(k)] is not linear. Preliminary investigation indicates that corrections in the values in k for the effect of clay content are needed to arrive at a linear relationship. Research to arrive at a functional form of this correction is continuing.

References

1. D. Irwin, *Arch and Monell Units, Patrick Draw–Table Rock Area, Sweetwater County, Wyoming—Upper Almond Sandstone Study,* Unpublished Union Pacific Resources Co. Data Files, 1976.
2. R. J. Weimer, Time–Stratigraphic Analysis and Petroleum Accumulations, Patrick Draw Field, Sweetwater County, Wyoming, *AAPG Bull.*, 50: 2150-2175 (1966).
3. D. G. McCubbin and M. J. Brady, Depositional Environment of the Almond Reservoirs, Patrick Draw Field, Wyoming, *Mt. Geol.*, 6: 3-26 (1969).
4. S. R. Jackson, L. Tomutsa, M. J. Szpakiewicz, M. M. Chang, M. M. Honarpour, and R. A. Schatzinger, Application of an Integrated Methodology for Construction of a Quantitative Transmissivity Model—Bell Creek Field, a Barrier Island Reservoir, *Proceedings of the Second International NIPER/DOE Reservoir Characterization Symposium, Dallas, Texas, June 25–28, 1989,* Academic Press, San Diego, Calif., 1991.
5. M. J. Szpakiewicz, R. Schatzinger, M. Honarpour, M. Tham, and R. Tillman, Geological and Engineering Evaluation of Barrier Island and Valley-Fill Lithotypes in Muddy Formation, Bell Creek Field, Montana, in *Petrogenesis and Petrophysics of Selected Sandstone Reservoirs of the Rocky Mountain Region,* E. B. Coalson (Ed.), pp. 159-182, The Rocky Mountain Association of Geologists, Denver, 1989.
6. M. J. Szpakiewicz, R. Schatzinger, S. Jackson, B. Sharma, A. Cheng, and M. Honarpour, *Selection of a Second Barrier Island Reservoir System for Expanding the Shoreline Barrier Reservoir Model and Refining NIPER Reservoir Characterization Methodology,* DOE Report NIPER-472, 1990.
7. M. J. Szpakiewicz and A. G. Collins, *Hydrochemical Study of the Upper Cretaceous and Lower Tertiary Formations in the Uinta, Piceance and Greater Green River Basins; Implications for Oil and Gas Related Problems,* DOE Report NIPER-95, 1985.
8. Frank Lim, Union Pacific Railroad Company, personal communication, 1990.
9. D. M. Richers, J. R. Reed, K. C. Horstman, G. D. Michels, R. N. Baker, L. Lundell, and W. Marrs, Landsat and Geochemical Study of Patrick Draw Oil Field, Sweetwater County, Wyoming, *AAPG Bull.*, 66: 903-922 (1982).
10. Jack Lane, personal communication at Union Pacific Railroad Company Field Office, Patrick Draw Field, 1990.

TORIS RESEARCH SUPPORT

Cooperative Agreement DE-FC22-83FE60149, Project BE2

National Institute for Petroleum and Energy Research
Bartlesville, Okla.

Contract Date: Oct. 1, 1983
Anticipated Completion: Sept. 30, 1991
Funding for FY 1991: $340,000

Principal Investigator:
James F. Pautz

Project Manager:
Chandra M. Nautiyal
Bartlesville Project Office

Reporting Period: Oct. 1–Dec. 31, 1990

Objective

The objective of this project is to provide research support to the Department of Energy (DOE) Program Manager for the Tertiary Oil Recovery Information System (TORIS) in the areas of enhanced oil recovery (EOR) project and reservoir database management and EOR project technology trend analysis.

Summary of Technical Progress

Trends in the type and number of EOR projects were analyzed for the period from 1980 to 1989. The analysis

was based on current literature and news media and the DOE/EOR Project Database, which contains information on more than 1348 projects. The National Institute for Petroleum and Energy Research (NIPER) maintains this database and analyzes trends in the data under the provisions of Cooperative Agreement No. DE-FC22-83FE60149.

The characteristics of the EOR projects were grouped by starting date and process type to identify trends in reservoir statistics and applications of process technologies. Twenty-two EOR project starts were identified for 1989 and 10 project starts for 1988. An obvious trend over recent years has been the decline in the number of project starts from 1981 until 1988, which corresponds to the oil price decline during that period (Fig. 1). There was a modest recovery of project starts in 1989, which lags the modest recovery of oil prices in 1987 that was reconfirmed in 1989. During the timeframe of 1980 to 1989, there has been a gradual improvement in costs of operation for EOR technology. The perceived average cost of EOR has gone down from a $30/bbl range to a low $20/bbl. The costs of operation seem to stay just at the price of oil or slightly above to result in marginal profitability. The use of polymer flooding has drastically decreased both in actual and relative numbers of project starts since the oil price drop in 1986. Production from polymer flooding is down more than 50%. Long-term plans for large, high-cost projects, such as CO_2 flooding in West Texas, steamflooding in California, and hydrocarbon flooding on the North Slope, have continued to be implemented. EOR process technologies have been refined to be more cost-effective, as shown by the continued application and rising production attributable to EOR.

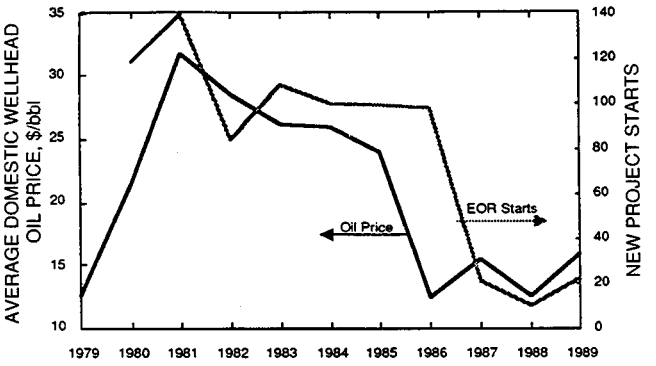

Fig. 1 Oil prices compared with enhanced oil recovery (EOR) project starts.

RESERVOIR DATABASE DEVELOPMENT: PHASE 1

Cooperative Agreement DE-FC22-83FE60149, Project SGP28

National Institute for Petroleum and Energy Research Bartlesville, Okla.

Contract Date: Aug. 18, 1989
Anticipated Completion: Jan. 31, 1991
Funding for FY 1991: $50,000

Principal Investigator:
James F. Pautz

Project Manager:
Chandra M. Nautiyal
Bartlesville Project Office

Reporting Period: Oct. 1–Dec. 31, 1990

Objectives

The objectives of Phase 1 research are to develop input and output criteria for a reservoir database and to prepare a detailed conceptual design of a RELIANCE database management system (DBMS) environment to meet those criteria.

Summary of Technical Progress

No significant progress was made on this project during the quarter.

ENHANCED OIL RECOVERY INCENTIVE PROJECTS SURVEY

Cooperative Agreement DE-FC22-83FE60149, Project SGP30

National Institute for Petroleum and Energy Research Bartlesville, Okla.

Contract Date: Aug. 18, 1989
Anticipated Completion: May 31, 1991
Funding for FY 1991: $36,500

Principal Investigator:
James F. Pautz

Project Manager:
Chandra M. Nautiyal
Bartlesville Project Office

Reporting Period: Oct. 1–Dec. 31, 1990

Objective

The objective of this project is to solicit completed FE-748 forms for the active incentive projects for calendar years 1987, 1988, and 1989. The data are to be reduced to an electronic media and validated.

Summary of Technical Progress

The Department of Energy encouraged oil companies and operators to undertake enhanced oil recovery (EOR) projects through an incentive program from 1979 to 1980. Those companies and operators who received an incentive are asked to submit an annual report. Initially, the companies were required to certify the projects as true EOR operations. A total of 423 certifications were received. When the Annual Report for Enhanced Oil Recovery Incentive Program details was published, the annual report requirements were defined as voluntary. Each year after 1982, operators have been requested to return a completed "Annual Report for Enhanced Oil Recovery Incentive Program," form FE-748. At present, many of the original projects have been terminated, completed, changed, combined with other projects, never started, or not reporting. For the 1986 reporting year, information was obtained on 150 projects. The information from these annual reports is used to maintain the EOR Project databases used by the Bartlesville Project Office.

At the end of 1986, 133 projects were still being tracked. Since the start of the project, 4 additional projects have been added for a total of 137 projects being tracked. Table 1 summarizes the status of these projects and the progress made on completing the survey.

Table 2 lists the projects for which no response was received for either 1987, 1988, and/or 1989.

TABLE 1

Status of the Enhanced Oil Recovery Projects Considered by SGP30 Survey

	Status		
	1987	1988	1989
Projects active	80	71	59
Projects deferred	13	13	13
Projects combined	1	4	4
Projects canceled	2	2	2
Projects completed	2	2	3
Projects terminated	33	37	36
Response refused by operator	2	2	8
No form received to date (no status)	4	6	12
Total	137	137	137

TABLE 2

Projects with Unknown Status for 1987, 1988, and 1989

Project No.	Operator in 1986	Status		
		1987	1988	1989
SF009	Woodstock Oil Corp.	Unknown contact	Unknown contact	Unknown contact
SF117	ORYX Energy Co.	Reported active	Reported active	Unknown
SF118	ORYX Energy Co.	Reported active	Reported active	Unknown
SF141	Mobil Oil Corp.	Reported active	Unknown	Unknown
SF164	Union Pacific Resources	Unknown	Unknown	Unknown
SF168	Geo. R. Brown Ptn.	Reported active	Reported active	Unknown
SF195	Mobil Oil Corp.	Reported active	Unknown	Unknown
SF206	Meridian Oil Inc.	Reported active	Reported active	Unknown
SF234	ORYX Energy Co.	Reported active	Reported active	Unknown
SF391	Mobil Oil Corp.	Reported active	Unknown	Unknown
SF392	Mobil Oil Corp.	Unknown	Unknown	Unknown
SFXX1	Placid Oil	Unknown contact	Unknown contact	Unknown contact

NATURAL RESOURCES INFORMATION SYSTEM FOR THE STATE OF OKLAHOMA

Contract No. DE-FG22-89BC14483

Oklahoma Geological Survey
University of Oklahoma
Norman, Okla.

Contract Date: June 22, 1989
Anticipated Completion: June 21, 1992
Government Award: $498,000
(Current year)

Principal Investigator:
Charles J. Mankin

Project Manager:
R. Michael Ray
Bartlesville Project Office

Reporting Period: Oct. 1–Dec. 31, 1990

Objective

The objective of this research program is to continue developing, editing, maintaining, using, and making publicly available the Natural Resources Information System (NRIS) for the state of Oklahoma. This contract funds the ongoing development work as a follow-on to earlier Grant No. DE-FG19-88BC14233. The Oklahoma Geological Survey (OGS), working with Geological Information Systems at the University of Oklahoma, has undertaken to construct this information system in response to the need for a computerized, centrally located library containing accurate, detailed information on the state's natural resources. Particular emphasis during this phase of development is being placed on computerizing information related to the energy needs of the nation, specifically oil and gas.

Summary of Technical Progress

The Oil and Gas Production Subsystem

The Oil and Gas Production (OGP) subsystem is composed of three major files: a Lease File, a Field File, and a County File. The Lease File contains production and formation records based on data obtained from the Oklahoma Tax Commission (OTC); data elements include lease name and number, location information, formations data, and monthly production totals. The Field File contains historical and current records for all 5100 active and inactive Oklahoma oil and gas fields, as identified by the Oklahoma Nomenclature Committee (ONC); data elements include field identification data, consolidation histories when relevant, discovery data, location information (county, section/township/range, and quarter/quarter section data), and monthly production aggregated (by location) from the records maintained on the Lease File. The County File has monthly oil and gas production data aggregated by county.

Processing for the OGP subsystem primarily consists of processing monthly computer tapes received from the OTC to update production totals for all three files and to add new records to the Lease Master File. At the beginning of this quarter, monthly production was on file for the period January 1983 to June 1990. New records for the Field Master File are added by manually coding and keying the results of ONC meetings. The Lease and Field Master Files are reconciled through combined computerized and manual efforts.

As reported previously, a primary thrust for the OGP subsystem must be toward enhancing the files through ongoing quality assurance efforts. Although the estimated error rate in the production input tapes received from the OTC is rather low, the sheer volume of data processed from these tapes creates a large number of errors on the Lease File. One result of these errors contained in the OTC source tapes is the significant number of production records that get added to the file with invalid "Producing Unit Numbers" (PUNs), commonly called "no-master" records. A series of computerized and manual processes has been developed to research company reporting patterns as part of the effort to allocate the no-master production to the appropriate leases. Significant efforts also are required to detect and resolve cases in which a monthly production total is unreasonably large for a lease; these usually are caused by decimal problems in the production reports or by the allocation of production to the wrong lease.

The July and August source data received from the OTC were added to the files. Also, efforts continued in processing and reviewing the OTC 1979–1982 production tapes. These older data contain a significant number of errors, including months of missing data, but overall most problems can be resolved, and the July 1991 data release will include production histories back to 1979.

The Lease File contains approximately 1,270,000 records, which represent 140,000 unique PUNs. About 90,000 of these PUNs have had production reported sometime during 1983 to 1990, and over 66,000 of them report 1989 and/or 1990 production.

Table 1 gives an overview of the progress and current status of production data quality assurance efforts by region and county. The effort expenditure on production data quality was increased during this quarter; this corresponds with preparations for the January 1991 data release. At the end of December, 7,736 no-master records had been resolved since the beginning of the contract, 5,016 had been added from OTC tapes, and 5,741 remained on file. Since production quality assurance efforts began in October 1988, almost 60,000 transactions have been generated to correct no-master and other types of production data problems.

TABLE 1

Progress and Current Status of Production Quality Assurance Efforts
Progress Summary (May 1989–December 1990)

	Counts of "No-Master" Records				Cumulative quality assurance transactions since October 1988
	Starting total, May 1989	Number added from OTC tapes, February 1989–August 1990	Number resolved	Ending total, December 1990	
North central					
047 Garfield	292	88	183	197	4692
053 Grant	154	52	77	129	2350
071 Kay	114	198	210	102	1152
073 Kingfisher	331	105	197	239	1888
081 Lincoln	123	68	74	117	331
083 Logan	141	67	93	115	521
103 Noble	145	5	61	89	612
109 Oklahoma	302	63	206	159	1282
119 Payne	106	62	92	76	369
Region subtotal	1708	708	1193	1223	13197
Northeast					
001 Adair	2	8	10	0	23
021 Cherokee	0	1	1	0	1
035 Craig	3	1	3	1	6
037 Creek	264	89	249	104	1356
097 Mayes	1	0	1	0	4
101 Muskogee	64	9	57	16	179
105 Nowata	60	12	51	21	154
107 Okfuskee	120	38	120	38	708
111 Okmulgee	170	44	134	80	896
113 Osage	115	10	71	54	460
115 Ottawa	1	3	2	2	2
117 Pawnee	160	83	207	36	745
131 Rogers	50	26	66	10	211
135 Sequoyah	12	4	13	3	36
143 Tulsa	72	24	69	27	351
145 Wagoner	47	11	28	30	119
147 Washington	76	13	63	26	296
Region subtotal	1217	376	1145	448	5547
Northwest					
003 Alfalfa	162	61	168	55	2402
007 Beaver	319	197	224	292	1846
025 Cimarron	37	32	35	34	224
043 Dewey	157	119	152	124	919
045 Ellis	144	120	127	137	587
059 Harper	254	168	267	155	2319
093 Major	334	171	309	196	4144
139 Texas	185	275	278	182	1978
151 Woods	72	93	88	77	794
153 Woodward	95	85	105	75	491
Region subtotal	1759	1321	1753	1327	15704

	Counts of "No-Master" Records				Cumulative quality assurance transactions since October 1988
	Starting total, May 1989	Number added from OTC tapes, February 1989–June 1990	Number resolved	Ending total, September 1990	
Southeast					
005 Atoka	4	4	5	3	34
013 Bryan	14	−5	2	7	44
023 Choctaw	0	0	0	0	0
027 Cleveland	52	0	35	17	220
029 Coal	17	16	23	10	154
049 Garvin	246	82	164	164	1096
061 Haskell	108	35	90	53	905
063 Hughes	160	77	169	68	768
069 Johnston	1	0	1	0	4
077 Latimer	148	150	221	77	1416
079 Le Flore	84	85	91	78	834
087 McClain	133	42	93	82	332
089 McCurtain	0	2	1	1	4
091 McIntosh	45	7	40	12	365
095 Marshall	25	10	28	7	211
099 Murray	28	17	34	11	125
121 Pittsburg	197	228	263	162	1421
123 Pontotoc	61	44	66	39	1449
125 Pottawatomie	105	80	110	75	631
127 Pushmataha	1	0	1	0	2
133 Seminole	106	39	75	70	467
Region subtotal	1535	913	1512	936	10482
Southwest					
009 Beckham	139	114	156	97	1049
011 Blaine	133	99	54	178	833
015 Caddo	268	225	259	234	1848
017 Canadian	264	123	188	199	1168
019 Carter	215	174	215	174	1254
031 Comanche	38	10	9	39	143
033 Cotton	21	25	20	26	34
039 Custer	234	177	235	176	1550
051 Grady	284	195	285	194	1708
055 Greer	57	42	95	4	165
057 Harmon	0	2	1	1	1
065 Jackson	2	1	2	1	6
067 Jefferson	34	9	14	29	60
075 Kiowa	17	13	6	24	13
085 Love	82	20	43	59	423
129 Roger Mills	184	280	312	152	2200
137 Stephens	181	135	140	176	1392
141 Tillman	3	0	2	1	5
149 Washita	86	54	97	43	922
Region subtotal	2242	1698	2133	1807	14774
Grand total	8461	5016	7736	5741	59704

Many of the 7,000 transactions this quarter were to correct problems in the 1983 and 1984 data; these years will also be stressed in the coming quarter since very few changes come through from the OTC for these years. The bar chart in Fig. 1 provides more perspective on the resolution rates. For all data years through 1989, progress has been made on reducing the number of no-master records. For 1990, eight new OTC tapes have been processed, and there are already almost 1,700 (plus about 250 that have been resolved) 1990 no-master records. The computerized and manual processes to perform the production quality assurance tasks help assure that the resolution rates will continue to improve, but the new problems added by each monthly OTC tape will keep effort expenditures high in this area. Nevertheless, it is anticipated that the 1983 and 1984 data will be "clean" for the July 1991 data release and that a similar announcement can be made concerning data years 1985 to 1989 in time for the July 1992 data release.

A second goal of the OGP subsystem work involves quality assurance efforts to "assign" leases to fields and derive field production totals from those lease assignments. These lease assignments are based on the official field outlines as designated by the Midcontinent Oil and Gas Association's ONC and documented in the "Blue Sheets" released by that committee. Some areas exist in which significant field extension drilling has taken place, but the ONC has had insufficient resources to update the field boundaries accordingly; therefore, at the beginning of 1990, almost 25% of the state's production was not allocated to any field(s) in the OGP subsystem.

Information packages for selected areas are produced each month from the NRIS data to assist the ONC in

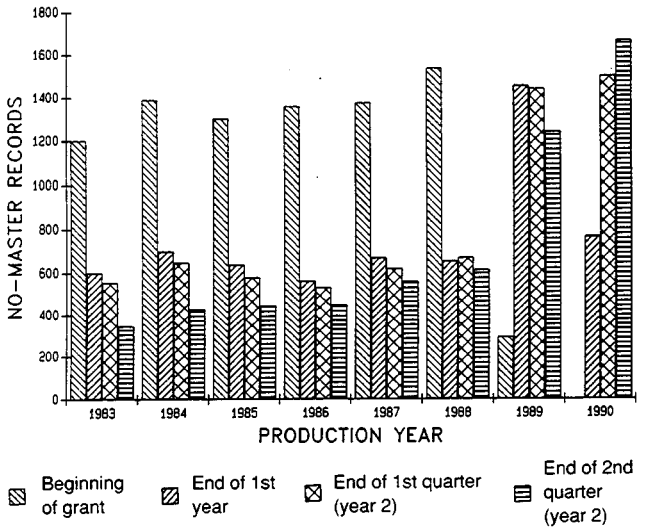

Fig. 1 Change in the no-master record totals.

updating its field outlines. This work has become a major component of the OGP quality assurance effort. The packages consist of maps and lists that depict producing leases located outside current field boundaries. On the basis of this input, the Committee set the goal of updating all gas field boundaries by June of 1991; oil-field boundaries will be emphasized the following year. Table 2 provides more detailed information about the current status of unassigned production by region and county. During this quarter, final approvals were voted and Blue Sheets were generated for fields in Blaine, Dewey, Custer, and Washita Counties. Areas that are in various stages of the ONC review process include Canadian, Grady, Harper, Hughes, and Pittsburg Counties, as well as the south central area. Overall, during this quarter, unassigned gas production was reduced to 18% of the annual average production.

Quality assurance efforts regarding the producing formations data comprise a third area of emphasis. During this quarter, significant progress was made in developing and testing a system of Producing Interval Codes to facilitate the aggregation of production volumes and the editing of the formations data reported by operators. The system was demonstrated during the previous quarter for selected OGS geologists, and the concept received initial approvals from that group. The first applications of the system were developed for four counties, and the edit review process for those counties is now complete. The goal is to have production by producing interval available to the public (at least for some areas) on the July 1991 data release.

Progress was also made on a fourth goal (mapping applications development). The latitude and longitude coordinates contained in Phillips Petroleum Company's Digital Land Grid Oklahoma Database are being used to map data from the NRIS production and well files. Funding for an IBM 486 PC with a large color monitor was provided by a private foundation (to be ordered by the end of this budget year), and GeoGraphix, Inc., donated a copy of their geologic mapping software to assist in NRIS mapping projects and to provide a link to the School of Geology, which also uses the GeoGraphix software.

Additional systems work included further progress on systems documentation, particularly the Well History File data dictionary.

The Well History File

The Well History File contains historical and current completion records for oil and gas wells reported to the Oklahoma Corporation Commission on Form 1002-A. At the start of the quarter, the Well History File contained 117,183 records for the southern half of Oklahoma. On a special project basis, supplemental data (where available) are added to the file from well logs, scout tickets, and core and sample documentation. Data elements on this file include demographic items (e.g., API well number, lease name and well number, location information, elevations, and dates of significant activities for the well), formation items (e.g., formation names, completion and test data, depths, and perforations), and reference information (e.g., for drilling samples, core samples, and well logs).

In addition to the standard Well History File processing, special activities are being undertaken to enhance the supplemental data on the file. Work is under way on a parallel track within the NRIS Project to organize and computerize information from the OGS Core and Sample Library and from the Ardmore Sample Cut Library. Through computer and manual reconciliation processes, relevant data are being added to the Well History File. As other data sources become available, they will be reviewed as a cost-effective means to add supplemental information to the well records.

A large portion of the Well History File work involves photocopying the completion reports for use in coding prior to data entry. All new completion reports are copied when received from the Oklahoma Corporation Commission; the originals are filed in the OGS's Well Log Library. Completion reports for areas of the state that have already been (or are being) worked are entered into the processing stream immediately. The others are filed for future processing. All historical completion reports are checked out of the Well Log Library and copied at the rate of about 8,000 to 12,000 forms per month; approximately 60% of these historical completion reports have now been copied.

Processing of the Oklahoma Corporation Commission's oil and gas well completion reports (Form 1002-A) is proceeding smoothly. Some delays were experienced during November and December because of holidays and vacations and as students adjusted their schedules to accommodate final exams. The stabilization of staffing in general, however, has contributed to significant current progress on the Well History File project.

Well records are being prescanned, keyed, and edited for the following south central counties: Cleveland, McClain, Pottawatomie, and Seminole. Over 15,000 well records

TABLE 2

Unassigned Production* by Region and County

	Gas production (annual average),† Mmcf			Liquid production (annual average),† Mbls		
	Total	Unassigned	Percent	Total	Unassigned	Percent
North central						
047 Garfield	50,734	7,607	15	2,636	439	17
053 Grant	15,860	10,840	68	2,697	1,637	61
071 Kay	3,125	240	8	1,420	94	7
073 Kingfisher	62,864	21,212	34	4,382	1,127	26
081 Lincoln	10,898	6,360	58	1,517	563	37
083 Logan	20,300	8,754	43	2,079	1,070	51
103 Noble	9,182	3,231	35	3,177	1,061	33
109 Oklahoma	25,804	15,413	60	3,513	1,655	47
119 Payne	4,875	1,076	22	2,023	426	21
Region subtotal	203,642	74,734	37	23,444	8,072	34
Northeast						
001 Adair	0	0	0	0	0	0
035 Craig	31	19	60	6	4	70
037 Creek	7,982	2,822	35	5,747	764	13
097 Mayes	2	2	100	33	33	100
101 Muskogee	1,343	782	58	287	45	15
105 Nowata	749	410	55	484	129	27
107 Okfuskee	6,341	3,141	50	1,042	415	40
111 Okmulgee	6,661	1,787	27	1,321	300	23
113 Osage	8,051	3,111	39	8,002	1,209	15
115 Ottawa	0	0	100	0	0	0
117 Pawnee	7,266	5,807	80	2,602	1,727	66
131 Rogers	367	341	93	148	78	53
135 Sequoyah	2,769	453	16	0	0	0
143 Tulsa	1,287	420	33	851	73	9
145 Wagoner	753	448	59	286	118	41
147 Washington	1,147	579	50	790	62	8
Region subtotal	44,752	20,124	45	21,601	4,957	23
Northwest						
003 Alfalfa	14,824	783	5	963	67	7
007 Beaver	86,131	32,149	37	2,984	1,663	56
025 Cimarron	11,846	3,962	33	627	352	56
043 Dewey	64,233	10,087	16	2,502	907	36
045 Ellis	35,548	2,803	8	1,154	184	16
059 Harper	51,532	7,037	14	404	171	42
093 Major	85,936	15,137	18	4,235	1,054	25
139 Texas	103,141	14,813	14	3,971	1,324	33
151 Woods	28,524	420	1	555	5	1
153 Woodward	31,140	628	2	464	14	3
Region subtotal	512,855	87,820	17	17,859	5,742	32
Southeast						
005 Atoka	735	522	71	2	1	27
013 Bryan	1,774	11	1	100	0	0
023 Choctaw	(3)	(3)	0	0	0	0
027 Cleveland	6,314	2,771	44	2,233	794	36
029 Coal	4,722	38	1	194	0	0
049 Garvin	44,900	6,141	14	6,900	1,223	18
061 Haskell	36,942	290	1	0	0	0
063 Hughes	13,470	7,983	59	1,223	574	47
069 Johnston	7	0	0	0	0	100
077 Latimer	87,324	702	1	0	0	0
079 Le Flore	22,199	384	2	0	0	0
087 McClain	23,511	5,308	23	3,660	1,254	34
089 McCurtain	0	0	100	0	0	0
091 McIntosh	7,899	3,529	45	6	5	86
095 Marshall	5,975	115	2	346	3	1
099 Murray	481	34	7	1,602	518	32
121 Pittsburg	67,964	8,980	13	0	0	50
123 Pontotoc	1,258	85	7	4,577	51	1
125 Pottawatomie	6,403	5,012	78	4,384	1,956	45
127 Pushmataha	0	0	0	0	0	0
133 Seminole	3,695	1,218	33	4,265	621	15
Region subtotal	335,572	43,119	13	29,492	6,999	24
Southwest						
009 Beckham	80,512	3,157	4	1,130	80	7
011 Blaine	93,349	15,029	16	1,272	465	37
015 Caddo	104,927	1,649	2	3,988	194	5
017 Canadian	108,548	44,599	41	2,921	1,919	66
019 Carter	18,549	5,690	31	14,183	1,169	8
031 Comanche	9,650	3,531	37	305	196	64
033 Cotton	241	60	25	387	55	14
039 Custer	127,681	681	1	2,349	13	1
051 Grady	110,433	42,821	39	7,232	1,825	25
055 Greer	256	50	20	14	2	14
057 Harmon	0	0	0	69	0	0
065 Jackson	0	0	0	102	23	23
067 Jefferson	367	316	86	1,077	739	69
075 Kiowa	237	39	16	109	41	38
085 Love	4,257	1,321	31	1,652	1,123	68
129 Roger Mills	150,989	3,356	2	1,125	73	7
137 Stephens	43,211	7,703	18	11,441	852	7
141 Tillman	0	0	0	127	76	60
149 Washita	63,759	418	1	771	2	0
Region subtotal	916,967	130,421	14	50,254	8,849	18
Grand total	2,013,789	356,218	18	142,650	34,619	24

*Production not assigned to any field.
†Annual averages based on January 1983–August 1990 production (as of 12/31/90).

were added to the file this quarter; thus, as of December 1990, 132,562 records were on file. The Well History File progress is shown in Table 3 by NRIS Regional Division. The current status of county coverage and the total record counts by county are shown in Figs. 2 and 3.

Special procedures have been implemented to further edit the location data recorded on the 1002-A forms, and various external sources are being researched when 1002-A locations are incomplete or inaccurate. Approximately 140 well records with location problems were corrected this quarter. Work was initiated to match Lease File records to well records by location and to assign OTC lease numbers to well records that can be matched. A computer program was written and tested that assigns latitude and longitude coordinates to well records, and it is anticipated that latitude/longitude data will be added to the Well History File for the July 1991 data release. An effort was made to locate missing 1002-As, and several forms were located in other libraries and added to the file.

This quarter supplemental data were manually added to records in the Ouachita Mountains area in southeastern Oklahoma; this brings the total supplemental record count

TABLE 3

Well History File Progress by NRIS Regional Division

Area of coverage	Well records		
	Start of grant	Start of quarter	Current
Southeast region	27,385	38,629	53,661
Southwest region	9,284	65,076	65,382
Northeast region	6,768	8,410	8,423
Northwest region	4,735	4,909	4,934
North central region	138	159	162
Total	48,310	117,183	132,562

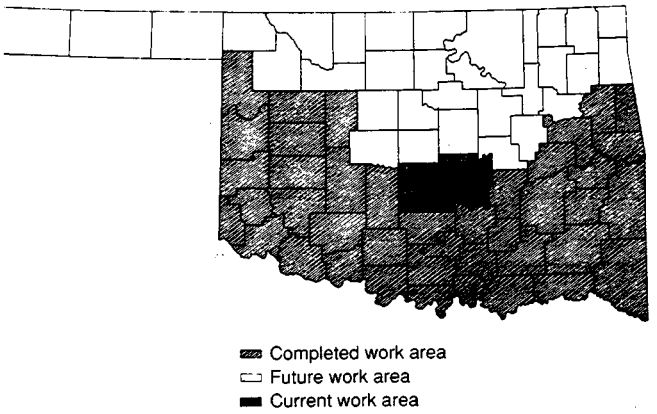

Fig. 2 Status of well history database project.

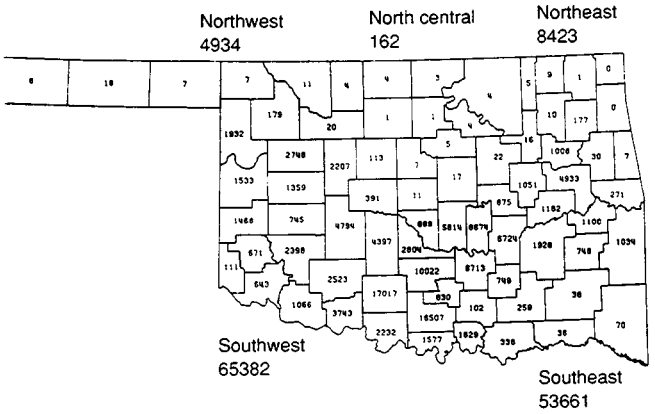

Fig. 3 Status of well history database project. Total well records, 132,562.

to 3783. As previously reported, a computer matching process is being developed to add supplemental data to the well records, including the core data that have been computerized for the OGS Core and Sample Library.

Public Data Release

Response to the release of NRIS data continues to increase as word spreads about its availability. For the OGS, NRIS data are playing a major role in the development of an Oklahoma Gas Atlas. Field and reservoir maps are being generated for the project, and a field chronology program has been developed to track the impacts of field consolidations. A presentation was given before faculty and staff of the University's Energy Center describing the Gas Atlas project and its interface with the NRIS database. Well data are being provided for an Environmental Science master's thesis that is still in progress. Details are being finalized for providing NRIS data on two Oklahoma basins to a consultant working on a special project for Petroconsultants. NRIS information was also provided to a Federal Regulatory Commission staff member working to gather information on the availability of natural gas data in the midcontinent region.

NRIS presentations were given to visitors from Argonne National Laboratory and to members of a committee studying the Geographical Information System requirements of Oklahoma State agencies. At least two poster sessions and two papers are to be presented at a March workshop titled "Petroleum-Reservoir Geology in the Southern Midcontinent" will include data from the NRIS system. The workshop is cosponsored by OGS and the Department of Energy's Bartlesville Project Office. Additionally, arrangements are being made to give an NRIS presentation to members of the Oklahoma City Chapter of the Computer-Oriented Geological Society.

Final discussions are under way with board members of the Oklahoma City Geological Society Library to provide the Library a subscription copy of the NRIS Well History File. This will allow members of the OCGS access to the 1002-A completion report information and will provide NRIS exposure to a fairly large base of independent Oklahoma geologists.

MICROBIAL TECHNOLOGY

DEVELOPMENT OF LUMINESCENT BACTERIA AS TRACERS FOR GEOLOGICAL RESERVOIR CHARACTERIZATION

Contract No. DE-AC22-90BC14666

Fairleigh Dickinson Laboratory
Abilene, Tex.

Contract Date: May 1990
Anticipated Completion: May 1991
Government Award: $40,057

Principal Investigator:
Jeannette W. King

Project Manager:
Edith C. Allison
Bartlesville Project Office

Reporting Period: Oct. 1–Dec. 31, 1990

Objectives

This research project resulted from recognition of the problem of being unable to accurately distinguish communication between wells in producing oil zones that may or may not be continuous. Such a determination is necessary when considering enhanced oil recovery (EOR) methods (whether waterflooding, carbon dioxide, or other methods) to increase sweep efficiency. Various kinds of chemical tracers are available, but they are expensive and many might be considered hazardous for underground aquifers. Other biological tracers are available but have not been developed for oil reservoir conditions. Bioluminescent bacteria seemed an obvious candidate because they thrive in saline waters (usually 3% salt) that have been contaminated by oil spills.

Summary of Technical Progress

A search of the literature has determined that bioluminescent bacteria have been studied primarily off the coast of California and in the Mediterranean Sea. Personal communications with investigators at the Catalina Marine Science, University of Houston Marine Science Center at Galveston, University of Texas at Port Aransas, University of West Florida in Pensacola, and the University of Miami Marine Science Center have determined that bioluminescent bacteria are prevalent in the Gulf of Mexico, the Pacific Ocean, and the Atlantic Ocean (citations of these occurrences of bioluminescent bacteria are included in the Bibliography). In the laboratory bioluminescent microorganisms are being tested to determine their use as cost-effective tracers in characterizing formations for EOR.

Work has continued as proposed, although trips to the coast to collect naturally occurring organisms have not been made because of unfavorable weather conditions.

A considerable amount of literature about the idiosyncracies of using these organisms in the laboratory and adapting them for other uses has been acquired. Growth media have been varied. Light intensity will be specifically measured when the photoelectric colorimeter is acquired for the laboratory. Hydrocarbon variations can be tolerated. Variations evidently affect the degree of luminescence.

A review of the literature and communication with marine microbiologists around the world confirmed that bioluminescent bacteria can be easily studied in vitro. Synthetic and seawater media are being used. Selection and monitoring are being done with a Millipore hydrosol apparatus.

Bioluminescent bacteria that have been acquired are being tested in the laboratory for easy monitoring and for adaption to oil reservoir conditions. Three different species, *Photobacterium phosphoreum* (a new subspecies), *Vibrio fischeri* (ATCC 7744), and *Vibrio fischeri* (25918), have been selected because of their various adaptive properties and capabilities. These are being adapted in the laboratory for simple use in the field.

Bibliography

Anderson, Raymond E., 1948, The Growth Requirements of Luminous Bacteria at Various Temperatures, *J. Cell. Comp. Physiol.*, 97-100.

Baumann, Paul, and Linda Baumann, 1977, Biology of the Marine Enterobacteria: Genera *Beneckea* and *Photobacterium*, *Annu. Rev. Microbiol.*, 31: 39-41.

Brown, D. E., F. H. Johnson, and D. A. Marsland, 1942, The Pressure, Temperature Relations of Bacterial Luminescence, *J. Cell. Comp. Physiol.*, 20: 151-168.

Doudoroff, Michael, 1942, Studies of the Luminous Bacteria. I. Nutritional Requirements of Some Species, with Special Reference to Methionine, *J. Bacteriol.*, 44: 451-459.

Eymers, Johanna G., and K. L. Van Schouwenburg, 1937, On the Luminescence of Bacteria. II. Determination of the Oxygen Consumed in the Light Emitting Process of *Photobacterium phosphoreum*, *Enzymologia*, 1: 328-340.

Farghaly, Abdel-Hamid, 1950, Factors Influencing the Growth and Light Production of Luminous Bacteria, *J. Cell. Comp. Physiol.*, 36: 165-183.

Giese, Arthur C., 1943, Studies on the Nutrition of Dim and Bright Variants of a Species of Luminous Bacteria, *J. Bacteriol.*, 46: 323-331.

Hendrie, Margaret S., W. Hodgiss, and J. M. Shewan, 1970, The Identification, Taxonomy and Classification of Luminous Bacteria, *J. Gen. Microbiol.*, 64: 151-169.

——, W. Hodgiss, and J. M. Shewan, 1971, Proposal for *Vibrio Marinus*, *Int. J. Syst. Bacteriol.*, 21: 218-220.

Johnson, Frank H., 1947, Bacterial Luminescence, *Adv. Enzymol.*, 7: 215-264.

McElroy, William D., and Abdel-Hamid Farghaly, 1948, Biochemical Mutants Affecting Growth and Light Production in Luminous Bacteria, *Arch. Biochem.*, 17: 379-390.

——, and David M. Kipnis, 1947, The Mechanism of Inhibition of Bioluminescence by Naphthoquinones, *J. Cell Comp. Physiol.*, 30: 359-380.

McKenney, Randolph E. B., 1902, Observations on the Conditions of Light Production in Luminous Bacteria, *Proceedings of the Biological Society of Washington*, XV: 213-234.

Nealson, Kenneth H., and J. Woodland Hastings, 1979, Bacterial Luminescence: Its Control and Ecological Significance, *Microbiol. Rev.*, 33: 149-518.

—— , and J. Woodland Hastings, 1977, Low Oxygen Is Optimal for Luciferase Synthesis in Some Bacteria, *Arch. Microbiol.*, 112: 9-16.

——, Terry Platt, and J. Woodland Hastings, 1970, Cellular Control of the Synthesis and Activity of the Bacterial Luminescent System, *J. Bacteriol.*, 104(1): 313-322.

Ruby, E. G., and J. G. Morin, 1979, Luminescent Enteric Bacteria of Marine Fishes: A Study of Their Distribution, Densities and Dispersion, *Appl. Environ. Microbiol.*, 38(3): 406-411.

Shilo, M., and T. Yetison, 1979, Physical Characteristics Underlying the Distribution Patterns of Luminous Bacteria in the Mediterranean Sea and the Gulf of Elat, *Appl. Environ. Microbiol.*, 38(4): 577-584.

POLYSACCHARIDES AND BACTERIAL PLUGGING

Contract No. DE-AC22-90BC14664

University of Michigan
Ann Arbor, Mich.

Contract Date: July 1, 1990
Anticipated Completion: June 30, 1993
Government Award: $50,000

Principal Investigator:
Scott Fogler

Project Manager:
Chandra Nautiyal
Bartlesville Project Office

Reporting Period: Oct. 1–Dec. 31, 1990

Objectives

The objectives of this research are to elucidate and model bacterial transport in porous media, to determine the importance of polysaccharides bridging as a retentive mechanism, and to identify key parameters that influence porous media plugging.

This project has been subdivided into three tasks. Task 1 is the determination of the growth kinetics of the *Leuconostoc* bacteria and how they are affected by nutrient feed and surface effects. Task 2 will quantify the importance of polysaccharide production as a cell retention mechanism. Task 3 is the elucidation of the rate of polysaccharide production and the combined effect of polysaccharide production and cell growth on plugging.

Summary of Technical Progress

Batch experiments have been conducted to determine if low sucrose concentrations limit cell growth. A reliable dextran assaying technique has been developed.

Effect of Low Sucrose Concentrations on Cell Growth

Batch experiments were conducted to compare the growth rate of the *Leuconostoc mesenteroids* cells on a medium containing no sucrose (a medium containing only yeast extract) with media containing low (1.25 and 6.2 g/L) sucrose concentrations. Figure 1 illustrates the cell density results from the batch experiments; Fig. 2 provides the respective sucrose concentrations data. The cell concentration was determined with a spectrophotometer that had been calibrated with plate counts. The cell concentration data suggest that the cells can reproduce with the use of only yeast extract as an organic source. Yeast extract is used in the medium receipt as a vitamin and amino acid supplement since *Leuconostoc mesenteroids* cells cannot metabolically synthesize the growth compounds they need for replication.

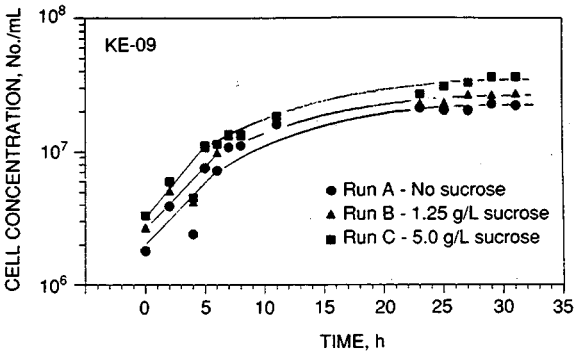

Fig. 1 Cell concentration.

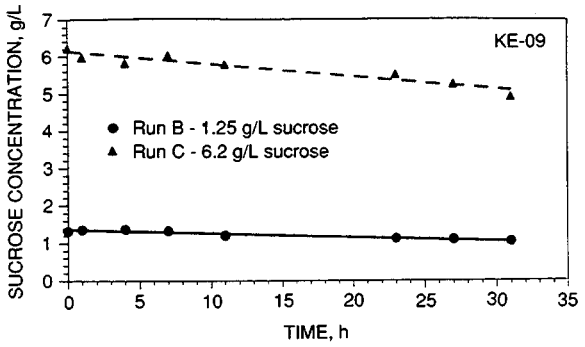

Fig. 2 Sucrose concentration.

The ability of the bacteria to grow solely on yeast extract infers that sucrose (or any other saccharides, such as fructose and glucose) is not the limiting growth nutrient. Hence the conventional models based on single limiting nutrients, such as the Monod model, cannot be used to describe cell growth and nutrient consumption. A new model must be developed for this purpose.

Two models are being considered to describe the growth of cells and consumption of sucrose and yeast extract. In both models it is assumed that the rate of cell growth with respect to time, in a batch reactor, is proportional to the cell concentration as traditionally given by Eq. 1. However, the specific growth differs from past models. Model I, Eq. 2, assumes that the bacteria overall specific growth rate is composed of two growth rates, μ_y and μ_s. The growth rates, μ_y and μ_s, are the respective growth rates of the bacteria on yeast extract and sucrose. Both of these individual growth rates can be related to their respective nutrient concentration by assuming that they follow a Monod kinetics as given by Eqs. 3 and 4:

$$\frac{dX}{dt} = \mu X \tag{1}$$

where

$$\mu = \mu_y + \mu_s \tag{2}$$

$$\mu_s = \mu_{max\,s} \frac{C_s}{K_s + C_s} \tag{3}$$

and

$$\mu_y = \mu_{max\,y} \frac{C_y}{K_y + C_y} \tag{4}$$

However, other models, proposed by Teisser, Moser, or Contois (as detailed by Bailey and Olis)[1] can be used to relate the dependence of the growth rate on nutrient concentrations.

Model I cannot account for zero growth of bacteria in the absence of yeast extract in the growth medium. The model predicts growth when yeast is eliminated from the feed and sucrose is the sole carbon source, whereas experimental results indicated that there is no bacterial growth under the same conditions. Thus it must be emphasized that the Model I fails when yeast extract is absent in the growth media.

The second model, which incorporates the concept of having two limiting nutrients, is given by Eq. 5.

$$\mu = \mu_{max}\, F(C_y)\, G(C_s) \tag{5}$$

where

$$F(C_y) = \frac{C_y}{K_y + C_y} \tag{6}$$

and

$$G(C_s) = \frac{C_s + B}{K_s + C_s} \tag{7}$$

This model assumes a Monod relationship between the growth rate and each nutrient. The additional constant B is

incorporated into $G(C_s)$ to describe the dependency of cell growth on the yeast extract. The constant B is defined as:

$$B = \frac{K_s \mu_{max\,y}}{\mu_{max}} \quad (8)$$

where $\mu_{max\,y}$ is the maximum growth rate of the cells on yeast extract alone (i.e., $C_s = 0$ and $C_y \gg K_y$) and μ_{max} is the maximum growth rate on yeast and sucrose (i.e., $C_s \gg K_s$ and $C_y \gg K_y$). This model will predict cell growth rate at low yeast concentration. An estimate of the constants for both models can be calculated from the data already present in this and the previous reports. Table 1 lists these parameters and their estimates.

TABLE 1

Parameter Estimates for Models I and II

Model I	$\mu_{max\,s} = 0.495\ hr^{-1}$ $\mu_{max\,y} = 0.205\ hr^{-1}$ $K_s = 1.24$ g/L $K_y = ?$
Model II	$\mu_{max} = 0.7\ hr^{-1}$ $\mu_{max\,y} = 0.205\ hr^{-1}$ $K_s = 1.24$ g/L $B = 0.36$ g/L $K_y = ?$

The following assumption will be examined next quarter: Determination of the parameters requires the assumption that yeast extract was in excess and the sucrose concentration did not change appreciably throughout the experiment.

Development of a Dextran Assay

The previous quarterly report stated that dextran, a polysaccharide, was separated from the cells by the procedures outlined by Jeanes et al.,[2] then analyzed using phenol–sulfuric acid assay.[3] In addition, it was reported that the assay did not provide reproducible results. With further investigation, a modified procedure detailed by Norris et al.[4] has been adopted as a reliable and reproducible assay. The results are shown in Fig. 3. Glucose and both low (87 000 daltons)- and high (2 000 000 daltons)-molecular-weight dextran were used as standards. As can be seen from the results, the linearity of the three curves and their overlap indicate that the technique can be used for the determination of polysaccharide production.

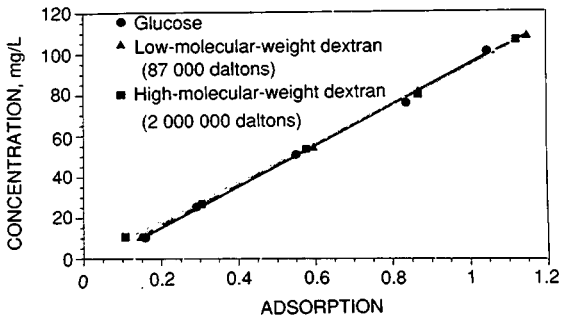

Fig. 3 Dextran calibration curve.

References

1. J. E. Bailey and D. F. Ollis, *Biochemical Engineering Fundamentals*, McGraw-Hill Book Co., Inc., New York, 1977.
2. Jeanes et al., Characterization and Classification of Dextrans from Ninety-Six Strains of Bacteria, *J. Am. Chem. Soc.*, 76: 5041-5052 (1954).
3. M. F. Chaplin and J. F. Kennedy, *Carbohydrate Analysis*, IER Press, Oxford, England, 1986.
4. J. R. Norris and D. W. Ribbons, *Methods in Microbiology*, Vol. 5B, Academic Press, New York, 1971.

MICROBIAL ENHANCEMENT OF OIL PRODUCTION FROM CARBONATE RESERVOIRS

Contract No. AC22-90BC14202

University of Oklahoma
Norman, Okla.

Contract Date: Jan. 23, 1990
Anticipated Completion: May 31, 1991
Government Award: $154,482

Principal Investigators:
Ralph S. Tanner
Roy M. Knapp
Michael J. McInerney
Emmanuel O. Udegbunam

Project Manager:
E. B. Nuckols
Metairie Site Office

Reporting Period: Oct. 1–Dec. 31, 1990

Objectives

The goal of this work is to evaluate the potential for microbial enhanced oil recovery (MEOR) in carbonate reservoirs. Specific objectives include a review of the literature pertinent to MEOR in carbonate reservoirs, a study of the microbial ecology of carbonate reservoirs, the isolation of microorganisms from these environments, examination of the effect of microorganisms and their end products of metabolism on carbonate pore structure, the

recovery of residual oil from carbonates in model core systems, and development of models to examine and predict MEOR processes in carbonate reservoirs.

Summary of Technical Progress

Oil Recovery from Carbonates

Experiments designed to study oil recovery mechanisms likely to mobilize residual oil from carbonates under varying wetting conditions are in progress. Residual oil saturation was obtained by mimicking the saturation history obtainable in reservoirs for different wetting conditions. Two types of model core systems that use the bacterial strain GSP-1 were employed: packs of Viola limestone chips and consolidated Bethany Falls limestone core plugs. Packs of Viola limestone chips (35-mesh size) are being used. Small packs (10 cm, 25-mL volume) of Viola limestone chips (35 mesh) treated with GSP-1 showed pressurization, biomass production, and considerable dissolution of the carbonate matrix, which was indicated by loss of chip volume. Data and results from a large pack are shown in Table 1 and Fig. 1. Work examining crude oil recovery from oil-wet Viola chips by GSP-1 is in progress.

TABLE 1

Viola Limestone Core Pack Data

Dimensions		
Length, 50 cm		
Diameter, 4.5 cm		
Bulk volume, 795 mL		
Core information		
Initial porosity, 33.95%		
Initial absolute permeability, 21.95 darcies		
Interstitial water saturation, 8.76%		
Residual oil saturation, 32%		
Microbial treatment data	**First treatment**	**Second treatment**
Post-treatment permeability	10.7	8.2
Highest pressure (gage psi)	6.7	12.4

Oil recovery from consolidated carbonates is also being pursued. Carbonate rock samples of the Bethany Falls formation were collected from McAdams Quarry near Mound City in eastern Kansas. This limestone, an oolitic grainstone to packstone with oomoldic porosity and heavy oil stains, has good reservoir properties that are locally preserved and easily accessible at McAdams Quarry. Permeability values ranged from 12 to 110 mD, whereas porosities varied from 6 to 20%.

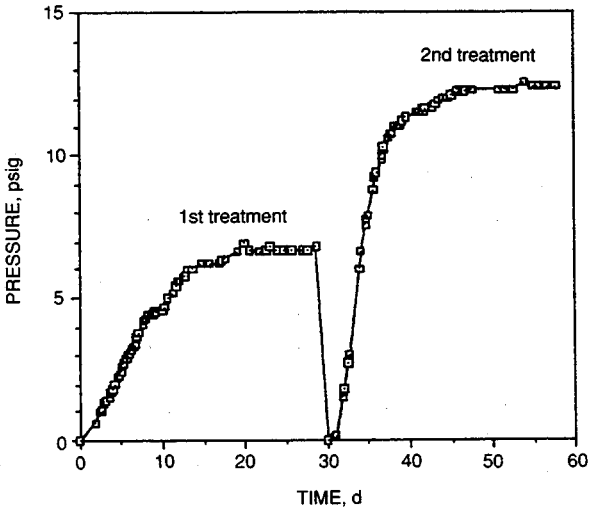

Fig. 1 Pressure vs. time data for large Viola chip pack. Data for first and second (30 d) treatment.

Effect of Bacterial Treatment on Carbonate Pore Structure

Core studies to examine the effect of microbial activity on the permeability and porosity of carbonates were initiated. A Bethany Falls core sample was incubated for 10 d with GSP-1. Characterization of the core sample before and after bacterial treatment indicated that change in porosity was slight. However, a marked increase in the percentage of larger pore openings was observed, which indicated considerable dissolution of the carbonate pore walls. Additional core plugs are being tested with GSP-1 and other bacterial strains, including *Clostridium acetobutylicum, Bacillus licheniformis* strain JF-2, and SP018, a polymer producer.

Microbial Transport in Carbonates

The transport of bacteria through carbonates was investigated with the use of GSP-1, a motile bacterium, as the test organism. GSP-1 penetrated both carbonate chip packs and consolidated core plugs. Penetration through 10-cm Viola chip packs (10 and 35 mesh) occurred in 40 h. Penetration through 2.54-cm Bethany Falls core plugs having permeabilities between 12 and 50 mD occurred within 18 h.

Effect of Adsorption on Substrate Availability

Effects of substrate adsorption in reservoirs are often overlooked when modeling and planning MEOR. As Bubela[1] pointed out, the possibility of substrate adsorption onto the pore walls of the reservoir rock is one of the parameters that should be factored in the assessment of a given reservoir in MEOR since paucity in substrate availability can interfere with the goals of an MEOR project.

Previous MEOR models[2,3] assumed adsorption isotherms for substrate adsorption without benefit of experimental work or knowledge of site-specific parameters for the assumed isotherms. Substrate adsorption behavior depends on the substrate composition and concentration, rock type, wetting conditions, and other physiochemical factors.

Study of the adsorption of glucose, ammonium, nitrate, and phosphate on surfaces of Viola limestone is near completion. Substantial adsorption of phosphate, ammonium, and glucose occurred on water-wetted Viola limestone. Ammonium ions adsorbed onto oil-wetted Viola limestone surfaces, but glucose and phosphate adsorption was not significant. Nitrate ions did not adsorb onto limestone surfaces under either condition. These results are summarized in Table 2. Desorption of these substrates from the limestone surface was also studied (Table 2). The desorptive process will determine whether the adsorbed species will be available to the bacterial population as the supended substrate concentration decreases with use. The results show that 96% of the adsorbed glucose desorbed when the chips were resuspended in brine. Only about 2.7% of the adsorbed phosphate ions and 25% of the adsorbed ammonium ions desorbed.

Adsorption from a multicomponent nutrient medium solution on water-wetted Viola limestone was also studied. The different substrates adsorbed to a lesser extent on the limestone surface when in combination. There was no nitrate adsorption.

Adsorption of substrate on water-wetted Ottawa III sand was also studied. Glucose or phosphate did not adsorb on water-wetted sand, but ammonium adsorption was considerable.

TABLE 2

Adsorption of Substrate Medium on Limestone*

Component	Initial concentration, mg/L	Original adsorbed, %	Adsorbed desorbing, %
Phosphate	10	78	2.7
Ammonium	200	50	25
Dextrose	100	12	94
Nitrate	23	0	0

*Adsorption expressed as milligrams of component adsorbed per gram of Viola chips. All assays were performed in 2% brine.

References

1. B. Bubela, Geobiology and Microbiologically Enhanced Oil Recovery, Chapter 4 of *Microbial Enhanced Oil Recovery*, E. C. Donaldson, G. V. Chiligarian, and T. F. Yen (Eds.), Elsevier Science Publishing, Inc., Amsterdam, 1989.
2. M. Y. Corapcioglu and A. Haridas, Microbial Transport in Soils and Groundwater: Numerical Model, *Adv. Water Resour.*, 8: 4 (December 1985).
3. M. R. Islam, *Mathematical Modeling of Microbial Enhanced Oil Recovery*, paper SPE 20480 presented at the 65th Annual Technical Conference and Exhibition in New Orleans, La., Sept. 23–26, 1990, Report CONF-900906, Society of Petroleum Engineers.

DEVELOPMENT OF IMPROVED MICROBIAL FLOODING METHODS

Cooperative Agreement DE-FC22-83FE60149, Project BE3

National Institute for Petroleum and Energy Research
Bartlesville, Okla.

Contract Date: Oct. 1, 1983
Anticipated Completion: Sept. 30, 1991
Funding for FY 1991: $300,000

Principal Investigator:
Rebecca S. Bryant

Project Manager:
Edith Allison
Bartlesville Project Office

Reporting Period: Oct. 1–Dec. 31, 1990

Objective

The objective of this project is to develop an engineering methodology for designing and applying microbial methods to improve oil recovery.

Summary of Technical Progress

One of the major constraints to microbial enhanced oil recovery (MEOR) technology has been the lack of simulation data to adequately describe and predict MEOR processes both in the laboratory and in the field. During the 1980s, researchers at the University of Oklahoma and the University of Southern California studied the transport of several different types of bacteria to produce one-dimensional (1-D) models. It became apparent that microbial transport in porous media was an extremely complex phenomenon that required laboratory and field data to adequately model. Although several attempts have been made to modify existing reservoir simulators to describe microbial processes, no model has yet fully incorporated all the complex phenomena that are believed to be important. Also, no model has integrated laboratory and field data for microbial transport processes. Thus an

accurate reservoir simulator for MEOR methods can best be developed through an integrated program of acquisition of laboratory and field data, with the feedback loop being the reservoir simulation model.

The unusual complexity of the mechanisms of oil recovery by microbial formulations will obviously require close coordination between laboratory mechanistic studies and oil displacement experiments under carefully controlled conditions to develop and validate a computer model.

NIPER has amassed a wealth of laboratory and field data on the mechanisms of oil mobilization of microbial formulations and the effects of various design parameters on oil recovery efficiency. Research with the use of laboratory experiments in FY90 began to define key mechanisms of oil mobilization. Work for FY91 will continue to develop the critical parameters, correlations, and mathematical models to describe the physical phenomena that are important in MEOR methods and the development of a mathematical computer simulator to model and predict the performance of microbial formulations in oil recovery applications.

Laboratory data from the National Institute for Petroleum and Energy Research (NIPER) will be used to develop correlations and mathematical models for specific phenomena, and linear coreflooding data will be used to test the simulator in an iterative process. The simulator development and laboratory testing aspects of this project will be carefully coordinated so that the results from testing the simulator with oil displacement experiments will be used to design laboratory experiments to clarify and quantify certain physical effects from which correlations that will be incorporated into the simulator will be refined and modified. The simulator will be the primary deliverable from this research. The overall goal of the project is to develop a method for predicting and evaluating microbial EOR processes in porous media.

For milestone 1, "Review All Laboratory Data and Make Necessary Modifications to the Plan Developed in FY90 for Laboratory Evaluation of MEOR Processes," a project meeting was held with members of the microbial experimental group and those currently participating in the mathematical simulation of MEOR processes. Several experiments were planned to evaluate microbial transport and to validate the 1-D microbial transport that is currently in use. A paper entitled "Modeling of Transport Phenomena of Microbial Systems in Porous Media" was presented in November at the annual AIChE meeting in Chicago, Ill. The presentation covered the development of a three-dimensional (3-D) three-phase, multiple-component numerical model to describe microbial transport phenomena in porous media. The model can accurately describe the observed transport of microbes, nutrients, and metabolites in coreflooding experiments.

For milestone 2, "Complete Development of Mathematical Descriptions of Microbial Oil Mobilization," a 1-D MEOR simulator was developed with the use of an extended method of lines (MOL) to solve the coupled model equations for predicting the propagation and distribution of microbes and nutrients and the permeability reduction caused by microbes in reservoir cores. Sensitivity runs with a 4-ft reservoir core were conducted to investigate the effect of grid block size and time step on simulation results. Results were stabilized after decreasing the grid block size to smaller than 0.025 ft and the time step to smaller than 0.004 d. Simulation results were comparable to those obtained from the use of a Crank–Nicolson method. Results obtained from these two methods will be compared with experimental microbial coreflood data to determine which method will better describe the coreflood data.

Experiments to obtain data to validate the numerical model were conducted. An experiment to determine the dispersion coefficient of microbial cells without nutrient in a Berea sandstone core was completed. A chemical tracer, fluorescein, was first injected into a brine-saturated 10-in. core. After the tracer was injected, a slug containing microbial cells with no nutrient present was injected. Figure 1 shows the results of these two injections. Apparently most of the microbial population traveled almost as fast as the tracer. The initial injected concentration of microorganisms was 1.2×10^9 cells/mL. However, the initial concentration of microorganisms compared with the effluent microbial concentration indicated that some of the cells were retained in the core, perhaps by adsorption.

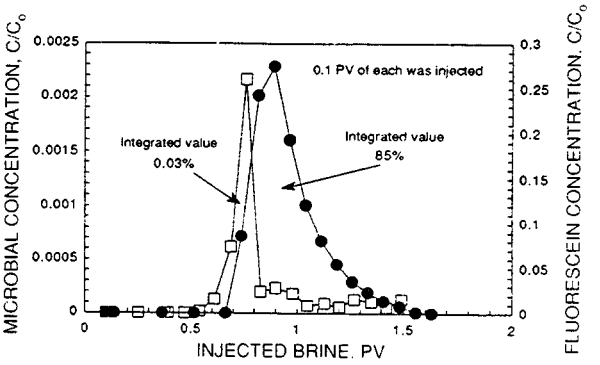

Fig. 1 Normalized concentrations of tracer and microorganisms in a 10-in. Berea sandstone core. —●—, fluorescein. —□—, cells.

The integration of the microbial concentration curve showed a very low recovery of cells. The simulator was used to match the tracer data (Fig. 2). Another experiment is being conducted at a different flow rate to determine if the dispersion coefficient will remain the same. A microbial transport experiment to determine adsorption effects is also being planned. A tracer experiment was conducted on a 4-ft Berea sandstone core that will be injected with microorganisms to simulate an injection strategy for validating the microbial simulation model. Approximately 97.7% of the tracer was recovered in the effluent (Fig. 3).

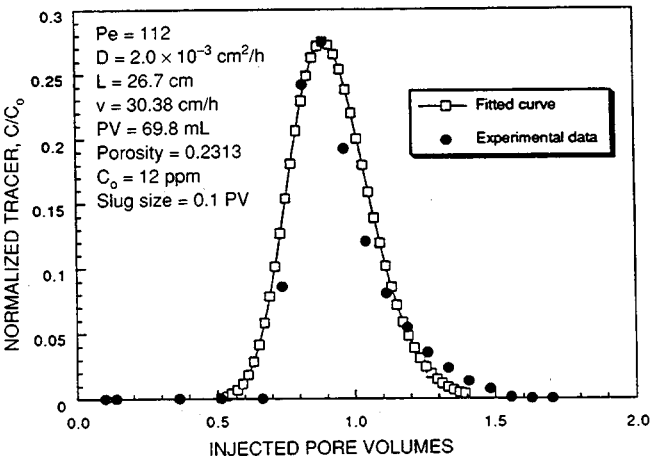

Fig. 2 Simulator match of experimental tracer data.

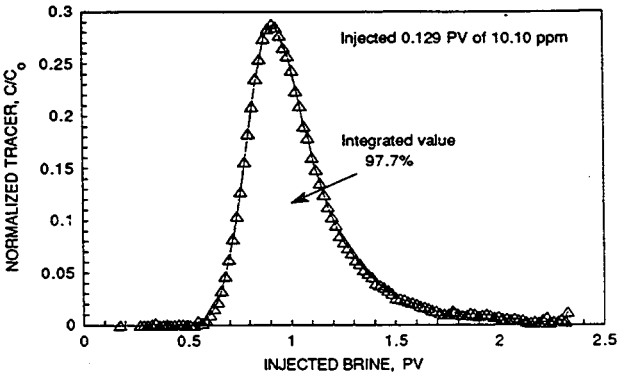

Fig. 3 Normalized concentration of tracer in a 4-ft Berea sandstone core.

Work for milestone 3, "Compare Oil Mobilization Mechanisms for Microbial Species Used for Permeability Modification With Those Used for Microscopic Oil Displacement," continued. A microbial coreflood was conducted with a microorganism that produced a polymer, and injection pressures were monitored. This microbial polymer-producing strain will be used to compare high- and low-permeability corefloods.

MICROBIAL-ENHANCED WATERFLOODING FIELD PROJECT

Cooperative Agreement DE-FC22-83FE60149, Project SGP13

National Institute for Petroleum and Energy Research
Bartlesville, Okla.

Contract Date: Oct. 1, 1983
Anticipated Completion: Sept. 30, 1991
Funding for FY 1991: $419,000

Principal Investigator:
Rebecca S. Bryant

Project Manager:
Edith Allison
Bartlesville Project Office

Reporting Period: Oct. 1–Dec. 31, 1990

Objectives

The objectives of this project are to determine the feasibility of improving oil recovery in an ongoing waterflood with the use of microorganisms and to expand the initial pilot and determine the economics of microbial-enhanced waterflooding. The scope of work includes continued monitoring of the Phoenix field site.

Summary of Technical Progress

The expanded microbial-enhanced oil recovery project site is located in S8-T24N-R17E of Rogers County, Okla. This site is part of Chelsea–Alluwe field in the Bartlesville formation and was initially developed soon after Delaware–Childers field. The site, which is owned by Phoenix Oil and Gas, Ltd., is being waterflooded. This field is in a very isolated area with virtually no other oil-producing leases nearby.

Fluorescein was injected as a tracer on June 6, 1990. Samples were taken from all 19 injection wells at 2-h intervals the first day. The injection wells nearest the centralized injection station (EL-2, WAL-3, and WM-13-10) exhibited a large tracer response that persisted throughout the sampling period, whereas some of the injection wells that were farther away did not show a maximum tracer response until the 2- or 4-h sampling.

Twenty-one producers were sampled 24 h after injection of tracer, daily, then weekly, and finally, once a month. Since the second day of sampling, the tracer response has never been higher than 0.30 ppm for any of the wells. The pattern of the fluorescein response seems to follow the same trend as that observed during the monitoring of the Mink Unit. There was an initial quick response of tracer from some of the nearest production wells; the response then leveled out to very low values.

Oil production from the Phoenix leases through October 1990 is shown in Fig. 1. Injection of the microbial formulation occurred on June 20, 1990, and nutrient is continuously injected. Since there are only five data points, no conclusions can be made at this time. Wellhead injection pressures and volumes continue to be monitored.

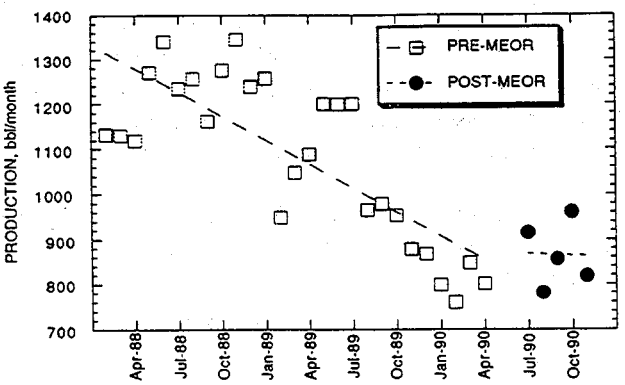

Fig. 1 Comparison of oil production before and after microbial injection. – –, y = 1332.4 + –17.672x R= 0.7814. - - - -, y = 910.42 + –1.383x R = 0.03012.

EFFECTS OF SELECTED THERMOPHILIC MICROORGANISMS ON CRUDE OILS AT ELEVATED TEMPERATURES AND PRESSURES

Contract No. DE-AC02-76CH00016

Brookhaven National Laboratory
Upton, Long Island, N.Y.

Contract Date: Mar. 1, 1989
Anticipated Completion: Sept. 30, 1990
Government Award: $155,000
(Current year)

Principal Investigators:
E. T. Premuzic
M. S. Lin

Project Manager:
Edith Allison
Bartlesville Project Office

Reporting Period: Oct. 1–Dec. 31, 1990

Objective

The objective of this program is to determine the chemical and physical effects of thermophilic organisms on crude oils and cores at elevated temperatures and pressures. Ultimately a database will be generated that will be used in technical and economic feasibility studies leading to field application.

Summary of Technical Progress

Studies dealing with the variations in the interaction between different types of microorganisms and crude oils have been continued. Earlier observations[1,2] have indicated that the composition of crude oils in terms of organic compounds present changes during the biotreatment in favor of lighter components. Concurrent with this biochemical alteration of crude oils, there is also a change in the composition of organic sulfur compounds. Most recent studies, details of which will be reported at the forthcoming meeting of the Society of Petroleum Engineers,[3] have shown that biotreatment of Boscan heavy crude oil from Venezuela with different microorganisms from the Brookhaven collection leads to significant chemical changes in the composition of the crude. Thus Boscan crude containing, on an average, about 5% sulfur was treated with BNL-4-22, BNL-4-23, and BNL-4-24 for 7 d, which resulted in an overall lowering of organic sulfur content by 10 to 25%. Although kinetic studies under optimum conditions have as yet to be carried out, BNL-4-22 removed 25% of the original sulfur present in the crude, which resulted in further detailed study. Biotreatment of Boscan crude oil with BNL-4-22 microorganism causes the following significant changes in the chemical composition of crude oil:

- Decrease in the total sulfur content.
- Decrease in the concentration of thianaphthalene organic compounds.
- Decrease in the C20 to C30 alkanes.
- Increase in the <20 type alkanes.
- An overall formation of lighter hydrocarbons.

Changes in the chemical composition of Boscan crude brought about by the biotreatment of the crude are consistent with those observed for Cerro Negro.[2] These changes, however, differ in chemical detail and further indicate the significance of variations in interactions of microbial species/crude oil types. These observations also imply that the biochemical mechanisms may differ with different microbial species and/or types of crude oils being biotreated.

Biochemical modification and/or removal of organic sulfur compounds from Cerro Negro and Boscan crudes by microorganisms from the BNL collection,[4] is "a first" and indicates that biotreatment of high sulfur content crude oils[4] may lead to a desulfurization process.

Experiments leading to improved designs of bioreactors are continuing. A prototype continuous-temperature-gradient incubator has been constructed, tested, and further modified. The most recent model can culture microbial strains in a continuous mode over a temperature range of

4 to 100°C (Ref. 5). This is a unique tool for the development of thermo-adapted bacteria capable of interaction with crude oils under different temperature regimes, including low and high extremes.

The summary FY 1990 Annual Report (BNL 45232) and the FY 1990 Annual Report (BNL 45368) have been completed and submitted.

References

1. E. T. Premuzic and M. S. Lin, Interaction Between Thermophilic Microorganisms and Crude Oil: Recent developments, *Resources, Conservation, and Recycling*, 5, 1991 (in press).
2. E. T. Premuzic and M. S. Lin, Prospects for Thermophilic Microorganism in Microbial Enhanced Oil Recovery (MEOR), in *Proceedings of the International Conference on MEOR, University of Oklahoma, Norman, Okla., May 27–June 1, 1990*, E. Donaldson (Ed.), Elsevier Press, 1990, in press.
3. E. T. Premuzic and M. S. Lin, Prospects for Thermophilic Microorganism in Microbial Enhanced Oil Recovery (MEOR), in *Proceedings of the SPE International Symposium on Oil Field Chemistry, Anaheim, California, Feb. 20–22, 1991.*
4. E. T. Premuzic and M. S. Lin, Patent pending, 1990.
5. E. T. Premuzic and M. S. Lin, Patent applied for, 1991.

ENHANCED OIL RECOVERY AND APPLIED GEOSCIENCE RESEARCH PROGRAM

Contract No. AC07-ID01570, Project 5AC3

Idaho National Engineering Laboratory
EG&G Idaho, Inc.,
Idaho Falls, Idaho

Contract Date: Oct. 1, 1988
Anticipated Completion: Sept. 30, 1995
Funding for FY 1990: $1,500,000

Principal Investigator:
C. P. Thomas

Project Managers:
I. Aoki
Idaho Operations Office

Edith Allison
Bartlesville Project Office

Reporting Period: Oct. 1–Dec. 31, 1990

Objectives

The objectives of this research program are to develop microbial enhanced oil recovery (MEOR) systems for application to reservoirs containing medium to heavy oils (12 to 20 °API) and to evaluate reservoir wettability and its effects on oil recovery.

The MEOR research goals include:

- Development of bacterial cultures that are effective for oil displacement under a broad range of reservoir conditions.
- Improved understanding of the mechanisms by which microbial systems displace oil under reservoir conditions.
- Determination of the feasibility of combining microbial systems with conventional enhanced oil recovery (EOR) processes, such as miscible and immiscible gas flooding, polymer and chemical flooding, and thermal methods.
- Development of an MEOR field process design and implementation of an industry cost-shared field demonstration project.

The goals of the reservoir wettability project are to develop:

- Better methods for assessment of reservoir core wettability.
- More certainty in relating laboratory core analysis procedures to field conditions.
- Better understanding of the effects of reservoir matrix properties and heterogeneity on wettability.
- Improved ability to predict and influence EOR response through control of wettability in reservoirs.

Summary of Technical Progress

MEOR Research

Organisms used in coreflood experimentation (*Bacillus licheniformis* JF-2) are routinely grown by inoculating 50 mL medium E supplemented with 1% sucrose with 100 µL of a fresh overnight culture (trypticase soy broth). The salinity is adjusted to 2.4% NaCl to model field conditions for the Moorcroft West Unit. Incubation is conducted aerobically at 30°C until the culture reaches an optical density of 1.0 +/–0.15 (approximately 50% of log phase). The cells are harvested by centrifugation (3000 rpm × 10 min at room temperature, with a Sorvall rotor SS34) and *resuspended* in fresh medium E with sucrose added to 1%. This procedure is followed to allow differentiation between metabolic products produced outside the core and those metabolites produced in the core. Under this regimen, only the cells themselves are used for inoculum, and therefore oil displacement that occurs is the result of either in situ production of metabolic products (surfactant, etc.) or the physical presence of the cells or both. Experiments were conducted in which the culture was grown and injected with no further treatment (hence cells + ex situ metabolites were added). These experiments indicate 4.3% original oil in place (OOIP) recovered with washed cells vs. 28.3% OOIP with unwashed cells + media (see Table 1). Coreflood experiments conducted at the Idaho National Energy

TABLE 1

**Microbial Enhanced Oil Recovery Coreflood Recovery Data*
(Washed vs. Unwashed Cells)**

Core†	Microbe‡	Oil§	VIS, cP	PERM, mD	S_{oi}, %PV	S_{orwf}, %PV	S_{ormf}, %PV	MEOR REC,¶ %OOIP	MEOR REC,** %OOIP ( )††
11	B L‡‡	LIC	288	109	79.3	39.2	35.8	2.6	4.3 (9.5)
26	B L§§	LIC	288	359	62.8	22.3	4.2	11.5	28.8 (25)

*Core parameters: OOIP, original oil in place; VIS, oil viscosity; PERM, absolute brine permeability of core; S_{oi}, initial oil saturation; S_{orwf}, waterflood residual oil saturation; S_{ormf}, microbial flood residual oil saturation; and PV, pore volume of core.

†For all corefloods, temperature = 23°C and brine = 2.4 wt % NaCl.

‡*Bacillus licheniformis* microbial system.

§Crude oil type: LIC, Lick Creek.

¶Microbial enhanced oil recovery at 6 PV of brine injected.

**Microbial enhanced oil recovery with brine injection until oil production ceases.

††PV of brine injected.

‡‡Washed cells resuspended in media E.

§§Unwashed cells in media E.

Laboratory (INEL) have been designed to model the in situ production of metabolites to more closely mimic the application of MEOR in the field.

The series of coreflood experiments developed to investigate parameters, such as crude oil type, crude oil viscosity, aging and incubation time, interfacial tension (IFT), and brine composition, continue. Results of the initial experimental corefloods in this experimental series were previously reported. All cores in the current set of experiments have now been flooded with the *B. licheniformis* microbial system, and the resulting data are shown in Table 2.

Five different oils, ranging in gravity from 17.5 to 38.1 °API at 60°F, were used in this set of experimental corefloods. All cores were coated with epoxy and fitted with end plates. The same coreflood apparatus used in previous coreflood experiments was used in this set of experiments. The dimensions of the unfired Berea sandstone cores were 1 in. in diameter and 6 in. in length. A 2.4 wt % NaCl brine solution was used to saturate the cores and to displace the oil as the cores were flooded. The brine solution was filtered through a 0.45 μm Millipore membrane and deaerated. All corefloods were performed at room temperature,

TABLE 2

Microbial Enhanced Oil Recovery Coreflood Recovery Data*

Core†	Microbe‡	Oil§	VIS, cP	PERM, mD	S_{oi}, %PV	S_{orwf}, %PV	S_{ormf}, %PV	MEOR REC,¶ %OOIP	MEOR REC,** %OOIP ( )††
22	B L‡‡	BUR	6	214	65.8	32.6	29.6	4.6	4.6 (12)
25	B L‡‡	SCH	54	85	72.3	39.5	37.9	1.4	2.2 (14.5)
23	B L‡‡	ALW	134	311	53.3	11.9	7.7	7.1	7.9 (6.5)
24	B L‡‡	MOO	142	115	72.3	39.4	38.3	1.3	1.4 (12)
26	B L§§	LIC	288	359	62.8	22.3	4.2	11.5	28.8 (25)

*Core parameters: OOIP, original oil in place; VIS, oil viscosity; PERM, absolute brine permeability of core; S_{oi}, initial oil saturation; S_{orwf}, waterflood residual oil saturation; S_{ormf}, microbial flood residual oil saturation; and PV, pore volume of core.

†For all corefloods, temperature = 23°C and brine = 2.4 wt % NaCl.

‡*Bacillus licheniformis* microbial system.

§Crude oil type: SOL, Soltrol 220; BUR, Burbank; SCH, Schuricht; AlW, Alworth; MOO, Moorcroft West; LIC, Lick Creek.

¶Oil recovery at 6 PV of brine injected.

**Oil recovery with brine injection until oil production ceases.

††Pore volumes of brine injected.

‡‡Washed cells resuspended in medium E.

§§Unwashed cells in medium E.

including the evacuation and saturation phase of the experimental work. The volume of injected microbes and nutrient was 60% pore volume (PV) for each core. All cores were incubated for 2 weeks at 37°C after the injection of the microbial system. The Lick Creek core was the only core inoculated with unwashed *B. licheniformis* cells in growth media (medium E). All other cores were inoculated with washed *B. licheniformis* cells in fresh medium E. Base-line (control) experiments were previously performed for each of the oils.

Coreflood experiments that use injection of only metabolites of *B. licheniformis* JF-2 are currently being performed. *Bacillus licheniformis* are grown by the previously described protocol, and the supernatant is harvested by centrifugation. The supernatant without cells is then injected into the cores. The investigation of waterflood residual oil recovery with the injection of metabolites followed by waterflood is continuing; four corefloods are now complete. Four different crude oils, ranging in gravity from 19.1 to 38.1 °API at 60°F, are being used in this experimental series.

All cores were prepared as previously described. *Bacillus licheniformis* metabolites were injected into the cores followed by brine injection. Brine injection was not initiated until the core, with the injected metabolites, was allowed to age 24 h at room temperature to allow for system stabilization. The volume of injected biosurfactant (metabolites) was equivalent to approximately 1 PV for each sequence in each core. The cores were then flooded with brine at the previous waterflood injection rate to an approximate 2-PV equivalent. The biosurfactant was also injected at the same rate. This procedure continued, alternating biosurfactant and brine injection, until five sequences of biosurfactant followed by brine had been injected (approximately 15 PV of total fluid).

Control experiments are being performed for this series of corefloods. The control cores are injected with brine only. Injection volumes and procedures are the same as those for the cores in which *B. licheniformis* metabolite was injected.

Oil has been displaced abiotically from Berea sandstone cores with cell-free culture supernatants of *B. licheniformis* JF-2. Results of completed corefloods in this series are shown in Table 3. The porosities of the cores used ranged from 22.0 to 23.4%. Oil recovery for the biosurfactant/brine injection ranged from 5.3 to 8.6% OOIP. Reduction in the residual oil saturation of each core was not experienced until approximately 7 PV of fluid was injected (approximately 3 PV of biosurfactant and 4 PV of brine). The reason for the observed trend in the biosurfactant flood oil recoveries will be investigated further as the experimental work with this series of corefloods continues. Experiments continue to compare microbial presence with absence in relation to oil recovery from Berea sandstone and to confirm the validity and implications of these results.

Field isolates anaerobically emulsify Schuricht crude oil with no detrimental degradation/transformation in the presence of 1% sucrose. Emulsification occurred faster in vials inoculated with field isolates than in those inoculated with *B. licheniformis* JF-2. Experiments continue to compare these field isolates with *B. licheniformis*.

Recovered oil samples were subjected to gas chromatography to analyze the extent of microbial degradation and/or transformation. Analysis was based on the comparison of the pristane/C_{17} and phytane/C_{18} ratios of experimental samples with those of abiotic controls as well as direct comparison of the chromatographic profiles. Data indicate no significant changes in the composition of the oil. The conclusion drawn is that, under anaerobic conditions in the presence of 1% sucrose as a carbon source, the oil is

TABLE 3

Biosurfactant Coreflood Recovery Data*
(No microbes injected)

Core†	Biosurfactant‡	Oil§	VIS, cP	PERM, mD	S_{oi}, %PV	S_{orwf}, %PV	S_{orbf}, %PV	Oil REC,¶ %OOIP
33	B L BIO	BUR	6	350	75.5	45.3	40.9	5.8
27	B L BIO	SCH	54	115	69.6	37.6	33.9	5.3
29	B L BIO	SCH	54	390	67.5	38.0	32.2	8.6
28	B L BIO	MOO	142	470	73.9	41.9	37.4	6.1

*Core parameters: OOIP, original oil in place; VIS, oil viscosity; PERM, absolute brine permeability of core; S_{oi}, initial oil saturation; S_{orwf}, waterflood residual oil saturation; S_{orbf}, biosurfactant flood residual oil saturation; PV, pore volume of core.

†For all corefloods, temperature = 23°C and brine = 2.4% wt % NaCl.

‡Metabolites of *Bacillus licheniformis* injected into core without dilution, no microbes injected.

§Crude oil type: BUR, Burbank; SCH, Schuricht; and MOO, Moorcroft West.

¶Oil recovery at approximately 15 PV of fluid injection (5 biosurfactant/brine sequences each consisting of 1 PV biosurfactant followed by 2 PV brine).

emulsified but is not subject to metabolic attack or extraneous transformations.

Continued experimental efforts with the interfacial tensiometer have resulted in calibration protocols. Two different cells, one containing a 0.22-mm capillary injector calibrated with a 0.0625-in. stainless steel ball and one containing a 1.58-mm injector calibrated with a 0.0937-in. stainless steel ball were used to measure the interfacial tension (IFT) of an *n*-butanol/water system. The published[1] IFT value for the system is 1.8 dynes/cm at 20°C. Data collected from current experiments indicate very good correlation with this value. The 0.22-mm injector-equipped cell resulted in a measured value at 23°C of 1.8672 dynes/cm (+/– 0.0690, n = 8), whereas the 1.58-mm equipped cell resulted in a value of 1.8947 dynes/cm (+/– 0.0514, n = 7).

Evaluation of Reservoir Wettability and Its Effects on Oil Recovery

Complex drilling fluids are an essential part of successful drilling operations. The choice of drilling fluids is generally dominated by geologic operating conditions. Drilling, like all field operations, can damage the contacted formation either by causing movement of fines or by chemical interactions between introduced fluid filtrate and reservoir rocks or fluids and the surrounding rock.[2] Potassium-based drilling mud is commonly used to inhibit clay damage and maintain hole stability. Oil-based mud can serve a similar purpose. Apart from occasional use of lease crude oil, most attempts to recover cores with unaltered wettability are performed with so-called bland water-based mud formulations. The design of water-based mud, which does not cause wettability alteration, has been a long-standing objective in core analysis. Initial studies focused mainly on changes in wettability of rocks that were initially very strongly water-wet.[3]

All core samples are exposed to some kind of drilling fluid during the coring process. If useful laboratory measurements of oil displacement behavior are to be made on the core samples in their recovered state (so-called fresh cores), knowledge of possible alterations in wettability because of the drilling fluid is required. The present study concentrates on typical water-based drilling mud. Muds designed for drilling under different conditions were included. In addition to using very strongly water-wet core samples, cores were treated with crude oil to obtain five designated ranges of initial wetting conditions from strongly water-wet to neutrally water-wet. Details of the procedure are available elsewhere.[4]

Drilling mud filtrates were prepared by filtration through mud cake. Individual drilling mud additives were also tested. These included typical surface-active agents (lignosulfonates, sulfonated asphalt, and Durenex) as well as several polymeric compounds, including carboxymethylcellulose (CMC), polyanionic cellulose (Drispac), starch (Dextrid), and Xanthan biopolymer (XC). The range of additive amount typically used in drilling mud formulations was covered by testing for wettability alteration at five levels of concentration. Changes in core properties were quantified by measurements of Amott wettability indexes made before and after exposure to mud filtrate or solutions of drilling mud components.

The investigation of alteration of initial wettability states of sandstone cores by flushing with drilling mud filtrates and studies of wettability changes in initially strongly water-wet cores caused by solutions of individual components of drilling muds indicate:

- Exposure to additives commonly found in water-based drilling muds can measurably affect the wettability of strongly water-wet cores. In some cases, the effects are more pronounced as concentration of the contaminant increases; in others, exposure even at low concentrations changes the wetting properties of strongly water-wet cores.
- Water-based drilling mud filtrates composed of mixtures of varying concentrations of these same additives have less effect on these same core properties when tested on initially strongly water-wet Berea sandstone. Some reduction in the Amott wettability index to water (I_w) was noted for all formulations.
- These same drilling mud filtrates have an overall leveling effect on the value of I_w as shown by tests of cores over a range of initial wetting conditions from strongly water-wet to neutral. Strongly water-wet cores become somewhat less water-wet. Neutral wet rocks tend to become slightly water-wet after exposure.

Significant changes in wetting properties, and sometimes also permeability, were caused by solutions of individual drilling mud constituents. Drilling fluid filtrates generally showed much less influence on wettability, and, in some cases, the measured wettability was essentially unchanged. In general, exposure to water-based drilling fluid filtrates tended to leave strongly water-wet samples less water-wet; cores that were initially close to neutral wettability became slightly water-wet. Results are presently being obtained for cores that are initially oil-wet.

Future work will include extension of the range of wettability conditions to oil-wet conditions by learning how to prepare cores with graded degrees of oil wetness and investigation of the reversibility of wettability alteration (for example, by flushing with brine) as a possibility for cores in which the mud filtrate causes wettability alteration.

References

1. A. W. Adamson, *Physical Chemistry of Surfaces*, 3rd ed., Interscience Publishers, New York, 1976.
2. R. F. Krueger, An Overview of Formation Damage and Well Productivity in Oilfield Operations, *J. Pet. Technol.*, 131-152 (February 1986).
3. E. Amott, Observations Relating to the Wettability of Porous Rock, *Trans. Soc. Pet. Eng. AIME*, 216: 156-162 (1959).

4. D. Jia, J. S. Buckley, and N. R. Morrow, *Control of Core Wettability with Crude Oil,* paper SPE 21041 presented at the Society of Petroleum Engineers 1991 International Symposium on Oilfield Chemistry, Anaheim, Calif., Feb. 20-22, 1991.

QUANTITATION OF MICROBIAL PRODUCTS AND THEIR EFFECTIVENESS IN ENHANCED OIL RECOVERY

Contract No. DE-AC22-90BC14662

University of Oklahoma
Norman, Okla.

Contract Date: Aug. 21, 1990
Anticipated Completion: Aug. 20, 1993
Government Award: $123,445

Principal Investigators:
Michael J. McInerney
Roy M. Knapp

Project Manager:
E. B. Nuckols
Metairie Site Office

Reporting Period: Oct. 1–Dec. 31, 1990

Objective

The objective of this study is to provide quantitative information on the effectiveness of microbial fermentation processes in recovering residual oil from consolidated sandstone cores. Quantitative and kinetic relationships will be developed which correlate the amount of substrate used to the amount of cells and products formed and the amount of residual oil recovered. This information will be used to develop numerical models of the interaction of microorganisms, their products, and oil recovery efficiency to assist researchers and operators in designing microbial systems to enhance oil recovery.

Quantitation of Microbial Products

The quantitation of products from carbohydrate by bacteria useful for enhanced oil recovery continued during this reporting period. The fermentation of glucose, the major monomeric component of most carbohydrates, by the halophilic anaerobic bacterium, strain TTL-30, and the facultatively anaerobic, halotolerant bacterium, strain SP018, was studied. Both bacteria have been used in laboratory studies of microbial selective plugging.

The metabolism and transport of strain TTL-30 were studied in three types of porous media: Ottawa sand (100 to 200 mesh size), Vassar Vertz crushed sandstone (45 mesh size), and Viola limestone (two mesh sizes, 10 and 35 mesh). The packs were 10 cm long and were saturated with a glucose–mineral salts medium. The metabolism of glucose by strain TTL-30 grown in the porous media was also compared with that of liquid cultures with the use of media of identical composition and inoculated with the same culture used to inoculate the cores. Table 1 shows the porosity and penetration rates of strain TTL-30 through the four kinds of porous material. Strain TTL-30 rapidly penetrated through each type of material, with the most rapid penetration observed in tubes packed with sand or 10-mesh limestone. A penetration rate of 0.5 cm/h is among the highest penetration rates observed in the absence of fluid flow.

TABLE 1

Transport of Strain TTL-30 Through Porous Media*

Core type	Porosity, %	Penetration rate, cm/h
Ottawa sand	35.7 ± 0.07	0.50 ± 0.00
Vertz sand	ND†	0.24 ± 0.00
Limestone (35 mesh size)	47.1 ± 0.27	0.24 ± 0.00
Limestone (10 mesh size)	51.6 ± 0.99	0.50 ± 0.00

*Values represent means ± standard deviations of duplicate cores.
†ND, not determined.

After 22 d of incubation under strictly anaerobic conditions, the packs were sacrificed, and the nature of fermentation end products in each pack was determined. Under identical experimental conditions, the nature and concentration of end products were also determined in liquid cultures. Acetate, ethanol, and formate were detected as end products both in liquid culture and in packs with different types of porous media (Table 2). Therefore the pathway

TABLE 2

Metabolism of Strain TTL-30 in Different Types of Porous Media*

Core type	Concentration, mM		
	Acetate	Ethanol	Formate
Ottawa sand	1.8	4.8	0.2
Vertz sand	4.0	2.5	0.3
Limestone (35 mesh size)	4.0	1.5	0.4
Limestone (10 mesh size)	4.0	2.0	0.5
Liquid culture	8.0	5.0	0.2

*Values represent means of duplicate cores.

used for glucose metabolism and energy production was the same in liquid culture and in porous material. This means that data obtained from experiments with liquid cultures will provide accurate estimates of the nature and concentrations of fermentation end products and of cell yields. Complete carbon recoveries were not obtained, so it is not possible to derive empirical stoichiometric equations that can be used in mathematical modeling. Experiments to obtain these equations are under way. One interesting point was that the cells penetrated through the packed cores without an appreciable consumption of glucose.

The fermentation of glucose by SP018 grown in a glucose–nitrate–mineral salts medium was studied. SP018 produced a variety of products from glucose. Organic acids were detected by high-pressure liquid chromatography, and the amount and identity of the volatile acids was confirmed by gas chromatography. Alcohols were detected and quantitated by gas chromatography. Fermentation products included ethanol, formate, acetate, butyrate, and lactate. The nature of the fermentation suggests that SP018 metabolizes glucose in a manner similar to some clostridia rather than members of the genus *Bacillus*.

Mathematical Modeling

Mathematical modeling efforts initially have focused on the transport of nutrients through a porous medium to determine an optimal injection protocol for a microbial process. Theoretical calculations and tracer experiments were conducted to estimate the extent of mixing and the slug size of the injected nutrients. The following are approximate solutions for predicting the convection–dispersion of nutrients in linear and radial systems.
For linear system

$$C_D = \frac{1}{2}\,\mathrm{erfc}\left[\frac{x_D - t_D}{2\,(t_D / N_{pc})^{1/2}}\right]$$

For radial system

$$C_D = \frac{1}{2}\,\mathrm{erfc}\left[\frac{r_D^2 - t_D}{4\,(r_D^3 / 3N_{pc})^{1/2}}\right]$$

where C_D = dimensionless concentration
x_D (or r_D) = distance
t_D = dimensionless time (or dimensionless PV)
N_{cp} = Peclet number

The superposition theory was applied to the slug-injection calculation since the convection–dispersion equations are linear. Figures 1 and 2 show the computed results that occur when nutrients were injected in six slugs of equal size followed by slugs of brine that were 2, 4, or 6 times as great as the volume of the nutrient slug. The simulation predicts that a large amount of mixing will occur. As the volume of the brine slug increased relative to the nutrient slug, a more uniform distribution of the nutrients throughout the formation was obtained. In radial flow systems, as compared with linear flow systems, the injection of nutrients followed by brine effectively swept the nutrients away from the well bore. This may prevent the loss of injectivity as a result of microbial growth in the vicinity of the well.

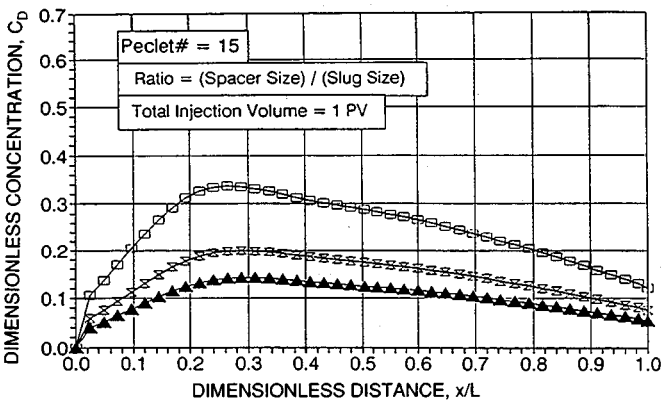

Fig. 1 Six-slug linear flow. —□—, ratio = 2. —⧖—, ratio = 4. —▲—, ratio = 6.

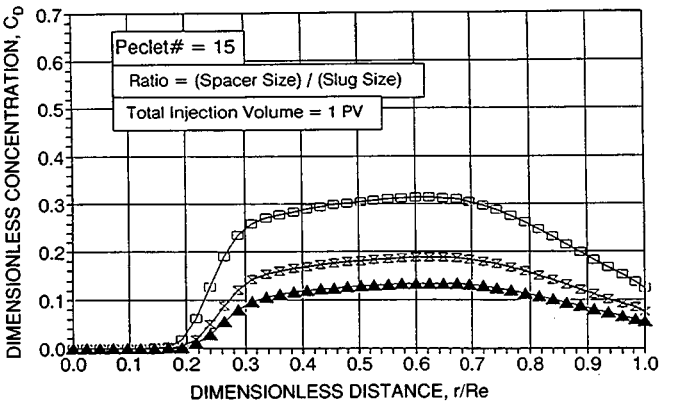

Fig. 2 Six-slug radial flow. —□—, ratio = 2. —⧖—, ratio = 4. —▲—, ratio = 6.

Core flow experiments were conducted to verify that mixing of the injected nutrient will occur. In these experiments, either one or two slugs of a sodium fluorocene solution was injected into a Berea sandstone core followed by brine injection (Figs. 3 and 4). The core flow experiments show that more mixing occurred with the injection of two slugs of sodium fluorocene than with the injection of one slug.

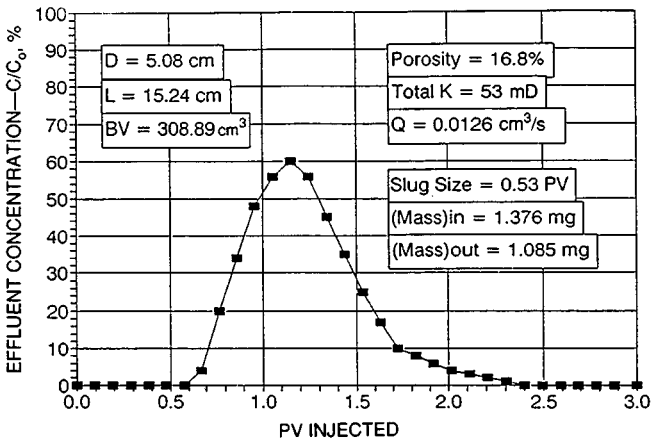

Fig. 3 One-slug tracer test.

These results suggest an optimal protocol for nutrient injection for a microbial process. Nutrients should be injected in slugs with as high a concentration and as low a volume as practical followed by the injection of brine slugs with at least twice the volume of the nutrient slug. This will sweep nutrients away from the well bore when radial flow conditions exist and provide mixing of the nutrients deep in the reservoir. The resulting concentration distribution depends on the relative size of the nutrient and the brine slugs and on the number of slugs used.

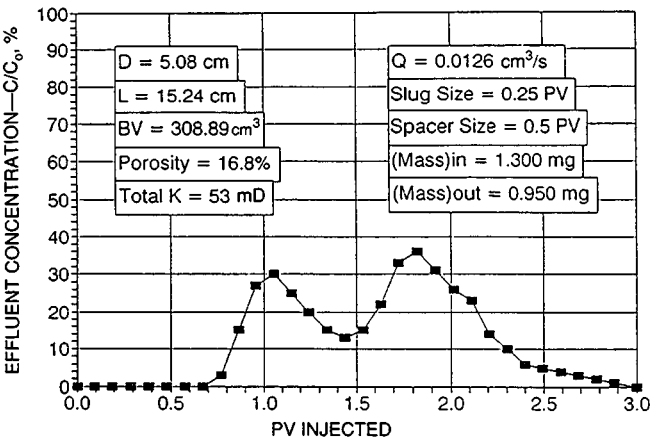

Fig. 4 Two-slug tracer test.

MICROBIAL FIELD PILOT STUDY

Contract No. DE-FG22-89BC14246

University of Oklahoma
Norman, Okla.

Contract Date: Nov. 22, 1988
Anticipated Completion: Dec. 31, 1991
Government Award: $202,272
(Current year)

Principal Investigators:
R. M. Knapp
M. J. McInerney
D. E. Menzie
J. L. Chisholm

Project Manager:
Edith Allison
Bartlesville Project Office

Reporting Period: Oct. 1–Dec. 31, 1990

Objective

The objective of this project is to perform a microbially enhanced oil recovery (MEOR) field pilot test in the Southeast Vassar Vertz Sand Unit (SEVVSU) in Payne County, Okla. Indigenous, anaerobic, nitrate-reducing bacteria will be stimulated to selectively plug flow paths that have been preferentially swept by a prior waterflood. This will force future floodwater to invade bypassed regions of the reservoir and increase sweep efficiency.

Summary of Technical Progress

Microbial Investigations

Previous studies[1] in the laboratory indicated that a molasses–ammonium nitrate nutrient mixture best stimulated the growth of microbial populations from the brines collected from the SEVVSU reservoir, Payne County, Okla. Tests were performed to evaluate the effect of varying concentrations of molasses and ammonium nitrate on the growth of the microbial populations. Brine collected from the pump manifold was amended with different concentrations of molasses and ammonium nitrate. The molasses concentration was varied from 1 to 5% (v/v), and for each molasses concentration the ammonium nitrate concentration was varied from 0.5 to 2.5% (w/v). Tubes were incubated for six weeks at 35°C, and growth was monitored spectrophotometrically as absorbance at 660 nm. The results of the experiment are shown in Fig. 1. Varying either the molasses or nitrate concentration did not significantly alter the amount of growth under any of the test conditions, which suggests that growth may be limited by the lack of some other essential nutrient in the brine–nutrient solution.

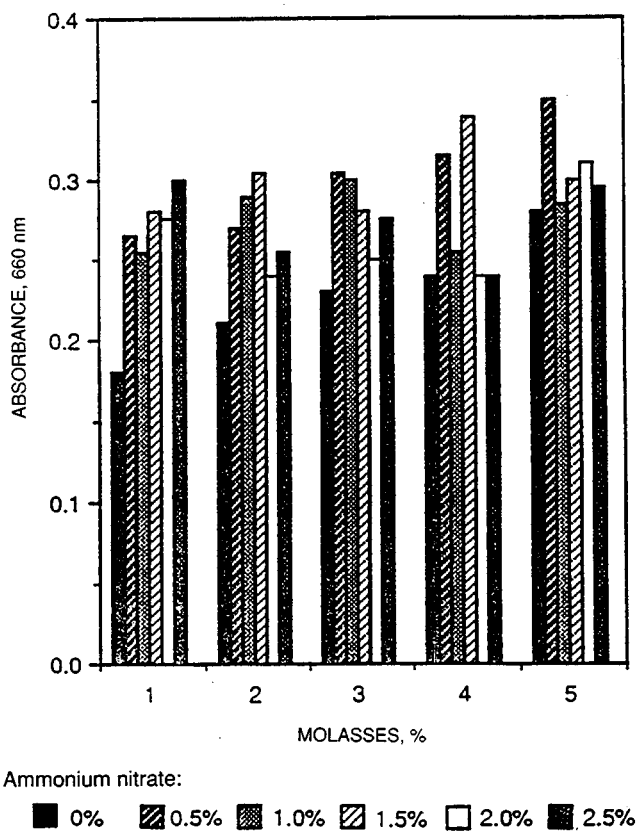

Fig. 1 Effect of molasses and ammonium nitrate on the growth of the microbial communities from Southeast Vassar Vertz Sand Unit (SEVVSU) brines.

In addition, the glucose fermentation products of five previously described[1] obligately anaerobic halophilic isolates from SEVVSU brines were analyzed. The isolates were grown in a mineral salts medium containing (g/L): PIPES (piperazine-N, N'-bis-[2-ethanesulfonic acid]) dipotassium salt, 1.5; NaCl, 120; glucose, 1; yeast extract, 0.25; resazurin, 0.001; trace mineral solution,[2] 20 mL; trace metal solution,[2] 10 mL; and a gas phase of N_2. The medium was prepared with strict anaerobic techniques.[3] At the beginning of the experiment and after 96 h of incubation at 35°C, volatile acids and alcohols in the liquid phase and CO_2 and H_2 in the vapor phase were analyzed. Volatile acids were analyzed with high-pressure liquid chromatography. Alcohols, CO_2, and H_2 were analyzed by gas chromatography. The fermentation products and carbon balances of the five isolates are shown in Table 1. All the isolates produced acetate, ethanol, CO_2, and H_2 as the end products of glucose fermentation. In addition, isolates WA and SA produced formate. Lactate, succinate, butyrate, propionate, valarate, or caproate were not detected.

Reservoir Characterization

The simulation of the SEVVSU reservoir with the Boast II black oil simulator is nearing the end of the history-matching phase. Two additional simulation runs have been performed for a more satisfactory match of observed vs. simulated water production. In particular, the model now reflects greatly reduced permeability between the portion containing the 8-2 and 8-3 wells and the main body of the reservoir. The match between observed and simulated field-wide water production is now within 5%. On a well-by-well basis, the match is within 15% with the higher volume wells more accurate. A discussion with Allen Erwin, Sullivan and Company, suggested that early water production from well 7-5 could be from another formation. An aquifer was coupled to the reservoir in this well's region to represent this formation.

Another reservoir simulator, the Eclipse 100 black-oil simulator, is being placed into service on the project. The geological model of the reservoir was constructed by digitizing maps from the current Boast II model. A grid system identical to the Boast II model was developed, and the reservoir properties were translated from maps to input files. Pressure–volume–temperature data are complete, and a recurrent production and injection data file is being prepared.

Field Pilot Operations

During the period Oct. 1, 1990, to Dec. 31, 1990, many of the physical arrangements for the field pilot test were completed. A formal contract between Sullivan and Company and the University of Oklahoma was executed during this quarter. Visits with Sullivan engineering staff have extended the agreement on various protocols for the field pilot and increased the understanding of both parties about reservoir properties, geometry, and operating history.

The wellbores and tubing of wells 5-1, 5-2, 7-1, and 7-2 were all cleaned during this quarter. Well 7-2 was acidized to increase formation injectivity. Downhole pumps, rods, beam pumping units, and flowmeters were installed on wells 5-1, 5-2, and 7-1. Three-phase, 440 V electricity has been connected to the pumping well locations and will be connected to the injection well site to power the Halliburton injection pump. Well 7-2 was connected to the field injection pump through a flowmeter and filter unit and began taking injection water in late December. The injection well is taking about 200 BPD at 300 psig surface pressure. It is expected to take 300 BPD at 500 psig.

Present plans call for a pressure falloff test in January. The three production wells are not currently pumping and have fluid to the surface. This allows casing pressures to be measured. During the falloff test, these wells will be monitored to infer directional permeability.

Once the falloff test is complete, injection will resume and the production wells will be placed on pump. After a stable flow pattern and pressure distribution are established, a sodium fluorescein tracer test will be performed.

Current nutrient plans are that 90 bbl of molasses will be mixed with 90 bbl of water containing around 6.5 tons of pelletized ammonium nitrate. This will be injected into the

TABLE 1

Glucose Fermentation Products of the Anaerobic Halophiles Isolated from Southeast Vassar Vertz Sand Unit Brines*

	Glucose consumed, mM	Products formed, mM						
		Ethanol	Acetate	Formate	CO_2	H_2	Carbon recovery, %	Hydrogen recovery, %
Isolate WA								
Exp. 1	9.67	13.45	5.39	3.25	18.31	4.63	102	101
Exp. 2	9.44	12.76	5.78	2.94	18.69	5.40	104	102
Isolate SA								
Exp. 1	10.39	10.6	7.44	3.40	18.08	5.54	92	89
Exp. 2	10.06	10.4	6.80	3.21	17.31	4.36	91	87
Isolate TA								
Exp. 1	10.06	13.90	6.74	ND†	17.73	4.89	97	100
Exp. 2	10.45	14.85	7.06	ND†	18.27	6.06	99	103
Isolate QB								
Exp. 1	5.56	5.96	8.11	ND†	9.49	2.00	113	108
Exp. 2	5.85	6.00	8.78	ND†	9.85	2.14	112	107
Isolate TTL-30								
Exp. 1	3.60	1.52	5.81	ND†	7.80	1.22	104	80
Exp. 2	4.04	1.69	6.18	ND†	8.75	1.33	101	77

*Cultures were grown in 160-mL serum bottles containing 30-mL mineral salts medium with 0.1% glucose, 0.025% yeast extract, and a gas phase of nitrogen. Volatile acids and alcohols in the liquid phase and CO_2 and H_2 in the gas phase were analyzed at the beginning of the experiment and after 96 h of incubation at 35°C.

†Not detected.

main injection flowline by the Halliburton pump at 2.5 gal/min. It will take about 2 d to inject the 200 bbl of nutrient mixture. This will be followed by 5 d of brine pad injection to disperse the nutrients within the reservoir. This process of nutrient injection followed by a pad of brine water will be repeated several times. Once nutrient injection treatments have been completed, the injection well will continue to take brine water while the field is monitored. After the last injection, a second tracer study will be run to determine if flow paths have changed.

The fluid from the producing wells will be metered for total fluid production. The produced fluid will be separated and total oil and brine production recorded. A mobile fluid sampling separator will be used on each well weekly to determine water cut.

References

1. R. M. Knapp, M. J. McInerney, D. E. Menzie, and J. L. Chisholm, Microbial Field Pilot Study, *Annual Report for the period November 22, 1989–December 31, 1989*, DOE/BC/14246-5, pp. 3-12, 1990.
2. R. S. Tanner, Monitoring Sulfate-Reducing Bacteria: Comparison of Enumeration Media, *J. Microbial. Methods*, 10: 83-90 (1989).
3. W. E. Balch and R. S. Wolfe, New Approach to the Cultivation of Methanogenic Bacteria: 2-Mercaptoethane Sulfonic Acid (HS-CoM) Dependent Growth of *Methanobacterium ruminatium* in a Pressurized Atmosphere, *Appl. Environ. Microbial.*, 32: 781-791 (1976).

MICROBIAL ENHANCED OIL RECOVERY RESEARCH

Contract No. DE-FG07-89BC14445

University of Texas at Austin
Austin, Tex.

Contract Date: Sept. 1, 1989
Anticipated Completion: Aug. 31, 1991
Government Award: $80,650
(Current year)

Principal Investigators:
Mukul M. Sharma
George Georgiou

Project Manager:
E. B. Nuckols
Metairie Project Office

Reporting Period: Oct. 1–Dec. 31, 1990

Objectives

The objective of this work is to develop an engineering framework for the exploitation of microorganisms to en-

hance oil recovery. Specific goals include (1) investigation of the mechanisms of microbially induced oil mobilization; (2) production, isolation, chemical characterization, and study of the physical properties of microbially produced surfactants; (3) model studies in sandstone cores for the characterization of the interactions between growing microbial cultures and oil reservoirs; (4) development of simulators for microbial enhanced oil recovery (MEOR); and (5) design of operational strategies for the sequential injection of microorganisms and nutrients in reservoirs.

Summary of Technical Progress

The production and purification of the biosurfactant from cultures of the microorganism *Bacillus licheniformis JF-2* were investigated, and the results from these studies are described here.

Introduction

A previous report showed that cultures of *B. licheniformis JF-2* produce a very effective surfactant under both aerobic and anaerobic conditions. The production of the surfactant-active compound is time dependent; after inoculation the interfacial tension (IFT) of the fermentation broth decreases until the cells reach the end of the exponential phase, at which point the IFT attains its minimum value. Subsequently, as growth decelerates and the cells enter stationary phase, the IFT of the broth increases rapidly; this indicates that the surfactant has been inactivated. The growth pattern of *B. licheniformis JF-2* under various conditions, the IFT of the broth as a function of fermentation time, and the production of metabolic by-products have been characterized in detail. An attempt has been made to isolate the surface-active compound(s) and characterize its chemical structure and phase behavior in tertiary hydrocarbon–brine–surfactant mixtures. Preliminary studies showed that the surfactant can be extracted from the clarified fermentation broth into ethyl acetate. A yellowish, viscous liquid was obtained after evaporation of the solvent. A solution of 1% of this liquid in 4% NaCl gave an IFT value against decane of around 5×10^{-3} mN/m, as measured by the spinning droplet technique.

The yield of active material from the ethyl acetate extraction was found to be very low. Therefore a variety of techniques for the efficient concentration and separation of the surfactant from the fermentation broth were studied.

Results

Four surfactant production cells were grown in 2-L Erlenmeyer flasks with a 500-mL working volume. The composition of the fermentation broth was 0.1% $(NH_4)_2SO_4$, 0.025% $MgSO_4$, 1% glucose in 100m*M* phosphate buffer consisting of KH_2PO_4, and K_2HPO_4 supplemented with a 1% (vol/vol) trace salt solution. The trace salt solution contained the following (g/L): EDTA, 1.0; $MnSO_4$, 3.0; $FeSO_4$, 0.1; $CaCl_2$, 0.1; $CoCl_2$, 0.1; $ZnSO_4$, 0.1; $CuSO_4$, 0.01; A1K $(SO_4)_2$, 0.01; H_3BO_4, 0.01; and Na_2MoO_4, 0.01. In most fermentations 0.5% NaCl was added. The progress of the fermentation was monitored by measuring the IFT against decane and the turbidity of the culture. It was found that the amount and age of inoculum are extremely important for the production of the biosurfactant. A fermentation protocol was devised that gave reproducibly low IFT values. After approximately 20 h of growth, the cells were removed by centrifugation, and the clarified supernatant was saved at 4°C for further purification.

A variety of techniques were used for the purification of the biosurfactant at a preparative scale. Although all these approaches did accomplish the isolation of surfactant to some extent, the recovery yield was generally low, typically 10%. Some of the results from different purification procedures are outlined in the following text.

Earlier reports have indicated that the surfactant from *B. licheniformis JF-2* can be precipitated at acidic pH. So that the efficiency of acid precipitation could be tested, the clarified fermentation broth was acidified to pH 2.0 with concentrated HCl and incubated at 4°C for at least overnight. The precipitate was recovered after centrifugation at $20,000 \times g$ for 20 min and extracted with methanol to obtain a partially purified surfactant sample. This technique was not very effective in separating the surfactant. The methanol soluble material did not show very low IFTs. In addition, neutralization of the supernatant after removal of the precipitate gave an IFT value close to that before acidification, which indicates that most of the active agent had not been removed.

Ammonium sulfate is a widely used salting-out agent for protein precipitation. The surfactant can be precipitated by the addition of ammonium sulfate at 25% of the saturation value. As a result the IFT of the supernatant increased from 0.332 to 13.250 mN/m. The precipitate, collected by filtration through a 0.45-μm membrane, was shown to be very active. The recovery yield of surfactant in this case has not been determined.

Organic extraction is a standard way of isolating active compounds from biological samples. In this case the supernatant following growth of the microorganisms was extracted with different organic solvents. The organic phase was isolated and evaporated to obtain the extracted material, which was then washed with a small amount of methanol to remove trace salts. At neutral pH, ethyl acetate performed slightly better than *n*-butanol and chloroform in extracting the surfactant from the broth. The recovery yield of the surfactant was around 5%. A relatively large quantity of organic solvent and prolonged contact time were essential for extraction. The yield of recovery can be increased by optimizing the pH or adding agents that enhance the partition of the surfactant into the organic phase.

On the basis of the fact that the surfactant can be precipitated by acidification, an anion exchange resin,

Amberlite IRA-400, was used. However, no significant adsorption of surfactant by the resin was observed even at pH 10.0 and 5% NaCl. Also, no adsorption of surfactant by Amberlite IRC-50, a cation exchange resin, was observed. On the contrary, activated carbon, Amberlite XAD-2, a hydrophobic non-ionic adsorbent that has been used for the isolation of rhamnolipid and various antibiotics from fermentation broths, and Amberlite XAD-7, a derivative of XAD-2 containing surface carboxylic esters, could adsorb surfactant from the fermentation broth efficiently. The capacity of these adsorbents was very high, in the range of 100 mL/g on the average. However, the adsorption was so strong that the adsorbed surfactant could not be eluted from the column with various organic solvents, including methanol, ethanol, acetone, ethyl acetate, and chloroform. This might indicate that strong hydrophobic interactions occur between the lipophilic domain of the surfactant molecule and the adsorbent surface. Fortunately, adsorption onto silica gel proved reversible: the adsorbed surfactant molecules could be readily eluted from the silica gel column with acetone. Upon evaporation of the acetone, active material could be obtained. However, the capacity of the silica gel was lower than that of the hydrophobic adsorbents. About 10% of the surfactant could be recovered by silica gel adsorption. The capacity of the column and recovery yield of surfactant could possibly be increased by appropriate pretreatment of the silica gel and washing with larger amount of acetone, respectively.

Following the primary extraction step, further purification was accomplished by preparative thin-layer chromatography or by gel filtration chromatography. Finally, a homogeneous compound was obtained by reverse-phase high-pressure liquid chromatography on a C_{18} column.

A STUDY OF THE INTERACTIONS BETWEEN MICROORGANISMS, MICROBIAL BY-PRODUCTS, AND OIL-BEARING FORMATION MATERIALS

Contract No. DE-AC22-90BC14665

Mississippi State University
Mississippi State, Miss.

Contract Date: June 1, 1990
Anticipated Completion: May 31, 1992
Government Award:

Principal Investigators:
Lewis R. Brown
Alex A. Vadie

Project Manager:
E. B. Nuckols
Metairie Site Office

Reporting Period: Oct. 1–Dec. 31, 1990

Objectives

The overall objective of this research is to develop basic information on the interaction between different species of microorganisms in oil-bearing formations and the interaction of rocks, microorganisms, and microbial by-products in oil-bearing formations. More specifically, this research addresses (1) the interaction between indigenous microbial species in the presence of exogenous nutrients and (2) the interaction of various microbial by-products with formation strata. The work has been divided into five tasks.

Summary of Technical Progress

In task 1 progress was made on the quantitation and identification of the microbial species indigenous to several different oil-bearing formations with special attention paid to determining whether ultramicrobacteria are present.

Core 5 was cut on Oct. 16, 1990, from Chevron Co. Well No. 679 of the EMSU oil field situated in Lea County, N. Mex. The core was obtained from 4300 to 4350 ft. The core was cut, packaged under anaerobic conditions, and received for analyses the same day. The microbiological analyses were conducted in accordance with the procedure adopted for core 4, i.e., the crushed core material was passed through a U.S.A. Standard Testing Sieve No. 40 (0.0165-in. opening) prior to mixing with the dilution water. Care was taken to ensure that particulate matter was included in all inocula, and small glass beads were added to some of the tubes of liquid media to increase the surface area available for colonization.

Aliphatic and aromatic profiles have been made for oil samples either from the core samples or from adjacent wells. Water samples have been analyzed for sodium, potassium, calcium, magnesium, iron, nickel, vanadium, zinc, chromium, copper, lead, nitrate, chloride, ammonia, nitrite, sulfate, hardness, orthophosphate, and total phosphate.

Acquisition of reservoir production and developmental data is in progress. Because of the proprietary nature of reservoir information, acquisition of certain data from respective oil companies is a very delicate, sensitive, and time-consuming matter.

Preparation for performing petrophysical and geological experiments on the cores is under way. Through a comprehensive and fundamental study of the geological nature of the cores, such as mineral composition, depositional envi-

TABLE 1

Number of Bacteria Per Gram of Core

Core No.	TSA Agar	Oil Agar	PI Agar	PCA Agar	CH_4-producing (H_4–CO_2) broth	CH_4-producing (formate) broth	NO_3 broth	NO_3–HC broth	SO_4–HC broth
1	20	240	–	0	0.7	0.0	0.0	0.0	240.0
2	–	492	–	–	92.0	>220.0	>220.0	18.6	48.0
3	640	20	80	–	>220.0	18.6	5.8	4.6	32.0
4	7200	136	1600	48	1.9	2.2	1.9	>220.0	1.2
5	–	–	–	–	0.0	0.6	0.6	58.0	>220.0

ronment, grain size, grain shape, grain orientation, particle packing, and rock diagenesis, substantial data and vital information will be available for implementation in the characterization of the reservoir rock. The cores also will be examined to generate petrophysical data, such as porosity, permeability, pore size, pore-size distribution, capillary pressure, rock interfacial tension, homogeneity, and isotropicity properties.

Core 1 was employed only to test procedures. Consequently, all other work is being conducted on cores 2 through 5. As indicated previously, the four cores (2 through 5) scheduled for this project have been subjected to analyses. Because of the length of time required to obtain the cores, work is slightly behind schedule but should be back on schedule within a few months.

The number of microorganisms obtained from the four cores is shown in Table 1. Heterotrophs and oil-degrading microorganisms were determined by plate count, whereas all other numbers were determined by the 3-tube most probable number technique (MPN).

Of the large number of pure culture isolates obtained from the various samples, 72 have been retained. The number of isolates and the medium from which they were obtained are as follows: 19 from Tryptic Soy Agar, 28 from Oil Agar, 3 from methane-producing isolates (with H_2–CO_2 atm.), 7 from methane-producing isolates (with formate), 6 from nitrate broth, 1 from nitrate-reducing, hydrocarbon-consuming broth, 2 from sulfate-reducing, hydrocarbon-consuming broth, and 6 from Plate Count Agar. All these isolates have been characterized morphologically, and selected cultures are being evaluated for their ability to use various carbon sources.

Several interesting observations have been made to date. First, no sulfate-reducing isolates have been obtained, even though the literature reports this type of organism as the most prevalent in oil reservoirs. The reason for this is not known, but note that none of the cores were from wells showing H_2S. Second, in each core only a few colonial types, rather than a great diversity of types, were found.

Task 2 is focused on determining the growth rates of and by-product formation by the indigenous microflora in pure and mixed cultures with the use of selected nutrients in flask cultures. Work has just begun on this task. Standardization of fatty acids is nearly complete. Media for various cultures have been prepared. Final selection of cultures to be used is currently being made.

Work will begin on task 3 Mar. 1, 1991, to determine the interaction between indigenous microbial by-products and the oil-bearing formation materials.

Task 4 is scheduled to begin May 1, 1991, to determine the growth rates of and by-products formation by the indigenous microflora in thin flat sandpacks prepared from formation materials and to determine the interaction between microbial by-products, the formation materials, and selected oil-recovery processes.

Task 5 is scheduled to begin Oct. 1, 1991, to determine the growth rates of and by-product formation by the indigenous microflora in live cores and to determine the interaction between microbial by-products, formation materials, and selected oil-recovery processes.

NEW MICROORGANISMS AND PROCESSES FOR MICROBIAL ENHANCED OIL RECOVERY

Contract No. DE-AC22-90BC14663

Injectech, Inc.
Ochelata, Okla.

Contract Date: Aug. 1, 1990
Anticipated Completion: July 31, 1992
Government Award: $189,482

Principal Investigators:
Penny L. Sperl
George T. Sperl

Project Manager:
Edith Allison
Bartlesville Project Office

Reporting Period: Oct. 1–Dec. 31, 1990

Objective

The objective of this research is to study the effect on microbial enhanced oil recovery (MEOR) and microbial-assisted waterfloods of microorganisms that use alternate electron acceptors. These alternative electron acceptors use as an energy source either carbonate, sulfate, or nitrate; these sources have the potential to cause a marked change in the microbial flora, the nature of the metabolic products, and the pressurization of the hydrocarbon formation by gas evolution. A three-phase evaluation will be made for each type of microbial population and electron acceptor (1) to identify mixed cultures that can grow under anaerobic conditions with either carbonate, sulfate, or nitrate as electron acceptors and with simple organic sources as electron donor sources, such as acetate, methanol, ethanol, propionate, and other volatile fatty acids (VFAs) normally found in production water; (2) to study mixed cultures of the preceding classes to minimize the requirements for added micronutrients; and (3) to study the effect of these cultures in classic Berea sandstone coreflood experiments and their effect on oil release.

Summary of Technical Progress

In the previous quarter of this project, certain aspects of the research were begun to prepare for the pursuit of some of the more detailed goals. Culture isolations were begun, and this work has proceeded quite successfully. Sources for the necessary equipment for coreflooding studies have been identified. A gas chromatograph (GC) was adapted for the detection of any and/or all biologically produced gases. This required reconfiguration of the GC's programs and columns. This is now complete and operating successfully. Any microbiological gas mixture containing any or all of the following can now be separated and quantified: methane, hydrogen sulfide, ammonia, nitrous oxide, nitrogen, hydrogen, oxygen, carbon monoxide, carbon dioxide, nitric oxide, and other short-chain hydrocarbons. This will allow the qualitative determination of the products of microbial growth and the quantitation of the gas mixtures necessary to keep the mixed cultures in a state of balance. Coreflood studies have not begun.

In this quarter *Thiobacillus denitrificans* and related denitrifying *Thiobacilli* could have potential for MEOR, especially in oil reservoirs that contain carbonate rock. All denitrifying *Thiobacillus* sp. tested will dissolve limestone and use this limestone as the sole source of carbon (Tables 1 and 2). In the examples cited, *T. denitrificans* ATCC 25259 and ATCC 23642, as well as some wild isolates from laboratory experiments and enrichment studies, including "moderately" thermophilic isolates (40°C), were used. These studies have been extended to 45°C, but growth of *T. denitrificans* under these temperature conditions is not good, even with isolates from the Soda Dam hot springs in New Mexico. The higher the temperature of the potential microorganisms for MEOR, the

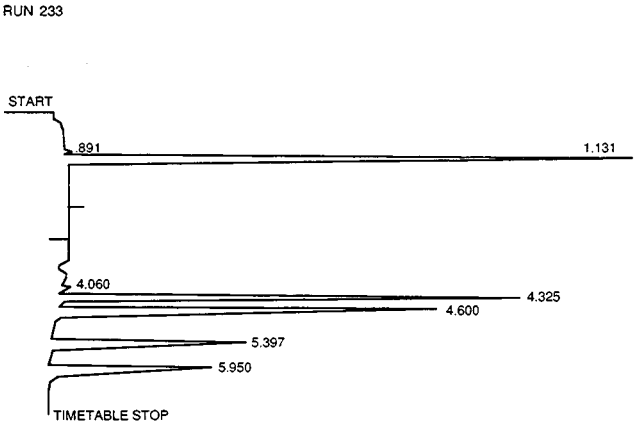

Closing signal file M: SIGNAL.BNC

RUN # 233 JAN 4, 1991 10:05:40

SIGNAL FILE: M:SIGNAL.BNC

MEOR GAS ANALYSIS

ESTD%-AREA

RT	TYPE	AREA	WIDTH	HEIGHT	CAL#	VOLUME %	NAME
.891	BB	110201	.368	4995		.000	
1.131	SBB	2633982	.062	702722	1R	4.453	CARBON DIOXIDE
4.060	PB	37748	.064	9823	2	3.289	HYDROGEN
4.325	SPB	2364610	.090	436364	3	5.520	OXYGEN
4.600	SPB	2364610	.090	436364	4	6.339	NITROGEN
5.397	BB	1377436	.113	203965	5	4.209	METHANE
5.950	PB	1891396	166	190081	6	5.251	CARBON MONOXIDE

Fig. 1 Standard gas mixture chromatography profile.

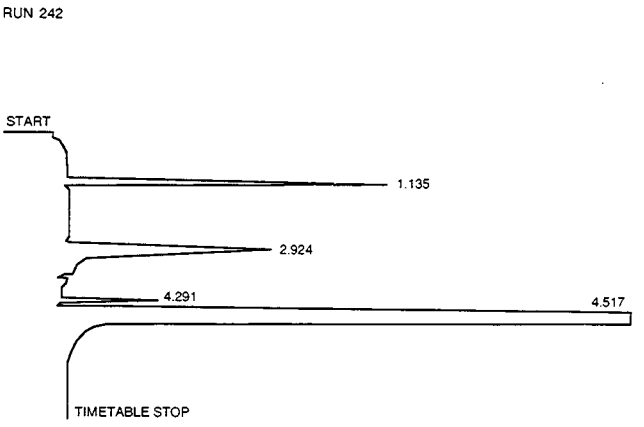

Closing signal file M: SIGNAL.BNC

RUN # 242 JAN 4, 1991 11:43:44

SIGNAL FILE: M:SIGNAL.BNC

MEOR GAS ANALYSIS

ESTD%-AREA

RT	TYPE	AREA	WIDTH	HEIGHT	CAL#	VOLUME %	NAME
1.135	BB	1231785	.072	285317	1R	2.082	CARBON DIOXIDE
2.924	BV	3357022	.284	196704	9	6.378	H_2S
4.291	PP	388924	.071	91562	3	1.117	OXYGEN
4.517	PB	31881776	.164	3240626	4	85.467	NITROGEN

Fig. 2 Gas chromatography profile of the gases produced by a typical sulfate-reducing bacterium.

TABLE 1

Dissolution of Crushed (≥100 Mesh) Limestone with Thiosulfate as Energy Source

Strain	% Dissolved
ATCC 25259	88.3
ATCC 23642	82.9
Buck Tail	85.0
Meadow Creek	86.1
1*N* HCl	87.4

TABLE 2

Dissolution of Solid Limestone in Medium 2

	Energy source		
Strain	Thiosulfate	Sulfur	Sulfide
ATCC 25259	740*	380	60
ATCC 23642	760	320	160
Buck Tail	723	370	30
Meadow Creek	635	330	35

*Milligrams per liter dissolved.

more applications they will have in reservoirs with high ambient temperatures.

It appears from these data that this limestone sample contains about 12 to 17% acid insoluble material (probably silicates).

In November cultures were set up to determine the gaseous products produced by denitrifying bacteria under conditions that might occur in an oil reservoir, i.e., reducing conditions (redox potential about –100 mV, H_2S, high nitrate concentrations). Three sulfur sources were tested as sources of energy: thiosulfate; sulfide; and metallic, elemental sulfur. The cultures were sparged with helium before they were sealed, although these procedures did not completely eliminate the presence of air in the cultures. The produced gases were then collected and subjected to chromatographic separations and quantitations. A key indicator of active denitrification is the production of nitrous oxide (N_2O) by the organisms. Copious N_2O was formed by most *T. denitrificans* strains when thiosulfate was used as an energy source. ATCC strains 25259 and 23644 both produced N_2O when elemental sulfur (S^0) was used and strains 29685, 23642, and 25259 produced N_2O when sulfide ($S^=$) was used as an energy source, although growth appeared to be minimal when compared with growth with thiosulfate. In addition, large amounts of nitrogen were produced by all cultures tested with each of these sulfur energy sources. As shown, H_2S is inhibitory and must be kept at low concentrations, but it may be added daily for good growth. Tests were run on the profiles of sulfate-reducing bacteria grown in the presence of the same medium as *T. denitrificans* but with added iron, organic acids (acetate, lactate, propionate, butyrate, and formate), and reduced power to about –200 mV. The gas produced under these conditions is primarily CO_2. When the cultures are acidified, significant levels of dissolved CO_2 are released from solution along with significant H_2S. Traces of ammonia are also formed in these cultures. It appears from these data that these cultures can be realistically mixed, and this will be attempted in the next quarter. It also appears that redox potential does have some effect on *T. denitrificans*, although the ranges where they are tolerant to redox potential overlaps well with the redox potential requirements for *Desulfovibrio* and related sulfate-reducing bacteria. No significant methane has been shown in any of the cultures. It could be simply that the media necessary for MEOR cannot support the growth of significant populations of methanogens, or it could be that the rather "loose" anaerobic conditions necessary for the successful cultivation of both denitrifying *Thiobacilli* and sulfate-reducing bacteria are not stringent enough to meet the requirements of typical methanogens.

The amount of limestone dissolved in a field is not critical since the simple opening of a new channel for water flow could have significant effects. In addition to the obvious effect of limestone dissolution, *T. denitrificans* could also have the effect of the typical MEOR microorganisms, such as selective plugging by the bug bodies of well-washed channels, production of considerable N_2 gas for well pressurization (enough N_2 gas is produced in some cultures that if the vessel is sealed tightly, then the gas pressure can actually cause a glass tube or bottle to explode), and production of increased CO_2 pressure through the dissolution of carbonate that is in equilibrium with CO_2. With optimization, about 1 g of limestone per liter of culture can be dissolved by *T. denitrificans* in the laboratory. An average waterflood injects 15,000 L of water per day, or about 15 kg of limestone can be dissolved per day, or 2 to 3 tons of carbonate could be dissolved in a year in a typical well if the microorganisms are continuously actively growing. This is not likely to happen, but the numbers do show the great potential of using *T. denitrificans* in MEOR processes. The limestone supplies the CO_2 necessary for the growth of *T. denitrificans* by the dissolution of carbonate, which is in equilibrium with dissolved CO_2. Ordinarily, CO_2 is supplied to *Thiobacilli* in the form of dissolved carbonate or bicarbonate. The dissolution of carbonate buffers the growth medium of the culture to a constant pH of 6.5, which is optimum for the growth of *T. denitrificans*. All acid produced from the oxidation of reduced sulfur compounds during growth is neutralized by the dissolution of limestone. The necessary nutrients added are ammonia and nitrate in the form of ammonium nitrate (which supplies both the alternate electron acceptor and a nitrogen source for the organisms),

a small amount of phosphate (just enough to satisfy the nutritional requirements of the microbes; otherwise the buffering capacity of the phosphate may interfere with the dissolution of the limestone), a reduced sulfur source necessary for the energy reactions of the cultures (this may theoretically be any of the following: sulfur, thiosulfate, tetrathionate or sulfide), and trace metals (most brines contain high enough concentrations of B, Zn, Cu, Co, Mn, Fe, Mo, W, Ni, and Se to satisfy the requirements of typical denitrifying microbes for trace elements). Under the best conditions, the only necessary materials that need to be injected into a well for MEOR processes would be ammonium nitrate, phosphate, and the microbes. Under the least ideal conditions, this list would include ammonium nitrate, phosphate, a reduced sulfur source, the microbes, and possibly some metal nutrients in very low concentrations.

In addition to the culture work done with *T. denitrificans*, strains of sulfate-reducing bacteria were also isolated and obtained. *Desulfovibrio desulfuricans* and *Desulfotomaculum* were obtained from the American Type Culture Collection and have been cultured at 40°C. These organisms were cultured on a minimal medium containing acetate, propionate, and butyrate as carbon sources. These fatty acids are the typical ones found dissolved in waters from most oil fields, and the concentrations used (100 to 750 ppm) are also typical. Strains from material obtained from the Trans-Alaska pipeline and other pipeline fouling material have also been isolated. The key to these organisms is that if *T. denitrificans* and *Desulfovibrio* can be mixed in a single culture, then the naturally occurring fatty acids will drive sulfur reduction, which will serve as the energy source for the denitrifying *Thiobacilli*. Thus the only necessary nutrients that will need to be added will be ammonium nitrate and some source of phosphate; all other nutrients will be supplied by naturally occurring chemicals in the formation and brines. In the next quarter an attempt will be made to mix these cultures. These organisms exist mixed in nature, but it is difficult to know whether or not they can be artificially mixed in a nontypical environment and both be active at the same time and form some type of stable community. There is a real possibility the eH may play a more important factor than originally thought. These questions will be answered in the next quarter.

The third group of microorganisms that may play an important role in our MEOR studies is the methanogenic microorganisms. At this point methanogens from pipelines have been identified which may be of use in our system. The mixture cited previously is theoretically capable of operating as a two-component system, but methanogens will eventually become a part of the microbial community, especially if CO_2 and H_2 are present. The source of reducing power should be the simple volatile fatty acids with CO_2 as the acceptor. Again, eH will be an important factor in the balance of the mixed microbial population, and if the eH is not strictly regulated, the first member of the community to suffer will be the methanogens.

In the third quarter, coreflooding experiments will begin with the use of each of these organisms individually and as mixtures, both grown separately and then mixed and grown in a mixed community.

ENVIRONMENTAL TECHNOLOGY

TECHNICAL ANALYSIS FOR UNDERGROUND INJECTION CONTROL

Cooperative Agreement DE-FC22-83FE60149, Project SGP23

National Institute for Petroleum and Energy Research
Bartlesville Okla.

Contract Date: Oct. 1, 1989
Anticipated Completion: Sept. 30, 1991
Funding for FY 1991: $74,500

Principal Investigator:
Michael P. Madden

Project Manager:
Alex Crawley
Bartlesville Project Office

Reporting Period: Oct. 1–Dec. 31, 1990

Objective

The objective of this project is to provide technical assistance to the Department of Energy (DOE) on matters related to underground injection control or other environmental topics related to oil and gas production.

Summary of Technical Progress

No request by the Bartlesville Project Office for technical assistance was made during this quarter. Only minimal effort and financial expenditures were directed to this project—for preparation of monthly and quarterly reports.